TIME-DEPENDENT BEHAVIOR OF PIN-BEARING BOLTED CONNECTIONS IN PULTRUDED FIBER REINFORCED POLYMER COMPOSITES UNDER NORMAL AND ELEVATED TEMPERATURES

A Dissertation
Presented to
The Academic Faculty

by

Javaid Anwar

In Partial Fulfillment
of the Requirements for the Degree
Doctor of Philosophy in the
School of Civil and Environmental Engineering

Georgia Institute of Technology
August 2017

Copyright © 2017 by Javaid Anwar

TIME-DEPENDENT BEHAVIOR OF PIN-BEARING BOLTED CONNECTIONS IN PULTRUDED FIBER REINFORCED POLYMER COMPOSITES UNDER NORMAL AND ELEVATED TEMPERATURES

Approved by:

Dr. David W. Scott, Advisor
School of Civil and Environmental Engineering
Georgia Institute of Technology

Dr. Russell T. Gentry
School of Architecture
Georgia Institute of Technology

Dr. Abdul-Hamid Zureick
School of Civil and Environmental Engineering
Georgia Institute of Technology

Dr. Lauren Stewart
School of Civil and Environmental Engineering
Georgia Institute of Technology

Dr. Rafi L. Muhanna
School of Civil and Environmental Engineering
Georgia Institute of Technology

Date Approved: May 3, 2017

To my parents, wife and children

ACKNOWLEDGEMENTS

All glory to Allah Almighty, the creator of the heavens, the earth, and everything between them. The creator of light, time, man, and woman. The ultimate source of knowledge and power. The one who gave me the ability to pursue my education, complete my work, and write this dissertation.

Although only my name appears on the cover of this dissertation, a great many people have contributed towards the fulfillment of this research. I owe my gratitude to all those who contributed to the completion of this work. My research advisor and my teacher, Dr. David W. Scott, has been instrumental in the completion of this research. His insightful comments, untiring guidance, extraordinary patience, and encouragement made this effort a success. I would also like to thank my dissertation committee members Dr. Abdul-Hamid Zureick, Dr. Rafi L. Muhanna, Dr. Russell T. Gentry, and Dr. Lauren Stewart, for their helpful comments and suggestions. Special thanks to the facility manager, Jeremy W. Mitchell, for his time and valuable suggestions about my experiments that were conducted in the Structural Engineering and Materials Laboratory at the Georgia Institute of Technology.

Finally, none of this would have been possible without my wife, my children, my parents, and siblings. They have been a constant source of love, concern, motivation, and strength throughout my Ph.D. program.

TABLE OF CONTENTS

LIST OF TABLES

LIST OF FIGURES

LIST OF SYMBOLS AND ABBREVIATIONS

A	Creep constant (function of temperature and bolt torque)
C_Δ	Geometry factor
C_M	Moisture condition factor
C_T	Temperature condition factor
E_L^t	Tensile modulus in the longitudinal direction of FRP, MPa (ksi)
F_L^{br}	Pin-bearing strength in the longitudinal direction of FRP, MPa (ksi)
F_L^t	Tensile strength in the longitudinal direction of FRP, MPa (ksi)
F_θ^{br}	Characteristic pin-bearing strength for the orientation of the resultant force at the bolt/FRP contact with respect to the direction of pultrusion, MPa (ksi)
L	Length of test specimen, mm (in)
P_t	Tensile load in bolt, kN (lbf)
R_{br}	Pin-bearing strength, kN (kip)
$R_{br}(t)$	Time-dependent pin-bearing strength, kN (kip)
R_n	Nominal connection strength, kN (kip)
R_u	Required connection strength due to factored loads, kN (kip)
T	Applied torque, N-m (lbf-in)
T_e	Elevated temperature, °C (°F)
T_o	Ambient (room) temperature, °C (°F)
T_g	Glass-transition temperature, °C (°F)
V_{csm}	Volume fraction of CSM fibers
V_{fil}	Volume fraction of fillers
V_{res}	Volume fraction of resin

V_{rov}	Volume fraction of roving fibers
V_v	Volume fraction of voids
V_X	Coefficient of variation
$X_{k(n)}$	Characteristic value
d	Nominal bolt diameter, mm (in)
d_n	Nominal bolt-hole diameter, mm (in)
e	Edge distance, mm (in)
k	Torque coefficient
$k_c(t)$	Time-dependent amplification factor accounting for creep
$k_{cr}(t)$	Deflection amplification factor
k_{def}	Deformation factor
k_n	Characteristic fractile factor
m	Stress-dependent and temperature-dependent coefficient
m_X	Mean of test results
n	Stress-independent and temperature-independent material constant
p	Creep constant (function of temperature and bolt torque)
q	Creep constant (function of temperature and bolt torque)
u	Total deformation, mm (in)
u_{fin}	Final deformation, mm (in)
u_{inst}	Instantaneous deformation, mm (in)
u_{st}	Instantaneous deflection due to gravity loads, mm (in)
w	Connection width, mm (in)
α	Characteristic extreme (scale) parameter of Weibull probability distribution function

β	Dispersion (or shape) parameter of Weibull probability distribution function
Δd	Bolt-hole deformation, mm (in)
Δd_{creep}	Creep component of the bolt-hole deformation, mm (in)
Δd_{inst}	Instantaneous deformation of the bolt-hole measured immediately upon loading, mm (in)
Δd_{total}	Total bolt-hole deformation, mm (in)
$(\Delta d/d)_o$	Percent bolt-hole deformation at the bearing failure load
$\dot{\Delta}_c$	Rate of creep component of percent hole elongation
$\varepsilon\,(t)$	Total time-dependent strain
ε_i	Stress-dependent initial elastic strain
$\dot{\varepsilon}_c$	Creep strain rate
ε_o	Initial strain to be defined after some loading period
λ	Time effect factor
σ_b	Applied bearing stress, MPa (ksi)
σ_{bu}	Maximum bearing stress, MPa (ksi)
σ_z	Transverse compressive stress, MPa (ksi)
σ_o	Pin-bearing strength, MPa (ksi)
ϕ	Resistance factor
ϕ_c	Resistance factor for connection
Ψ_1	Factor accounting for bolt-hole clearance
Ψ_2	Factor accounting for temperature
Ω	Data confidence factor

SUMMARY

Whereas numerous studies have focused on the influence of various connection parameters on the short-term response of bolted connections in pultruded fiber-reinforced polymer (FRP) composites, few have examined their long-term behavior. This dissertation examines the short- and long-term response of an E-glass/polyester pultruded FRP material subjected to single pin-bearing loads. The investigation involves experiments on single-bolt tension connections under a double-lap shear configuration at normal and elevated service temperatures. Elevated temperature tests are conducted at 43.3, and 60°C (110, and 140°F). First, the effect of specific connection parameters including diameter-to-thickness ratios, bolt-hole clearances, and bolt tightening torques on the bearing strength of a connection are evaluated. Then, time-dependent pin-bearing tests are conducted at various load levels selected based on the short-term test results. Sustained load tests are carried out on material coupons for time durations of up to 1,000 hours. Based on short- and long-term test results, a semi-empirical predictive model is proposed for the time-dependent behavior of the pultruded FRP materials subjected to single pin-bearing loads. Finally, an equation is proposed to estimate the time-dependent pin-bearing strength of a connection that considers the effect of temperature and connection conditions.

CHAPTER 1

INTRODUCTION

1.1 Research Motivation

Fiber-reinforced polymeric (FRP) composites represent a growing class of materials used in civil engineering applications including new construction as well as the repair of existing structures. FRP members can offer significant advantages such as high strength-to-weight and stiffness-to-weight ratios, resistance to corrosion, design flexibility, and ease of installation. The aforementioned properties make FRP composites competitive with traditional construction materials such as structural steel and reinforced concrete in many applications. Amongst various manufacturing processes for FRP composites, the pultrusion process is among the most cost efficient. Pultrusion is a process that combines pulling and extrusion, in which continuous fibers are pulled through a resin bath, formed into a shape, and then pulled through a heated die in which polymerization of the resin into a hardened form occurs and full section emerges. A schematic illustration of the pultrusion process is shown in Figure 1.1 [1].

The successful assembly of structural systems made of FRP materials requires connections between elements; these connections must be considered when assessing the overall behavior of the structure. Bolted connections (schematic shown in Figure 1.2) are a common method of joining FRP members. The strength and failure modes of bolted connections are influenced by a variety of factors including connection parameters, environmental conditions, and loading type. As discussed by Mottram and Turvey [2], the

scope of testing needed to evaluate the number of connection variables is large enough to be possibly impractical to undertake. Similarly, the behavior of bolted connections under sustained loading is a complex phenomenon due to the viscoelastic behavior of many FRP materials. There exist significant gaps in the understanding of the time-dependent behavior of pultruded FRP members, which limits the effectiveness of design criteria developed for these advanced materials. It is therefore imperative to study this behavior in order to develop and validate design criteria to be used with these materials.

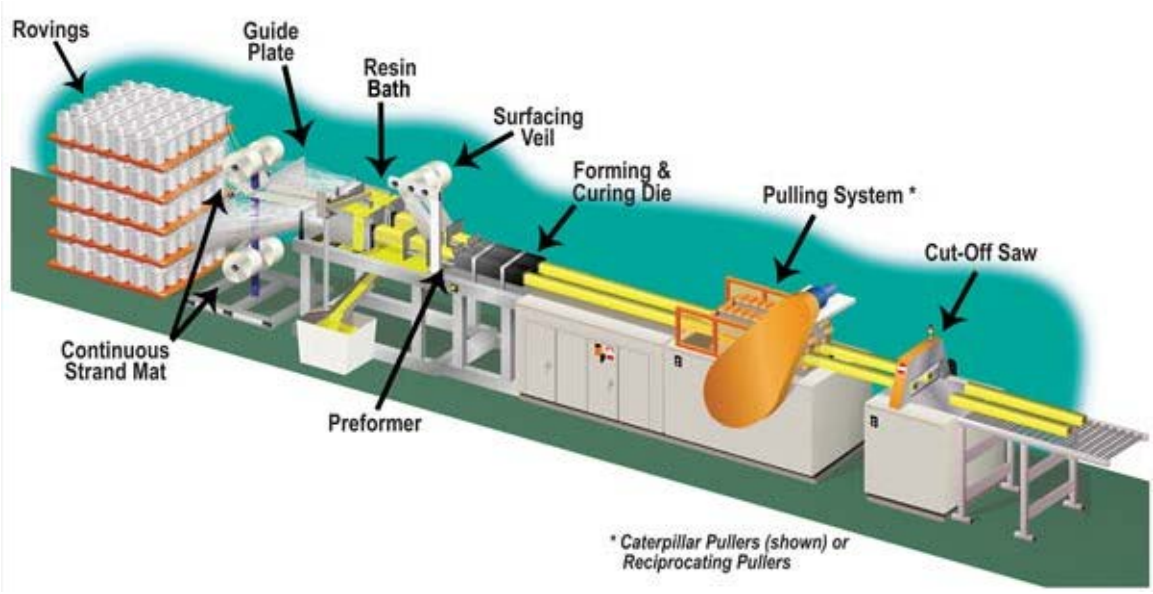

Figure 1.1 Schematic illustration of pultrusion process (reprinted with permission) [1].

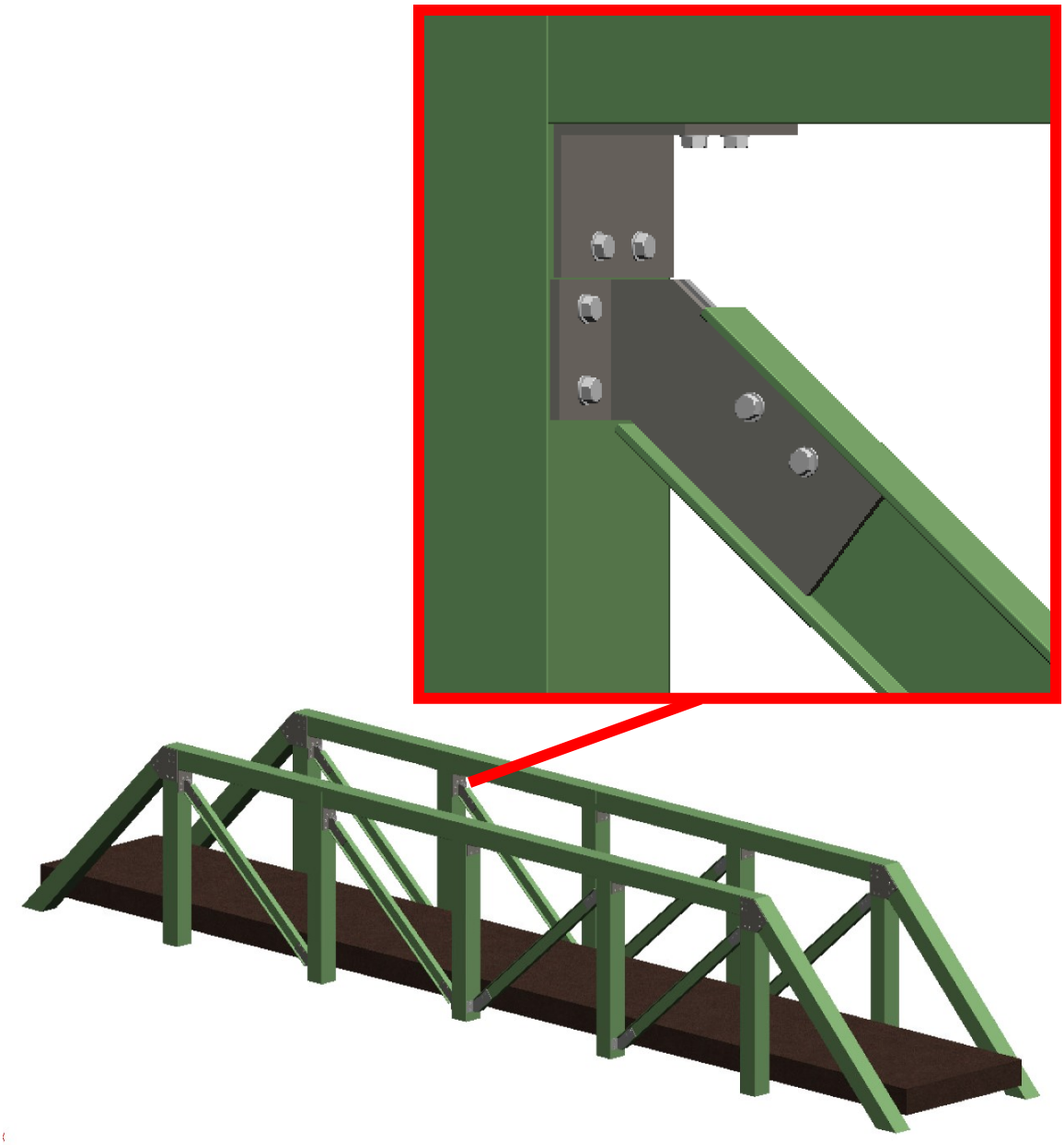

Figure 1.2 Schematic illustration of bolted connections in FRP bridge.

1.2 Scope and Objectives

The primary objective of this research program is to investigate the pin-bearing behavior of E-glass/polyester pultruded FRP composite materials. The investigation involves single bolt connections subjected to in-plane loading in tension under a double-lap shear configuration. First, short-term pin-bearing tests are carried out at normal and elevated service temperatures to investigate the effects of specific connection parameters on bearing strength. Then, time-dependent pin-bearing tests are conducted at various load levels selected based on the short-term test results. Bearing deflections in the FRP material at the pin are recorded for time durations of up to 1,000 hours. These time dependent tests include consideration of normal and elevated service temperatures. Based on short- and long-term test results, a semi-empirical predictive model is proposed for the time-dependent behavior of the pultruded FRP materials subjected to single pin-bearing loads. Specifically, the objectives of this research are:

a. To examine the influence of specific connection parameters (*d/t* ratio, bolt-hole clearance and bolt tightening torque) on the short-term pin-bearing strength at normal and elevated service temperatures.

b. To investigate the behavior of pin-bearing connection under constant sustained loads at various load levels, specific bolt-hole clearances and specific bolt tightening torques at normal and elevated service temperatures.

c. To propose a suitable predictive model for the time-dependent behavior of pin-bearing connection based on semi-empirical modeling, and experimental results.

d. To develop a suitable equation to estimate the time-dependent pin-bearing strength of a connection including the effect of temperature and connection conditions.

CHAPTER 2

PREVIOUS WORK

Connections in pultruded profiles can generally be divided into three categories; bolted, adhesively bonded and combined (bolted and bonded) connections. Adhesively bonded connections generally fail in a brittle manner whereas combined connections are more ductile and are efficient when a high degree of restraint is desirable [3]. Bolted connections are often preferred in civil engineering applications because of practicality, ease of installation in the field, dismantling and simple inspection procedures. The major disadvantage of bolted connections is the presence of holes that cause stress concentrations. Also, holes disrupt the continuity of the fiber reinforcement, which may promote localized failure modes like delamination at the hole edge due to large through-thickness stress gradients [4].

A large body of work exists regarding the pin-bearing behavior of FRP composite materials. Although very limited research has been performed specifically related to the long-term response of pin-bearing connections under sustained loading, a large array of work pertaining to different factors that affect the short-term bearing behavior of connections can be found in the literature. Thoppul et al. [5] presented a review on mechanics of bolted connections and Gand et al. [6] presented a state-of-the-art review on the behavior of FRP composites and identified knowledge gaps. More recently, Coelho and Mottram [7] presented a detailed review of the behavior of FRP connections and joints. The literature review presented in this study pertains to plate-to-plate connections and does not include beam-to-column joints. The factors deemed pertinent to this study are highlighted.

2.1 Failure Modes

The double-lap single bolt tension connections in pultruded profiles may fail in one of four distinct failure modes as shown in Figure 2.1; bearing, cleavage, shear-out, or net-tension. The bearing failure mode occurs due to localized crushing of the FRP where the bolt shank contacts the cylindrical surface of the bolt hole. The other failure modes are associated with shear and tension stresses exceeding the corresponding material strengths along planes parallel or normal to the tension direction [8]. These four modes are for concentric tension loading either parallel or normal to the direction of pultrusion. Mixed modes are possible when the connection force is off-axis [2]. Amongst these failure modes, bearing is the only benign failure mode, characterized by progressive damage growth, which develops slowly and hence is typically most desirable. Other failure modes often occur abruptly and fail without warning. The controlling failure mode is typically dictated by particular geometric parameters; edge distance *e*, bolt diameter *d*, and connection width *w*. Table 2.1 [8] shows typical *e/d* and *w/d* ratios associated with the four distinct failure modes of single-bolt tension connections in pultruded glass fiber reinforced polymer (GFRP) plate.

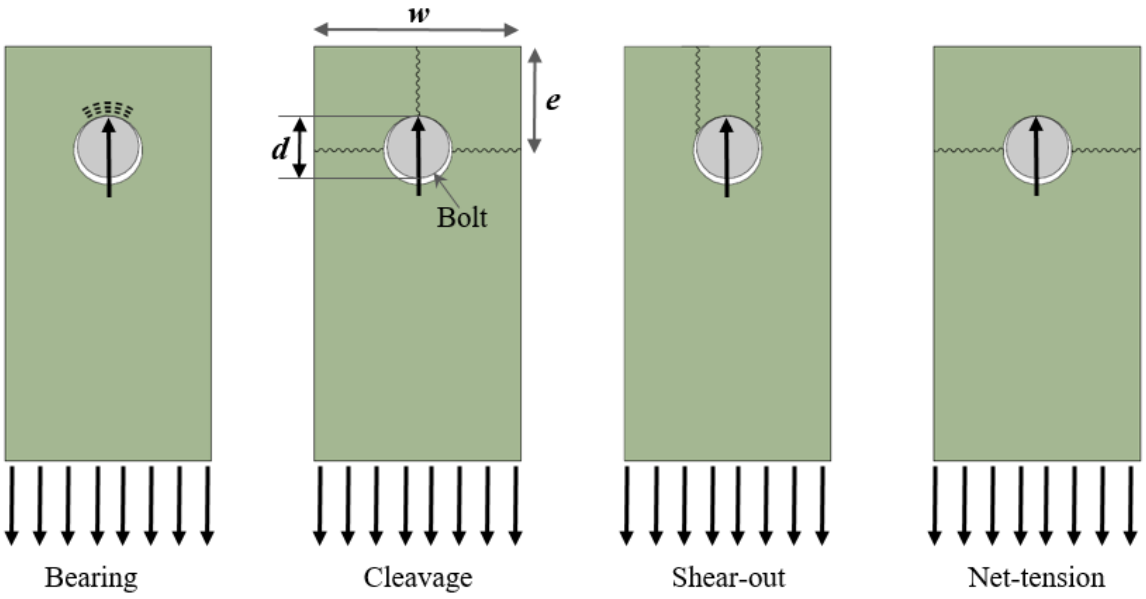

Figure 2.1 Potential failure modes in double-lap single-bolt FRP connections (after [8]).

Table 2.1 Typical *e/d* and *w/d* ratios associated with the four basic failure modes of single-bolt tension connections in 6.4 mm (1/4 in) thick pultruded GFRP plate at ambient temperature with roving and tension directions coincident (after [8]).

Failure mode	***e/d***	***w/d***
Bearing	5	7
Cleavage	2	5
Shear-out	2	10
Tension	7	3

2.2 Pin-Bearing Strength

Pin-bearing strength (R_{br}) is typically computed as the projected area of the bolt bearing times characteristic pin-bearing strength (F_{θ}^{br}) [9,10], given by Equation (2.1).

$$R_{br} = tdF_{\theta}^{br} \tag{2.1}$$

where

R_{br} = pin-bearing strength, kN (kip)

t = thickness of the FRP component and/or member, mm (in)

d = nominal diameter of bolt, mm (in)

F_{θ}^{br} = characteristic pin-bearing strength for the orientation of the resultant force at the bolt/FRP contact with respect to the direction of pultrusion, MPa (ksi)

By definition pin-bearing strength is the mean stress at bearing failure. However, the failure load is defined when there is no lateral restraint in the connection. For the bearing strength to be the pin value there must be no tightening of the bolt. A review of test methods reveals a lack of consistency in how pin-bearing strengths of pultruded materials are measured [11,12]. The lack of consistency comes from various factors including but not limited to the definition of failure load, bolt-hole clearance, lateral restraint, and testing procedures.

The definition of failure load can be examined in different ways from the load-extension plot obtained during a bearing strength test. Figure 2.2 shows a typical load-extension plot that allows various ways of defining the failure load [13]; these potential failure loads are defined in Table 2.2. Mottram and Zafari [12] explained that failure loads

(*d*) to (*g*) have not been observed in pin-bearing strength tests of pultruded materials. Failure load (*c*) depends on the gauge length used to measure the bolt-hole elongation. Failure load (*b*) is not observed in pin-bearing strength tests with coincident direction of loading and direction of pultrusion. Hence, through the process of elimination, the authors' concluded that pin-bearing strength should always be determined using failure load (a), i.e. the maximum load.

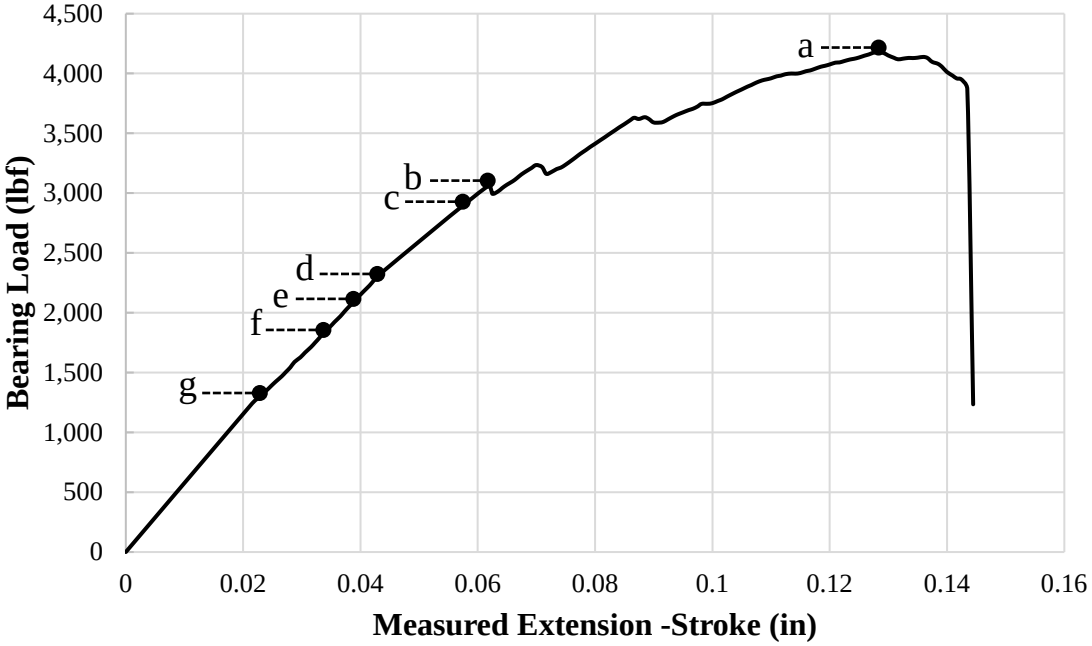

Figure 2.2 Representative load-extension plot showing various ways to define failure load (after [13]).

Table 2.2 Potential failure loads (after [12,13]).

Failure load	Description
a	The maximum load. Typically, considerable damage will have occurred in reaching this load.
b	The first peak in the load/extension plot. Damage sustained up to this load is not insignificant.
c	The load corresponding to a specified amount of hole elongation.
d	The load at which the load/extension curve first deviates from linearity. The point at which this occurs is usually difficult to establish.
e	The load at which cracking first becomes audible. Specimens examined at this point would show visible cracks around the loaded side of the bolt hole.
f	The load at which cracking is initiated. This load is probably quite low and very difficult to determine.
g	The load at which cracks become visible outside the washers.

2.3 Review of Test Methods

A brief review of existing test methods is presented to highlight the differences in measuring pin-bearing strength. ASTM Standard D953-10 [14] provides a method to compute the bearing strength of plastics. The tensile test Procedure A in the standard specifies the testing of connection under a double lap shear configuration. Maximum bolt-hole clearance is 0.075 mm (0.003 in) for 6.325 mm (1/4 in) diameter bolt. In other words, maximum bolt-hole diameter (d_n) is 1.012 times bolt diameter, i.e. a maximum bolt-clearance of 0.012 d_n. The *e/d* and *w/d* ratios are specified as 3 and 3.7 respectively for a

6.325 mm (1/4 in) diameter bolt. Bearing strength corresponds to the bearing stress at which the bearing hole has undergone displacement equal to 4 % of its initial diameter.

ASTM Standard D5961-10 [15] provides a method to evaluate the bearing response of polymer matrix composite laminates. This standard allows testing under both double lap shear and single lap shear configurations. The specimen is specified to have a close-tolerance bearing hole and lightly lateral applied torque (2.2 to 3.4 N-m (19.5 to 30 lbf-in)). The *e/d* and *w/d* ratios are specified as 3 and 6 respectively for a 6 mm (1/4 in) diameter bolt. Ultimate bearing strength is determined from the maximum load carried by the specimen. The standard also offers a methodology for determining offset bearing strength. The specimen is loaded until a maximum load is reached and the applied force has subsequently dropped off approximately 30% from the maximum, or displacement equal to one-half the hole diameter has occurred.

The ASCE Load & Resistance Factor Design (LRFD) Pre-Standard (2010) [10] specifies bolt diameters in the range of 9.53 mm (3/8 in) up to and including 25.4 mm (1 in). Hardened flat circular washers are specified to have an outer diameter at least twice the nominal bolt diameter. Bolts are to be torqued to the snug-tightened condition. The nominal bolt-hole diameter (d_n) is specified to be a minimum 1.6 mm (1/16 in) larger than the nominal bolt diameter. In other words, the bolt-hole clearance is in the range $0.06d_n$ to $0.14d_n$ for bolt size ranging from 25.4 to 9.53 mm (1 in to 3/8 in). Statistical analyses are to be conducted per ASTM D7290.

2.4 Connection Parameters Influencing Pin-Bearing Strength

2.4.1 Fiber Orientation

When the direction of pultrusion and connection force are coincident, the pin-bearing strength is highest. If the connection force is perpendicular to the pultrusion direction, the pin-bearing strength is lowest. Rosner and Rizkalla [16] tested 102 single-bolt connections under a double-lap shear configuration. The GFRP used in the study consisted of E-glass fibers and polyester matrix. High-strength bolts having 19 mm (0.75 in) diameter were used having sufficient length such that bolt shank was in contact with the hole and not the bolt threads. Connections were tightened to a torque of 32.5 N-m (24 Ibf-ft) and bolt-hole clearance of 1.6 mm (1/16 in). It was observed that on average the bearing strength of connections was reduced by 18 and 24% when the fiber direction with respect to loading was 45° and 90° respectively, as compared to coincident loading. Turvey [17] conducted 54 tests on single-bolt tension connections in pultruded glass reinforced plastic (GRP), to study the influence of angle between pultrusion and loading direction, and the joint geometry. The 6.4 mm (1/4 in) thick GRP plate used in the study consisted of E-glass fibers, continuous filament mat (CFM) and polyester resin. Tests were conducted on 10 mm (0.39 in) tight fitting holes, and the bolts were lightly torqued to 3 N-m (2.2 lbf-ft). A total of 18 tests were conducted each for 30°, 45°, and 90° between the pultrusion and loading direction. The author observed that for off-axis angles greater than 30°, the tension failure mode dominated and cracks propagated parallel to the rovings.

2.4.2 *e/d* and *w/d* Ratio

In addition to investigating the influence of fiber orientation, Rosner and Rizkalla [16] also studied the effect of geometric parameters including the connection width *w*, the edge distance *e*, and the thickness *t*. The controlling failure mode was typically dictated by specific geometric parameters. The authors demonstrated that for coincident fiber orientation and loading, the geometric parameter *w* significantly influenced the capacity of a connection, and the corresponding mode of failure. For coincident fiber orientation and loading, the bearing strength of the connection increased with increases in *e/d* and *w/d* ratios up to a value of 5. The authors recommended minimum *e/d* and *w/d* ratios of 5.

2.4.3 Lateral Restraint/Bolt Torque

Stewart [18] showed that for steel bolts loaded in tension as a result of applied torque *T*, the resultant tensile load in bolt P_t is given by Equation (2.2). The relationship between the applied torque and the induced tension is variable, since most of the applied torque is consumed by friction. In the study, the author has shown that the torque coefficient *k* was substantially constant at a value of 0.2 for all bolt diameters and for both coarse and fine threads.

$$T = kdP_t \tag{2.2}$$

Collings [19] further established the relationship between torque and constraint stress. For a standard washer the diameter was assumed to be 2.2 times the diameter of the hole and the simplified expression for lateral constraint expressed as transverse compressive stress (σ_z) was given by Equation (2.3).

$$\sigma_z = 1.658 \frac{T}{d^3} \tag{2.3}$$

Collings conducted tests on laminates consisting of carbon fibers and epoxy resin systems. Amongst other factors Collings also investigated the effect of lateral constraint on bearing strength. Laminates$(0° \pm 45°)$ balanced about the mid-plane were tested in tension. It was observed that the effects of *d/t* on bearing strength were negligible for high lateral pressure (22 MPa (3.19 ksi)) as shown in Figure 2.3.

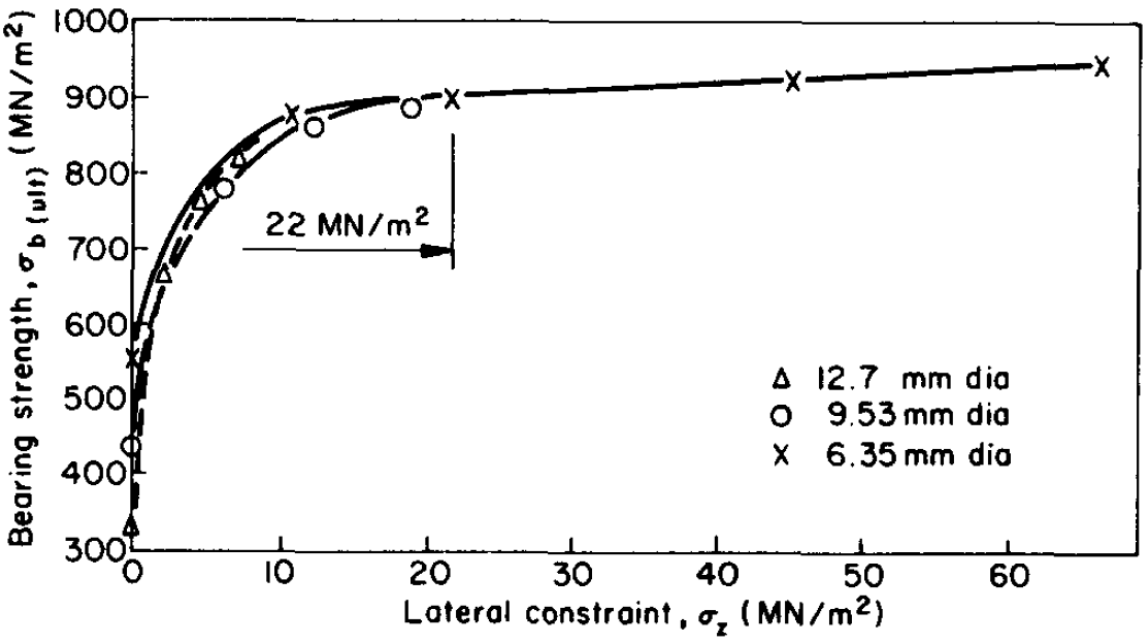

Figure 2.3 Variation of bearing strength with lateral restraint - $(0° \pm 45°)$ laminate (reprinted with permission) [19].

Stockdale and Matthews [20] conducted tests on bolted connections in composite materials. Flat plate specimens having 2 mm (0.08 in) thickness were made from E-glass fibers preimpregnated with Shell (DX231/DX137)® resin. Two different layups each having seven layers were investigated for 6.3 mm (1/4 in) diameter holes. Washers having an outside diameter of 16 mm (0.63 in) were used and tests were conducted for bolt clampup loads of 0, 4.9, 9.8, and 14.7 kN (0, 1.1, 2.2, and 3.3 kips). The main conclusion of this study was that bearing failure load increased with an increase in bolt clampup load.

Kretsis and Matthews [21] conducted experiments on GFRP laminates with single-hole bolted joints. Different fiber/resin combinations and layups were used in the experimental program. It was observed that the strength of laterally unrestrained specimens was less than "finger-tight" specimens by a range of 20-30%. Similar to Colling's conclusion, the authors observed that bearing strength increased asymptotically with an increase in lateral pressure.

Cooper and Turvey [22] conducted 81 tests to study the effect of joint geometry and bolt clamping torque on the failure load, failure mode and stiffness of double lap, single-bolt joints (10 mm (0.39 in) diameter). The material consisted of E-glass fibers in a polyester epoxy resin and filler (e.g. clay or calcium carbonate) matrix. Connections were tested in tension at three clamping conditions: the pin bearing condition (zero bolt clamping torque with no lateral constraint), the lightly clamped condition (3 N-m (27 lbf-in) bolt clamping torque) and the fully clamped condition (30 N-m (266 lbf-in)) bolt clamping torque). It was observed that as the bolt torque was increased from zero to 3 N-m (27 lbf-in) and 30 N-m (266 lbf-in), the bearing failure load increased by 45 and 80% respectively.

Yuan and Liu [23] conducted experiments on bolted connections in GFRP flat sheets having E-glass fibers and polyester matrix. The specimens were 9.5 mm (3/8 in) thick, 102 mm (4 in) wide and 343 mm (13.5 in) long. Close-fit, single-bolt connections were tested in a double-lap shear configuration with a *w/d* ratio of 7. Tests were conducted at different torque levels ranging from 0 to 34 N-m (0 to 301 lbf-in). Connections were tested as per ASTM D953-97 [24] Procedure A. It was concluded that ultimate load capacity increased with increasing bolt torque. In the authors' opinion an applied torque level of 35 N-m (310 lbf-in) was considered optimum as large torques tended to damage the material.

The ASCE Pre-Standard [10] specifies that bolts in bearing-type FRP connections need only be tightened to the snug-tightened condition. This condition has been defined by researchers as the tightness that exists when all parts in a joint are in firm, but not necessarily continuous contact [2]. Also, over-tightening of the bolt is not recommended to prevent through-thickness crushing of the FRP material. To prevent the likelihood of material crushing, the EUROCOMP Design Code and Handbook [25] specifies that the clamping force should not be higher than one-third of the through-thickness crushing strength of the material and never exceed 68 MPa (9.86 ksi).

2.4.4 *d/t* Ratio

One of the goals of Collings' [19] investigation was to study the effect of *d/t* ratio on bearing strength. Laminates ($0°/\pm45°$) balanced about the mid-plane were tested in tension. It was observed that for laterally unrestrained specimens, the bearing strength reduced with increasing *d/t* ratio as shown in Figure 2.4.

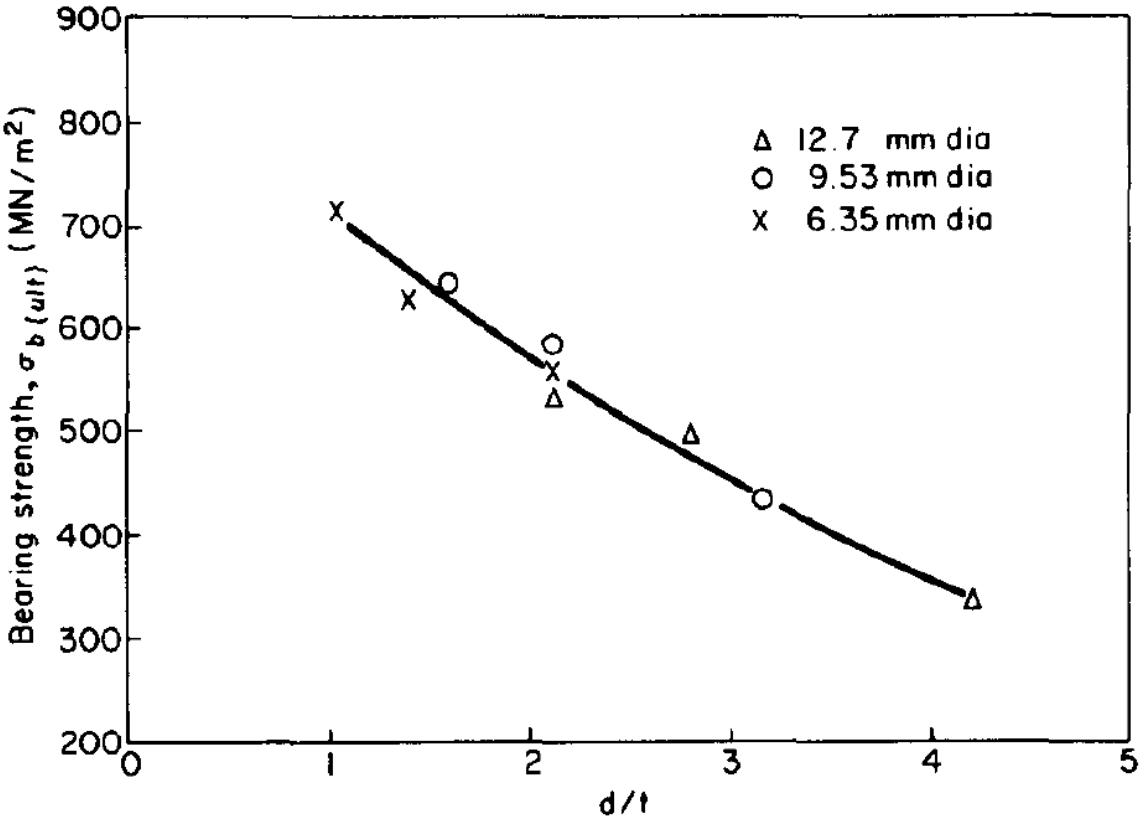

Figure 2.4 Variation of bearing strength with *d/t* ratio - (0° $\pm$ 45°) laminate, laterally unrestrained (reprinted with permission) [19].

Similarly, the experimental results of Kretsis and Matthews [21] also indicated that the ultimate bearing strength for "finger-tight" bolts reduced considerably with increasing *d/t* ratio. Mottram and Zafari [12] conducted experiments on a 6.35 mm (1/4 in) thick pultruded material having E-glass fibers and vinylester matrix. The results showed that for small clearance size (0.2 mm (0.008 in)), pin-bearing strength decreased (linearly) by about 15% with increasing *d/t* ratio. However, this trend was not obvious when the clearance size was higher (1 mm (0.04 in)). In the authors' opinion this observation needs further

characterization work. The results of this study are shown in Figure 2.5. The figure shows a variation of characteristic pin-bearing strength with *d/t* ratio. These characteristic values were computed in accordance with Annex D7 to Eurocode 0 [26].

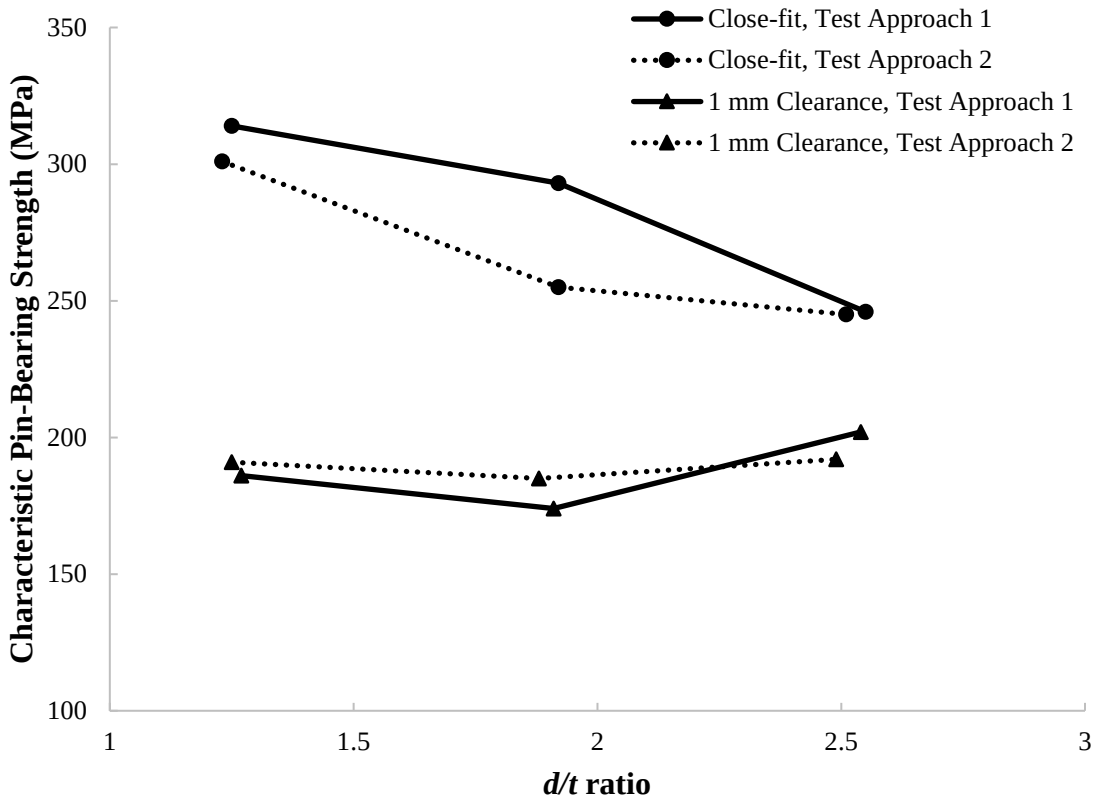

Figure 2.5 Characteristic pin-bearing strength vs *d/t* ratio (after [12]).

2.4.5 Confinement Area

Stockdale and Matthews [20] also investigated the effect of washer size in addition to the influence of bolt clampup loads. The material description and test parameters for this study are presented in Section 2.4.3. With all other parameters held constant, tests were conducted for washer diameters of 9.5, 16 and 21 mm (0.37, 0.63 and 0.83 in). Compared to the pinned-condition (no clamping), an approximately 40% increase in failure load was observed for specimens with washers and a "finger-tight" condition. In the authors' opinion failure load was approximately proportional to the ratio of washer outside to inside diameter at constant clamping pressures.

Abd-El-Naby and Hollaway [27] studied the effects of the area and the material used for clamping on the bearing strength of single-bolt connections. The material used was manufactured from E-glass fibers, polyester resin and filler. Single-bolt (9.5 mm (3/8 in) diameter) tests were carried out where the bolts were subjected to small clamping torque equivalent to a 'finger-tight' condition. Connections were tested at three clamping conditions: the first condition used tight-fitting steel washers having an outer diameter equal to 2.2 times the inner diameter, the second condition used steel plates that covered all the potential damage area, and the third condition used smooth composite plates covering the same area. It was observed that strength increased as the confinement area increased. However, no definite difference was observed in strengths for the latter conditions.

Sun et al. [28] investigated the response of connections under varying clampup loads, varying clamped area and varying layup of FRP material. The material used in the

study was carbon/epoxy unidirectional preimpregnated tapes. The authors observed that failure load increased as the size of clamped area increased.

Khashaba et al. [29] studied glass-fiber reinforced epoxy laminates (5.2 mm (0.2 in) thick) and investigated the effect of tightening torque (0, 5, 10 and 15 N-m (0, 44, 88 and 133 lbf-in)) and washer outer diameter size (14, 18, 22 and 27 mm (0.55, 0.71, 0.87 and 1.06 in)). The washer inner diameter was set as 1.04 times bolt diameter, i.e. 6.24 mm (1/4 in). It was observed that the stiffness of the joint increased with decreasing washer size and the load–displacement plots became increasingly non-linear.

2.4.6 Bolt-Hole Clearance

Naik and Crews [30] used an inverse formulation with finite element analysis for single bolt connections in graphite/epoxy laminate. In the study two bolt-hole clearances (0.8 and 1.6%) were analyzed and compared to the reference case of a snug-fit connection - no clearance between the hole and the bolt. It was concluded that bolt hole clearance influenced the stresses and deformation of the bearing hole. The authors' asserted that the contact arc between the bolt and the bolt-hole reduced with increase in bolt-hole clearance. For 1.6% bolt hole clearance with bearing stress of 475 MPa (69 ksi), the peak radial stress was 36% higher and contact angle was about 30% smaller as compared to the reference case without clearance. Also, at bearing stresses of 1,000 MPa (145 ksi) the bolt-hole elongation for a 1.6% bolt-hole clearance was 16% greater than the reference case.

Yuan et al. [31] studied the effect of bolt hole clearance on the behavior and ultimate load capacity of bolted connections. The material used in the study consisted of E-Glass fibers and polyester matrix and the thickness of specimens was 9.53 mm (3/8 in).

High-strength stainless steel bolts (12.7 mm (1/2 in) diameter) were used and tested at the zero torque condition. To ensure a bearing failure mode, the *w/d* and *e/d* ratios were selected as 8 and 4 respectively. It was observed that the toughness of the bolted connection, ultimate load, and load at incipient failure reduced with an increase in bolt-hole clearance. Also, for the small hole clearance (less than 0.8 mm (0.03 in)), no significant effect was observed on the ultimate load.

Lee et al. [32] investigated the effect of geometric parameters on the mechanical behavior of single-bolt pultruded FRP connections under tension. In this study, an E-glass/polyester material was used and specimens were cut from standard structural shapes. The authors investigated the effect of parameters including width of the connection, edge distance, bolt-hole clearance, and plate thickness. Based on the results of investigation on the effect of bolt-hole clearance, the authors concluded that the failure load of the specimens with 2 mm (0.08 in) bolt-hole clearance was 22% lower than that of specimens with 1 mm (0.04 in) bolt-hole clearance. The results showed that the effect of bolt-hole clearance over 2 mm (0.08 in) was insignificant.

2.4.7 Fastener Parameters

Erki [33] investigated the effects of fastener strength and stiffness on the load carrying capacity of connections. Twenty-eight connections were tested in tension and thirty-five in compression. All tests were conducted under double-lap single bolt configuration on pultruded GFRP plates. The material consisted of glass fibers and polyester matrix with a fiber volume fraction of approximately 40-45%. The outer plates were 13 mm (1/2 in) in thickness and inner plate 25 mm (1 in) thick. The fasteners used

were GFRP threaded rods, steel threaded rods and smooth shank steel bolts, all having 19 mm (3/4 in) diameter. All tests were conducted with 1.6 mm (1/16 in) clearance holes. It was concluded that if the fastener is stronger than the plate material, failure modes and maximum capacity are dictated by the mechanical properties of the FRP plates. If the fastener is weaker than the plate material, the failure modes and maximum capacity are mainly influenced by the fastener with little damage to the FRP plates.

2.4.8 Number of Bolts/Rows

Abd-El-Naby and Hollaway [34] discussed the load distribution between bolts in two-bolt connections in a pultruded material manufactured from E-glass fibers with a polyester resin. The investigation involved testing of connections with two bolts in series, studying the effect of changing the relative stiffness of the plates forming the connection, as well as the effect of different failure modes. For the specimens that failed in bearing, the authors concluded that the load distribution was uniform; i.e. the load per bolt was equal to the strength of a single-bolt joint. Also, the authors concluded that for the bearing failure mode, the efficiency of the multiple fastener connection was similar to that of a geometrically equivalent single bolt connection. Hassan et al. [35] studied the effect of certain parameters (width of member, edge distance, bolt pattern, number of bolts and fiber orientation) that influence the strength and failure mode of bolted connections. The important conclusion of the study was that an increase in the ultimate capacity of the connection was not directly proportional to an increase in number of bolts used.

2.5 Response of Bolted Connections under Sustained Loads

Limited research can be found in the literature pertaining to the viscoelastic behavior of bolted connections. Those investigations that have been performed have focused on the behavior of laminated composites (typically used in the aerospace industry) as opposed to pultruded materials. The failure of pultruded FRP structural elements under sustained load is often governed by a creep-rupture phenomenon. The time to failure of an element depends on the sustained stress level, temperature and the presence of moisture, with increases in each factor giving rise to shortened times to failure [10].

Shivakumar and Crews [36] investigated relaxation in bolt clampup force for double-lap bolted connections in an FRP laminate. The connection consisted of a graphite/epoxy (T300/5208) laminate with a 32 ply quasi-isotropic layup. The bolt diameter was 6.35 mm (1/4 in) and initial applied torque was 5.65 N-m (50 lbf-in). This clampup force was then measured periodically over a 100-day test period. The experiments were conducted for different temperature and moisture conditions. It was concluded that the clampup force relaxed even at room temperature and dry conditions. Based on experimental results and finite element analysis, bolt clampup relaxation was predicted as approximately 8, 13, 20 and 30% for exposure durations of 1 day, 1 month, 1 year, and 20 years respectively.

Kallmeyer and Stephens [37] investigated the creep response of FRP laminates subjected to bolt-bearing loads at ambient and elevated temperatures. The specimen used in the study was a 16 ply quasi-isotropic ($[45/0/-45/90]_{2s}$) laminate composed of graphite fiber and bismaleimide matrix and had a nominal thickness of 2.16 mm (1/12 in). Single-bolt connections were tested in tension under a double-lap shear configuration by a pair of

6.35 mm (1/4 in) thick steel plates. To ensure a bearing failure mode *w/d* and *e/d* ratios were selected as 8 and 6 respectively. Two levels of tightening torque were studied; 5.65 N-m (50 lbf-in) representing moderate torque, and a "finger-tight" condition. Creep tests were conducted up to 200 hours at load levels of 60-90 % of average ultimate monotonic bearing strength at temperatures of 23, 100 and 150°C (73.4, 212 and 302°F). The creep test results indicated significant time-dependent hole elongations at increased stress levels and temperatures. Also, an increase in the creep rate of hole elongation was observed when bolt tightening torque was reduced from moderate to "finger-tight" level. The creep test results demonstrated more scatter in the data for a "finger-tight" condition compared to a torque level of 5.65 N-m. The authors attributed this scatter in creep results to the lateral applied torque, and the bolt-hole clearance. The study highlights the importance of considering the time-dependent response of composites in the design of bolted connections. The authors proposed an empirical expression to model the connection creep rate as a function of time and applied bearing stress. The authors assumed the relationship between the rate of percent hole elongation, the normalized bearing stress and time as shown in Equation (2.4).

$$\dot{\Delta}_c = A\left(\frac{\sigma_b}{\sigma_{bu}}\right)^p t^q \tag{2.4}$$

where

$\dot{\Delta}_c$	=	rate of creep component of percent hole elongation
σ_b	=	applied bearing stress, MPa (ksi)
σ_{bu}	=	maximum bearing stress, MPa (ksi)
$A, p \; and \; q$	=	constants (function of temperature and bolt torque)

The ASCE Pre-Standard [10] defines the strength of connections including a time effect factor as given by Equation (2.5).

$$R_u \leq \lambda \phi R_n C_\Delta C_M C_T \tag{2.5}$$

where

R_u = required connection strength due to factored loads, kN (kip)

ϕ = resistance factor

λ = time effect factor

R_n = nominal connection strength, kN (kip)

C_Δ = geometry factor

C_M = moisture condition factor

C_T = temperature condition factor

When the nominal connection strength R_n is governed by the pin bearing strength R_{br}, it is calculated as given by Equation (2.1), and the resistance factor ϕ_c is taken as 0.8. The ASCE Pre-Standard [10] specifies values for time effect factor λ as given in Table 2.3.

Table 2.3 Time effect factors λ (after [10]).

Load Combination	Time Effect Factor λ
1.4D (permanent load)	0.4
1.2D + 1.6L + 0.5(L_r or S or R)	0.8 when L is from occupancy
	0.6 when L is from storage
	1.0 when L is from impact
1.2D + 1.6(L_r or S or R) + (0.5L or 0.5W)	0.75
1.2D + 1.0W + 0.5L + 0.5(L_r or S or R)	1
1.2D + 1.0E + 0.5L + 0.2S	1
0.9D + 1.0W	1
0.9D + 1.0E	1
Load Combinations including flood loads	0.75
Load Combinations including atmospheric ice loads	0.75

The adjustment factors C_M and C_T are specified in the ASCE Pre-Standard [10] and shown here in Table 2.4. The adjustment factor C_T is applied to calculate adjusted member resistance to account for effects of service temperatures falling in the range between 32ºC (90ºF) and 60ºC (140ºF). The factor C_T has been calculated so that the product $C_M C_T$ represents approximately the combined effect of moisture and temperature.

Table 2.4 Adjustment factors, C_M and C_T, for end use conditions (after [10]).

Reference Property	**Moisture** C_M	**Temperature (°F)** C_T **for (90<T≤140)**
Vinyl ester material		
Strength	0.85	$1.7 - 0.008T$
Elastic Modulus	0.95	$1.5 - 0.006T$
Polyester material		
Strength	0.80	$1.9 - 0.010T$
Elastic Modulus	0.90	$1.7 - 0.008T$

2.6 Response of Bolted Connections at Elevated Temperatures

Turvey and Wang [38] studied the influence of temperature on the structural integrity of bolted connections. The material used in the study was 6.4 mm (1/4 in) pultruded GRP plate having E-glass fibers and polyester matrix. In the study single-bolt tension connections were tested with bolt diameter of 10 mm (0.39 in). Tests were conducted at temperatures of ambient (20-25°C (68-77°F)), 40°C (104°F), 60°C (140°F), and 80°C (176°F). The experimental program involved testing of both coincident and mutually orthogonal pultrusion and tension axis. For thermal pre-conditioning, the connections were allowed to soak unstressed at the target temperature for 30 minutes. The results demonstrated a reduction in failure load with increase in temperature. The authors observed that in many instances, the mode of failure at ambient temperature and elevated

temperatures was different. The test results also showed that a relative reduction in failure load due to elevated temperature was smaller when the pultrusion and tension axis were orthogonal than when they were coincident.

Turvey and Wang [39] investigated the influence of hot-wet conditions on single-bolt tension connections under a double-lap configuration. The experimental program involved testing of “finger-tight” connections, with a nominal diameter of the bolt of 10 mm (0.39 in) and bolt-hole clearance of 0.2 mm (0.008 in). The material used in the study was EXTREN 500 series pultruded GRP plate having a thickness of 6.4 mm (1/4 in). Based on the manufacturer’s design guidelines [40] which predict a decrease of 50% in strength for the material subjected to a temperature of 65.6°C (150°F), the authors conducted tests at ambient temperature (20-24°C (68-75°F)), 60°C (140°F), and 80°C (176°F). The authors also investigated two water immersion periods of 6.5 and 13 weeks to study the influence of moisture on the material properties. Connections designed to fail in bearing exhibited a 63% drop in load carrying capacity for the specimens immersed in water for 6.5 weeks at 60°C (140°F), compared to the dry ambient conditions tests. The authors also recommended not to use the type of material used in the study in bolted connections where temperatures above 60°C (140°F) may be expected.

Turvey and Wang [41] conducted a study on thermal pre-conditioning of bolted tension connections in pultruded GRP plate at three elevated temperatures of 40°C (104°F), 60°C (140°F), and 80°C (176°F). Based on experiments and finite element analysis, the authors concluded that a thermal preconditioning period of 30 minutes duration was more than adequate for all of the pultruded GRP material in the connection to reach the required test temperature. Wu et al. [42] presented an experimental and analytical modeling study

of the strength of pultruded FRP single-bolt (ordinary steel and novel blind bolting) double-lap connections subjected to tension loading at elevated temperatures. The material used in the study consisted of E-glass fibers and polyester resin matrix having a plate thickness of 5.5 mm (0.22 in). A total of 36 single-bolt connections were tested under a lateral applied torque of 3 N-m (26.6 lbf-in). Temperature-dependent mechanical properties were determined from dynamic mechanical analysis (DMA) and the decomposition temperature was found from thermogravimetric analysis (TGA). As recommended by Turvey and Wang [41], the specimens were "soaked" unstressed for 30 minutes at the target temperature and then loaded to ultimate failure. Six test temperatures were selected in the investigation; 23, 60, 100, 140, 180, and 220°C (73.4, 140, 212, 284, 356, and 428°F). The authors observed the maximum load reduction of 85% in both methods of mechanical fastening as the test temperature increased from 23°C (73.4°F) to 220°C (428°F). Elevated temperatures also influenced the load-displacement response of a connection. With the increase in temperature the load-displacement curves became increasingly non-linear before reaching the maximum load.

One of the goals of the investigation by Kallmeyer and Stephens [37], was to study the influence of elevated temperatures (23, 100 and 150°C (73.4, 212 and 302°F)) on single-bole tension connections in a quasi-isotropic laminate. The monotonic tension tests conducted at a bolt clampup torque of 5.65 N-m (50 lbf-in) demonstrated that the material exhibited more sensitivity to temperature in the deformation response of the connection compared to the strength. The creep tests were conducted for time periods of up to 200 hours. In addition to the bolt clampup torque, temperature was observed to have significant effects on the creep response. At a stress level of 90% of ultimate bearing strength and

lateral applied torque of 5.65 N-m (50 lbf-in), test specimens ruptured within 100 hours. The authors observed that with an increase in temperature the creep rate increased and the rupture time decreased.

CHAPTER 3

MATERIAL PROPERTIES AND TEST PARAMETERS

3.1 Material Description

The pultruded material used in the study consisted of E-glass continuous strand mat (CSM), E-glass fiberglass rovings, a synthetic surfacing veil and an isophthalic polyester resin. Specimens were cut from 101.6 mm (4 in) wide square tube structural elements (Figure 3.1) with a wall thickness of 6.35 mm (0.25 in). The volume fraction of constituents using sections from the same lot was determined by Kang [43] via the modified ignition loss method proposed by Ye et al. [44]. First, resin weight was determined by burning the samples in a furnace for a period of 4 hours to eliminate the resin, and the difference between the weight of sample before and after burning was assumed to be the resin weight. Then, rovings and CSM fiber reinforcements were collected in separate beakers and fillers were resolved by using Sulfuric and Nitric acids. The difference in weights determined the filler weight, and subtracting the beaker weights determined the weights of rovings and CSM fiber reinforcements. Finally, the volume fraction of constituents was determined from the relationship between weight, density and volume. Table 3.1 shows the relative proportions of the constituent materials [43]. Engindeniz and Zureick [45] conducted tests to determine the glass-transition temperature (T_g) of the material using sections from the same lot. The authors used dynamic mechanical analysis (DMA), and differential scanning calorimetry (DSC) and determined the T_g of the material to be 102°C (215.6°F).

Figure 3.1 FRP structural profile – 101.6 mm (4 in) square tube.

Table 3.1 Volume fraction of constituents (after [43]).

Constituent	**Roving** V_{rov} **(%)**	**CSM** V_{csm} **(%)**	**Resin** V_{res} **(%)**	**Filler** V_{fil} **(%)**	**Void** V_v **(%)**
Mean	23.1	12.2	53.7	9.3	1.7
Standard Deviation	1.4	0.8	1.2	1.1	0.2
% COV	6.2	6.7	2.3	12.0	12.9

3.2 Tensile Properties

A total of 12 tests were conducted to determine tensile properties in accordance with ASTM D3039-14 [46]. As suggested by Mottram [47] and Wang & Zureick [48], prismatic coupons without end tabs were used in the tests. The width of the test specimen was 2.54 cm (1 in) and gage length was 20.3 cm (8 in) with an added length of approximately 12.7 cm (5 in) to ensure adequate seating in the pneumatic grips. The tests were conducted using a computer-controlled hydraulic load actuator at a constant head displacement rate of 1.27 mm/min (0.05 in/min). Figure 3.2 shows the tension test setup; specific details for the equipment used are given in Appendix D. A single uniaxial extensometer was used to measure the longitudinal strain in the coupon. Figure 3.3 shows a typical specimen at failure. Figure 3.4 shows a representative stress-strain diagram for the tension tests. Specimen dimension and test results are shown in Table 3.2 and a summary of test results is shown in Table 3.3. In the tables F_L^t and E_L^t represent tensile strength and modulus in the longitudinal direction of the FRP, respectively. Tensile modulus (E_L^t) was computed from the slope of stress-strain curve between 4,000 με and 8,000 με. The results of two tests (test number 2 and 9) were discarded due to the slippage of the extensometer during the test. A comparison of tensile properties determined by other researchers for specimens from the same lot is given in Table 3.4.

Figure 3.2 Test setup to measure tensile properties.

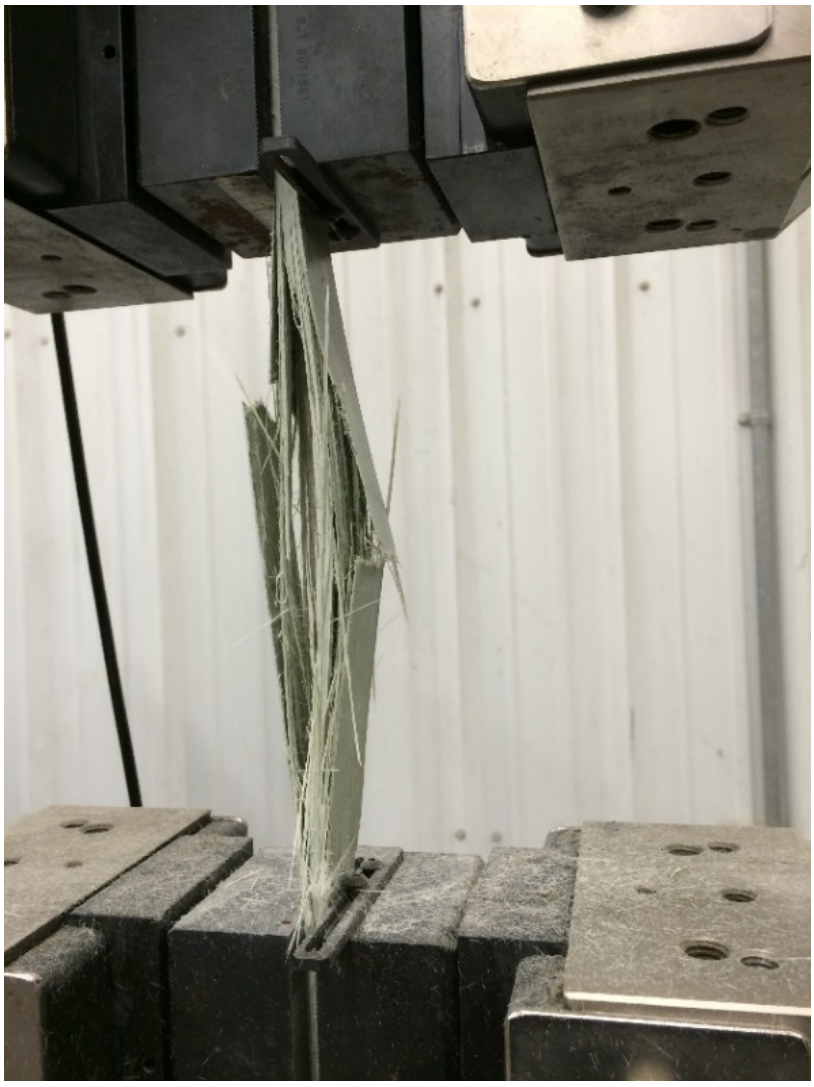

Figure 3.3 Test specimen at failure – tension test.

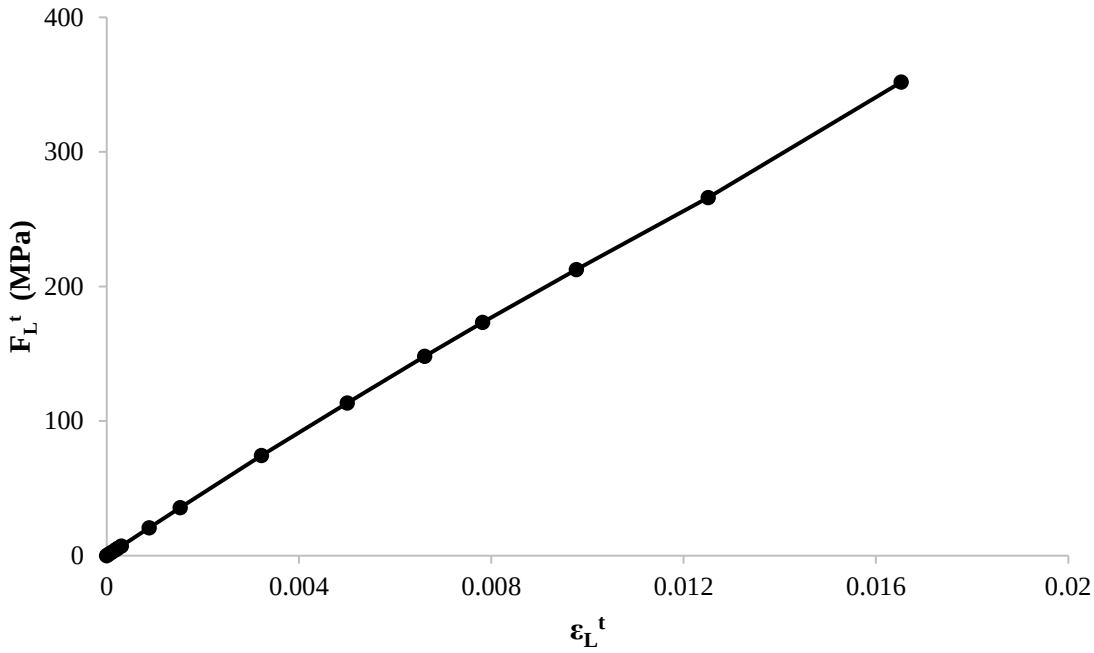

Figure 3.4 Representative stress-strain diagram for tension tests.

Table 3.2 Tensile test specimen dimension and test results.

Test	Width		Thickness		Gauge Length		F_L^t		E_L^t	
	mm	in	mm	in	mm	in	MPa	psi	MPa	psi
Test 1	26.3	1.04	6.5	0.26	205.5	8.09	378.9	54955	21.8	3162
Test 2	25.8	1.02	6.5	0.26	204.8	8.06	386.6	56075	21.2	3076
Test 3	26.2	1.03	6.5	0.26	204.8	8.06	395.0	57287	21.1	3065
Test 4	26.7	1.05	6.5	0.26	204.8	8.06	388.3	56325	22.3	3231
Test 5	25.2	0.99	6.2	0.24	203.2	8.00	315.3	45732	21.0	3044
Test 6	26.0	1.02	6.6	0.26	203.2	8.00	351.8	51021	21.3	3088
Test 7	24.9	0.98	6.2	0.24	203.2	8.00	344.7	49997	19.6	2849
Test 8	26.4	1.04	6.1	0.24	203.2	8.00	323.6	46940	21.7	3144
Test 9	26.3	1.03	6.1	0.24	203.2	8.00	348.2	50496	33.6	4879
Test 10	26.1	1.03	6.1	0.24	203.2	8.00	361.1	52370	21.3	3089
Test 11	25.9	1.02	6.1	0.24	203.2	8.00	375.6	54471	24.2	3509
Test 12	26.0	1.02	6.1	0.24	203.2	8.00	351.0	50913	23.3	3385

Table 3.3 Tensile properties of FRP specimens.

Property	F_L^t		E_L^t	
	MPa	psi	GPa	ksi
Mean	358.5	52,000	21.8	3,156
Standard Deviation	26.5	3,839	1.3	185
% COV	7.4		5.8	

Table 3.4 Comparison of tensile properties of FRP specimens from previous research.

Property	Sample Size	F_L^t		E_L^t	
		MPa	**psi**	**GPa**	**ksi**
Kang [43]					
Mean	30	372.8	54,100	23.8	3,445
Standard Deviation		25.6	3,700	1.5	218
% COV		6.9		6.3	
Smith [49]					
Mean	15	376.8	54,648	22.8	3,300
Standard Deviation		34.4	4,986	1.7	244
% COV		9.1		7.4	
Current Investigation					
Mean	10	358.5	52,000	21.8	3,156
Standard Deviation		26.5	3,839	1.3	185
% COV		7.4		5.8	

3.3 Pin-Bearing Test Parameters

In light of the review presented in Chapter 2, the following parameters were identified to investigate the behavior of a bolted connection subject to a pin bearing mode of failure.

a. Geometric parameters: The geometry of the test specimen was selected such that the expected mode of failure was always bearing as opposed to cleavage, shear-out, or net-tension. As discussed earlier, bearing is the only benign failure mode that develops slowly and hence is typically most desirable. Tests conducted at various *e/d* and *w/d* ratios showed that specimens failed consistently in bearing failure mode at e*/d* and *w/d* ratios of 8 and 6 respectively. Figure 3.5 shows the representative load-stroke plot for *e/d* ratios of 3 and 8. Figure 3.6 shows the bearing failure mode at e*/d* and *w/d* ratios of 8 and 6 respectively.

b. Connection configuration: Single-bolt tension connections under a double-lap shear configuration were selected to isolate the potential influences associated with multi-bolt, and single-lap shear connections. The response of a connection varies with the number of bolts and rows. Similarly, single-lap shear loading is not concentric and can impart bending effects.

c. Material configuration: Direction of fibers directly influence the strength of a connection. For consistency, all the tests were conducted with loading along the direction of pultrusion.

d. Fastener parameters: High strength steel bolts were used having sufficient length such that the bolt shank was in contact with the FRP and not the bolt

threads. These were readily available high strength steel bolts (Grade 9) having hexagonal cap screw, minimum wedge tensile strength of 1,241 MPa (180,000 psi), and mechanical properties conforming to ASTM F-606 [50] except wedge tensile strength.

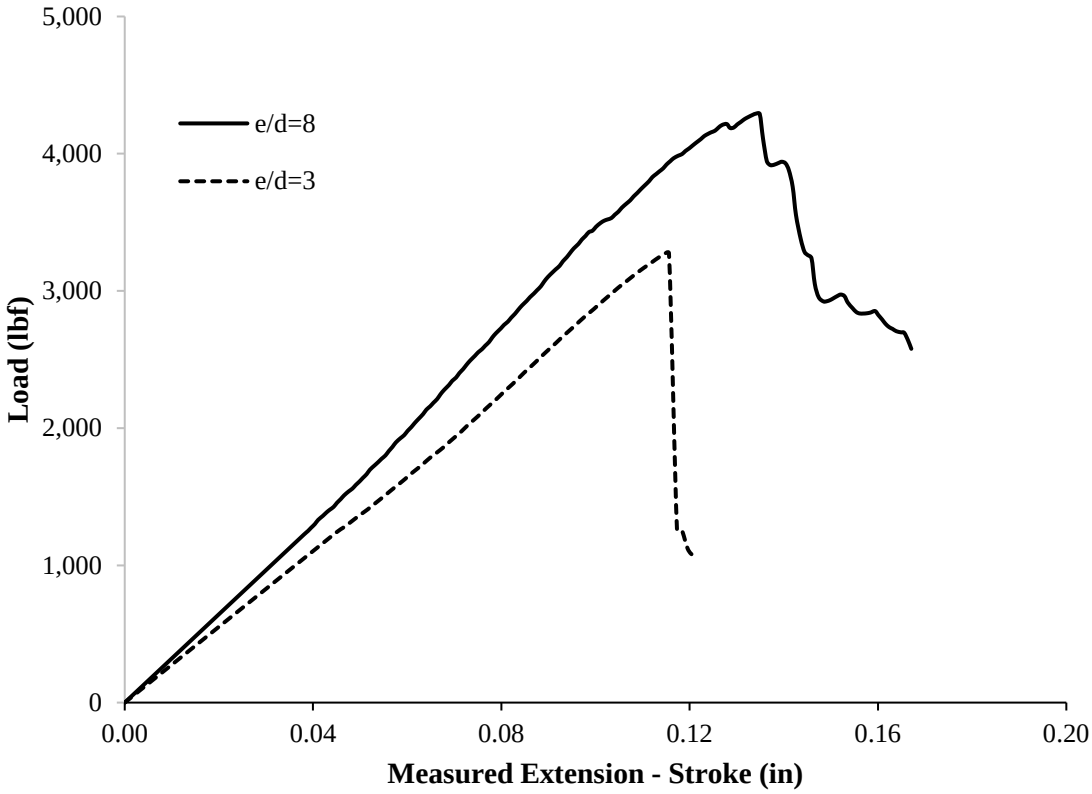

Figure 3.5 Representative load-extension plot for *e/d* ratio of 3 and 8.

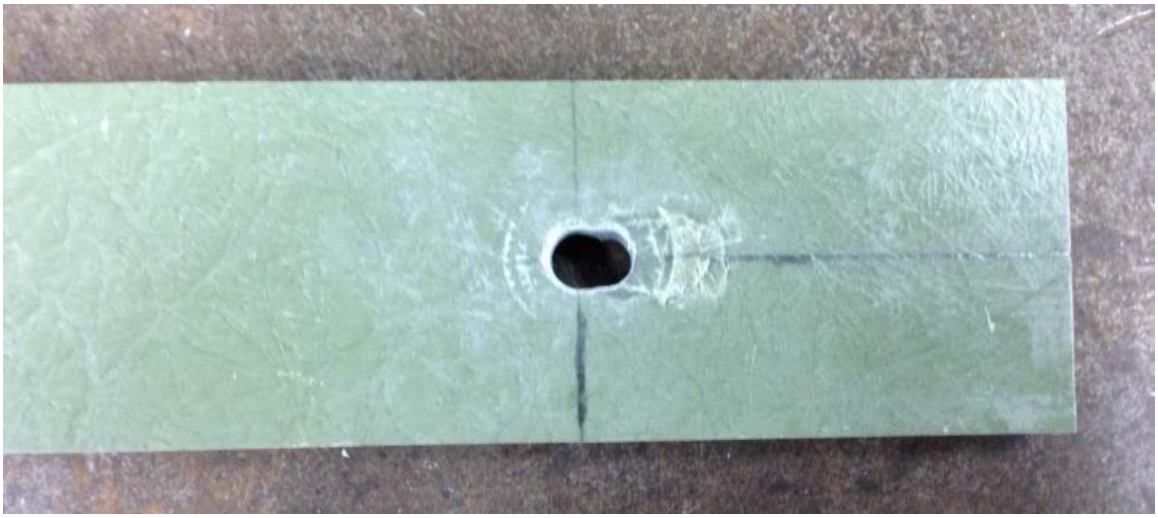

Figure 3.6 Bearing failure mode for *e/d* and *w/d* ratios of 8 and 6 respectively.

Figure 3.7 shows the specimen geometry and loading configuration used in the experimental study. As discussed earlier in Chapter 2, for true pin bearing behavior there must be no tightening of the bolt. Therefore, to represent pin-bearing behavior a connection with no lateral restraint was selected for study. In this research a test specimen with a "laterally unrestrained" condition is defined as having no restraint on either side such that the specimen is free to deform laterally. For the torqued specimen tests, the lateral pressure was applied through a dial-gauge type torque wrench. Similarly, with regards to bolt-hole clearance, a test specimen with a "close fit" condition is defined as a hole with small clearance ($\leq$ 0.3 mm (0.01 in)).

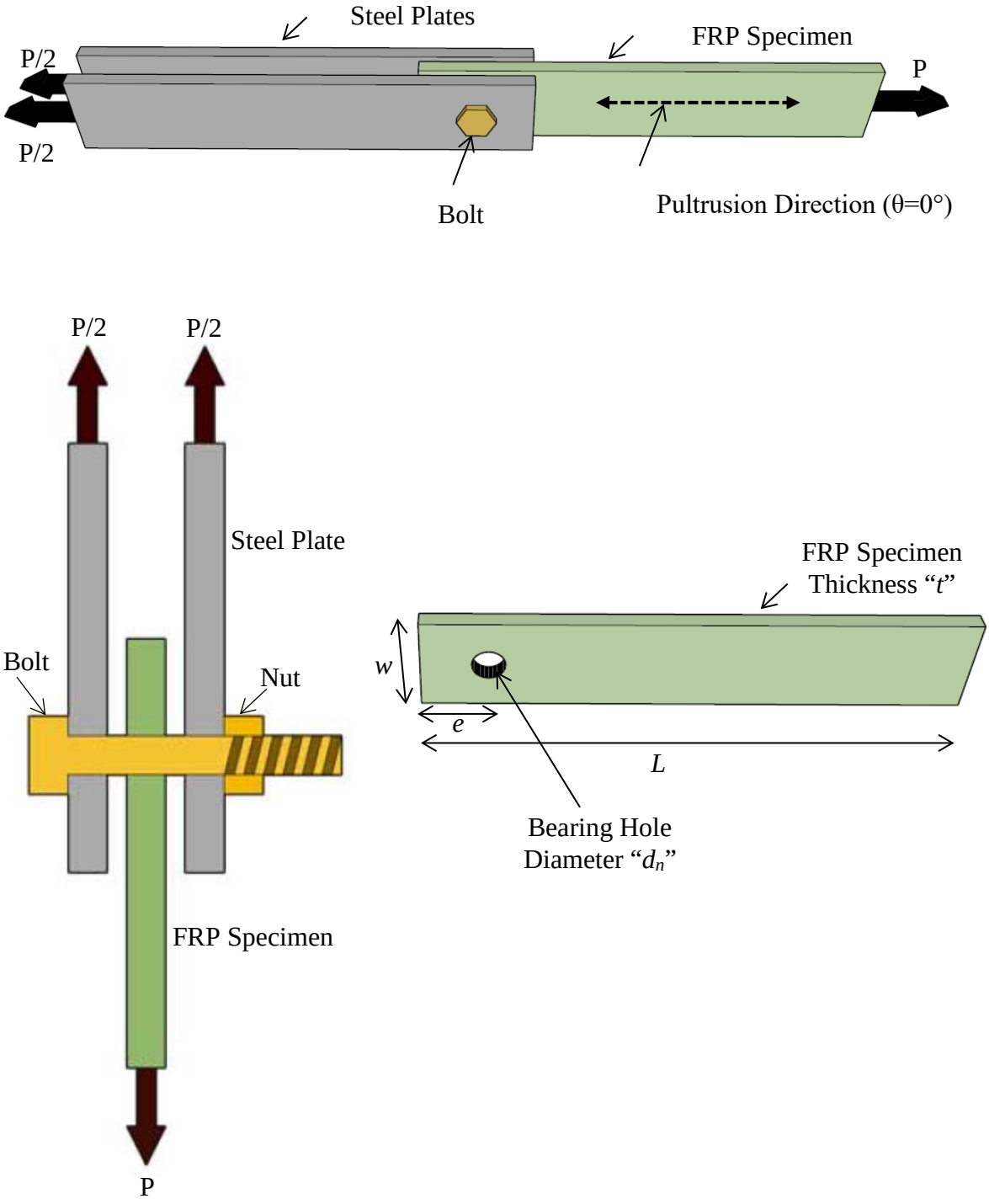

Figure 3.7 Loading apparatus and specimen geometry.

CHAPTER 4

SHORT-TERM PIN-BEARING TESTS

4.1 Objective

As discussed in Chapter 2, a large variety of connection parameters can significantly influence pin-bearing strength. However, limited work has been done on studying the effects of specific connection parameters on the pin-bearing strength; *d/t* ratio, bolt hole clearance, and bolt tightening torque. Therefore, it was deemed pertinent to study these parameters in the current research investigation.

4.2 Test Matrix

As discussed in Chapter 3, to ensure bearing failure modes e*/d* and *w/d* ratios have been selected as 8 and 6 respectively. Table 4.1 gives specimen geometry for the short-term pin-bearing tests; the test matrix employed for the short-term investigation is given in Table 4.2 and Table 4.3. As will be discussed in Chapter 6, for statistical analysis a total of 10 tests were conducted under each category. As shown in Table 4.2, the effect of *d/t* ratio was investigated for two different categories at ambient (room) temperature (24°C (75°F)); the response of the connection under specific lateral restraint conditions and at specific bolt-hole clearances. For the lateral restraint, two different conditions were considered; the laterally unrestrained condition (representing pin-bearing behavior) and moderate torque values, calculated based on the work done previously on the subject [19,22,25]. Similarly, for bolt-hole clearance, two different conditions were considered; the close-fit condition

and a 1.6 mm (1/16 in) clearance. The bolt-hole clearance is a practical consideration and is generally taken as 1.6 mm (1/16 in) for constructability [9].

As shown in Table 4.3, the effect of elevated service temperatures was investigated for the case of laterally-unrestrained, close-fit connection, and *d/t* ratio of 1. The tests were conducted at ambient (room) temperature 24°C (75°F), 43.3°C (110°F), and 60°C (140°F). These temperatures were selected based on manufacturer guidelines, previous work, and expected service conditions. The manufacturer's design guidelines for the material do not recommend its use at temperatures above 65.5°C (150°F). As discussed earlier, Turvey and Wang [39] recommended that pultruded material like GRP should not be used in bolted connections where temperatures above 60°C (140°F) may be expected. Zureick and Kahn [51] showed that composite components can experience temperatures that are at least 15°C (59°F) higher than the air temperature when in-service structures are exposed to direct sunlight. In real world situations such as attics and crawlspaces for buildings in comparatively hot climates, ventilation experts assert that temperatures in these spaces can easily reach 60°C (140°F) in the summer months[52].

Table 4.1 Specimen geometry - short-term pin-bearing tests.

d/t	***e*** **mm (in)**	***d*** **mm (in)**	***w*** **mm (in)**	***L*** ***mm (in)***	***e/d***	***w/d***
1	50.8 (2)	6.35 (0.25)	38.1 (1.5)	178 (7)	8	6
1.5	76.2 (3)	9.53 (0.375)	57.2 (2.25)	229 (9)	8	6
2	101.6 (4)	12.7 (0.5)	76.2 (3)	305 (12)	8	6

Table 4.2 Test matrix - short-term pin-bearing tests at ambient (room) temperature (24°C (75°F)).

Lateral restraint	Unrestrained	Unrestrained	Torqued	Torqued
Bolt-hole clearance	Close-fit	1.6 mm (1/16 in)	Close-fit	1.6 mm (1/16 in)
***d/t* ratio**	1	1	1	1
	1.5	1.5	1.5	1.5
	2	2	2	2

Table 4.3 Test matrix - short-term pin-bearing tests at elevated temperatures.

Temperature	**Ambient Temperature (24°C (75°F))**	**43.3°C (110°F)**	**60°C (140°F)**
Lateral restraint	Unrestrained	Unrestrained	Unrestrained
Bolt-hole clearance	Close-fit	Close-fit	Close-fit
***d/t* ratio**	1	1	1

4.3 Test Setup and Procedure

Tests were conducted using a computer-controlled hydraulic load actuator at a constant head displacement rate of 1.27 mm/min (0.05 in/min). Pneumatic grips were used on one end of the FRP sample while the other end was connected to steel plates via a single pin. Figure 4.1 shows the typical test setup; specific details for the equipment used are given in Appendix D. In the light of the discussion presented in Section 2.2, the bearing failure load was taken as the maximum load on the load-extension curve where subsequently the force drops off approximately 30% from the maximum. The corresponding bearing strength (F_L^{br}) of the connection was computed by dividing the maximum load by the initial projected area of the bolt-hole. For measuring bolt-hole elongation, the measured cross-head extension represents the total deformation of the specimen. However, the average stress at the bearing failure load is in general significantly less when compared to the tensile strength of the specimen. For instance, as will be demonstrated later in the test results, for the case of a close-fit laterally unrestrained connection having a *d/t* ratio of 1, at bearing failure load of 14.3 kN (3.2 kips) the specimen experiences a stress of 59 MPA (8.6 ksi) which is only about 16% of the tensile strength (358.5 MPA (52 ksi)) of the specimen. Therefore, the measured extension was assumed to represent the deformation of the bolt-hole only and is denoted by Δd. The percent bolt-hole deformation $(\Delta d/d)_o$ at the bearing failure load was computed by dividing bolt-hole elongation by original bolt-hole diameter.

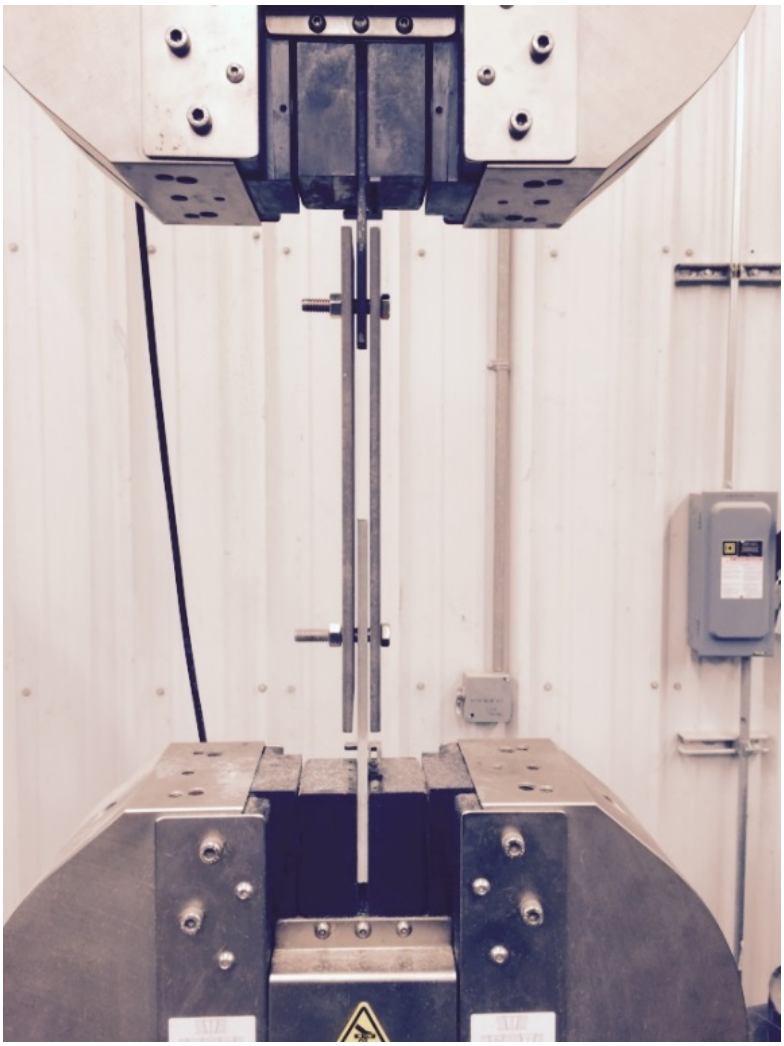

Figure 4.1 Test setup – short-term pin-bearing tests.

4.4 Results and Discussion – Tests at Ambient (Room) Temperature

4.4.1 Close-fit, Laterally Unrestrained Specimens

It was observed in all tests that as the load increased, the bolt shank indented into the hole and the material in the vicinity of the hole started crushing. Since the material was free to deform laterally, deformation of the material near the hole transverse to the direction of loading – referred to as "blooming" - was observed. This behavior typically directly preceded the onset of bearing failure. A schematic illustration of "blooming" near the bolt-hole is shown in Figure 4.2, and a representative test specimen at failure is shown in Figure 4.3. The test data demonstrated that it can be modeled with a linear function up to the maximum load. An immediate significant drop in the load without recovery was observed after reaching the maximum value, which for the purposes of this investigation was defined as bearing failure in the specimen. A representative load-extension plot is shown in Figure 4.4 and load-extension curves for all the tests are shown in Appendix A. As expected, all the connections failed in bearing which is characterized by localized crushing of the FRP material where the bolt shank contacts the cylindrical surface of the bolt-hole. The corresponding bearing strength (F_L^{br}) of the connection was computed by dividing the maximum load by the initial projected area of the hole. Test results are provided in Table 4.4 and a summary showing standard deviation (SD) and coefficient of variation are given in Table 4.5. The mean percent bolt-hole deformation $(\Delta d/d)_o$ at the bearing failure load was computed as 28.7, 29.8, and 35.2% for *d/t* ratios of 1, 1.5, and 2 respectively. Figure 4.5 shows the variation of mean pin-bearing strength with *d/t* ratio. The results demonstrate that pin-bearing strength decreases with an increase in *d/t* ratio.

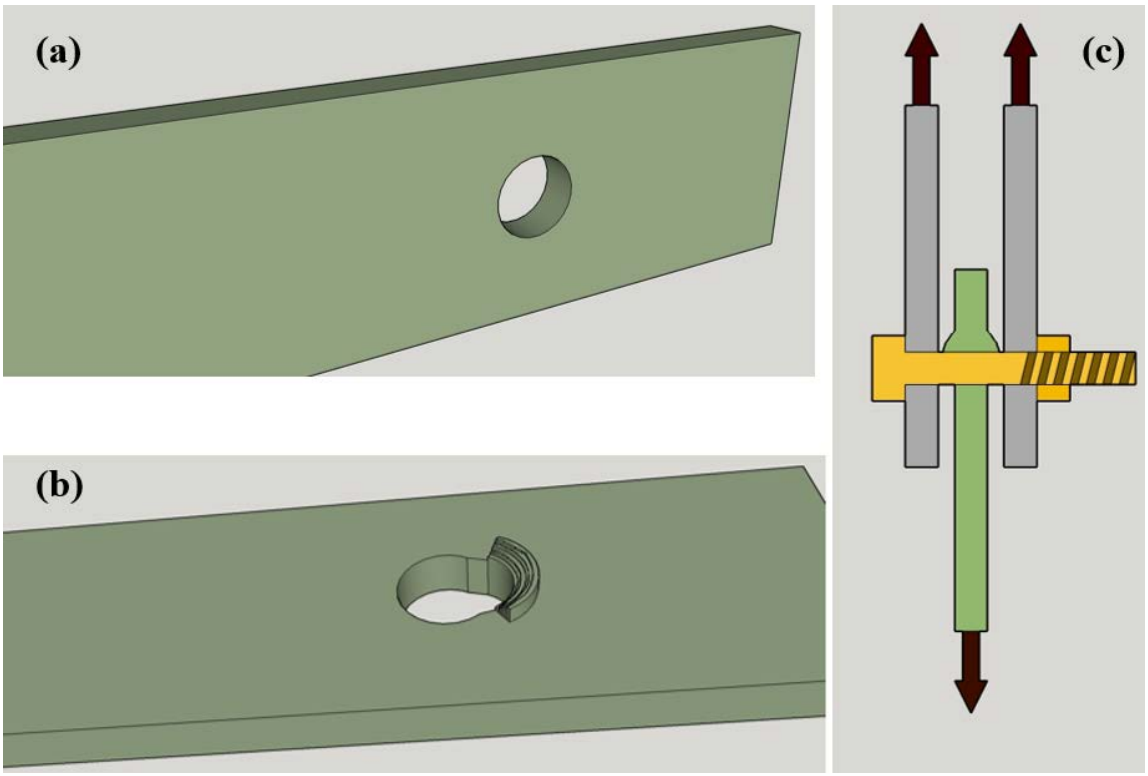

Figure 4.2 "Blooming" of the bolt-hole. (a) unloaded specimen, (b) bearing failure mode at failure, and (c) side elevation of the specimen at failure.

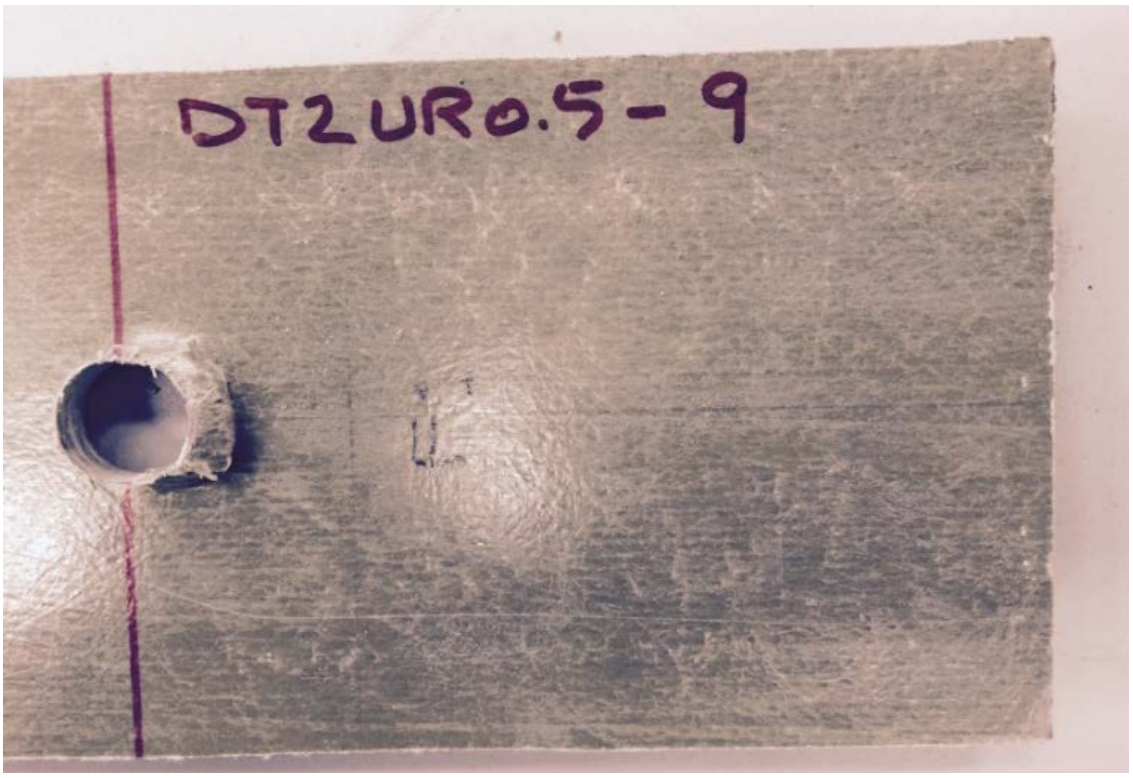

Figure 4.3 Representative test specimen at failure - close-fit, laterally unrestrained specimen.

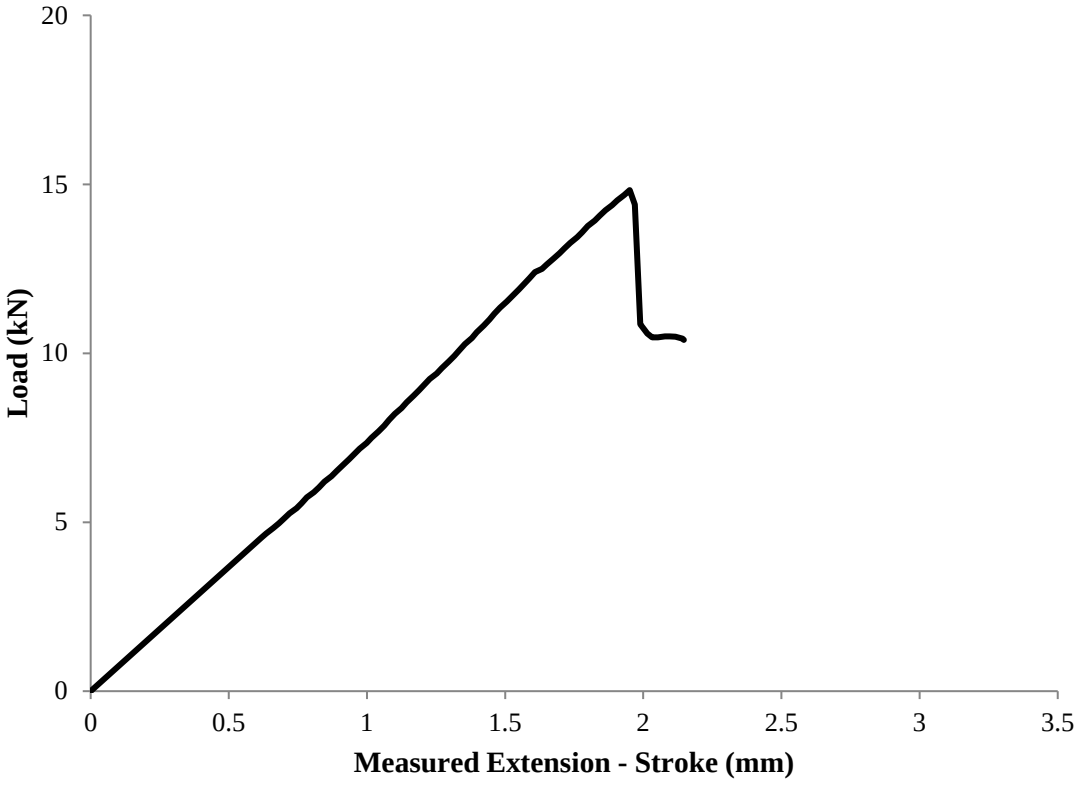

Figure 4.4 Representative load-extension curve – close-fit, laterally unrestrained specimen (6.35 mm (1/4 in) diameter bolt).

Table 4.4 Pin-bearing test results - close-fit, laterally unrestrained specimens.

Test	Bearing Load kN (lbf)			Bearing Stress MPa (psi)		
	***d/t* = 1**	***d/t* = 1.5**	***d/t* = 2**	***d/t* = 1**	***d/t* = 1.5**	***d/t* = 2**
Test 1	14.19 (3,190)	18.64 (4,190)	18.79 (4,223)	352 (51,039)	308 (44,697)	233 (33,786)
Test 2	14.83 (3,333)	18.57 (4,175)	18.79 (4,224)	368 (53,334)	307 (44,532)	233 (33,793)
Test 3	14.90 (3,351)	19.72 (4,434)	16.51 (3,712)	370 (53,610)	326 (47,295)	205 (29,692)
Test 4	14.91 (3,352)	20.21 (4,543)	22.74 (5,112)	370 (53,631)	334 (48,456)	282 (40,897)
Test 5	14.89 (3,347)	17.17 (3,860)	21.34 (4,797)	369 (53,555)	284 (41,170)	265 (38,377)
Test 6	15.40 (3,462)	19.24 (4,325)	21.05 (4,733)	382 (55,385)	318 (46,136)	261 (37,862)
Test 7	14.25 (3,204)	17.13 (3,850)	21.48 (4,829)	353 (51,264)	283 (41,071)	266 (38,629)
Test 8	12.67 (2,847)	19.35 (4,351)	23.09 (5,191)	314 (45,557)	320 (46,409)	286 (41,528)
Test 9	13.12 (2,950)	18.09 (4,067)	21.89 (4,922)	325 (47,204)	299 (43,380)	271 (39,374)
Test 10	13.50 (3,035)	21.24 (4,775)	21.75 (4,889)	335 (48,561)	351 (50,935)	270 (39,108)

Table 4.5 Summary - pin-bearing test results for close-fit, laterally unrestrained specimens.

***d/t* ratio**	**Sample Size**	**Mean Strength**		**SD**		**%COV**
		MPa	**psi**	**MPa**	**psi**	
1	10	354	51,310	22	3,230	6.3
1.5	10	313	45,410	21	3,110	6.8
2	10	257	37,300	26	3,710	10.0

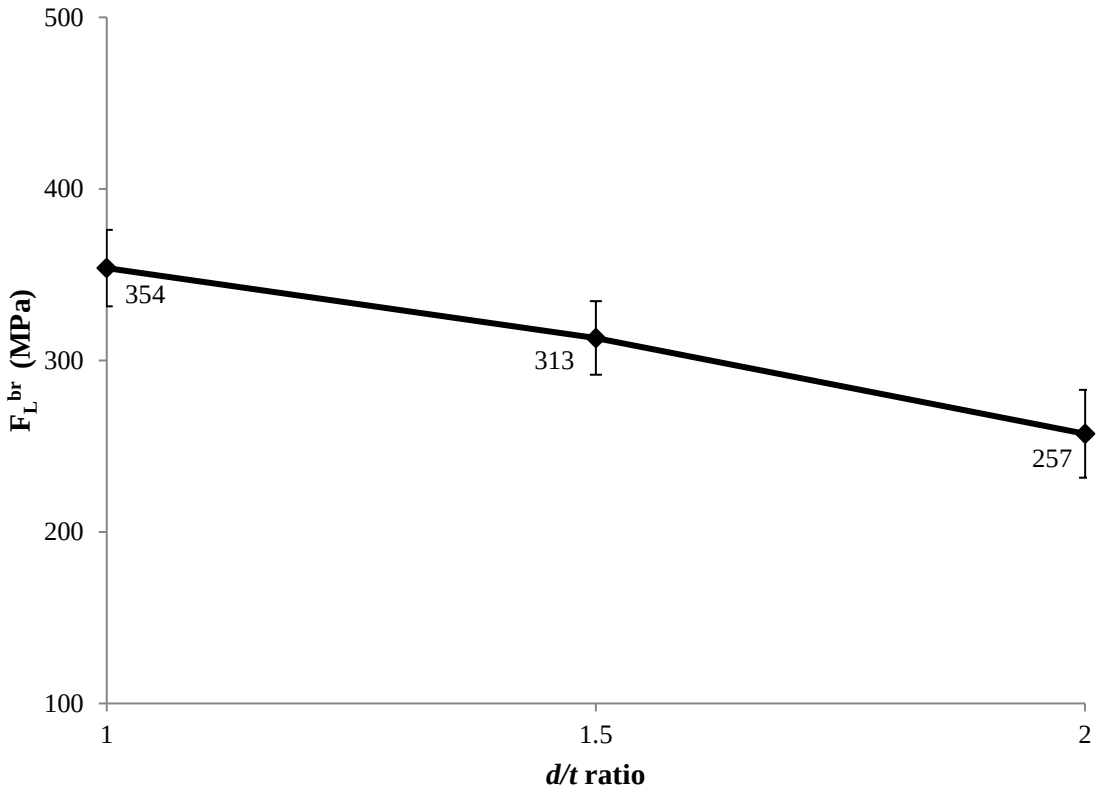

Figure 4.5 Mean pin-bearing strength vs *d/t* ratio for close-fit, laterally unrestrained specimens.

4.4.2 1.6 mm (1/16 in) Bolt-Hole Clearance, Laterally Unrestrained Specimens

The behavior of connections under this category was similar to the connections with close-fit condition. At the onset of failure, the "blooming" of the hole was observed as shown in Figure 4.6. The test data can be modeled with a linear function up to the maximum load. After reaching the maximum load an immediate drop in the load without recovery was observed indicating bearing failure. As intended, all the connections failed in bearing. A representative load-extension curve is shown in Figure 4.7. Load-extension curves for all

tests are shown in Appendix A. Test results are provided in Table 4.6 and a summary of results showing standard deviation, and coefficient of variation are given in Table 4.7. The mean percent bolt-hole deformation $(\Delta d/d)_o$ at the bearing failure load was computed as 14.4, 11.5, and 10.2% for *d/t* ratios of 1, 1.5, and 2 respectively. Figure 4.8 shows the variation of mean pin-bearing strength with *d/t* ratio. The results demonstrate that pin-bearing strength decreases with increasing *d/t* ratio.

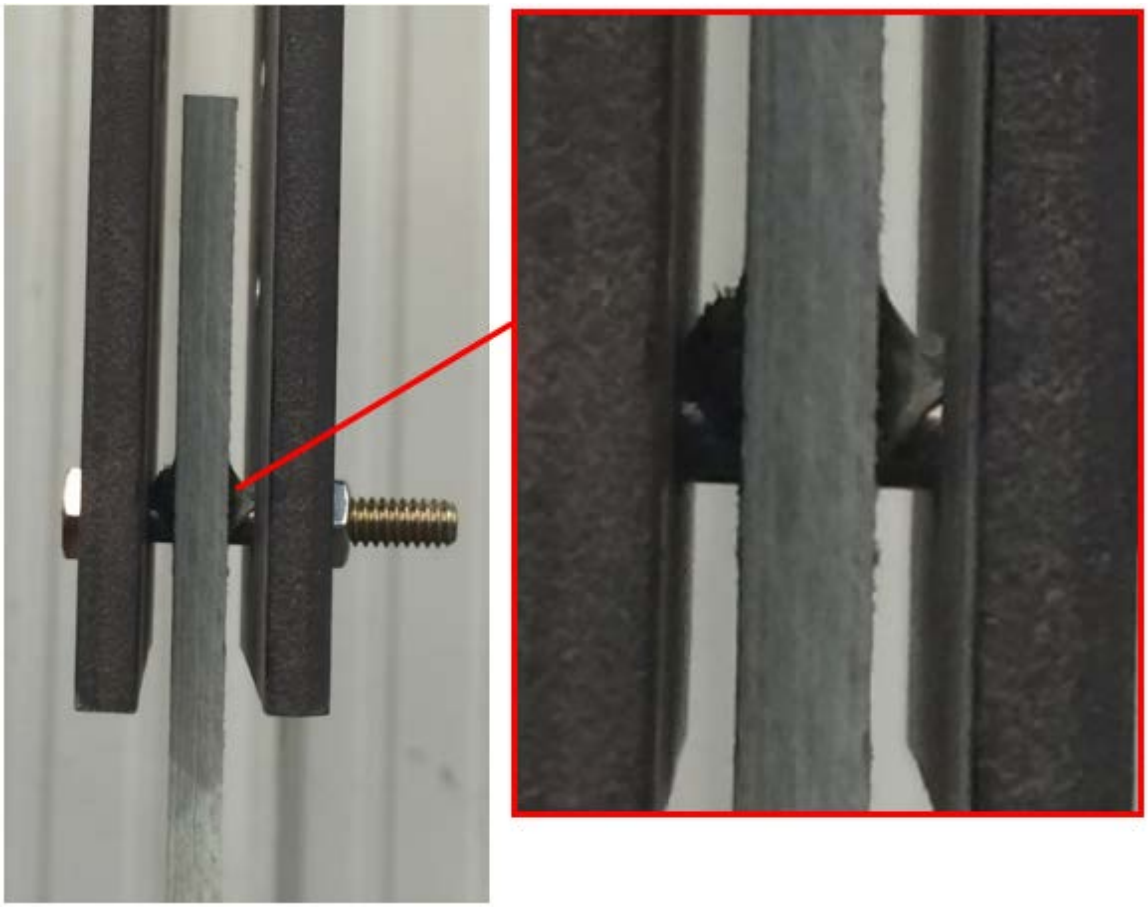

Figure 4.6 "Blooming" of the connection - 1.6 mm (1/16 in) bolt-hole clearance, laterally unrestrained specimens.

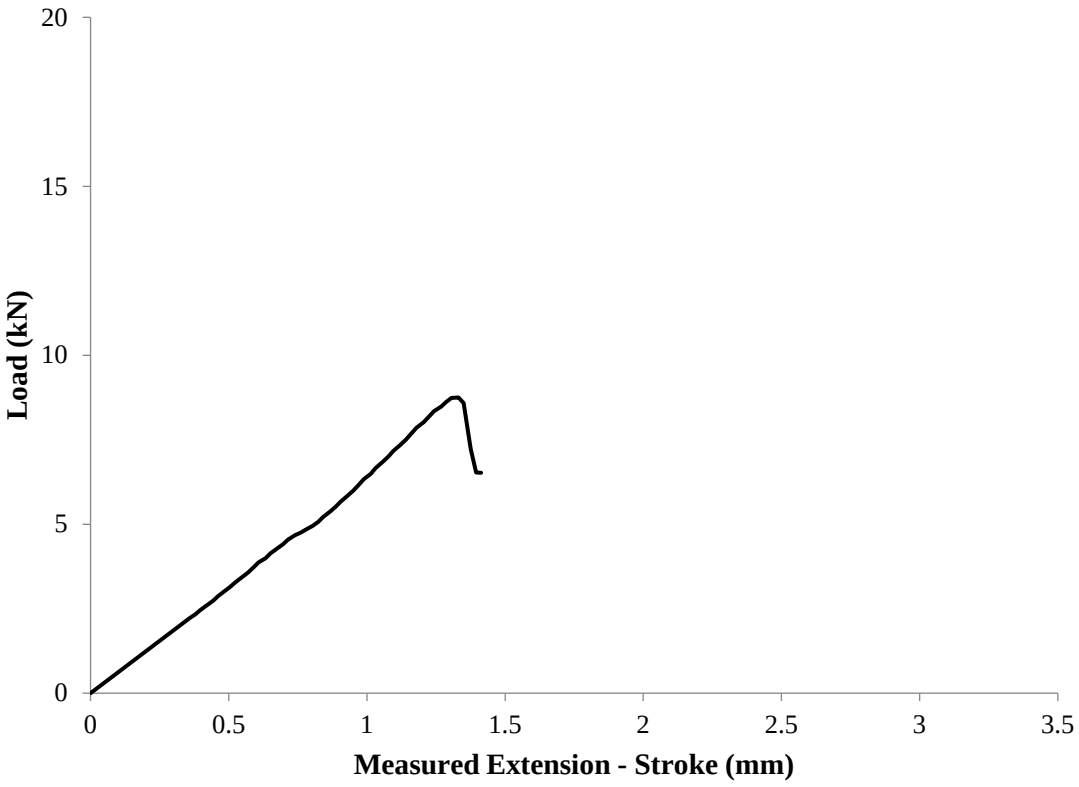

Figure 4.7 Representative load-extension curve – 1.6 mm (1/16 in) bolt-hole clearance, laterally unrestrained specimen (6.35 mm (1/4 in) diameter bolt).

Table 4.6 Pin-bearing test results - 1.6 mm (1/16 in) bolt-hole clearance, laterally unrestrained specimens.

Test	Bearing Load kN (lbf)			Bearing Stress MPa (psi)		
	***d/t* = 1**	***d/t* = 1.5**	***d/t* = 2**	***d/t* = 1**	***d/t* = 1.5**	***d/t* = 2**
Test 1	8.75 (1,967)	10.40 (2,339)	14.93 (3,357)	217 (31,472)	172 (24,949)	185 (26,857)
Test 2	7.40 (1,664)	10.74 (2,414)	15.02 (3,376)	184 (26,626)	178 (25,750)	186 (27,011)
Test 3	8.39 (1,886)	12.04 (2,708)	14.35 (3,226)	208 (30,172)	199 (28,880)	178 (25,808)
Test 4	8.02 (1,803)	10.99 (2,470)	12.36 (2,779)	199 (28,842)	182 (26,347)	153 (22,234)
Test 5	7.55 (1,698)	12.57 (2,826)	13.69 (3,078)	187 (27,166)	208 (30,145)	170 (24,626)
Test 6	7.79 (1,750)	11.27 (2,533)	13.53 (3,043)	193 (28,004)	186 (27,019)	168 (24,341)
Test 7	7.73 (1,737)	9.88 (2,221)	14.32 (3,218)	192 (27,789)	163 (23,695)	178 (25,746)
Test 8	8.23 (1,851)	10.72 (2,410)	15.56 (3,497)	204 (29,609)	177 (25,706)	193 (27,978)
Test 9	7.89 (1,773)	10.91 (2,452)	13.17 (2,960)	196 (28,370)	180 (26,158)	163 (23,679)
Test 10	7.91 (1,777)	12.60 (2,833)	13.86 (3,116)	196 (28,440)	208 (30,220)	172 (24,931)

Table 4.7 Summary - pin-bearing test results for 1.6 mm (1/16 in) bolt-hole clearance, laterally unrestrained specimens.

***d/t* ratio**	**Sample Size**	**Mean Strength**		**SD**		**%COV**
		MPa	**psi**	**MPa**	**psi**	
1	10	198	28,650	10	1,450	5.0
1.5	10	185	26,890	15	2,190	8.1
2	10	175	25,320	12	1,720	6.8

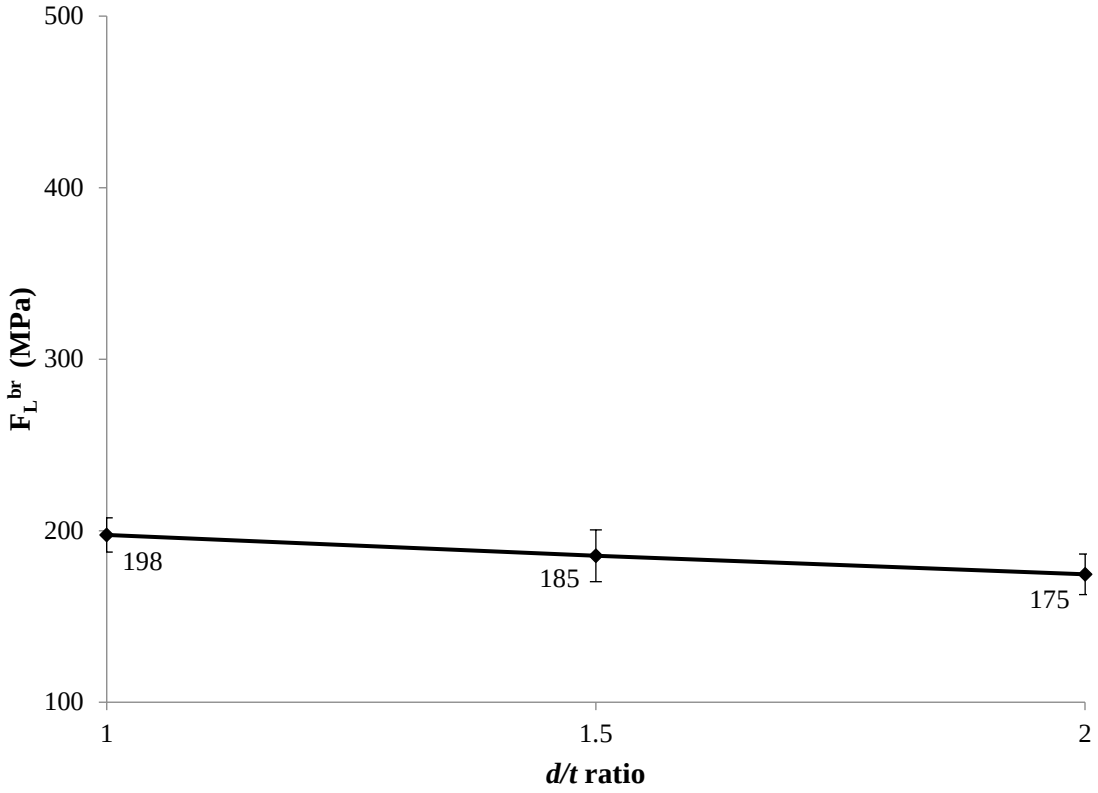

Figure 4.8 Mean pin-bearing strength vs *d/t* ratio for 1.6 mm (1/16 in) bolt-hole clearance, laterally unrestrained specimens.

4.4.3 Close-fit, Moderately Torqued Specimens

The amount of lateral compressive stress provided by the applied torque depends on bolt-hole diameter, washer size, and torque coefficient *k* (discussed in Section 2.4.3). For a 6.35 mm (1/4 in) diameter bolt, ASTM D5961-10 [15] mentions light lateral applied torque values of 2.2 to 3.4 N-m (19.5 to 30 lbf-in), and Kallmeyer and Stephens [37] used a value of 5.65 N-m (50 lbf-in) to represent moderate torque. A torque value of 5.65 N-m was selected for the present work to represent moderate toque for a 6.35 mm (1/4 in)

diameter bolt. The lateral constraint stress was then computed in accordance with previous research as discussed in Section 2.4.3. For the same lateral constraint stress, torque values of 14.9, and 35.3 N-m (132 and 313 lbf-in) were then computed to represent moderate torque for 9.53 and 12.7 mm (3/8 and 1/2 in) diameter bolts respectively. The torque coefficient *k* was assumed to be 0.2; this assumption was made for the reasons presented in Section 2.4.3. Details for the moderate torque specimens are given in Table 4.8. The washers used conformed to ASTM F436-11 [53]. These were readily available "loose-fit" washers of the type typically used in construction. The bolts were torqued using a standard dial torque wrench and all the bolts were kept in a conditioned environment that remained unchanged.

Table 4.8 Moderate torque values for test specimens.

Bolt diameter (*d*) mm (in)	**Washer size**	**Torque (*T*) N-m (lbf-in)**	**Lateral constraint (σ_z) MPa (psi)**
6.35 (1/4)	2.2 *d*	5.65 (50)	36.6 (5306)
9.53 (3/8)	2 *d*	14.9 (132)	
12.7 (1/2)	2 *d*	35.3 (313)	

As the specimens were constrained laterally, “blooming” of the material in the vicinity of the loaded pin was suppressed by the washers. This resulted in an increased load carrying capacity. Figure 4.9 shows the swelling of the area outside the region constrained by washers indicating failure. A representative load-extension curve is given in Figure 4.10, which shows bilinear behavior in the moderately torqued connection. Initially the behavior of a connection can be modeled by a linear function until the point significant reduction in initial stiffness as previously observed by Hart-Smith [54]. Cooper and Turvey [22] defined this point of stiffness reduction as *damage load*. In all tested specimens, the second linear region of the load-extension plot was observed to be comparatively shorter than the first one. Load-extension curves for all the tests are shown in Appendix A. Test results are provided in Table 4.9 and a summary of results showing standard deviation and coefficient of variation are given in Table 4.10. The mean percent bolt-hole deformation $(\Delta d/d)_o$ at the bearing failure load was computed as 47.8, 36.9, and 33.2% for *d/t* ratios of 1, 1.5, and 2 respectively. Figure 4.11 shows the variation of mean pin-bearing strength with *d/t* ratio. The results indicate that no significant relationship exists between pin-bearing strength and *d/t* ratio.

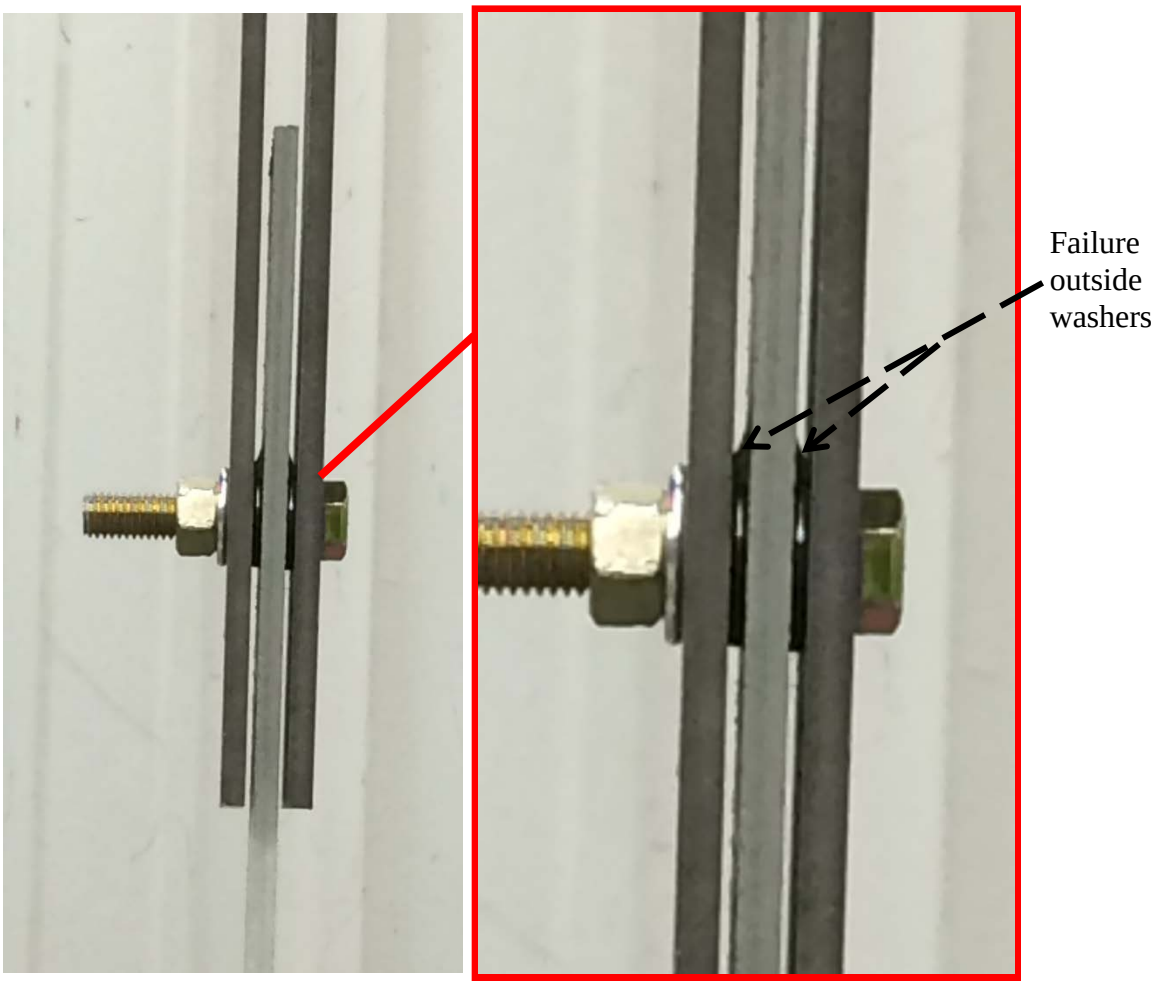

Figure 4.9 Failure outside the area constrained by washers - close-fit, moderately torqued specimens.

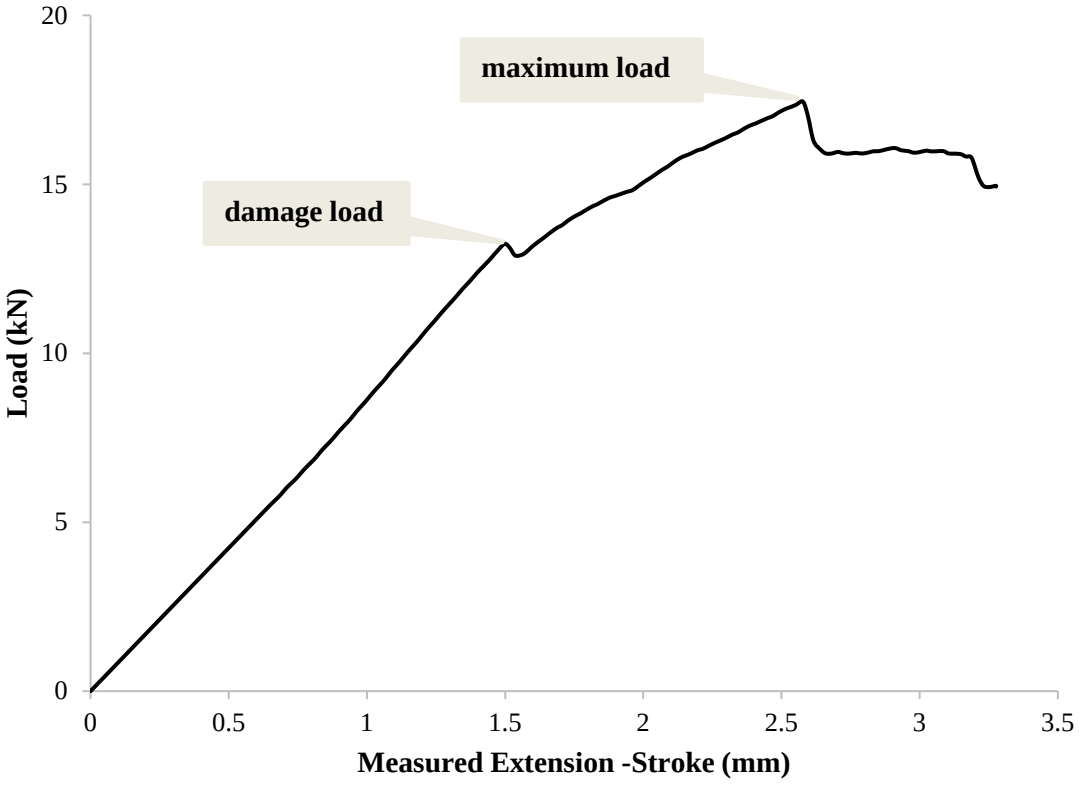

Figure 4.10 Representative load-extension curve – close-fit, moderately torqued specimen (6.35 mm (1/4 in) diameter bolt).

Table 4.9 Pin-bearing test results - close-fit, moderately torqued specimens.

Test	Bearing Load kN (lbf)			Bearing Stress MPa (psi)		
	***d/t* = 1**	***d/t* = 1.5**	***d/t* = 2**	***d/t* = 1**	***d/t* = 1.5**	***d/t* = 2**
Test 1	19.74 (4,437)	30.75 (6,914)	35.65 (8,016)	489 (70,992)	508 (73,746)	442 (64,124)
Test 2	16.93 (3,805)	29.91 (6,724)	34.17 (7,681)	420 (60,881)	495 (71,722)	424 (61,446)
Test 3	17.59 (3,955)	28.80 (6,475)	35.78 (8,045)	436 (63,287)	476 (69,067)	444 (64,358)
Test 4	18.60 (4,181)	29.86 (6,712)	35.95 (8,083)	461 (66,903)	494 (71,599)	446 (64,662)
Test 5	15.97 (3,591)	29.13 (6,549)	33.65 (7,565)	396 (57,461)	482 (69,861)	417 (60,523)
Test 6	16.37 (3,681)	29.56 (6,646)	36.32 (8,166)	406 (58,889)	489 (70,886)	450 (65,328)
Test 7	16.76 (3,767)	28.13 (6,323)	36.66 (8,242)	416 (60,279)	465 (67,443)	455 (65,936)
Test 8	17.44 (3,921)	27.77 (6,244)	35.45 (7,970)	433 (62,743)	459 (66,598)	440 (63,757)
Test 9	17.52 (3,940)	28.25 (6,350)	35.74 (8,035)	435 (63,035)	467 (67,733)	443 (64,277)
Test 10	16.37 (3,681)	29.21 (6,567)	36.73 (8,257)	406 (58,898)	483 (70,045)	455 (66,053)

Table 4.10 Summary - pin-bearing test results for close-fit moderately torqued specimens.

***d/t* ratio**	**Sample Size**	**Mean Strength**		**SD**		**%COV**
		MPa	**psi**	**MPa**	**psi**	
1	10	430	62,340	28	4,100	6.6
1.5	10	482	69,870	15	2,220	3.2
2	10	442	64,050	12	1,800	2.8

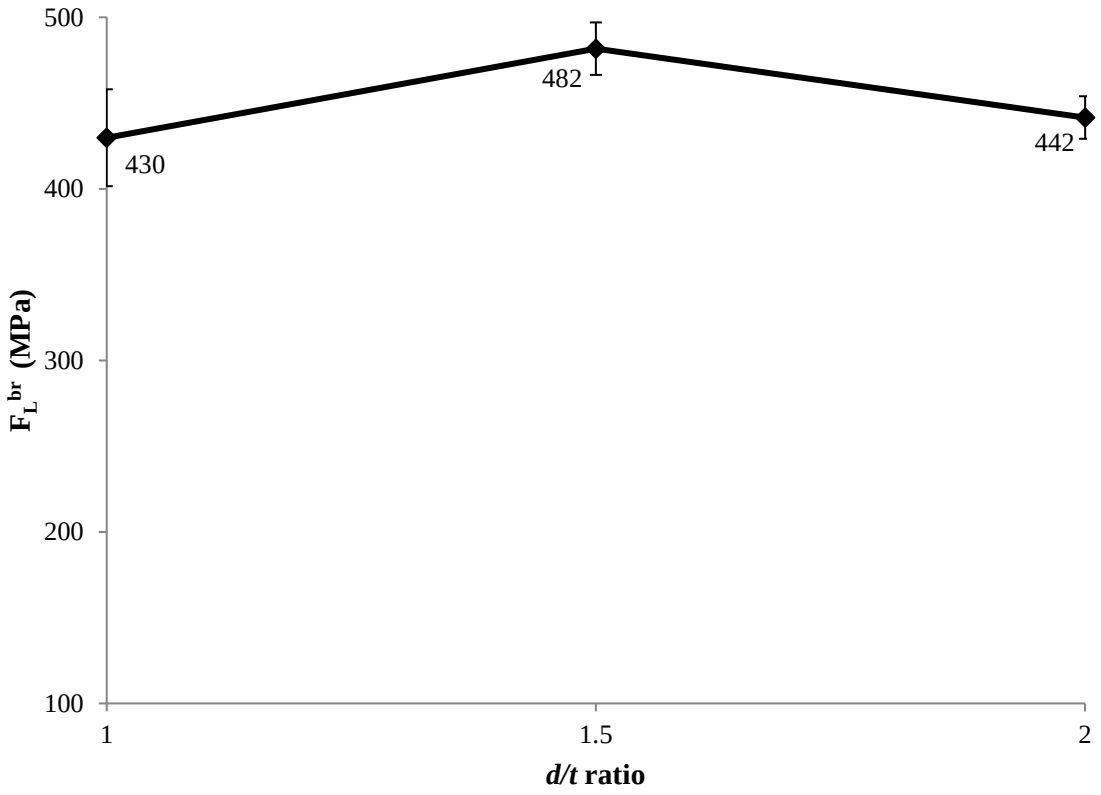

Figure 4.11 Mean pin-bearing strength vs *d/t* ratio for close-fit moderately torqued specimens.

Figure 4.12 shows a representative test specimen at failure. The specimen failed in bearing after reaching the maximum (failure) load; this was accompanied by an increase in bolt-hole deformation due to significant movement of the bolt in the connection.

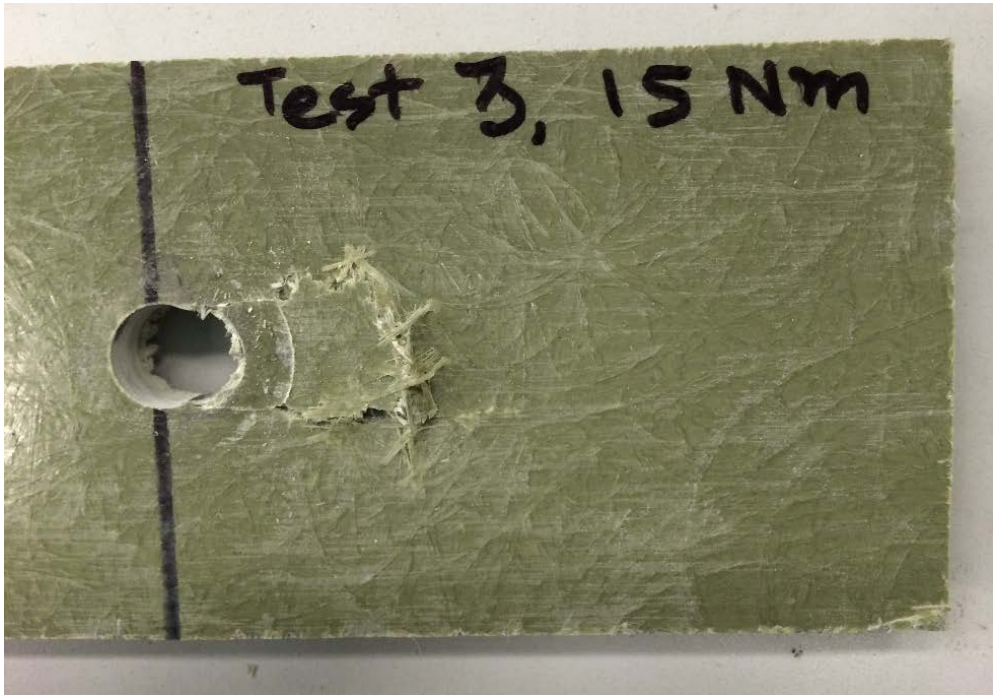

Figure 4.12 Representative test specimen at failure – close-fit, moderately torqued specimen.

4.4.4 1.6 mm (1/16 in) Bolt-Hole Clearance, Moderately Torqued Specimens

All the specimens were torqued as discussed in Section 4.4.3. Similar to the case of close-fit, moderately torqued specimens, the presence of lateral restraint increased the load carrying capacity of the connection. Also, the bilinear approximation models the behavior of a connection, displaying a reduction in stiffness after reaching the “damage load.” A

representative load-extension curve is shown in Figure 4.13. Load-extension curves for all the tests are shown in Appendix A. Test results are provided in Table 4.11 and a summary of results showing standard deviation and coefficient of variation are given in Table 4.12. The mean percent bolt-hole deformation $(\Delta d/d)_o$ at the bearing failure load was computed as 33.4, 29.5, and 24.6% for *d/t* ratios of 1, 1.5, and 2 respectively. Figure 4.14 shows the variation of mean pin-bearing strength with *d/t* ratio. The results indicate that no significant relationship exist between pin-bearing strength and *d/t* ratio.

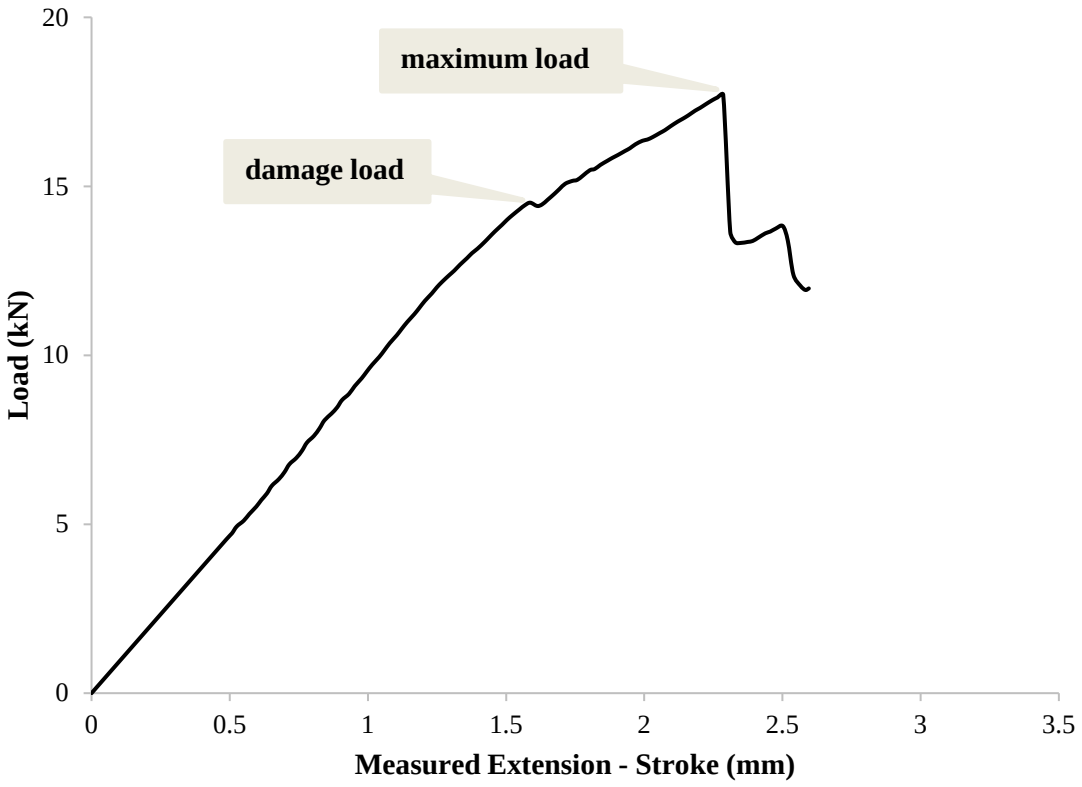

Figure 4.13 Representative load-extension curve – 1.6 mm (1/16 in) bolt-hole clearance, moderately torqued specimen (6.35 mm (1/4 in) diameter bolt).

Table 4.11 Pin-bearing test results – 1.6 mm (1/16 in) bolt-hole clearance, moderately torqued specimens.

Test	Bearing Load kN (lbf)			Bearing Stress MPa (psi)		
	***d/t* = 1**	***d/t* = 1.5**	***d/t* = 2**	***d/t* = 1**	***d/t* = 1.5**	***d/t* = 2**
Test 1	17.69 (3,978)	24.32 (5,468)	32.50 (7,307)	439 (63,644)	402 (58,322)	403 (58,455)
Test 2	19.08 (4,289)	23.08 (5,189)	30.37 (6,827)	473 (68,617)	382 (55,346)	377 (54,617)
Test 3	16.97 (3,814)	23.88 (5,369)	32.87 (7,390)	421 (61,026)	395 (57,265)	408 (59,116)
Test 4	18.27 (4,106)	22.56 (5,072)	28.57 (6,422)	453 (65,702)	373 (54,105)	354 (51,379)
Test 5	17.20 (3,867)	21.53 (4,841)	31.11 (6,994)	427 (61,868)	356 (51,639)	386 (55,953)
Test 6	17.71 (3,981)	21.96 (4,938)	29.68 (6,672)	439 (63,703)	363 (52,668)	368 (53,376)
Test 7	17.47 (3,927)	23.22 (5,219)	33.65 (7,564)	433 (62,835)	384 (55,672)	417 (60,515)
Test 8	17.65 (3,969)	25.14 (5,652)	29.43 (6,616)	438 (63,502)	416 (60,283)	365 (52,927)
Test 9	19.20 (4,316)	23.81 (5,353)	30.98 (6,964)	476 (69,053)	394 (57,099)	384 (55,711)
Test 10	19.14 (4,303)	23.37 (5,253)	32.45 (7,295)	475 (68,856)	386 (56,036)	402 (58,361)

Table 4.12 Summary - pin-bearing test results for 1.6 mm (1/16 in) bolt-hole clearance, moderately torqued specimens.

***d/t* ratio**	**Sample Size**	**Mean Strength**		**SD**		**%COV**
		MPa	**psi**	**MPa**	**psi**	
1	10	447	64,880	21	3,000	4.6
1.5	10	385	55,840	18	2,590	4.6
2	10	386	56,040	21	3,010	5.4

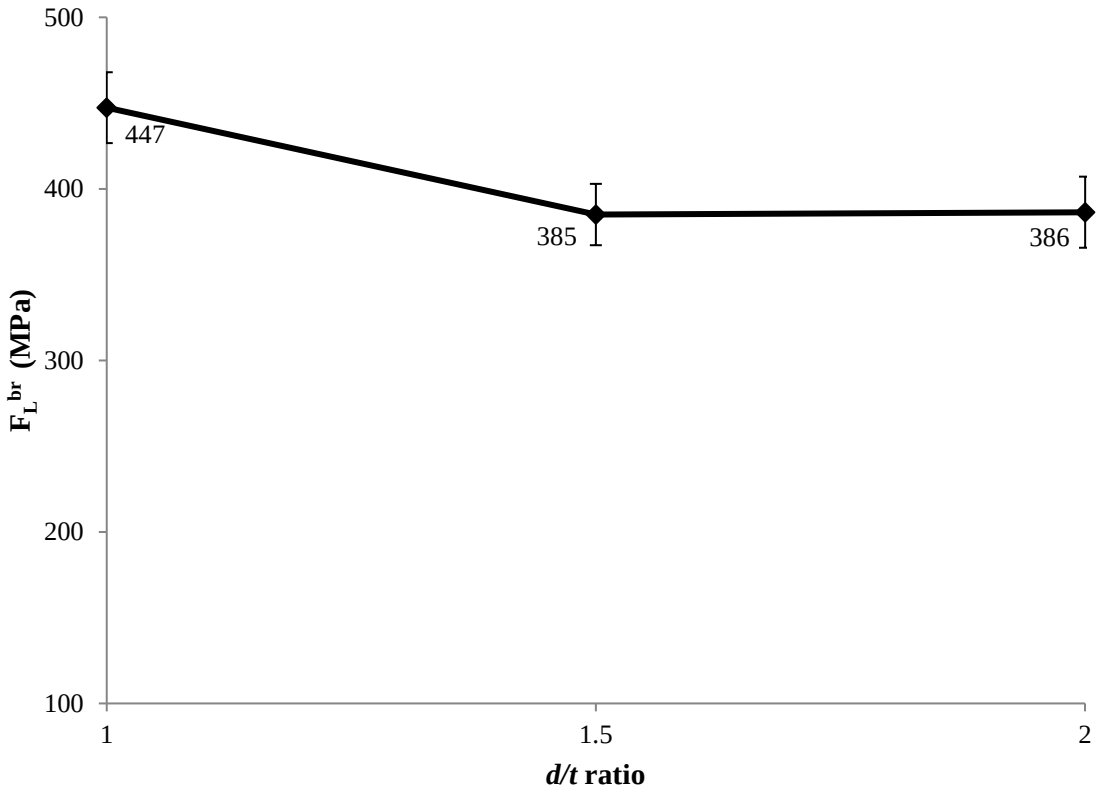

Figure 4.14 Mean pin-bearing strength vs *d/t* ratio for 1.6 mm (1/16 in) bolt-hole clearance, moderately torqued specimens.

4.4.5 Summary

Figure 4.15 shows the variation of strength as a function of *d/t* for the FRP materials used in this investigation. In the figure, the mean pin-bearing strengths are normalized with respect to pin-bearing strength at a *d/t* of 1. The results indicate that for laterally unrestrained connections, whether close-fit or having large bolt-hole clearance (1.6 mm (1//16 in), the pin-bearing strength is reduced with increasing *d/t* ratio for this pultruded material. However for moderately torqued connections, whether close-fit or having large bolt-hole clearance (1.6 mm (1//16 in), no specific relationship can be established between pin-bearing strength and *d/t* ratio.

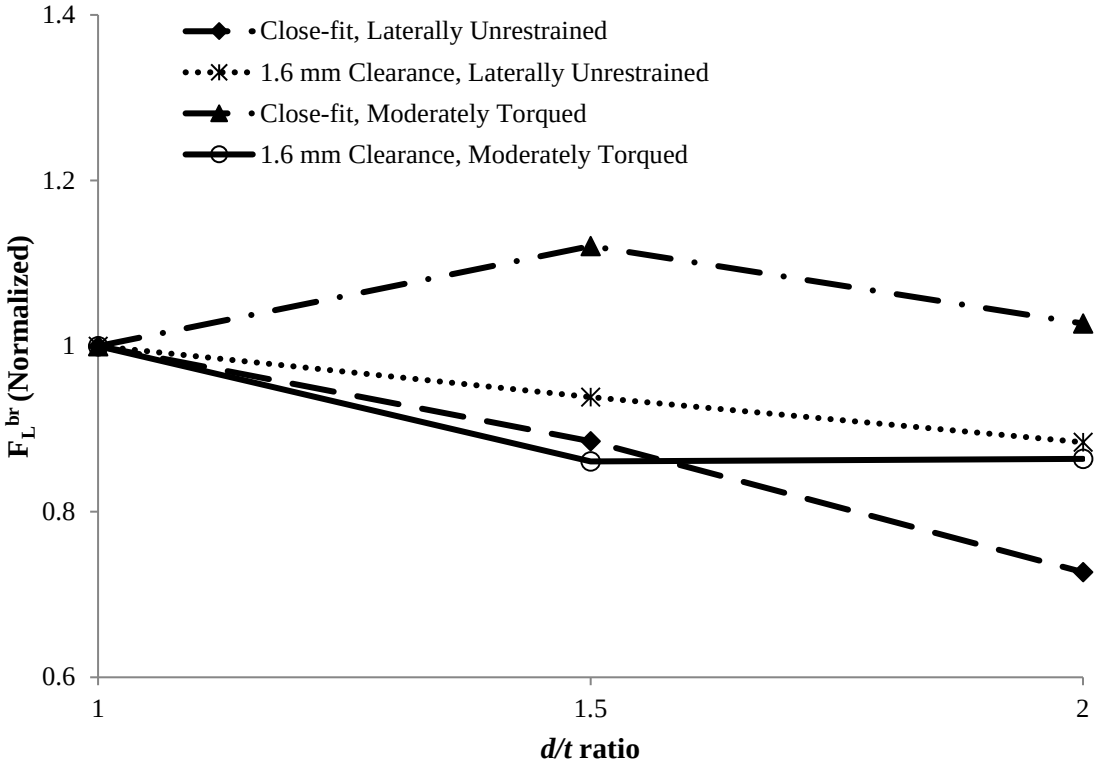

$$F_L^{br}(Normalized) = \frac{F_L^{br}}{F_L^{br}\ for\ d/t = 1}$$

Connection Parameter	$F_L^{br}(Normalized)$ *d/t* ratio		
	1	**1.5**	**2**
Close-fit, laterally unrestrained	1	0.88	0.73
1.6 mm (1/16 in) clearance, laterally unrestrained	1	0.94	0.88
Cloe-fit, moderately torqued	1	1.12	1.03
1.6 mm (1/16 in) clearance, moderately torqued	1	0.86	0.86

Figure 4.15 Summary – variation of normalized mean pin-bearing strength with *d/t* ratio.

4.5 Short-Term Tests at Elevated Temperatures

The mechanical properties of many FRP composites degrade significantly under elevated temperatures. As shown in Figure 4.16 the stiffness of the composite reduces with increasing temperature and the material softens above its glass transition temperature [51]. Researchers have thoroughly examined the influence of temperature on the mechanical properties of FRP materials; however limited studies have focused on investigating the response of bolted connections in pultruded FRP materials under elevated temperatures. A detailed discussion on the influence of elevated temperatures was presented in Section 2.6. In the present investigation, short-term tests were conducted at elevated temperatures as per the test matrix presented in Table 4.3, and the results are discussed in the following sections.

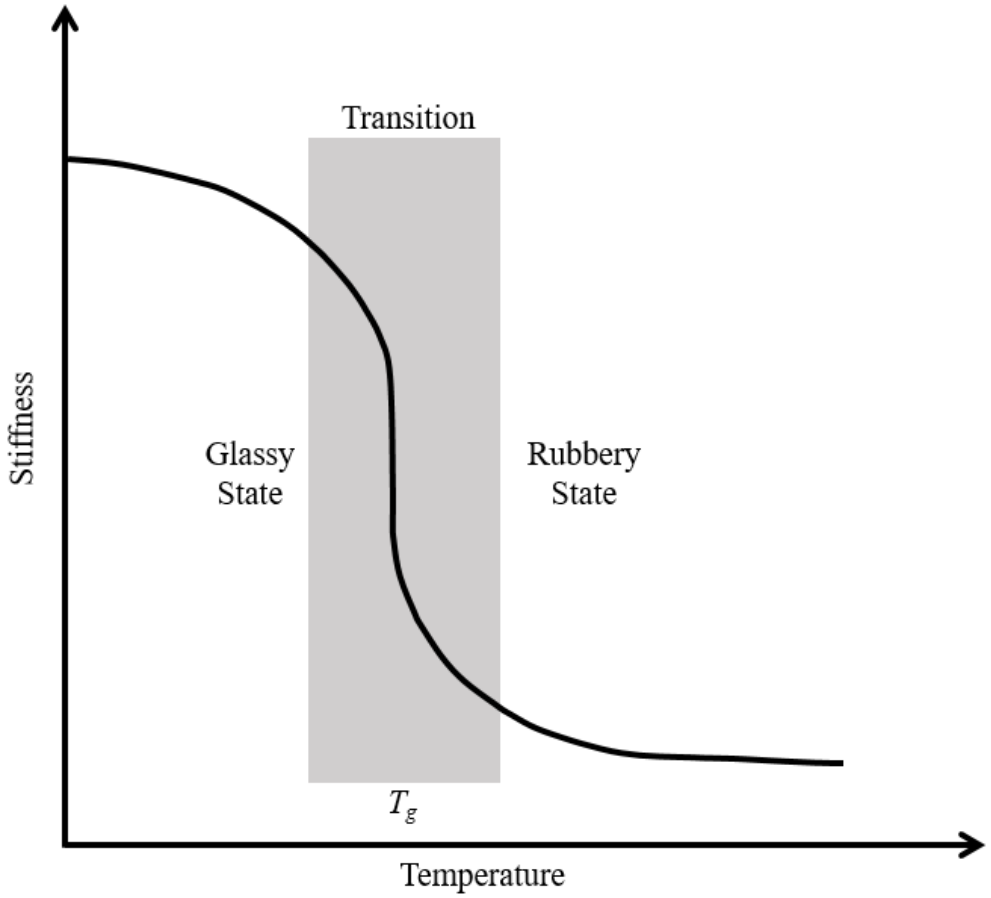

Figure 4.16 Effect of temperature on the stiffness of composites (after [51]).

Close-fit laterally unrestrained specimens were used to investigate short-term pin-bearing behavior at elevated temperatures. Temperatures of 24°C, 43.3°C and 60°C (75°F, 110°F and 140°F) were selected for the reasons discussed in Section 4.2. To achieve the desired temperature in the connection, the specimen is allowed to soak unstressed for a certain time period, known as thermal preconditioning. For this thermal preconditioning, previous experiments have shown that the material in the connection of the GRP plate reaches the required test temperature within a 30-minute soaking period [41].

To measure the short-term pin-bearing strength at elevated temperatures, an environmental chamber (shown in Figure 4.17, and Figure 4.18) was constructed and placed in the computer controlled hydraulic load actuator. The environmental chamber was constructed from 38.1 mm (1.5 in) thick duct board. The chamber was heated using a finned strip-heater and temperature was controlled by a digital thermostat. Details of the specific equipment used are given in Appendix D. After installing the specimen in the fixture, the door was closed and the inside temperature was increased to the desired temperature and the unstressed specimen was then conditioned for 30 minutes. A total of 10 tests were conducted at each temperature; 24°C (room temperature), 43.3°C and 60°C (75°F, 110°F, and 140°F). The results are shown in Table 4.13 through Table 4.15. A summary of results is given in Table 4.16. The test results show that the mean pin-bearing strength reduces from 263 MPa (38,120 psi) at ambient (room) temperature (24°C (75°F)) to 177 MPa (25,690 psi) at 43.3°C (110°F), and to 147 MPa (21,270 psi) at 60°C (140°F), exhibiting a reduction of 32.6 and 44.2% respectively. Figure 4.19 shows the representative test specimen at failure and Figure 4.20 shows the representative load-extension curves at 24°C (75°F) (ambient temperature), 43.3°C and 60°C (75°F, 110°F, and 140°F). Load-extension curves for all the tests are shown in Appendix A. The mean percent bolt-hole deformation $(\Delta d/d)_o$ at the bearing failure load, was computed as 27.9, and 24.3% at 43.3°C and 60°C (110°F, and 140°F) respectively.

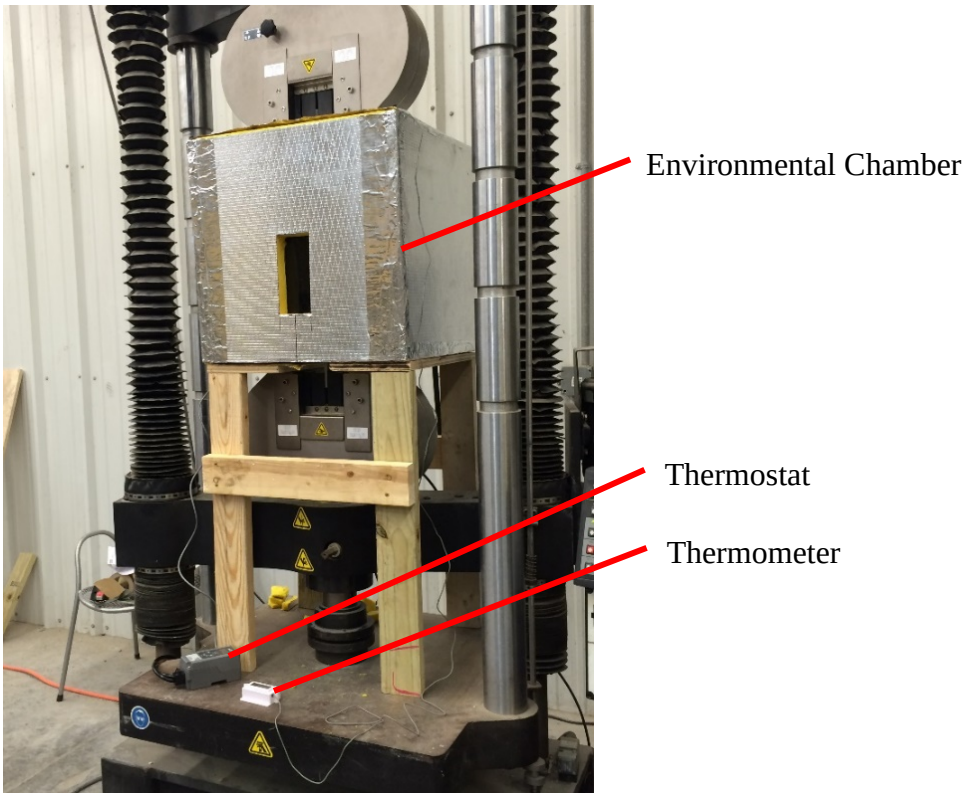

Figure 4.17 Test setup – elevated temperature tests (isometric view).

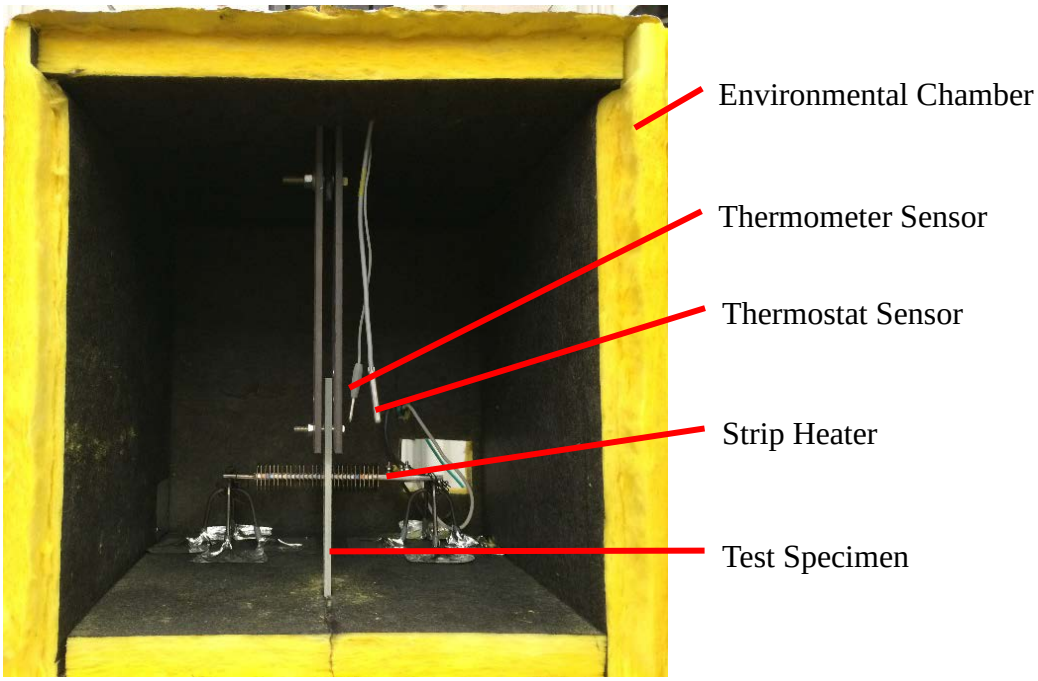

Figure 4.18 Test setup – elevated temperature tests (environmental chamber inner view).

Table 4.13 Short-term pin-bearing strength tests at ambient (room) temperature (24°C (75°F)).

Test	**Bearing Load kN (lbf)**	**Bearing Strength MPa (psi)**
Test 1	9.65 (2,168)	239 (34,694)
Test 2	8.86 (1,992)	220 (31,872)
Test 3	10.97 (2,466)	272 (39,457)
Test 4	11.89 (2,673)	295 (42,763)
Test 5	10.48 (2,356)	260 (37,691)
Test 6	10.23 (2,300)	254 (36,794)
Test 7	11.35 (2,550)	281 (40,808)
Test 8	10.64 (2,391)	264 (38,256)
Test 9	11.35 (2,552)	282 (40,833)
Test 10	10.57 (2,377)	262 (38,032)
Mean	10.60 (2,380)	263 (38,120)
SD	0.88 (198)	22 (3,170)
%COV	8.3	

Table 4.14 Short-term pin-bearing strength tests at 43.3°C (110°F).

Test	**Bearing Load kN (lbf)**	**Bearing Strength MPa (psi)**
Test 1	7.66 (1,722)	190 (27,549)
Test 2	6.99 (1,571)	173 (25,129)
Test 3	7.02 (1,577)	174 (25,240)
Test 4	7.11 (1,599)	176 (25,580)
Test 5	6.66 (1,498)	165 (23,964)
Test 6	7.59 (1,707)	188 (27,313)
Test 7	7.09 (1,594)	176 (25,510)
Test 8	7.78 (1,750)	193 (28,002)
Test 9	6.83 (1,536)	169 (24,569)
Test 10	6.69 (1,503)	166 (24,048)
Mean	7.16 (1,610)	177 (25,690)
SD	0.40 (91)	10 (1,450)
%COV	5.6	

Table 4.15 Short-term pin-bearing strength tests at 60°C (140°F).

Test	**Bearing Load kN (lbf)**	**Bearing Strength MPa (psi)**
Test 1	5.24 (1,179)	130 (18,863)
Test 2	5.53 (1,243)	137 (19,892)
Test 3	5.76 (1,296)	143 (20,728)
Test 4	6.73 (1,512)	167 (24,197)
Test 5	5.32 (1,197)	132 (19,147)
Test 6	6.26 (1,407)	155 (22,505)
Test 7	6.16 (1,386)	153 (22,172)
Test 8	6.13 (1,377)	152 (22,035)
Test 9	6.31 (1,419)	157 (22,699)
Test 10	5.68 (1,278)	141 (20,446)
Mean	5.91 (1,330)	147 (21,270)
SD	0.48 (108)	12 (1,720)
%COV	8.1	

Table 4.16 Summary of short-term test results at elevated temperatures – close-fit, laterally unrestrained specimens.

Temperature °C (°F)	Sample Size	Mean Strength		COV (%)	Max Strength Reduction (%)
		MPa	psi		
24 (75)	10	263	38,120	8.3	0
43.3 (110)	10	177	25,690	5.6	32.6
60 (140)	10	147	21,270	8.1	44.2

Figure 4.19 Representative test specimen at failure – short-term test at 60°C (140°F).

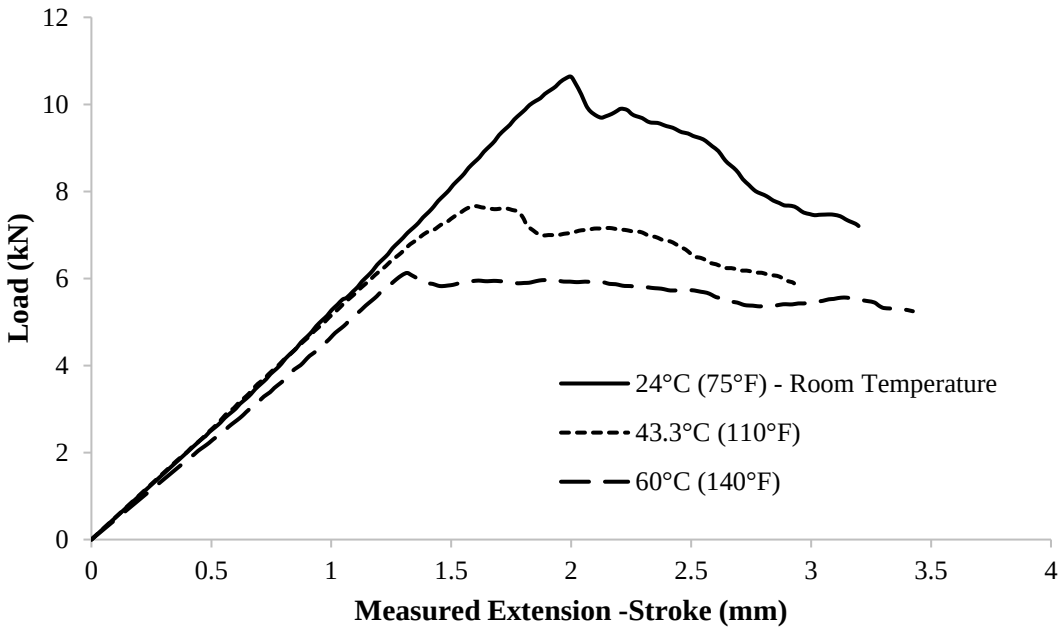

Figure 4.20 Representative load-extension curves at various temperatures - close-fit, laterally unrestrained specimens.

4.6 Summary

Figure 4.21 shows the mean pin-bearing strength as a function of *d/t* for the parametric investigation carried out at room temperature. Similarly, Figure 4.22 shows the influence of temperature on the pin-bearing strength. The COV for the pin-bearing tests varied from 2.8 to 10%. The mean percent bolt-hole deformation $(\Delta d/d)_o$ at the bearing failure load is shown in Table 4.17.

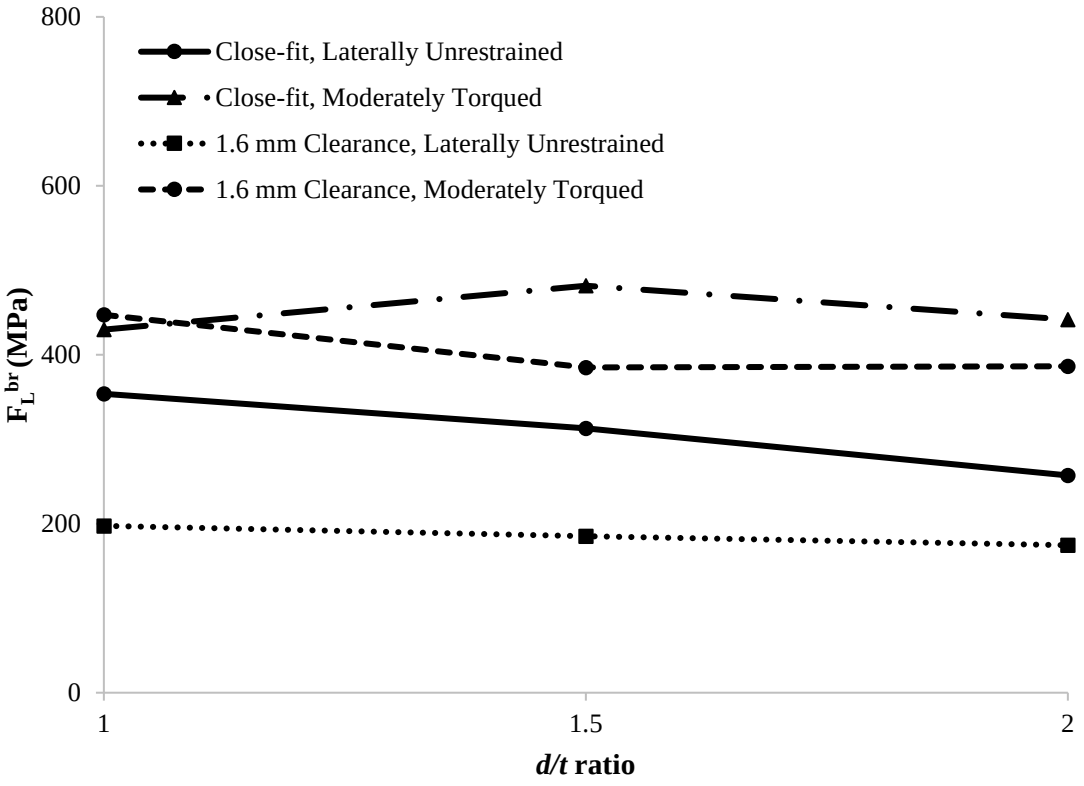

Figure 4.21 Summary – variation of mean pin-bearing strength with *d/t* ratio.

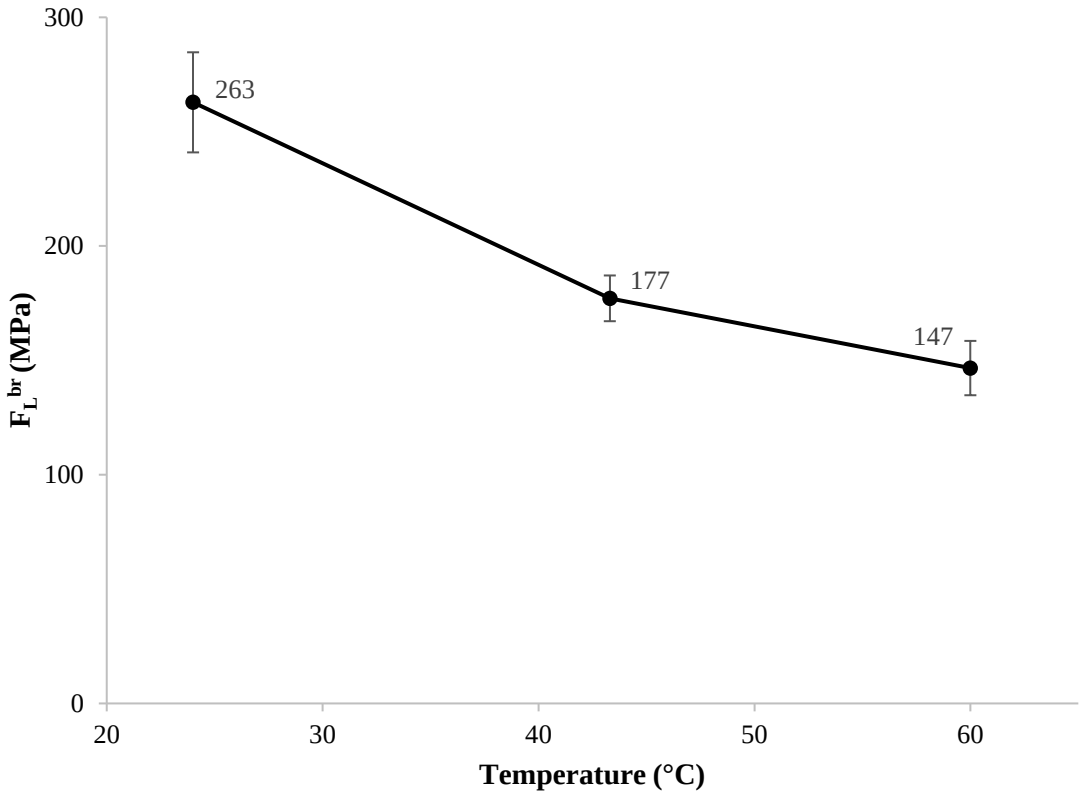

Figure 4.22 Reduction in mean pin-bearing strength with increase in temperature - close-fit, laterally unrestrained specimens.

Table 4.17 Mean percent bolt-hole deformation $(\Delta d/d)_o$ at the bearing failure load.

Test	*d/t* ratio	Temperature °C (°F)	$(\Delta d/d)_o$ %	COV %
Close-fit, laterally unrestrained	1	24 (75)	28.7	8.8
	1.5	24 (75)	29.8	7.2
	2	24 (75)	35.2	8.7
1.6 mm (1/16 in) bolt-hole clearance, laterally unrestrained	1	24 (75)	14.4	12.1
	1.5	24 (75)	11.5	12.2
	2	24 (75)	10.2	5.5
Close-fit, moderately torqued	1	24 (75)	47.8	12.9
	1.5	24 (75)	36.9	9.4
	2	24 (75)	33.2	6.7
1.6 mm (1/16 in) bolt-hole clearance, moderately torqued	1	24 (75)	33.4	11.2
	1.5	24 (75)	29.5	9.7
	2	24 (75)	24.6	7.2
Close-fit, laterally unrestrained	1	43.3 (110)	27.9	12.0
Close-fit, laterally unrestrained	1	60 (140)	24.3	17.4

4.7 Conclusions

The effects of specific connection parameters; *d/t* ratio, bolt hole clearance, and bolt tightening torque on pin-bearing strength were investigated at normal and elevated service temperatures. The following conclusions can be drawn from this parametric investigation:

a. For laterally unrestrained connections, whether close-fit or having large bolt-hole clearance (1.6 mm (1/16 in)), pin-bearing strength reduces with increasing *d/t* ratio.

b. For close-fit moderately torqued connections, and 1.6 mm (1/16 in) bolt-hole clearance moderately torqued connections, no significant relationship exists between pin-bearing strength and *d/t* ratio.

c. For a given *d/t* ratio, an increase in bolt-hole clearance reduces pin-bearing strength.

d. Similarly, an increase in lateral restraint increases the pin-bearing strength significantly.

e. The pin-bearing strength for these types of pultruded material is significantly decreased at moderately elevated temperatures.

f. The percent bolt-hole deformation $(\Delta d/d)_o$ at the bearing failure load reduces with an increase in bolt-hole clearance and temperature, while $(\Delta d/d)_o$ increases with an increase in lateral applied torque.

The results of the short-term investigation demonstrate the importance of bolt-hole clearance, lateral restraint, and service temperature on the performance of bolted connections in FRP members. However, the influence of these parameters on time-dependent behavior must also be investigated in order to properly characterize and predict the long-term performance of bolted connections for these types of materials. The time-dependent response of the bearing connections under sustained loads is the subject of the next phase of this investigation.

CHAPTER 5

RESPONSE OF PIN-BEARING CONNECTIONS UNDER SUSTAINED LOADS

5.1 Objective

This chapter presents the results of an experimental investigation into the behavior of single pin-bearing connections under constant sustained loads at various load levels, specific bolt-hole clearances and specific bolt tightening torques for both normal and elevated service temperatures.

5.2 Development of Test Matrix

The short-term test results demonstrated that in addition to other connection parameters such as connection geometry and environmental conditions, the bolt-diameter to thickness (*d/t*) ratio significantly influences the strength of a connection. Therefore, for consistency all the tests under sustained loading were conducted with a *d/t* ratio of 1. All the specimens used in the investigation were nominally 6.35 mm (0.25 in) thick, 38.1 mm (1.5 in) wide, and 406 mm (16 in) long. One 6.35 mm (0.25 in) diameter hole was drilled 50.8 mm (2 in) away from both ends of the specimen, thus achieving *d/t*, *e/d*, and *w/d* ratios of 1, 8, and 6 respectively. Figure 5.1 shows the specimen geometry used in the investigation. The response of single bolt tension connections under sustained loading was investigated to study the influence of bolt-hole clearance, lateral applied torque, and elevated service temperature.

Table 5.1 and Table 5.2 show the formulated test matrix for experiments under sustained loading. The duration of the creep tests was selected such that the experimental data could be effectively approximated using available models in the literature. Generally, the creep constants required for modeling long-term response are computed from the experimental data plotted on logarithmic scale. Therefore, to have at least three decades on the logarithmic scale, a test duration of 1,000 hours was selected. The sustained load levels were selected based on published design guidance and the fact that the characteristic strength is less than the mean strength. The ASCE Pre-Standard [10] specifies values for time effect factor (shown in Table 2.3) ranging from 0.4 to 1.0. Also, as will be presented later in Chapter 6, characteristic strength is less than mean strength, and the design of bolted connections is based on the characteristic strength. Therefore, the sustained load levels ranging from 50% to 80% of mean pin-bearing strength were selected to be investigated. In Table 5.1 and Table 5.2, tests shown in the shaded cells were initially designed but later not conducted. As will be demonstrated later by the experimental results, for creep tests conducted at a sustained load level of 50% of mean pin-bearing strength, the results demonstrated an increase in bolt-hole deformation with time for all connection conditions when compared with Case-I (close-fit laterally, laterally unrestrained specimens at ambient temperature). Also, for Case-I at a sustained load level of 80% of mean bearing strength, the specimens failed during the test duration. Therefore, based on the preliminary conclusion that lateral restraint, bolt-hole clearance, and elevated temperatures further aggravates the connection response when compared with Case-I, tests at a sustained load level of 80% mean pin-bearing strength for these cases were not conducted. The number of tests conducted under each category are shown in Table 5.3.

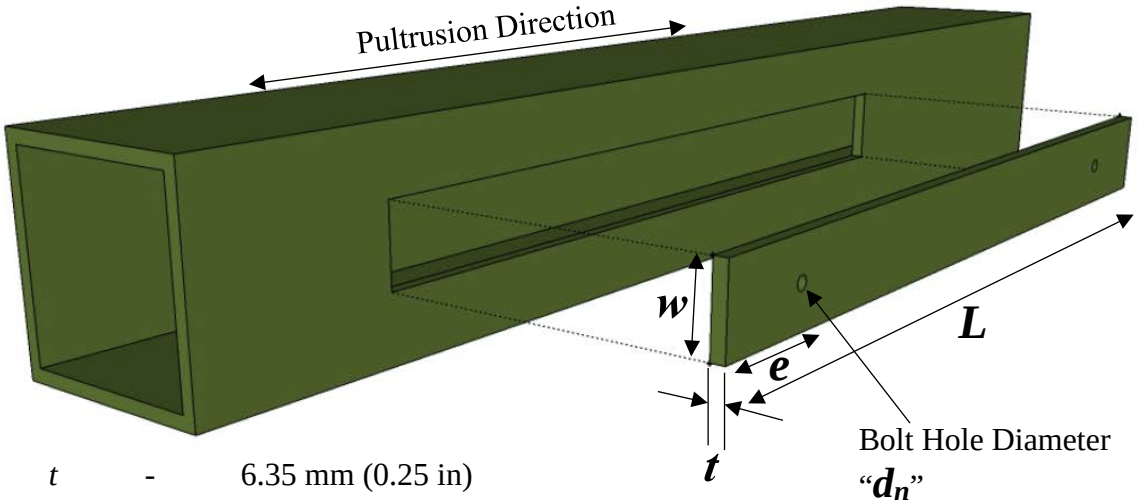

t	-	6.35 mm (0.25 in)
w	-	38.1 mm (1.5 in)
e	-	50.8 mm (2 in)
L	-	406 mm (16 in)

Figure 5.1 Specimen geometry – creep tests.

Table 5.1 Test matrix – pin-bearing tests under sustained loads at ambient (room) temperature (24°C (75°F)).

Sustained Load Level (% of Mean)	Case-I	Case-II	Case-III
	No Lateral Restraint Close-fit	Moderate Torque Close-fit	No Lateral Restraint 1.6 mm (1/16 in) Clearance
Creep Tests at Room Temperature			
50%	6 weeks	6 weeks	6 weeks
65%	6 weeks		
70%	6 weeks	6 weeks	6 weeks
80%	6 weeks	6 weeks	6 weeks
Duration	24 weeks	12 weeks	12 weeks

Table 5.2 Test matrix – pin-bearing tests under sustained loads at elevated temperatures.

Sustained Load Level (% of Mean)	Temperature	
	43.3°C (110°F)	60°C (140°F)
Case-I - Close-fit, No Lateral Restraint		
50%	6 weeks	6 weeks
70%	6 weeks	6 weeks
80%	6 weeks	6 weeks
Duration	12 weeks	12 weeks

Table 5.3 Test matrix – number of pin-bearing tests under sustained loads.

Sustained Load Level (% of Mean)	**Case-I**		**Case-II**	**Case-III**
	No Lateral Restraint **Close-fit**		**Moderate Torque** **Close-fit**	**No Lateral Restraint** **1.6 mm (1/16 in) Clearance**
Creep Tests at Ambient (Room) Temperature				
50%	3		6	4
65%	6		-	-
70%	3		5	3
80%	5		-	-
Creep Tests at Elevated Service Temperatures				
	Temperature			
	43.3°C (110°F)	60°C (140°F)		
50%	4	3	-	-
70%	3	3	-	-

5.3 Test Setup

Bolt-hole deformations in the FRP material at the pin were recorded for time durations of up to 1,000 hours at normal and elevated service temperatures. Single bolt tension connections were tested under a double-lap shear configuration. Axial load was applied to the single-bolt connection using a static lever-arm test setup as shown in Figure 5.2; specific details of the equipment used are given in Appendix D. The lever-arm magnified the load applied to the specimen by a factor of 10. The test setup calibration was carried out by comparing the load vs strain plot on the creep test rig to that of the connection plate in a servohydraulic test machine. A comparison of the two plots shown in Figure 5.3 confirms the load transfer ratio of 1:10. A steel plate and high-strength steel bolts were used to minimize deformations in the fixture. These high-strength steel bolts (Grade 9) were readily available having a hexagonal cap screw, minimum wedge tensile strength of 1,240 MPa (180,000 psi), and mechanical properties conforming to ASTM F-606 [50] except wedge tensile strength. Two strain gauges were placed on both sides of the steel plate at the bottom of the fixture to ensure that the test specimen was properly aligned prior to the application of load to avoid bending along the length of the test specimen. Two deflection gauges with a precision of 0.00254 mm (0.0001 in) were affixed to the specimen as shown in Figure 5.2 for measuring deformation at the bolt holes. Deflections were recorded every 6 minutes for first hour, every 15 minutes for next three hours, every hour for the following 24 hours, and every day thereafter up to 1,000 hours.

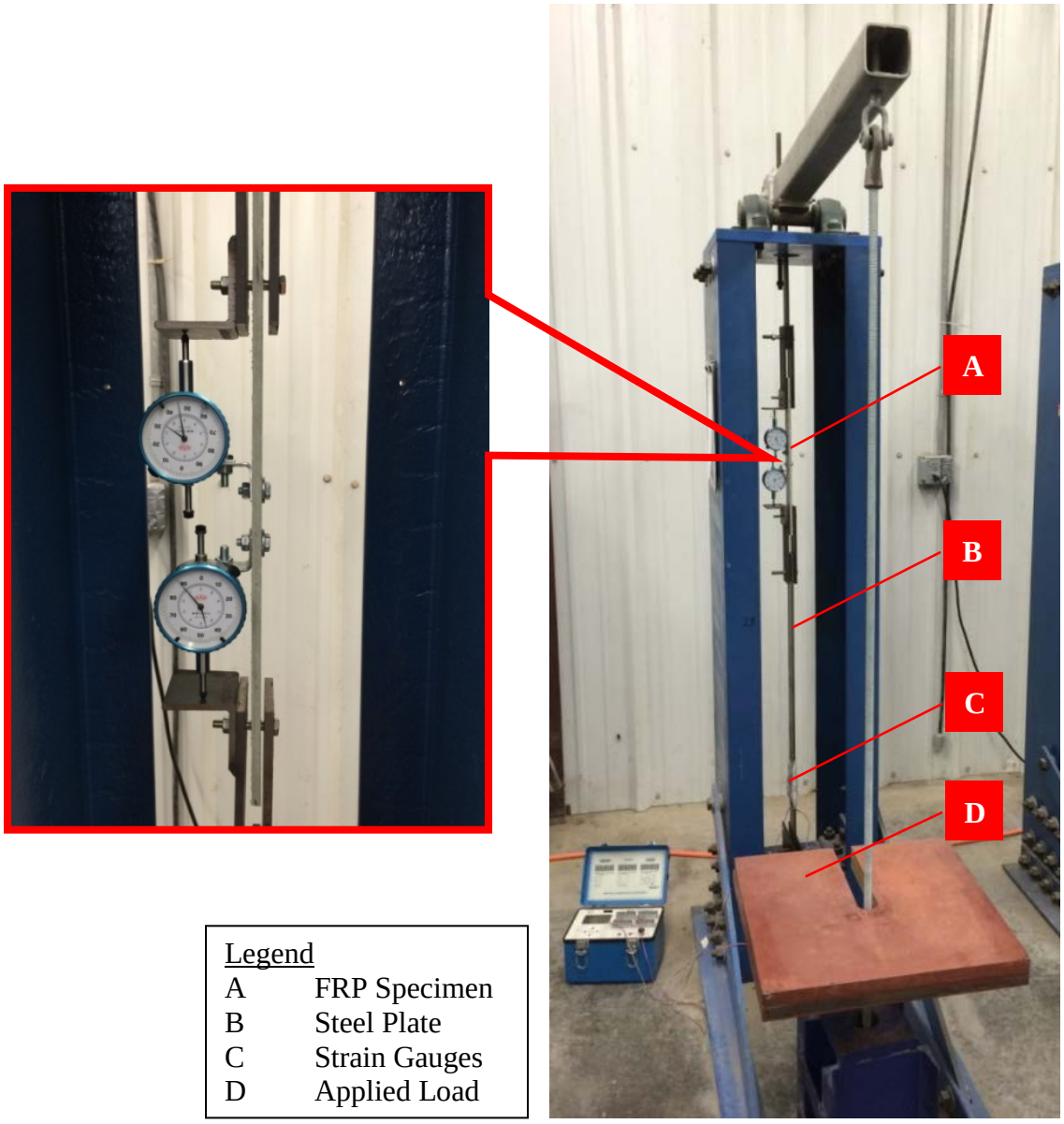

Figure 5.2 Creep test setup.

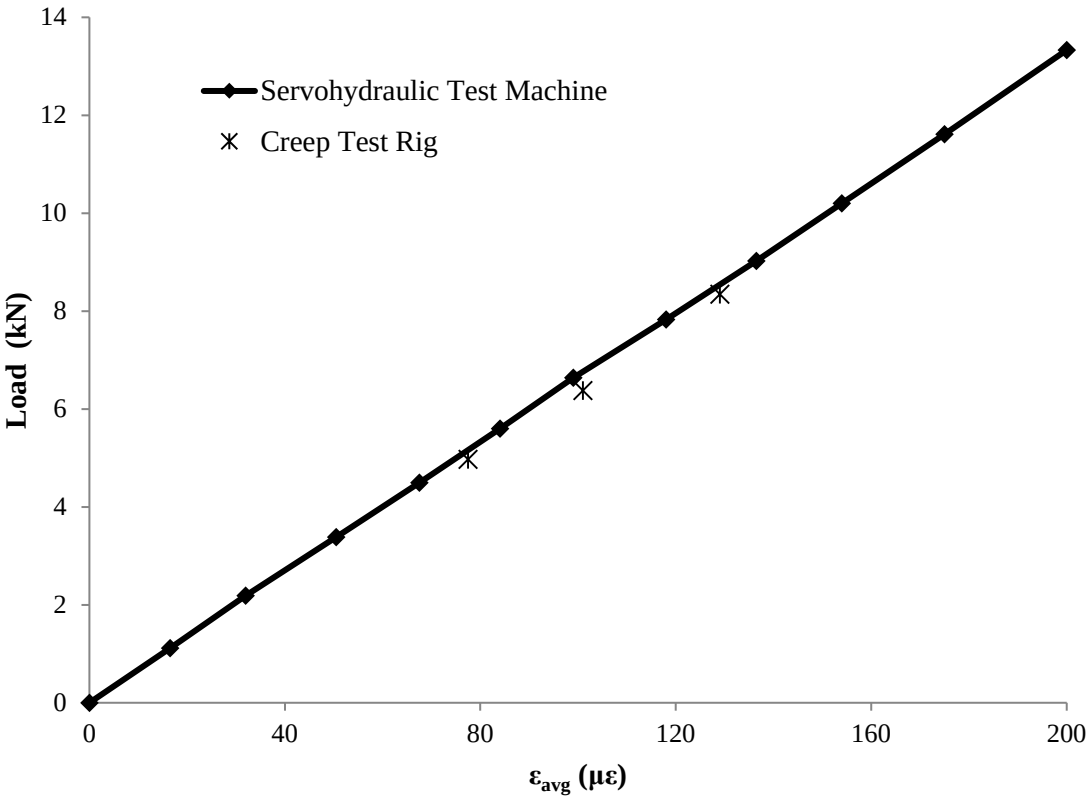

Figure 5.3 Creep test setup calibration.

5.4 Results and Discussion – Tests at Ambient (Room) Temperature

5.4.1 Case-I - Close-fit, Laterally Unrestrained Specimens

As discussed in Chapter 4, short-term pin-bearing strength tests were conducted for the close-fit, laterally unrestrained condition with a *d/t* ratio of 1. The resultant mean bearing strength was determined to be 10.6 kN (2,380 lbf) and served as the basis for the load levels used in the time-dependent tests. Test results for specimens subjected to various load levels are discussed in the following sections. Figure 5.4 shows a typical instrumentation setup for tests conducted on laterally unrestrained specimens.

Figure 5.4 Instrumentation setup – Case-I - close-fit, laterally unrestrained specimens.

5.4.1.1 Case-I - Sustained Load Level - 80% of Mean Bearing Strength

Five tests were conducted at a sustained load level of 80% of the mean bearing strength. Table 5.4 provides time to failure for the tests, where failure was assumed when bolt-hole deformation reached 50% of the bolt-hole diameter – 3.2 mm (1/8 in). Figure 5.5 shows the representative test specimens at failure. These failures at relatively short time

durations demonstrate that the viscoelastic response of bolted connections in FRP materials must be accounted for to achieve a safe practical design.

Figure 5.5 Representative test specimens at failure – stress level of 80% of mean bearing strength (Case-I - close-fit, laterally unrestrained specimens).

Table 5.4 Time to failure – sustained load level of 80% of mean bearing strength (Case-I - close-fit, laterally unrestrained specimens).

Test	Time to failure (hours)
1	150
2	0.28
3	2.92
4	21.0
5	121

5.4.1.2 Case-I - Sustained Load Level – 50, 65, and 70% of Mean Bearing Strength

Creep tests were conducted at load levels representing 50, 65, and 70% of mean bearing strength. None of the specimens tested failed during the duration of the tests. Visual examination of the bolt-holes at the end of tests revealed slight "blooming" as discussed earlier and illustrated in Figure 4.2, in the region where the bolt shank was in contact with the FRP material. The total bolt-hole deformation (Δd_{total}) recorded in the creep tests was decomposed into two parts as given in Equation (5.1). In general, bearing hole deformation was more pronounced for the specimens subjected to higher sustained stress levels.

$$\Delta d_{total} = \Delta d_{inst} + \Delta d_{creep} \tag{5.1}$$

where

Δd_{total} = total bolt-hole deformation, mm (in)

Δd_{inst} = instantaneous deformation of the bolt-hole measured immediately upon loading, mm (in)

Δd_{creep} = creep component of the bolt-hole deformation, mm (in)

Results of the sustained load tests are summarized in Table 5.5, which shows the creep component of the percent bolt-hole deformation ($\Delta d_{creep}/d$). The variation in the test data indicates that deformation in the connection is highly dependent on the specific fiber/matrix composition directly adjacent to the bolt-hole. Since the fiber geometry is not completely uniform in the material, it will certainly influence the viscoelastic response of the test specimen. Another reason for this variation may be the absence of lateral restraint. Since lateral restraint confines the potential damage area adjacent to the hole, the deformation of the holes with washers under even a small amount of torque is expected to be more generally uniform.

Table 5.5 Creep component of the percent bolt-hole elongation at 1,000 hours - Case-I - close-fit, laterally unrestrained specimens.

Sustained Load Level (% of Mean)	$\Delta d_{creep}/d$ **(%)**					
	Test 1	**Test 2**	**Test 3**	**Test 4**	**Test 5**	**Test 6**
50%	0.78	0.72	1.06			
65%	2.92	1.6	1.04	1.24	0.88	0.52
70%	0.96	5.46	1.92			

The results of tests under sustained loading are shown in Figure 5.6, expressed as mean values of the creep component of the percent bolt-hole deformation. The results of individual tests are shown in Appendix B. These results clearly demonstrate the increase in deformation of the bolt-hole under the sustained loading. The results show that the creep deformations increased at a continuously decreasing rate up to about 400 hours of loading. Beyond this point, the deformations increased at a fairly constant and comparatively low rate. All the test specimens exhibited some degree of viscoelastic deformation.

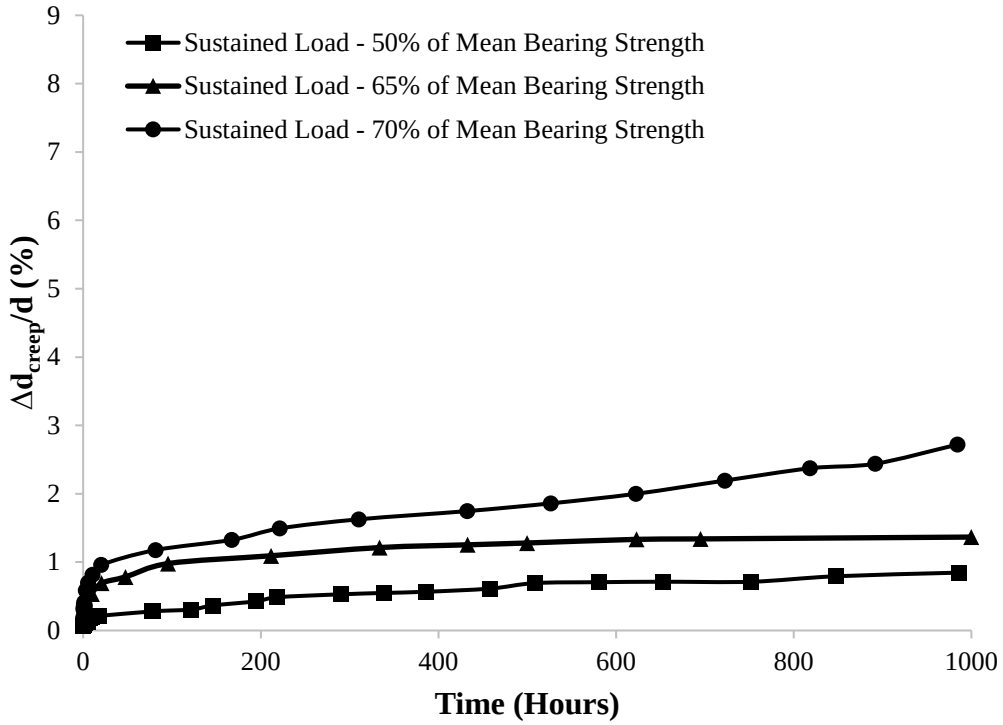

Figure 5.6 Creep test results – mean values of creep component of the percent bolt-hole deformation (Case-I - close-fit, laterally unrestrained specimens).

Figure 5.7 shows the creep test results for a sustained load level of 70% of mean bearing strength. The curve showing the mean values of the experimental results demonstrate rapid increase in bolt-hole deformation, particularly after about 600 hours of loading. This observation might be an indication that the material is in a tertiary creep stage. However, the results of individual tests demonstrate that in two tests the bolt-hole deformation increased at a fairly steady rate after about 400 hours of loading. One test demonstrated a continuous increase in bolt-hole deformation during the duration of the test. This observation suggests that the rapid increase in bolt-hole deformation observed in mean

curve may be due to the scatter in the data from one single test, and is not necessarily an indication of tertiary creep.

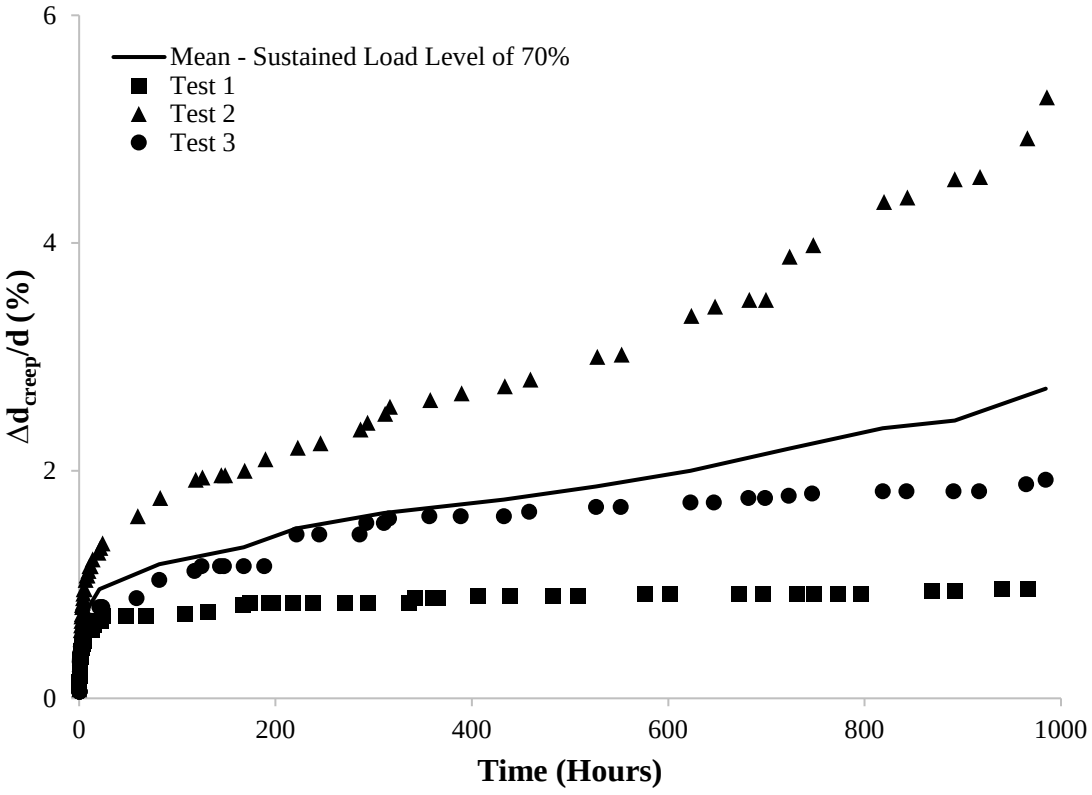

Figure 5.7 Creep test results – creep component of the percent bolt-hole deformation – sustained load level of 70% of mean bearing strength (Case-I - close-fit, laterally unrestrained specimens).

5.4.2 Case-II - Close-fit, Moderately Torqued Specimens

As discussed in Section 4.4.3, a torque value of 5.65 N-m (50 lbf-in) was selected to represent moderate torque for a 6.35 mm (1/4 in) diameter bolt. This torque was applied using a standard torque wrench. The washers used conformed to ASTM F436-11 [53] specifications. These were readily available "loose-fit" washers of the type typically used in construction. The washers had an outer diameter of 2.2*d*, and were used on both sides of the FRP connection as shown in Figure 5.8. Short-term pin-bearing strength tests were conducted and the resultant mean bearing strength used in the investigation was 17.3 kN (3,900 lbf). Test results at specific load levels are discussed in the following sections.

Figure 5.8 Creep test setup – Case-II - close-fit, moderately torqued specimens.

5.4.2.1 Case-II - Sustained Load Level – 70% of Mean Bearing Strength

Five tests were conducted at a sustained stress level of 70% of mean bearing strength. Three tests failed at time durations of 15, 316, and 575 hours, where failure was assumed when bolt-hole deformation reached 50% of the bolt-hole diameter – 3.2 mm (1/8 in). The tests demonstrated that the deformation of the specimen was constrained by the washers in the immediate vicinity of the bearing hole. However, since the material was free to deform laterally outside the washers, noticeable “blooming” of the specimen was observed as shown in Figure 5.9 and Figure 5.10.

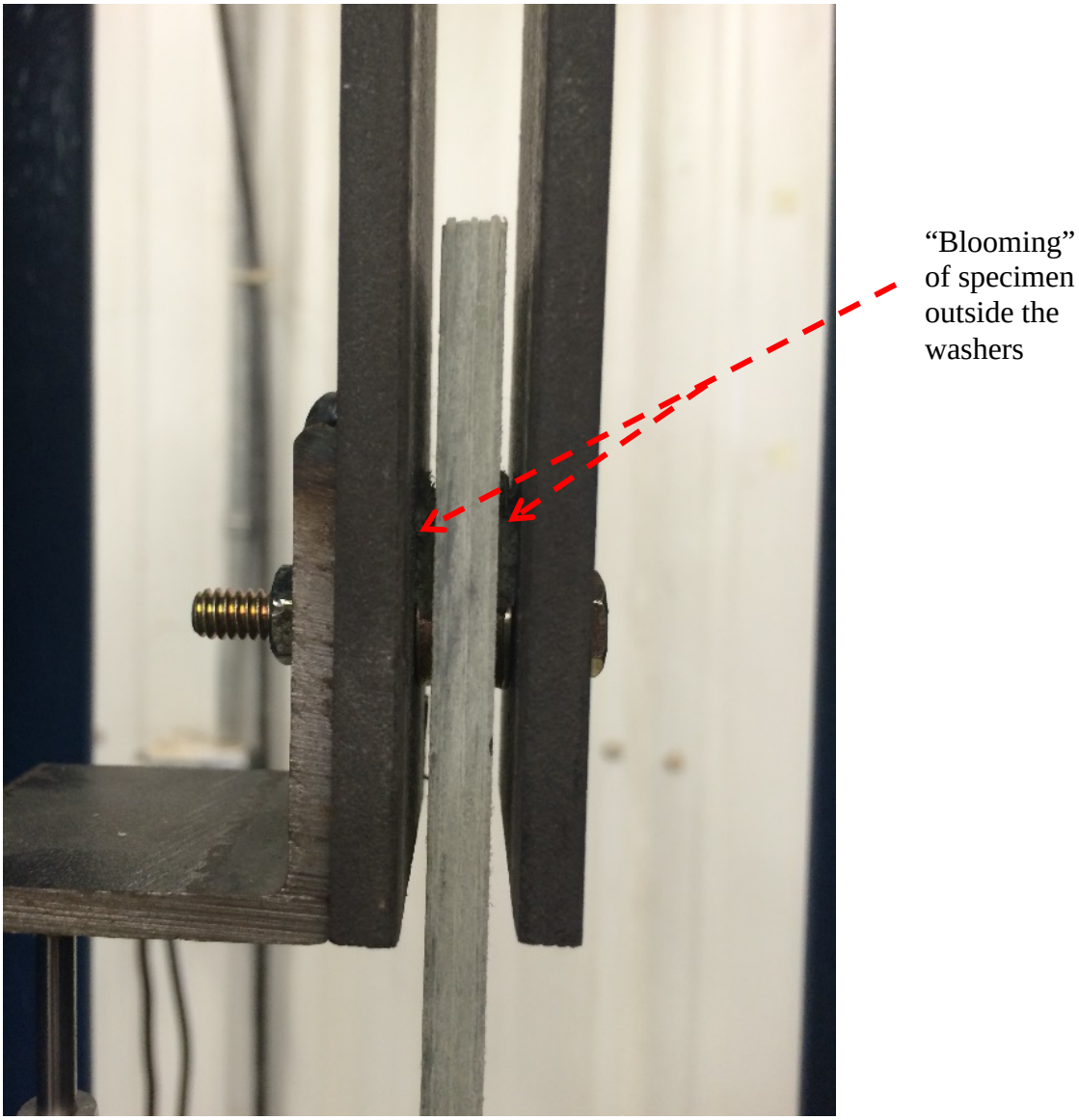

Figure 5.9 Side view of test specimen at failure – sustained load level of 70% of mean bearing strength (Case-II - close-fit, moderately torqued specimens).

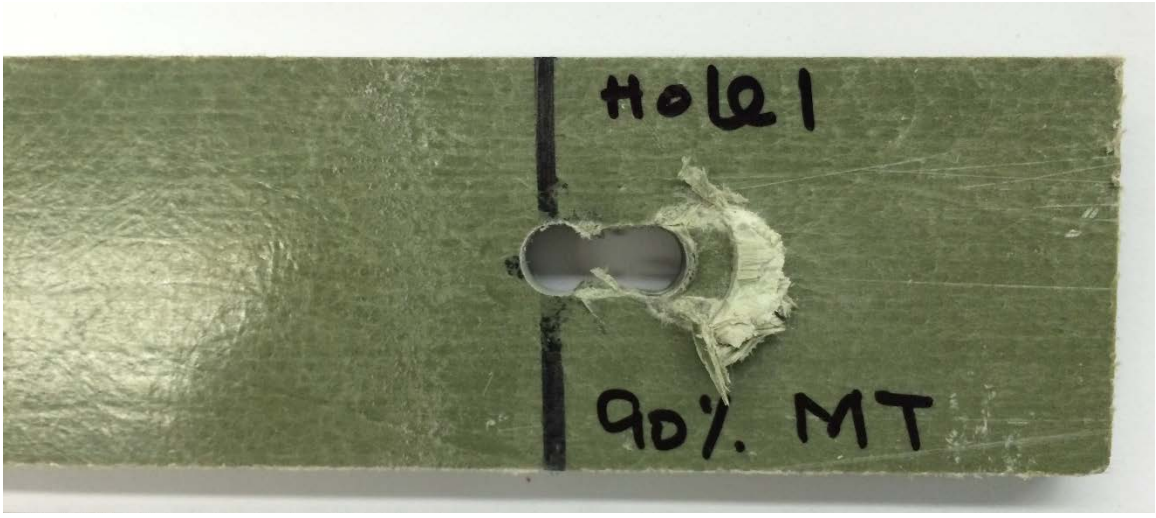

Figure 5.10 Top view of test specimen at failure – sustained load level of 70% of mean bearing strength (Case-II - close-fit, moderately torqued specimens).

At a sustained stress level of 70% of mean bearing strength, two out of five tests did not fail during the duration of the test. The creep component of the percent bolt-hole deformation ($\Delta d_{creep}/d$) for these tests was recorded as 6.96, and 6.88%. The test results are shown in Figure 5.11, expressed as the mean value of the creep component of the percent bolt-hole deformation. Results of individual tests under this category are shown in Appendix B. The results showed that variation in test data is comparatively small when compared to the tests in Case-I (close-fit, laterally unrestrained specimens). This indicates that lateral restraint confines the potential damage area and hence reduces the variation in the test results resulting from a non-uniform distribution of fibers in the vicinity of bolt-hole. Creep deformation increased at a continuously decreasing rate up to 1,000 hours of loading whereas in Case-I, increase in creep deformations remained fairly constant or insignificant after about 400 hours of loading. Also, the observation that three tests failed

prior during the test duration suggests that the beneficial effect of increased bearing strength achieved by providing lateral restraint is lost or reduced significantly under sustained loading. Mottram [55] conducted bolt tension relaxation tests and found that the loss in pretension in pultruded FRP connections is > 40% in 10 years. This will be discussed in more detail in Section 5.6.

5.4.2.2 Case-II - Sustained Load Level – 50% of Mean Bearing Strength

For the tests conducted at a sustained load level of 50% of mean bearing strength, none of the specimens tested failed during the duration of the tests. Visual examination of the bolt holes at the end of test did not show any significant damage to the bearing hole. The results of the tests are shown in Figure 5.11, expressed as the mean value of the creep component of the percent bolt-hole deformation. Results of individual tests are shown in Appendix B. Test results are summarized in Table 5.6, which shows the creep component of the percent bolt-hole deformation ($\Delta d_{creep}/d$). Comparing these test results with the creep tests on specimens with no lateral restraint (Case-I, sustained load level of 50% of mean bearing strength), two observations can be made. First, in contrast to the creep tests on specimens with no lateral restraint the relative variation in the test data is small - similar to what was seen at higher stress levels. Second, deformations at 1,000 hours for this case are in general more than the specimens with no lateral restraint. This observation indicates that due to viscoelastic relaxation, the clamping force provided by lateral restraint relaxes under sustained loads. These results are discussed in detail in Section 5.6.

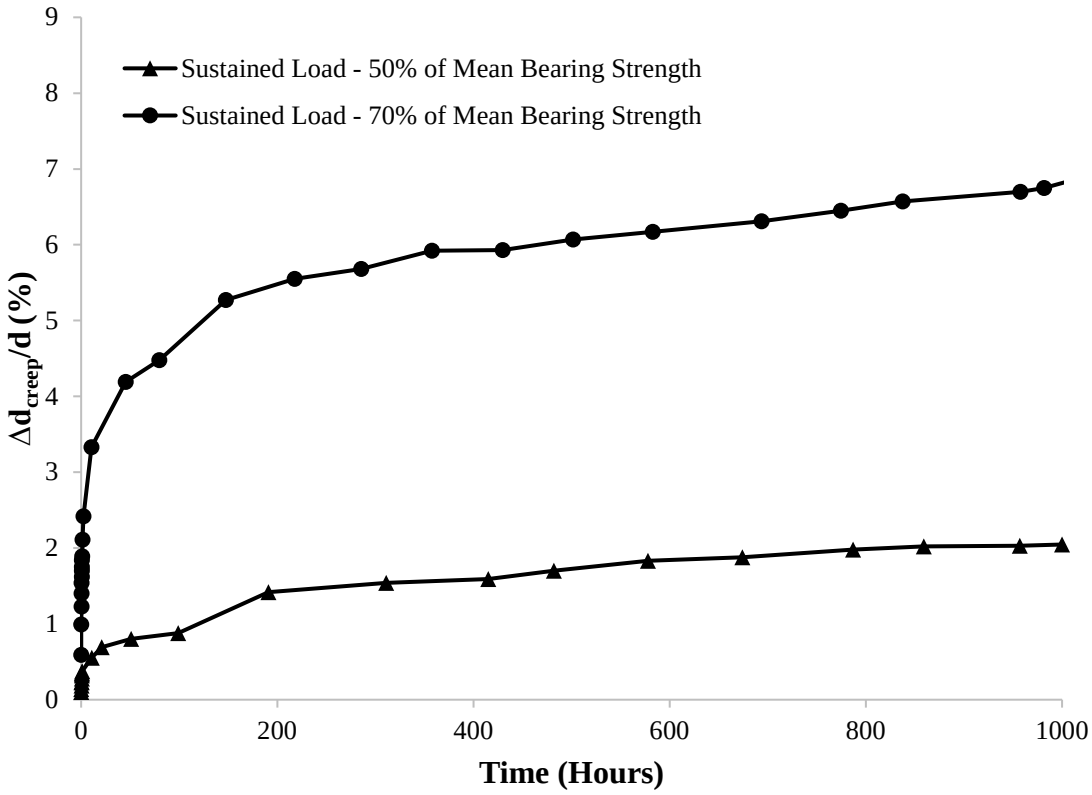

Figure 5.11 Creep test results – mean values of creep component of the percent bolt-hole deformation (Case-II - close-fit, moderately torqued specimens).

Table 5.6 Creep component of the percent bolt-hole elongation at 1,000 hours - Case- II - close-fit, moderately torqued specimens.

Sustained Load Level (50% of Mean)	$\Delta d_{creep}/d$ **(%)**
Test 1	1.46
Test 2	2.10
Test 3	2.00
Test 4	2.24
Test 5	1.88
Test 6	2.60

5.4.3 Case-III - 1.6 mm (1/16 in) Bolt-Hole Clearance, Laterally Unrestrained Specimens

For specimens tested in this configuration, a 1.6 mm (1/16 in) bolt-hole clearance was achieved by drilling the bearing hole using a standard paddle bit. Short-term pin-bearing strength tests resulted in a mean bearing strength of 8.00 kN (1,790 lbf) and served as the basis for the load levels used in this series of time dependent tests. Results at specific load levels are discussed in the following sections.

5.4.3.1 Case-III - Sustained Load Level – 70% of Mean Bearing Strength

Three tests were conducted at a sustained load level of 70% of mean bearing strength. The specimens failed at 12, 12, and 80 minutes. Failure was assumed when bolt-hole deformation reached 50% of the bolt-hole diameter. These test results show that the bolt-hole clearance not only lowers the pin-bearing strength when compared to the close-fit connection, but also significantly affects the creep response. Figure 5.12 shows a representative test specimen at failure. As discussed earlier, the bolt-hole clearance is a practical consideration and is generally taken as 1.6 mm (1/16 in) for constructability [9]. This aspect is missing from the test standards; for instance, ASTM D953-10 [14] specifies a maximum bolt-hole clearance of 0.075 mm (0.003 in) for 6.325 mm (1/4 in) diameter bolts, and ASTM D5961-10 [15] specifies a close-tolerance bearing hole.

Figure 5.12 Creep test specimen at failure – stress level of 70% of mean bearing strength - (Case-III - 1.6 mm (1/16 in) bolt-hole clearance, laterally unrestrained specimens).

5.4.3.2 Case-III - Sustained Load Level – 50% of Mean Bearing Strength

For the creep tests conducted at a sustained load level of 50% of mean bearing strength, none of the tested specimens failed during the duration of the tests. The mean of the creep component of the percent bolt-hole deformation is shown Figure 5.13. Results of individual tests are shown in Appendix B. Results of the creep tests are summarized in Table 5.7. In general, the behavior of connections with 1.6 mm (1/16 in) bolt-hole clearance was similar to that for connections with a close-fit condition under the same load level. Clearly, bearing-hole deformations increase under sustained loading. Also, the variation in the test data is observed to be more in this category when compared to the close-fit

connection subjected to a sustained load level of 50% of mean bearing strength. Kallmeyer and Stephens [37] indicated that bolt-hole clearance could be one of the potential causes of scatter in their creep test results. Also, as discussed earlier in Section 2.4.6, Naik and Crews [30] asserted that bolt-hole clearance significantly influenced the stresses and deformation of the bearing hole under monotonic loading. It can be reasoned that the cause of this variation in the test data might lie in the movement of the bolt in the connection. Contrary to the close-fit connection, the bolt-hole clearance allows relatively more free space. This presence of free space in the connection offers a weak zone and hence presents less resistance to deformation depending upon the specific fiber/matrix composition in the vicinity of bearing hole. This observation, however needs further characterization. In addition, earlier in Section 5.4.2, it was observed that relative variation in the test data for connections with lateral constraints was small compared to the laterally unrestrained connections. These observations may be an indication that variation in the test data, in addition to the lay-up of fibers and lateral constraint, is also significantly affected by bolt-hole clearance.

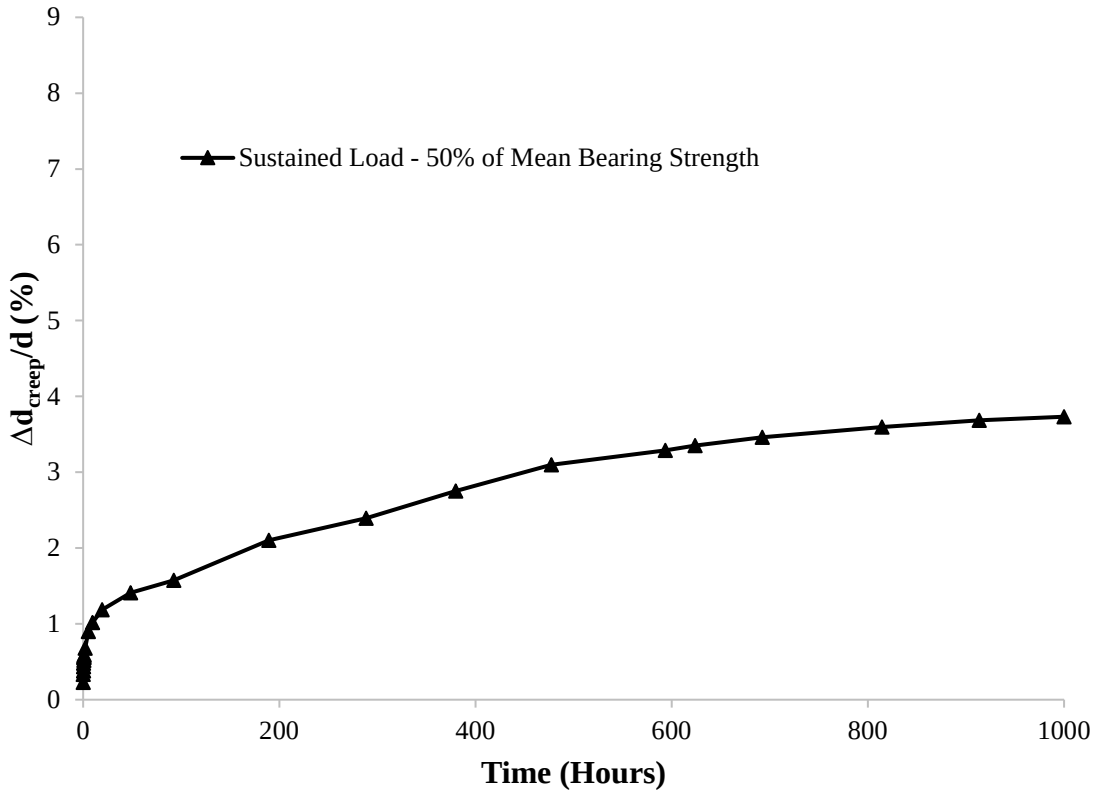

Figure 5.13 Creep test results – mean values of creep component of the percent bolt-hole deformation (Case- III - 1.6 mm (1/16 in) bolt-hole clearance, laterally unrestrained specimens).

Table 5.7 Creep component of the percent bolt-hole elongation at 1,000 hours - Case- III - 1.6 mm (1/16 in) bolt-hole clearance, laterally unrestrained specimens.

Sustained Load Level (50% of Mean)	$\Delta d_{creep}/d$ **(%)**
Test 1	1.56
Test 2	4.10
Test 3	7.08
Test 4	2.30

5.5 Long-Term Tests at Elevated Temperatures

A series of close-fit laterally unrestrained specimens were subjected to sustained loads at elevated temperatures to compare to the time-dependent response under normal laboratory conditions. As was done in the short-term investigation, the connection response under sustained loads was investigated for elevated temperatures of 43.3°C and 60°C (110°F and 140°F). These temperatures were selected based on manufacturer guidelines, previous work, expected service conditions, and reasons discussed in Section 4.2. The tests were conducted in an environmental chamber located in the Structural Engineering and Materials Laboratory (SEML) at the Georgia Institute of Technology. The walk-in temperature and humidity chamber has a temperature range of -35°C to 85°C (-31°F to 185°F). The chamber has a stainless steel interior with 127 mm (5 in) thick Urethane Foam insulation. Temperatures inside the chamber are controlled and monitored through the control panel located outside the chamber. Figure 5.14 shows the lever arm test rigs placed inside the environmental chamber. As with the short-term investigation, a 30-minute soaking period was selected for thermal pre-conditioning of the test specimens. To achieve this, first the temperature inside the chamber was increased to the desired level. Then, the test specimens were placed inside the creep test rigs. Finally, the specimens were loaded after 30 minutes. Results at specific temperatures and specific load levels are discussed in the following sections.

Figure 5.14 Creep test setup – tests under elevated temperatures.

As discussed in Chapter 4, short-term pin-bearing strength tests were conducted at a *d/t* ratio of 1 and temperatures of 43.3°C, and 60°C (110°F, and 140°F). The resultant mean pin-bearing strength values served as the basis for the load levels used in the time-dependent tests. Three tests were conducted at a sustained load level of 70% of mean pin-bearing strength at 43.3°C (110°F). The tests failed at time durations of 15, 27, and 117 hours, where failure was assumed when bolt-hole deformation reached 50% of the bolt-hole diameter. Similarly, all three tests conducted at a sustained load level of 70% of mean

pin-bearing strength at 60°C (140°F) failed at time durations of 5, 165, and 249 hours. The test results also demonstrate a large variation in the response of the connections. As discussed earlier in Sections 5.4.1.2 and 5.4.2.1, the non-uniform lay-up of fibers and absence of lateral restraint can significantly influence the behavior of a connection. Nevertheless, these results clearly highlight the influence of temperature on the behavior of a connection under sustained loading, and must be accounted for in the design of bolted connections. Earlier in Section 5.4.1.2 test results indicated that at a sustained load level of 70% of mean pin-bearing strength none of the specimens failed during the duration of tests at ambient (room) temperature. Also, the sustained load levels representing 70% of mean pin-bearing strength at 43.3°C, and 60°C (110°F, and 140°F) are only 70% and 55% respectively, of the same load level at ambient (room) temperature. The results demonstrate that increases in temperature not only affect the short-term pin-bearing strength, but also significantly influence the behavior of a connection under sustained loading.

Creep tests were also conducted at a sustained load level of 50% of mean pin-bearing strength at 43.3°C, and 60°C (110°F, and 140°F), and none of the tested specimens failed during the duration of testing. The mean of the creep component of the percent bolt-hole deformation is shown in Figure 5.15, and result of each test is shown in Appendix B. Results of the creep tests are summarized in Table 5.8. Comparing these results with the tests conducted at room temperature, presented earlier in Section 5.4.1.2, the results demonstrate that deformation of the single pin-bearing connection increases with increasing in temperature. Increasing the test temperature from ambient to 43.3°C and 60°C (110°F and 140°F) increased the bolt-hole deformation at 1,000 hours by approximately 300% and 900%, respectively.

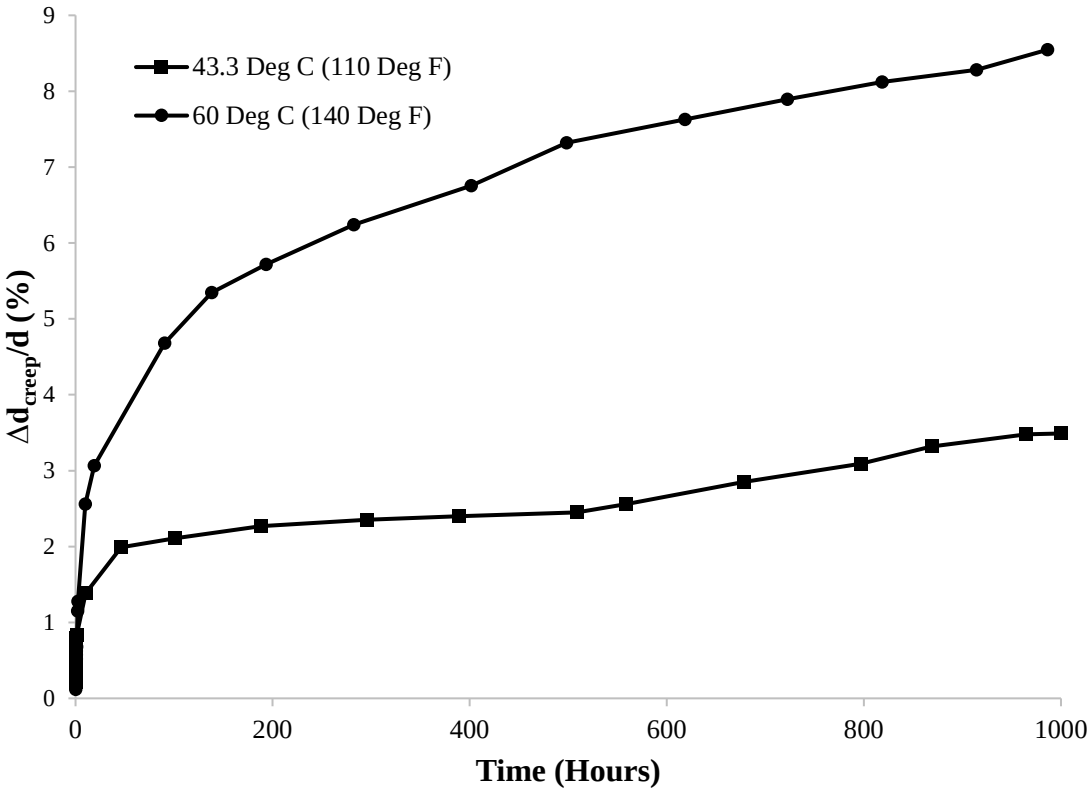

Figure 5.15 Creep test results – mean values of creep component of the percent bolt-hole deformation at sustained load level of 50% of mean bearing strength (elevated temperature tests) - close-fit, laterally unrestrained specimens.

Table 5.8 Creep component of the percent bolt-hole elongation at 1,000 hours and at sustained load level of 50% of mean bearing strength (elevated temperature tests) - close-fit, laterally unrestrained specimens.

Sustained Load Level (50% of Mean)	$\Delta d_{creep}/d$ **(%)**	
	43.3°C (110°F)	**60°C (140°F)**
Test 1	2.40	8.68
Test 2	2.68	8.88
Test 3	5.08	8.20
Test 4	3.80	

5.6 Summary

Creep test results for all the tests are summarized in Table 5.9, which shows the mean value of the creep component of the percent bolt-hole deformation ($\Delta d_{creep}/d$) at 1,000 hours. Figure 5.16 shows the mean value of creep component of the percent bolt-hole deformation at 1,000 hours for a sustained load level of 50% of mean bearing strength. Observations from the creep tests are summarized in the following.

a. For close-fit laterally unrestrained connections, at a sustained load level of 80% of mean pin-bearing strength all the tests failing at a relatively short duration (discussed in Section 5.4.1.1) highlights the importance of considering viscoelastic behavior in the design of FRP materials. The test results demonstrate that although viscoelastic behavior is an important consideration in the design of FRP materials, this behavior becomes more pronounced in FRP bolted connections due to presence of bolt-holes that disrupt continuity of the fibers giving rise to stress concentrations. Also, for a sustained load level of 70% of mean bearing strength, the results demonstrate that the connection failed prior to reaching specified test duration of 1,000 hours in all the cases except for Case-I (close-fit, laterally unrestrained connection).

b. The bolt-hole deformations at 1,000 hours for close-fit moderately torqued connections are in general observed to be more than the specimens with no lateral restraint. For a close-fit moderately torqued connection at a sustained load level of 50% of the mean bearing strength, the bolt-hole deformation at 1,000 hours increased by approximately 140% when compared with a

laterally unrestrained connection. These results show that the beneficial effect of an apparent increase in pin-bearing strength is lost under sustained loading. The fact that FRP composites creep suggests that there will be relaxation in the confining stress that is provided by the lateral restraint.

c. The short-term pin-bearing test results presented in Chapter 4 demonstrated that specimens with a bolt-hole clearance of 1.6 mm (1/16 in) exhibited a lower pin-bearing strength when compared with close-fit connections. The creep test results demonstrate that connections with bolt-hole clearances commonly used in construction demonstrate significantly increased deformation under sustained loading when compared with a close-fit connection. For instance, at a sustained load level of 50% of the mean bearing strength for a connection having 1.6 mm (1/16 in) bolt-hole clearance, the bolt-hole deformation at 1,000 hours increased by approximately 340% when compared with a close-fit connection. The reason for increased bolt-hole deformation under sustained loading may lie in the weak zone occurring as a result of bolt-hole clearance. The presence of bolt-hole clearance results in reduced contact area between the bolt and the bolt-hole when compared with a close-fit connection [5,30]. This leads to higher compressive stresses at the contact interface resulting in reduced bearing capacity and more deformation under sustained loads. The test standards such as ASTM D953-10 [14] and ASTM D5961-10 [15] do not include specifications for 1.6 mm (1/16 in) bolt-hole clearance which is a practical consideration, although tests have shown that bolt-hole clearance

significantly influences both the short- and long-term response of a connection.

d. As would be expected, both short- and long-term test results demonstrated that FRP composite materials behave differently under elevated temperatures. At a sustained load level of 50% of the mean bearing strength the bolt-hole deformation at 1,000 hours increased by approximately 300% and 900% when the test temperature was increased from ambient to 43.3 and 60°C (110 and 140°F) respectively. It can be reasoned that at elevated temperatures the rate of creep of fibers increases and the ability of matrix to transfer loads reduces, thus causing increased deformation.

e. One other observation from the creep tests is the variation in the test data. The non-uniform lay-up of fiber/matrix composition in the vicinity of the bearing hole contributes towards this variation which increases when there is bolt-hole clearance and when the temperature increases. The lateral restraint confines the potential damage area and hence the relative variation in the test data is reduced.

Table 5.9 Creep test results – mean values of creep component of the percent bolt-hole deformation ($\Delta d_{creep}/d$) at 1,000 hours.

Sustained Load Level (% of Mean)	**($\Delta d_{creep}/d$) (%)**			
	Case-I		**Case-II**	**Case-III**
	No Lateral Restraint **Close-fit**		**Moderate Torque** **Close-fit**	**No Lateral Restraint** **1.6 mm (1/16 in) Clearance**
Creep Tests at Ambient (Room) Temperature				
50%	0.85		2.05	3.73
65%	1.37		-	-
70%	2.78		Failed	Failed
80%	Failed		-	-
Creep Tests at Elevated Service Temperatures				
	Temperature			
	43.3°C (110°F)	60°C (140°F)		
50%	3.49	8.59	-	-
70%	Failed	Failed	-	-

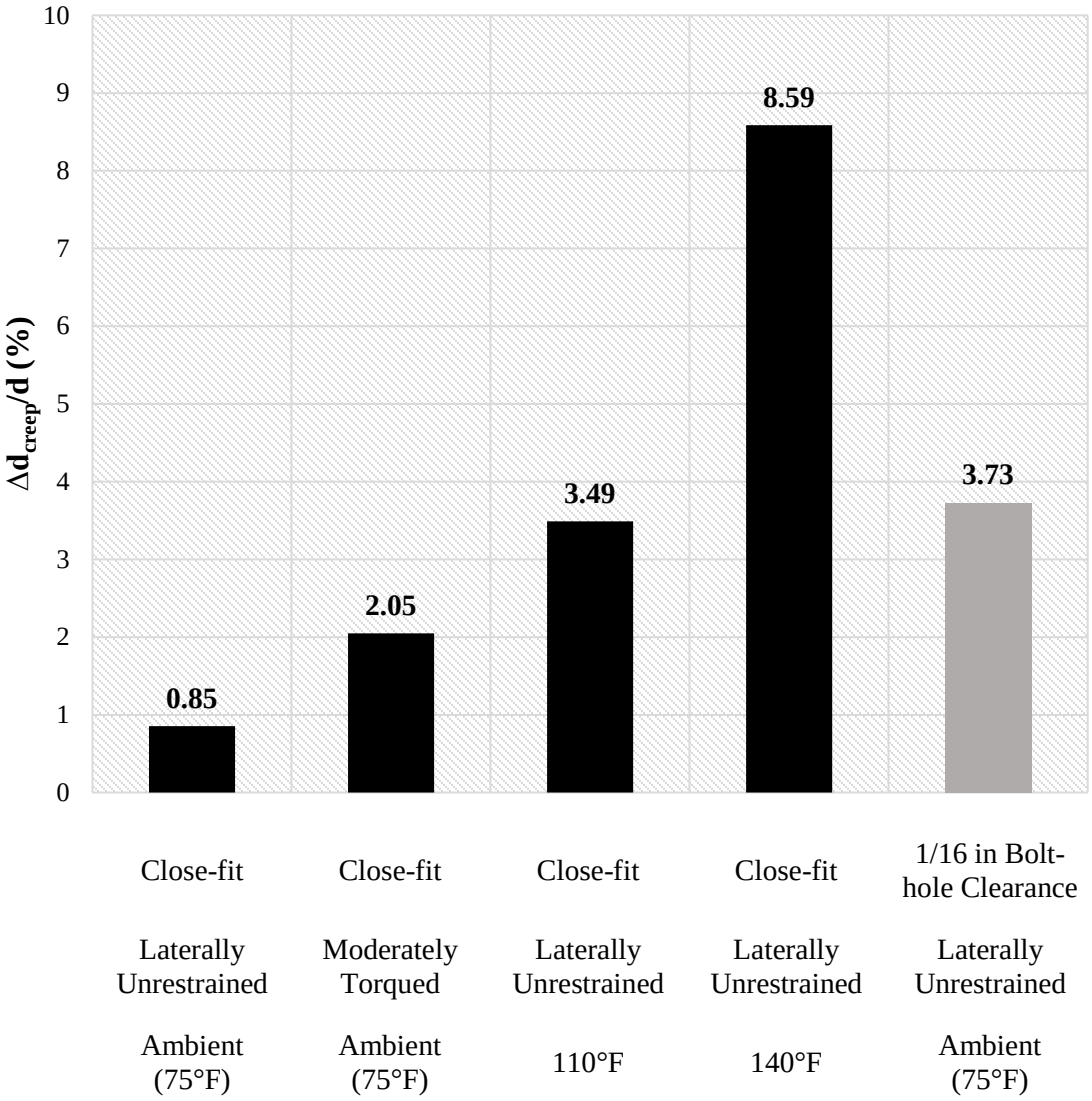

Figure 5.16 Mean value of creep component of the percent bolt-hole deformation at 1,000 hours – sustained load level of 50% of mean bearing strength.

5.7 Conclusions

The behavior of single pin-bearing connections under constant sustained loads was investigated at a *d/t* ratio of 1 for various load levels, specific bolt-hole clearances and specific bolt tightening torques at normal and elevated service temperatures. The following conclusions can be drawn from this parametric investigation.

a. The viscoelastic behavior of FRP materials does influence the behavior of bolted connections under sustained loading and hence must be accounted for in design criteria. This viscoelastic behavior becomes more pronounced with increases in relative stress level.

b. Comparing test results of Case-I and Case-II, it is observed that the perceived increased bearing strength achieved by providing lateral restraint is lost or reduced significantly under sustained loading. Therefore, pin-bearing strength in the design of bolted connections should always be computed when there is no lateral restraint in the connection. This aspect must be included in the test standards and any design criteria.

c. Bolt-hole clearance not only influences the short-term pin-bearing strength, but also significantly affects the response under sustained loading. A provision of bolt-hole clearance is a practical design consideration and must be included in the test standards. The design of bolted connections should also include the effect of bolt-hole clearance in computing the strength of a connection.

d. Similarly, elevated service temperatures significantly influence both the short- and long-term response of a connection in pultruded FRP materials.

e. The test results indicate that the absolute value of pin-bearing strength after incorporating all the factors should always be less than 70% of mean pin-bearing strength.

CHAPTER 6

DEVELOPMENT OF PREDICTIVE MODELS FOR THE TIME-DEPENDENT BEHAVIOR OF PIN-BEARING CONNECTIONS

6.1 Statistical Analysis of Material Properties

In the design of bolted connections, the capacity of a connection is computed based on characteristic strength instead of mean strength. Therefore, before developing a suitable predictive model, it is necessary to characterize the properties of the material used in this research. Zureick et al. [56] presented a detailed comparison of different probability distribution functions for characterization of FRP material properties. To characterize the engineering properties of FRP composite materials, the authors examined three probability distribution functions; Weibull, lognormal, and normal distributions. Alqam et al. [57] compared the two- and three-parameter Weibull distribution and showed that although three-parameter Weibull distribution is more robust, the third (location) parameter does not improve the characterization of the data in FRP composite materials. Therefore, Zureick et al. [56] examined two-parameter rather than three-parameter Weibull distribution. The authors recommended a two-parameter Weibull probability distribution for modeling both strength and stiffness properties of the FRP. Also, the 5th-percentile value is recommended for determining the FRP properties being consistent with many other civil engineering applications. Owing to the small sample size of typical data samples, this value is recommended to be reduced by incorporating a data confidence factor which yields an 80^{th} percent lower confidence level of the 5th-percentile value of the test data.

In order to compute characteristic properties in the present investigation, two different approaches were considered. One approach followed the procedure given in ASTM D7290-11 [58] which assumes a two-parameter Weibull probability distribution. The second approach followed guidance given in Annex D7 to Eurocode 0 [26], which assumes a Gaussian distribution. In ASTM D7290-11, the characteristic value is defined as a statistically-based material property representing the 80% lower confidence bound on the 5th-percentile value of a specified population. The expression for two-parameter Weibull probability distribution is shown in Equation (6.1) [56,58].

$$f(x;\alpha,\beta) = \left(\frac{\beta}{\alpha}\right)\left(\frac{x}{\alpha}\right)^{\beta-1} exp\left[-\left(\frac{x}{\alpha}\right)^{\beta}\right] \tag{6.1}$$

where

β = dispersion (or shape) parameter

α = characteristic extreme (scale) parameter

The nominal value of the test data is then computed as the 5th-percentile of the two-parameter Weibull distribution. To account for statistical uncertainties due to the small sample size, the nominal value is multiplied by a data confidence factor (Ω) to obtain the characteristic value. For an 80% confidence level of the 5th-percentile, values of Ω are specified for various sample sizes and coefficient of variation (COV). Values of Ω are given for a smallest sample size of 10.

On the other hand, in the procedure set forth in the Eurocode [26], characteristic properties are determined assuming a Gaussian distribution. The characteristic value ($X_{k(n)}$) is determined as shown in Equation (6.2).

$$X_{k(n)} = m_X\,(1 - k_n V_X) \tag{6.2}$$

where

m_X = mean of the *n* sample results

k_n = characteristic fractile factor

V_X = coefficient of variation of *X*

Based on normal distribution, values of k_n for the 5% characteristic value are specified in Table D1 of the Eurocode and are reproduced here in Table 6.1.

Table 6.1 Values of k_n for the 5% characteristic value (after [26]).

n	1	2	3	4	5	6	8	10	20	30	∞
V_X known	2.31	2.01	1.89	1.83	1.80	1.77	1.74	1.72	1.68	1.67	1.64
V_X unknown	-	-	3.37	2.63	2.33	2.18	2.00	1.92	1.76	1.73	1.64

Selected test results were examined to evaluate both procedures and it was found that each gave a similar estimate of the characteristic values. Table 6.2 shows the comparison of the two procedures. However, unlike ASTM D7290-11, the Eurocode approach is not sensitive to any outliers in the data. Detection of outliers may be important because FRP is inhomogeneous at a microscopic level; the pin-bearing response of FRP materials is highly dependent on the lay-up of fibers in the vicinity of drilled holes. This

results in a greater variation in test results compared to similar tests on a homogeneous material like steel. Hence, the Weibull distribution was assumed for the population and characteristic strengths were computed in accordance with ASTM D7290-11. As discussed earlier, values of data confidence factor (Ω) are given in ASTM 7290-11 with 10 being the smallest sample size to be considered. Also, the variation in the properties of FRP materials is generally between 5 to 15%. Therefore, a minimum of 10 short-term material property tests were conducted for each investigation in this research. Figure 6.1 shows the cumulative distribution function of the test data, which for the Weibull distribution is given by Equation (6.3).

$$F(x;\alpha,\beta) = 1 - exp\left[-\left(\frac{x}{\alpha}\right)^{\beta}\right] \tag{6.3}$$

Table 6.2 Comparison of characteristic pin-bearing strength values computed using ASTM D7290-11 and Eurocode approaches – close-fit, laterally unrestrained specimen tests.

***d/t* ratio**	***d/t* = 1**	***d/t* = 1.5**	***d/t* = 2**
Mean strength (MPa)	354	313	257
Standard Deviation (MPa)	22.3	21.4	25.6
Characteristic strength (MPa)			
ASTM D7290-11 approach	299	248	199
Eurocode approach	311	272	208

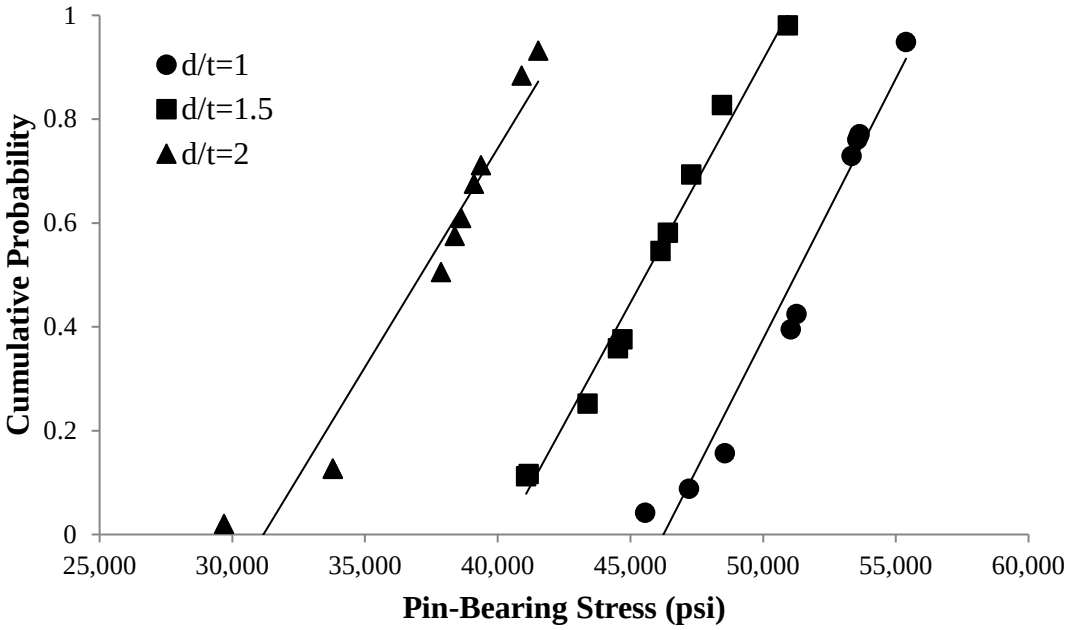

Figure 6.1 Cumulative distribution function (CDF) – Weibull distribution (close-fit, laterally unrestrained specimen tests).

Table 6.3 and Table 6.4 show the characteristic strengths for the short-term pin-bearing strength investigation evaluated in accordance with ASTM D7290-11. Similarly, for creep tests Table 6.5 shows the sustained load level expressed as percentage of mean and as an equivalent percentage of characteristic strength. The table for instance shows that a sustained load level representing 80% of mean strength is approximately the same as 100% of characteristic strength.

Table 6.3 Short-term pin-bearing test results - ambient (room) temperature (24°C (75°F)).

***d/t* ratio**	**Bearing Strength**					
	Mean		**Minimum**		**Characteristic**	
	MPa	**psi**	**MPa**	**psi**	**MPa**	**psi**
Close-fit, Laterally Unrestrained						
1	354	51,310	314	45,560	299	43,320
1.5	313	45,410	283	41,070	248	36,020
2	257	37,300	205	29,690	199	28,910
Close-fit, Moderate Torque						
1	430	62,340	396	57,460	333	48,270
1.5	482	69,870	459	66,600	427	61,880
2	442	64,050	417	60,520	400	58,080
1.6 mm (1/16 in) Bolt-hole Clearance, Laterally Unrestrained						
1	198	28,650	184	26,630	164	23,790
1.5	185	26,890	163	23,700	140	20,330
2	175	25,320	153	22,230	141	20,490
1.6 mm (1/16 in) Bolt-hole Clearance, Moderate Torque						
1	447	64,880	421	61,030	383	55,550
1.5	385	55,840	356	51,640	331	47,950
2	386	56,040	354	51,380	327	47,400

Table 6.4 Short-term pin-bearing test results – elevated temperatures.

Temperature	Bearing Strength					
	Mean		Minimum		Characteristic	
	MPa	psi	MPa	psi	MPa	psi
Close-fit, Laterally Unrestrained, *d/t* ratio of 1						
Ambient 24°C (75°F)	263	38,120	220	31,870	206	29,870
43.3°C (110°F)	177	25,690	165	23,960	146	21,150
60°C (140°F)	147	21,270	130	18,860	112	16,310

Table 6.5 Sustained load levels expressed as percentage of reference strength.

Reference Strength	Sustained Load Level			
% of Mean	50	65	70	80
% of Characteristic	60	80	90	100

6.2 Models for Long-Term Behavior

There are a number of models available in the literature to predict the long-term performance of FRP composite materials. At the microscopic level, De Silva [59] presented a detailed theoretical analysis of creep in FRP composites based on phenomenological parameters of the individual components. The paper describes three processes governing creep of FRP composites. First, relaxation of shear stresses at the fiber ends causing load redistribution; second, stress relaxation of the matrix causing load transfer to the fibers and third, the creep of fibers. Scott et al. [60] published a detailed review of the various models pertaining to time-dependent response of FRP materials. Similarly, Lee [61] presented a detailed account of creep and the time-dependent response of FRP composites. Based on work done by previous researchers, the following models are evaluated for their suitability to accurately predict the long-term performance of pin-bearing connections for the material used in this investigation.

6.2.1 Findley's Power Law Model

The time-dependent response of the material can be modeled using the power law developed by Findley [62]. Scott and Zureick [63] used the same model in their study on a similar pultruded FRP material and found it to provide a reasonable approximation for creep deformation for the material loaded in uniaxial compression. The relatively low fiber volume fraction of the material in the present study supports the assumption that creep deformation would be primarily matrix driven; hence the Findley power law can be applied. In the simplest form the Findley power law can be written as shown in Equation (6.4):

$$\varepsilon\,(\mathrm{t}) = \varepsilon_i + mt^n \tag{6.4}$$

where

$\varepsilon\,(\mathrm{t})$	=	total time-dependent strain
ε_i	=	stress-dependent initial elastic strain
m	=	stress-dependent and temperature-dependent coefficient
n	=	stress-independent and temperature-independent material constant
t	=	time after loading

The evaluation of empirical constants needed to formulate the power law may be found from the experimental creep data. Rearranging Equation (6.4) and taking the log of both sides results in Equation (6.5):

$$log[\varepsilon\,(\mathrm{t}) - \varepsilon_o] = logm + nlogt \tag{6.5}$$

Plotting Equation (6.5) on logarithmic scales yields a straight line. The intercept at 1-hour duration represents the value of *m* and the slope of the straight line yields *n*. To apply this model to the present study, the relative bolt-hole deformation is expressed as shown in Equation (6.6). Based on this model, the percent hole deformation can be estimated for a given service life.

$$log\left[\frac{\Delta d\ (t)}{d} - \frac{\Delta d_i}{d}\right] = logm + nlogt \tag{6.6}$$

Figure 6.2 shows the creep data plotted on a logarithmic scale for the close-fit, laterally unrestrained specimens under a sustained load level of 70% of mean pin-bearing strength. The resultant values of constants *m* and *n* are shown in Table 6.6. Experimental

creep data and the approximation using Findley's model is shown in Figure 6.3, expressed as creep component of the percent bolt-hole deformation ($\Delta d_{creep}/d$) (explained in Section 5.4.1.2).

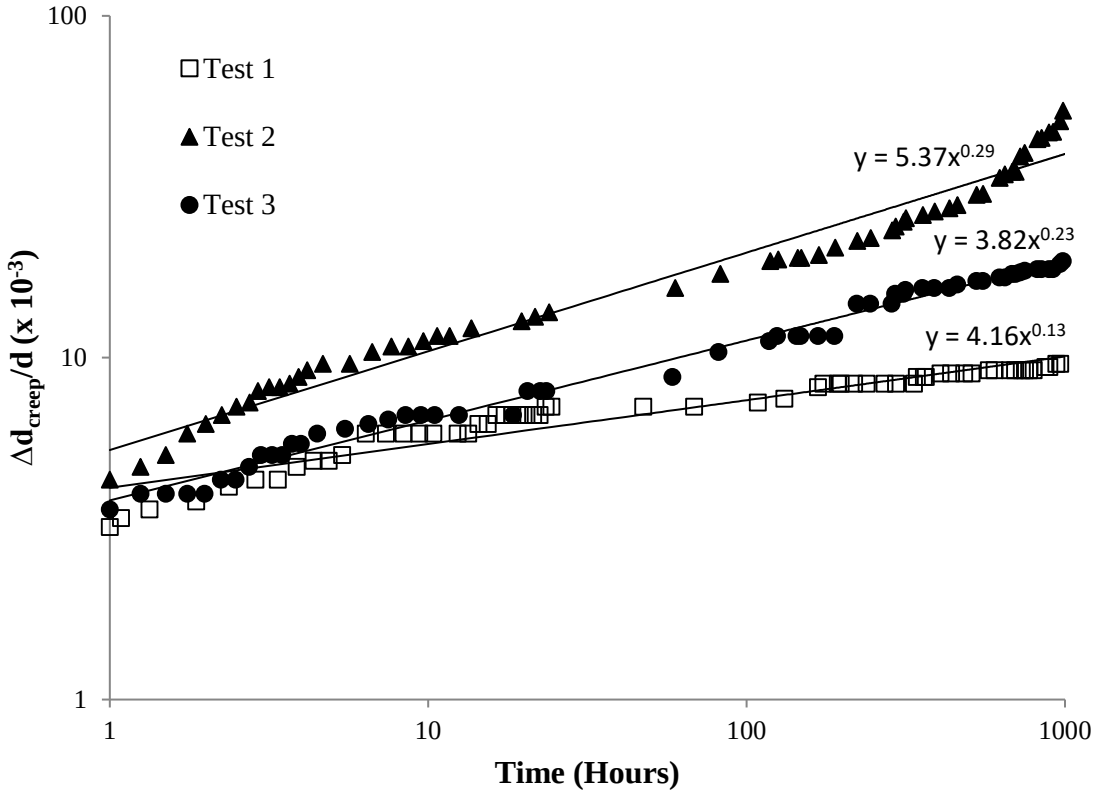

Figure 6.2 Evaluation of constants *m* and *n* - stress level of 70% of mean pin-bearing strength (close-fit, laterally unrestrained specimens).

Table 6.6 Creep constants *m* and *n* - stress level of 70% of mean pin-bearing strength (close-fit, laterally unrestrained specimens).

Test	***m*** **(Δd/d x 10^{-3})**	***n***
Test 1	4.16	0.13
Test 2	5.37	0.29
Test 3	3.82	0.23
Average	**4.45**	**0.22**

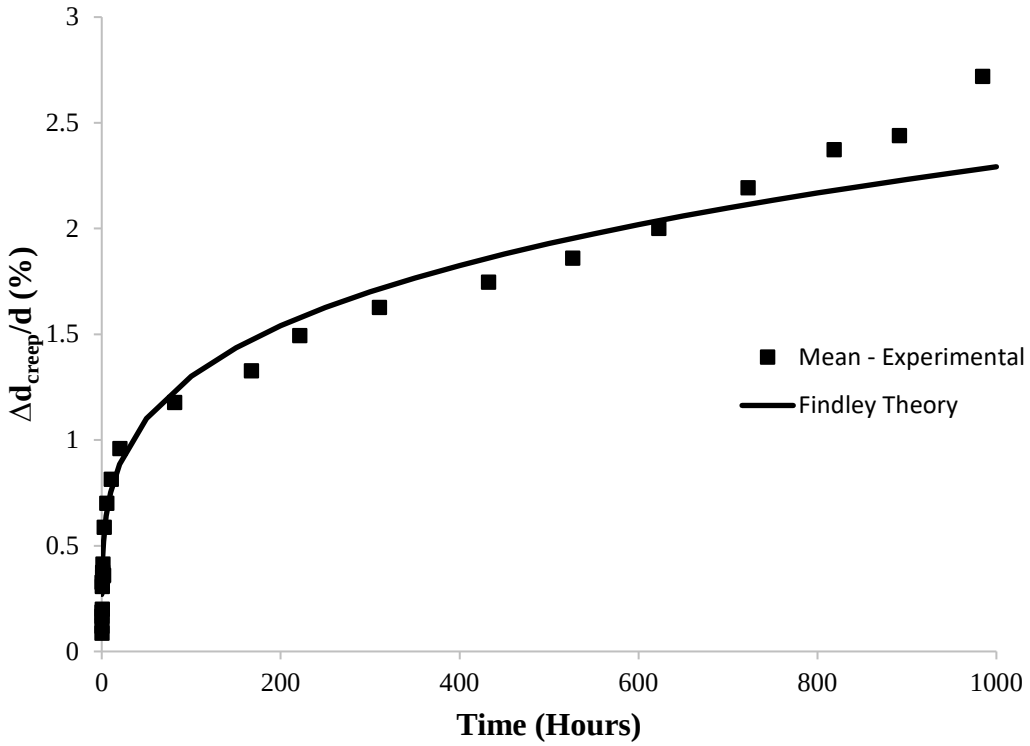

Figure 6.3 Experimental creep data and Findley's model - stress level of 70% of mean pin-bearing strength (close-fit, laterally unrestrained specimens).

6.2.2 General Power Law Model

Kallmeyer and Stephens [37] investigated the creep response of FRP laminates subjected to bolt-bearing loads at ambient and elevated temperatures. The authors proposed an empirical expression to model the connection creep rate as a function of time and applied bearing stress. In the study, the creep strain rate is assumed to be represented by Equation (6.7):

$$\dot{\varepsilon}_c = A\sigma^p t^q \tag{6.7}$$

where

$\dot{\varepsilon}_c$ = creep strain rate

$A, p \text{ and } q$ = constants that are functions of temperature

The rate of percent hole elongation is assumed to be related to normalized bearing stress and time by the relationship given in Equation (6.8):

$$\left(\frac{\Delta \dot{d_{creep}}}{d}\right) = A\left(\frac{\sigma_b}{\sigma_{bu}}\right)^p t^q \tag{6.8}$$

where

$\frac{\Delta \dot{d_{creep}}}{d}$ = rate of creep component of percent hole elongation

σ_b = applied bearing stress, MPa (ksi)

σ_{bu} = maximum bearing stress, MPa (ksi)

$A, p \text{ and } q$ = constants (function of temperature and bolt torque)

Based on the creep test results and the relationship given in Equation (6.9),

$$\frac{d}{dt} log_{10}\, t = \frac{1}{t \ln 10} = 0.4343\, t^{-1} \tag{6.9}$$

the authors' assumed the value of $q = -1$, independent of temperature and bolt torque. The logarithmic rate of percent hole elongation was measured at each temperature, bearing stress and clampup torque, then plotted against the normalized bearing stress and fit with power law expression given in Equation (6.10):

$$\frac{d\left(\Delta d_{creep}/d\right)}{d(\log t)} = A'\left(\frac{\sigma_b}{\sigma_{bu}}\right)^{p'} \tag{6.10}$$

where

$\Delta d_{creep}/d$ = creep component of percent hole elongation

Based on the comparison between the experimental results and proposed model, the authors' asserted that the proposed power law is a reasonable approximation for predicting the creep response of bolted laminate connections. For the present investigation, test results of close-fit, laterally unrestrained specimens were modeled using this approach. Figure 6.4 and Table 6.7 show the relationship between logarithmic rate of percent hole-elongation and normalized bearing strength for the case of close-fit, laterally unrestrained specimens.

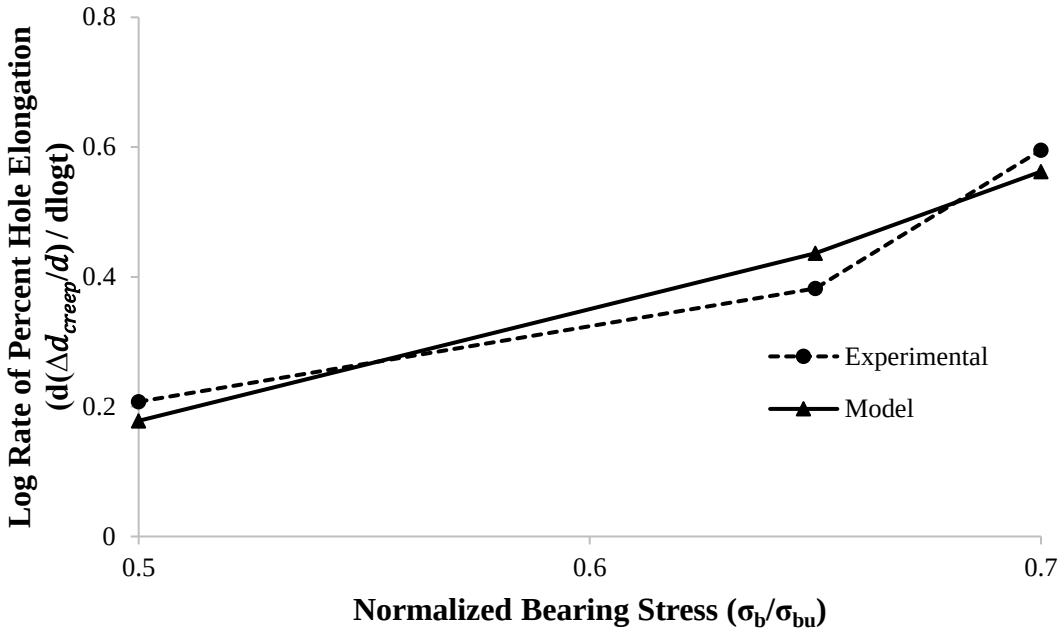

Figure 6.4 Experimental creep data and General Power Law model - close-fit, laterally unrestrained specimens.

Table 6.7 Experimental creep data and General Power Law model - close-fit, laterally unrestrained specimens.

$\frac{\sigma_b}{\sigma_{bu}}$	$\frac{d(\Delta d_{creep}/d)}{d(\log t)}$	
	Experimental	**Model**
0.50	0.21	0.18
0.65	0.38	0.44
0.70	0.60	0.56

$A = 0.83, p = 3.41, q = -1$

Based on this model, the percent-hole elongation can now be approximated at any time duration. Computation of the percent-hole elongation at 1,000 hours for sustained load level of 70% of mean pin-bearing strength is shown below. Figure 6.5 shows the experimental creep data and the approximation using the General Power Law model.

$$\left(\frac{\Delta \dot{d_{creep}}}{d}\right) = 0.83\ (0.9)^{3.41} t^{-1} \tag{6.11}$$

$$\left(\frac{\Delta \dot{d_{creep}}}{d}\right) = \frac{0.244}{t} \tag{6.12}$$

$$\frac{\Delta d_{creep}}{d} = \int_{0.1}^{1000} \frac{0.244}{t} dt = 2.25 \tag{6.13}$$

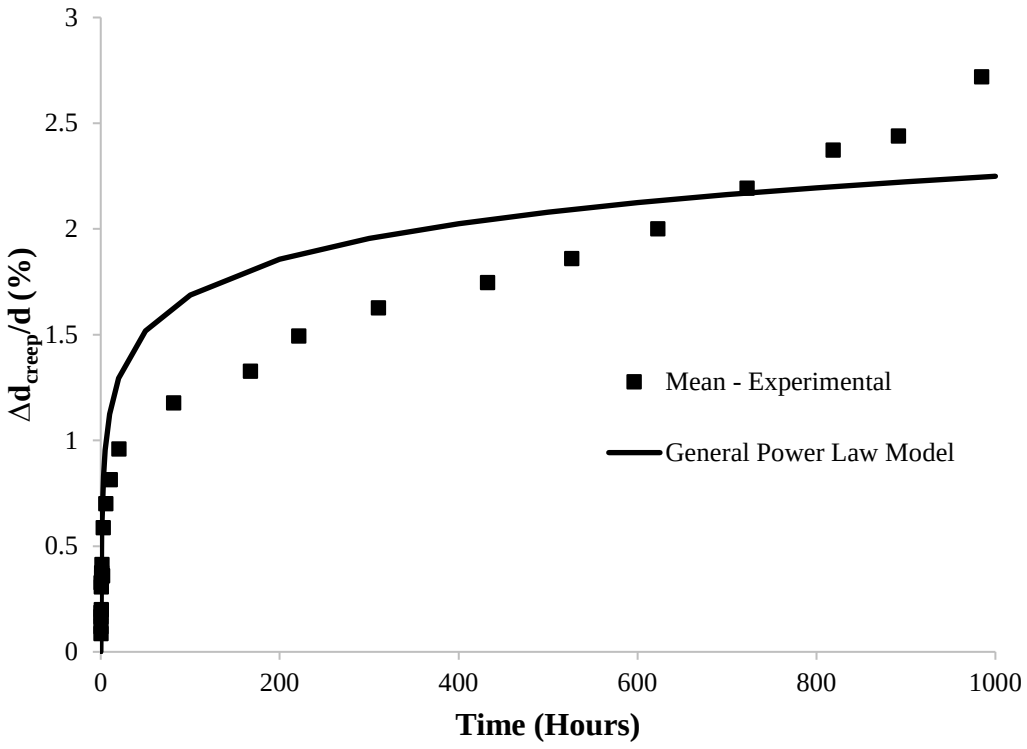

Figure 6.5 Experimental creep data and General Power Law model - stress level of 70% of mean pin-bearing strength (close-fit, laterally unrestrained specimens).

6.2.3 Comparison of Models

In Findley's model, the approach treats each experiment separately and yields an independent curve for each test. On the contrary, in the General Power Law model, the data needs to be averaged before finding the creep constants. Figure 6.6 shows the comparison of experimental and modeling results at 1,000 hours of loading at a sustained load level of 70% of short-term mean pin-bearing strength. The results demonstrate that both the models provide a reasonable approximation for computing creep deformation of the pin-bearing bolted connection for the pultruded FRP used in this investigation. However, from Figure 6.3 and Figure 6.5 it is observed that Findley theory more closely follows the experimental data when compared with General Power Law model. For consistency, all the remaining tests were modeled using the Findley approach as presented in the following section.

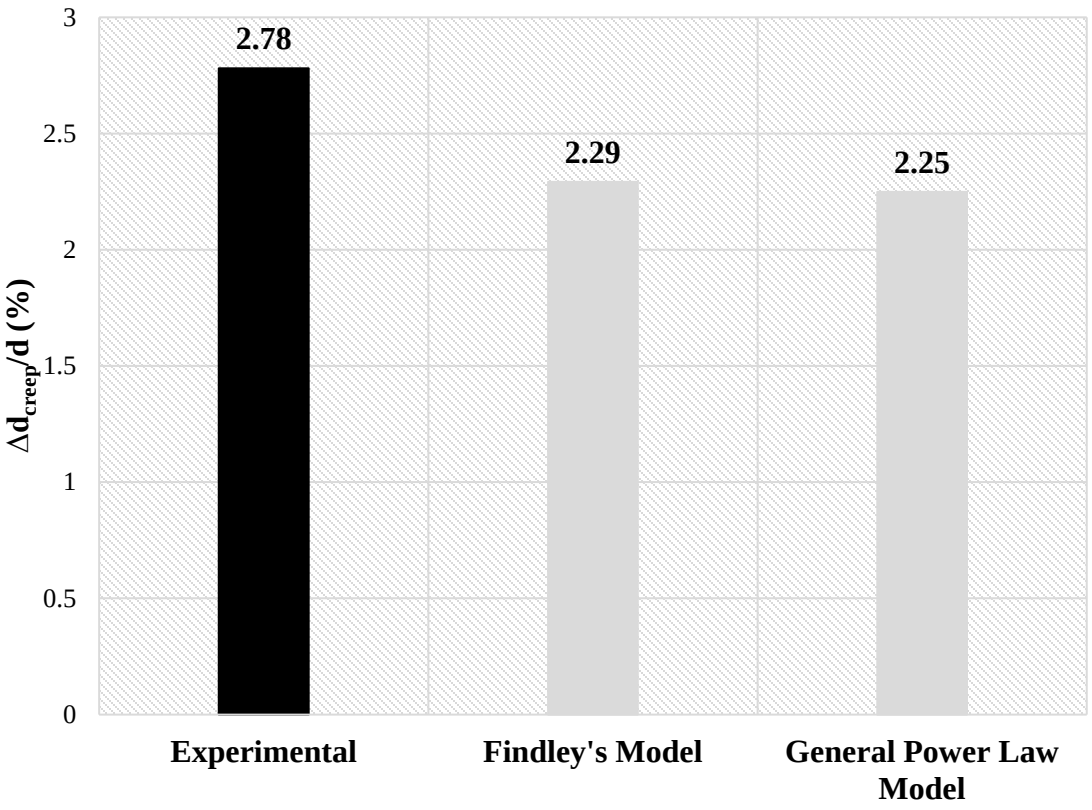

Figure 6.6 Creep component of the percent bolt-hole deformation at 1,000 hours - stress level of 70% of mean pin-bearing strength (close-fit, laterally unrestrained specimens).

6.2.4 Modeling Long-Term Behavior Using Findley's Power Law

The experimental creep data was modeled using the Findley power law as described in Section 6.2.1. The mean value of creep component of the percent bolt-hole deformation ($\Delta d_{creep}/d$) and predictive mean creep curves formulated using Findley's Power Law model are shown in Figure 6.7 to Figure 6.10. The results of individual tests and approximation using Findley theory are tabulated and shown in Appendix C.

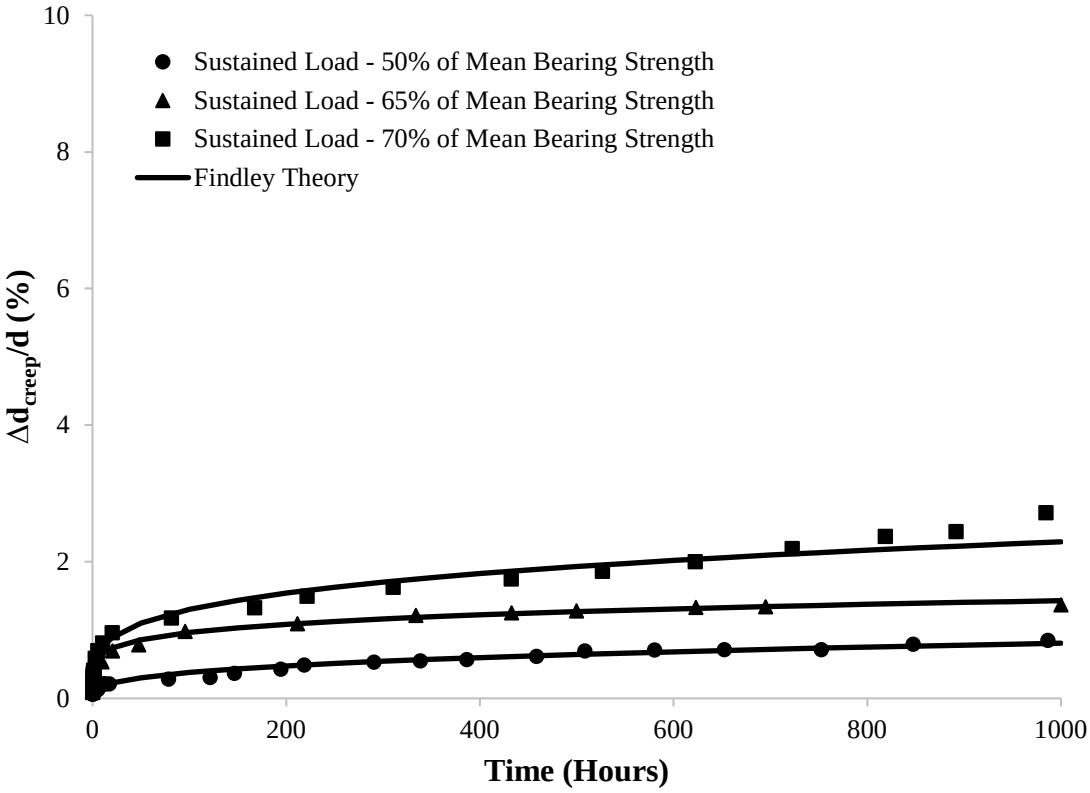

Figure 6.7 Creep component of the percent bolt-hole deformation - close-fit, laterally unrestrained specimens.

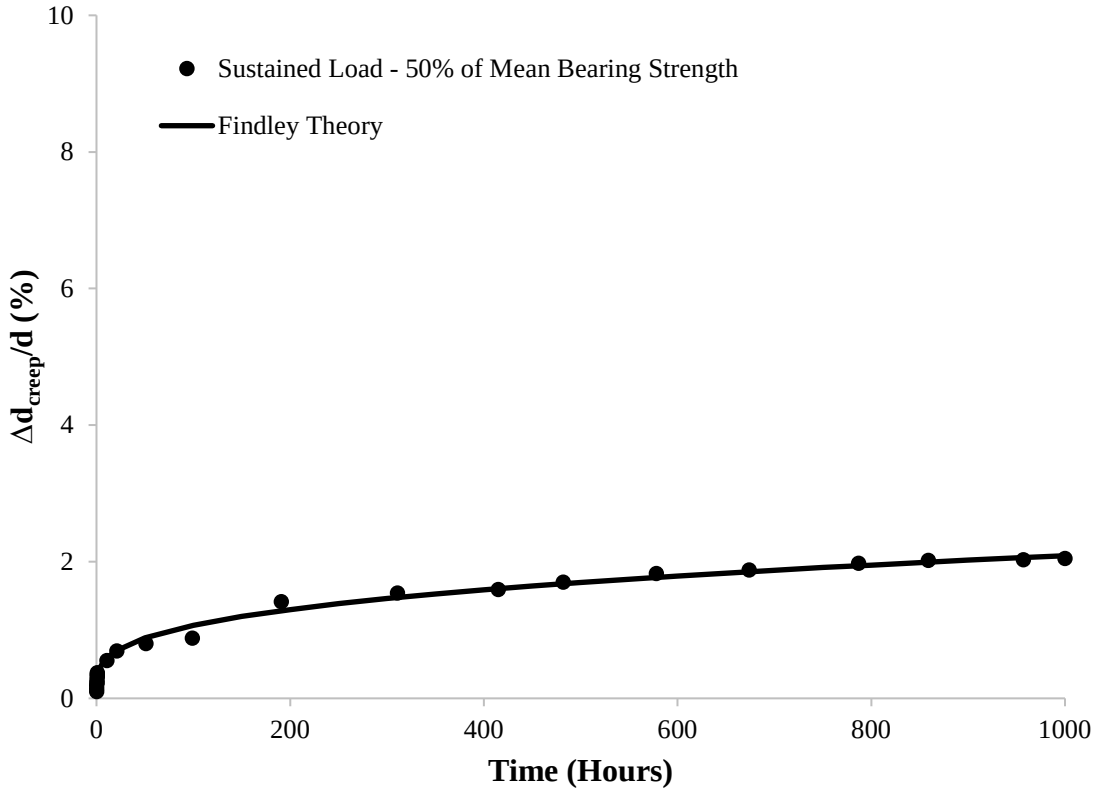

Figure 6.8 Creep component of the percent bolt-hole deformation - close-fit, moderately torqued specimens.

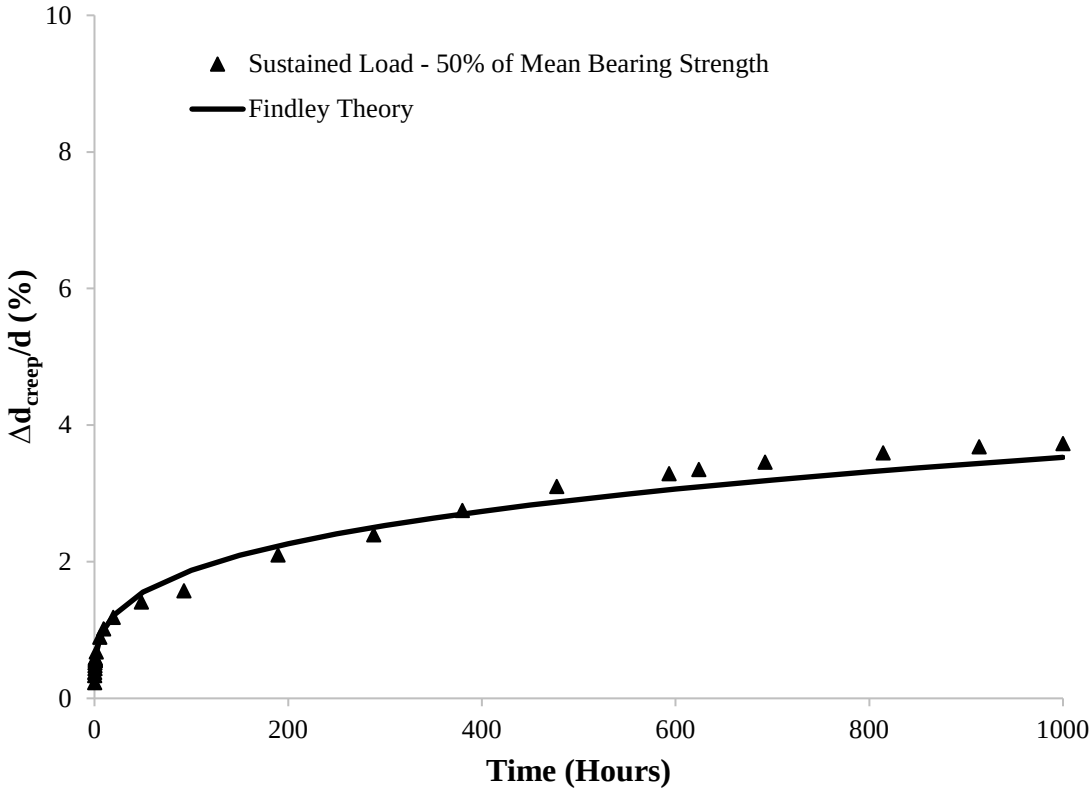

Figure 6.9 Creep component of the percent bolt-hole deformation - 1.6 mm (1/16 in) bolt-hole clearance, laterally unrestrained specimens.

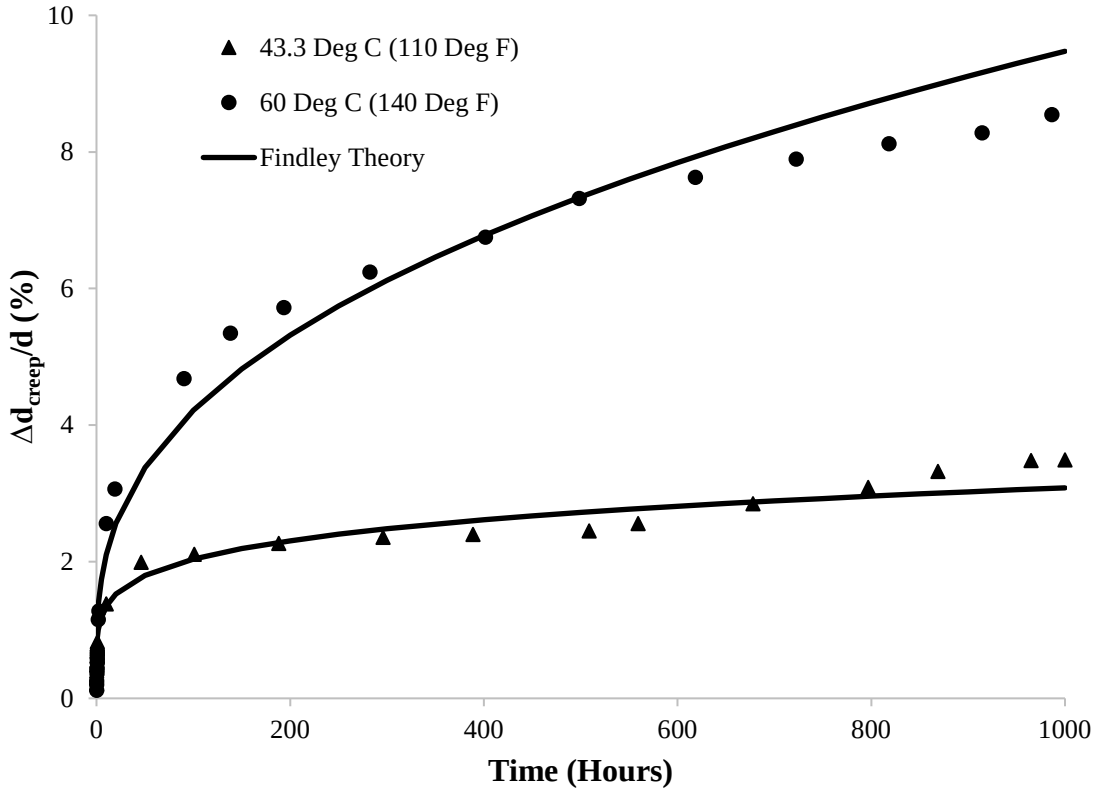

Figure 6.10 Creep component of the percent bolt-hole deformation – sustained load level of 50% of mean bearing strength for close-fit, laterally unrestrained tests at elevated temperatures.

6.3 Development of Predictive Model for the Time-Dependent Behavior of Pin-Bearing Connections

6.3.1 Background

In the design procedures developed for wood using a serviceability limit state, EN 1995-1-1:2004 Eurocode 5 (EC5) [64] specifies that final deformation can be estimated by Equation (6.14):

$$u_{fin} = u_{inst}\,(1 + k_{def}) \tag{6.14}$$

where

u_{fin} = final deformation, mm (in)

u_{inst} = instantaneous deformation, mm (in)

k_{def} = deformation factor

The deformation factor k_{def} adjusts the instantaneous deflection, values for which are given in EC5; depending on service class, these values range from a minimum of 0.6 to a maximum of 4.0. Fan and Enjily [65] stated that these values of k_{def} are based on the limited test data available and entirely on bending test data. The authors' defined k_{def} as the ratio of the increase in deflection with time under the load to the initial elastic deflection. Similarly, Van De Kuilen [66] defined k_{def} as shown in Equation (6.15):

$$k_{def} = \frac{\varepsilon\,(\mathrm{t}) - \varepsilon_0}{\varepsilon_o} \tag{6.15}$$

where

$\varepsilon\,(\mathrm{t})$ = total strain at a given time

ε_o = the initial strain to be defined after some loading period

Similarly, for serviceability limit states in the design of pultruded FRP structures, the ASCE Pre-Standard [10] specifies Equation (6.16) to calculate the total deflection u:

$$u = u_{st}\, k_{cr}(t) \tag{6.16}$$

where

u_{st} = instantaneous deflection due to gravity loads, mm (in)

$k_{cr}(t)$ = deflection amplification factor

The deflection amplification factor $k_{cr}(t)$ is given by Equation (6.17). This time-dependent creep factor is based on Findley's model [62] with constants determined from experimental creep data presented by Zureick [67].

$$k_{cr}(t) = 1 + t^{1/4}/6 \tag{6.17}$$

where

t = required service period of service, expressed in years

6.3.2 Development of Predictive Model for Pin-Bearing Connections

Based on the results of this investigation, it is possible to develop a suitable predictive model for estimating long-term bolt-hole deformation. A simplified equation for long-term deformation may be expressed as

$$\Delta d_{total} = \Delta d_{inst}(1 + k_c(t)) \tag{6.18}$$

where

Δd_{total} = total bolt-hole deformation, mm (in)

Δd_{inst} = instantaneous deformation of the bolt-hole resulting immediately upon loading, mm (in)

Equation (6.18) can be normalized relative to the original bolt-hole diameter as

$$\frac{\Delta d_{total}}{d} = \frac{\Delta d_{inst}}{d}(1 + k_c(t)) \tag{6.19}$$

The time-dependent amplification factor $k_c(t)$ is a function of short-term and viscoelastic material properties, as well as the applied stress level. In Equation (6.19), $k_c(t)$ represents the creep component of the overall normalized bolt-hole deformation. This factor may be approximated as a power law function that is inversely proportional to the deformation response of the material under short-term loading:

$$k_c(t) = \frac{t^n \left(\frac{\sigma_b}{\sigma_{bu}}\right)}{\left(\frac{\Delta d}{d}\right)_o^{n/2}} \tag{6.20}$$

where

$k_c(t)$ = time-dependent amplification factor accounting for creep expressed in %

t = time after loading in hours

n = stress-independent and temperature-independent material constant

$\left(\frac{\Delta d}{d}\right)_o$ = bolt-hole deformation at the maximum load from short-term pin-bearing tests (expressed as percent bolt-hole deformation

$\left(\frac{\sigma_b}{\sigma_{bu}}\right)$ = applied sustained stress level expressed as percentage of characteristic pin-bearing strength

Earlier in Chapter 4, pin-bearing strength was denoted by F_L^{br} in the experimental results. This nomenclature was specific to the experimental program of the research investigation. To generalize this term, the pin-bearing strength is denoted by σ_{bu} in the development of the predictive model. The mean percent bolt-hole deformation at the maximum load from the short-term pin-bearing tests $\left(\frac{\Delta d}{d}\right)_o$ for a *d/t* ratio of 1 for close-fit, laterally unrestrained specimens was determined as 28.7% (≈ 30%), as given in Table 4.17. Similarly, the mean value of stress-independent and temperature independent material constant (n) was determined as 0.22, as given in Table 6.6. Using the mean values of these parameters determined from the present investigation, Equation (6.20) may be expressed in the following form:

$$k_c(t) = \frac{t^{0.22}\left(\frac{\sigma_b}{\sigma_{bu}}\right)}{30^{0.11}} \tag{6.21}$$

Based on Equation (6.21), the amplification factor is plotted together with the experimental results and shown in Figure 6.11. The figure shows that the most conservative estimate of the factor $k_c(t)$, is achieved when the applied load level is 100% of the characteristic pin-bearing strength. As would be expected, the bolt-hole deformation increases with increases in applied load level and will be maximum when this load level is 100% of the characteristic pin-bearing strength. Therefore, at this load level the formulation will yield the maximum value of the amplification factor implying the most conservative estimate.

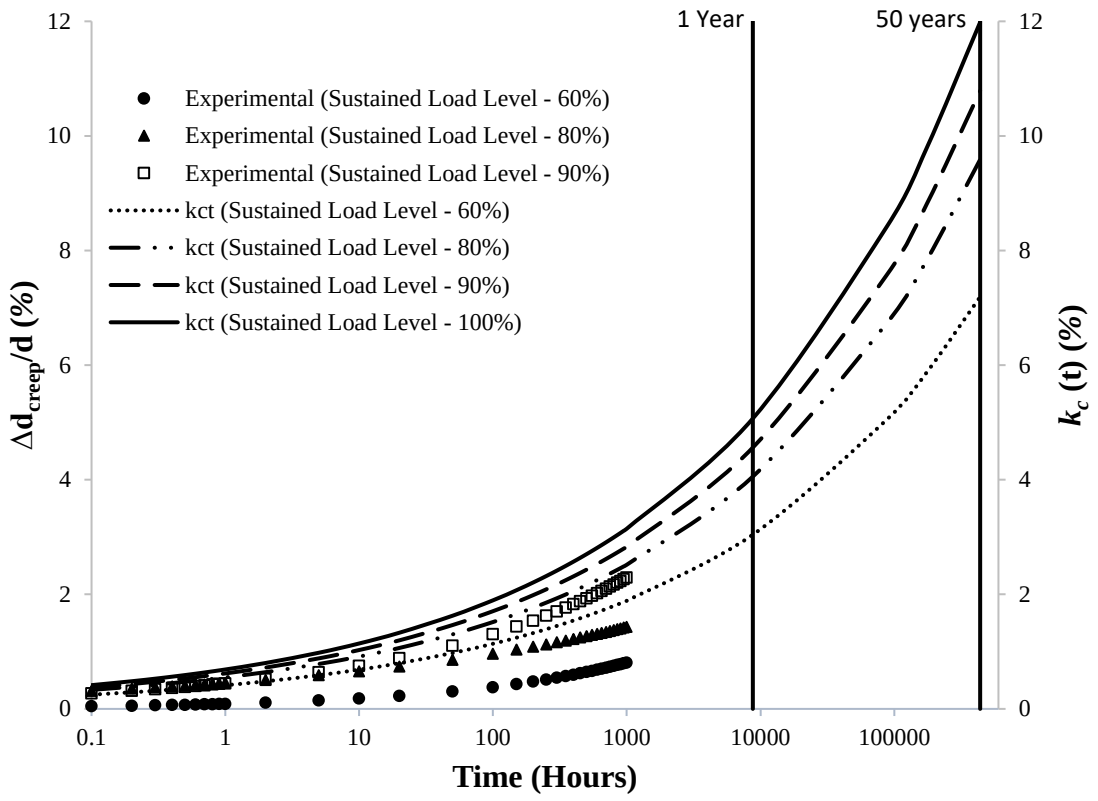

Figure 6.11 Predicted and experimental creep curves (sustained load level expressed as percentage of characteristic strength) - close-fit, laterally unrestrained specimens.

To account for bolt-hole clearance, Equation (6.21) may be modified as follows:

$$\Psi_1 k_c(t) = \Psi_1 \frac{t^{0.22}\left(\frac{\sigma_b}{\sigma_{bu}}\right)}{30^{0.11}} \tag{6.22}$$

where

Ψ_1 = factor accounting for bolt-hole clearance

Ψ_1=1.0 for close-fit connection

Ψ_1=2.0 for 1.6 mm (1/16 in) bolt-hole clearance

The value of factor Ψ_1 is determined from the ratios of short-term pin-bearing strength investigation presented earlier in Chapter 4 and summarized in Table 6.3. For a connection having a 1.6 mm (1/16 in) bolt-hole clearance, Ψ_1 is determined as follows:

$$\Psi_1 = \frac{\sigma_o\ (close - fit)}{\sigma_o(1.6\ mm\ (1/16\ in)\ \ bolt - hole\ clearance)} \tag{6.23}$$

$$= \frac{43{,}320\ psi}{23{,}790\ psi} = 1.82 \approx 2$$

where

σ_o = pin-bearing strength, MPa (psi)

The short-term pin-bearing strength investigation presented in Chapter 4 demonstrated that the pin-bearing strength of a connection with 1.6 mm (1/16 in) bolt-hole clearance reduced by approximately 50% when compared with a close-fit connection. Similarly, creep tests presented in Chapter 5 demonstrated that at a sustained load level of 60% of characteristic pin-bearing strength, the bolt-hole deformation of a connection with 1.6 mm (1/16 in) bolt-hole clearance at 1,000 hours increased by approximately 340% when compared with a close-fit connection. Therefore, the conclusion that bolt-hole clearance reduces the pin-bearing strength and increases the bolt-hole deformation under sustained loads implies that

the amplification factor $k_c(t)$ given in Equation (6.21) needs to be modified by incorporating a suitable factor to account for bolt-hole clearance. Based on Equation (6.22), Figure 6.12 shows the amplification factor $\Psi_1 k_c(t)$ plotted together with experimental results for a sustained load level of 60% of short-term characteristic pin-bearing strength. The creep curves show that the amplification factor $\Psi_1 k_c(t)$ from Equation (6.22) provides a reasonably conservative estimate of the creep response of the FRP materials used in this investigation.

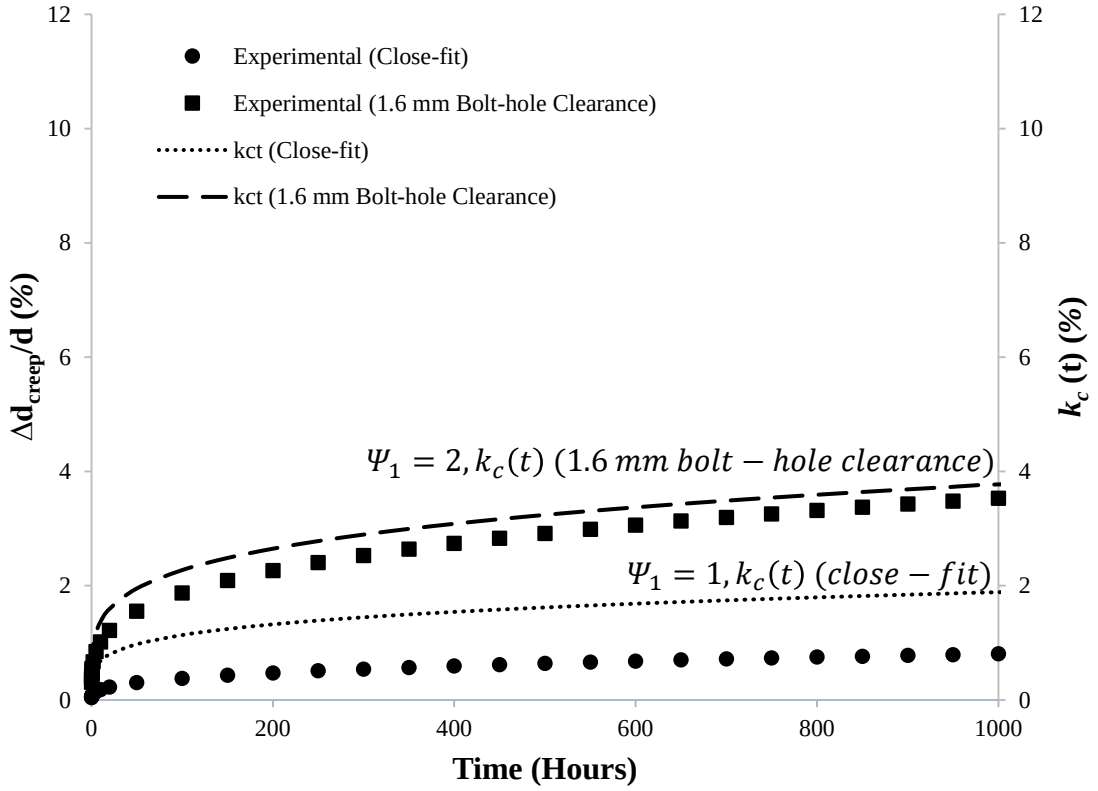

Figure 6.12 Predicted and experimental creep curves for sustained load level of 60% of short-term characteristic pin-bearing strength – laterally unrestrained specimens.

To account for temperature, Equation (6.21) may further be modified as follows:

$$\Psi_1\Psi_2 k_c(t) = \Psi_1\Psi_2 \frac{t^{0.22}\left(\frac{\sigma_b}{\sigma_{bu}}\right)}{30^{0.11}} \tag{6.24}$$

where

Ψ_2 = factor accounting for temperature

Ψ_2=1.0 for room temperature (24°C (75°F))

Ψ_2=2.5 for 43.3°C (110°F) temperature

Ψ_2=5.5 for 60°C (140°F) temperature

The value of factor Ψ_2 is defined as follows and determined from the short-term pin-bearing strength investigation presented earlier in Chapter 4 and summarized in Table 6.4:

$$\Psi_2 = \frac{\sigma_{o\ at\ T_o}}{\sigma_{o\ at\ T_e}} x \frac{(\Delta d/d)_{o\ at\ T_o}}{(\Delta d/d)_{o\ at\ T_e}} x \frac{T_e}{T_o} \tag{6.25}$$

where

T_o = ambient (room) temperature expressed in °C

T_e = elevated temperature expressed in °C

σ_o = pin-bearing strength, MPa (psi)

For 43.3°C (110°F),

$$\Psi_2 = \frac{29{,}870\ psi}{21{,}150\ psi} x \frac{28.7}{27.9} x \frac{43.3}{24} = 2.62 \approx 2.5$$

For 60°C (140°F),

$$\Psi_2 = \frac{29{,}870\ psi}{16{,}310\ psi} x \frac{28.7}{24.3} x \frac{60}{24} = 5.40 \approx 5.5$$

As discussed earlier in Chapter 4 and Chapter 5, the elevated service temperatures caused a reduction in the pin-bearing strength and increased bolt-hole deformation under sustained loads when compared with the response of a connection at ambient temperature conditions. Increasing the test temperature from ambient to 43.3, and 60°C (110, and 140°F) increased the bolt-hole deformation at 1,000 hours by approximately 300%, and 900%, respectively. Therefore, the amplification factor $k_c(t)$ given in Equation (6.21) needs to be modified by incorporating a suitable factor to account for elevated service temperatures. Based on Equation (6.24), Figure 6.13 shows the amplification factor plotted together with experimental results for a sustained load level of 60% of the short-term characteristic pin-bearing strength. The creep curves show that the amplification factor $\Psi_2 k_c(t)$ from Equation (6.24) provides a reasonably conservative estimate of the creep response of the FRP materials used in this investigation.

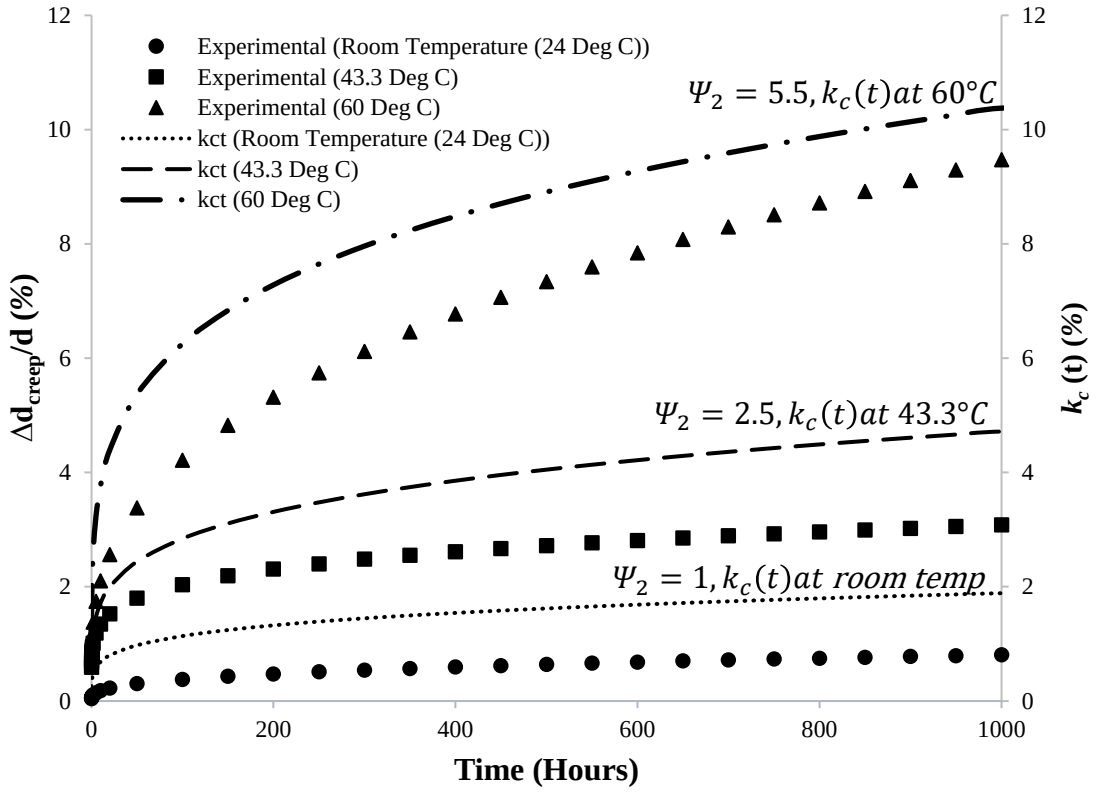

Figure 6.13 Predicted and experimental creep curves for sustained load level of 60% of short-term characteristic pin-bearing strength – close-fit, laterally unrestrained specimens.

By specifying time t in years instead of hours, expressing the factor $k_c(t)$ in decimal form instead of as a percentage, and simplifying Equation (6.21), $k_c(t)$ may be expressed as:

$$k_c(t) = \frac{t^{0.22}}{20} \tag{6.26}$$

To account for bolt-hole clearance and temperature, Equation (6.26) may be expressed as:

$$\Psi_1 \Psi_2 k_c(t) = \Psi_1 \Psi_2 \frac{t^{0.22}}{20} \tag{6.27}$$

This formulation allows the time-dependent pin-bearing strength $R_{br}(t)$ to be estimated as shown in Equation (6.28):

$$R_{br}(t) = R_{br}(1 - \Psi_1 \Psi_2 k_c(t)) \tag{6.28}$$

where

R_{br} = short-term pin-bearing strength, kN (kip)

Figure 6.14 and Figure 6.15 shows the predicted reduction in bearing strength over time for various bolt-hole clearances and temperature conditions. The figures indicate that by the end of a 50-year service life for a given structure, the bearing strength of a connection at room temperature having a 1.6 mm (1/16 in) bolt-hole clearance reduces by approximately 25%.

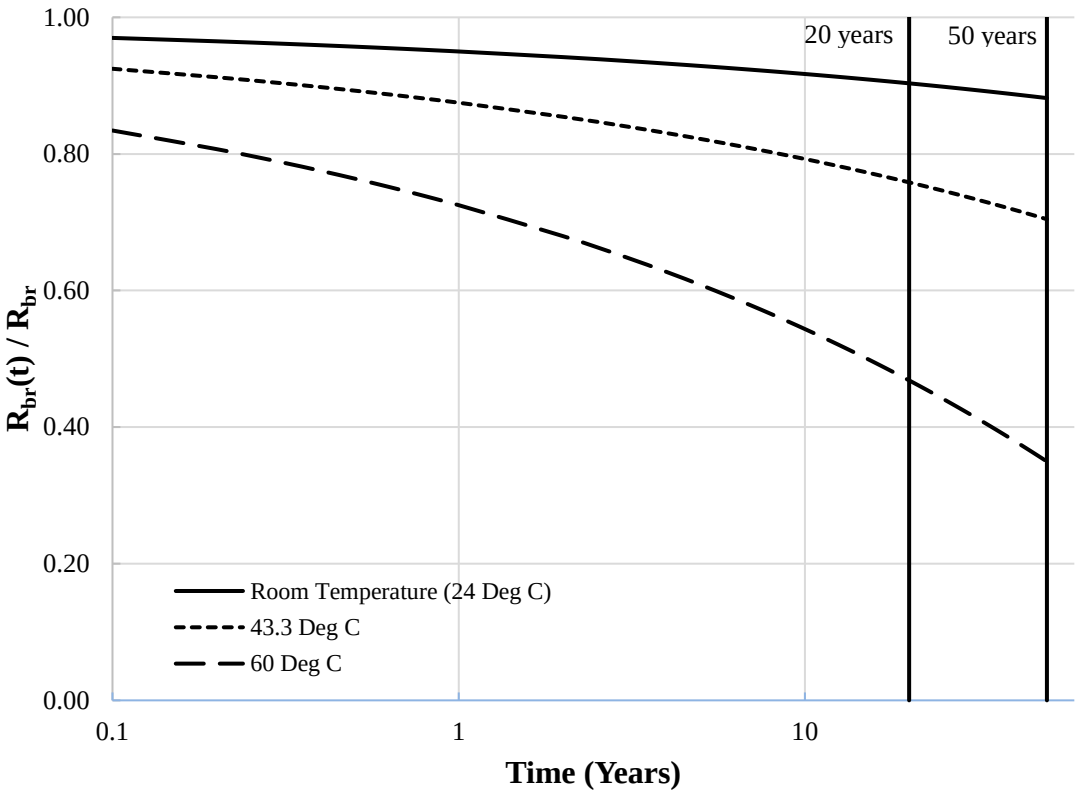

Figure 6.14 Reduction in pin-bearing strength with time – close-fit, laterally unrestrained connection.

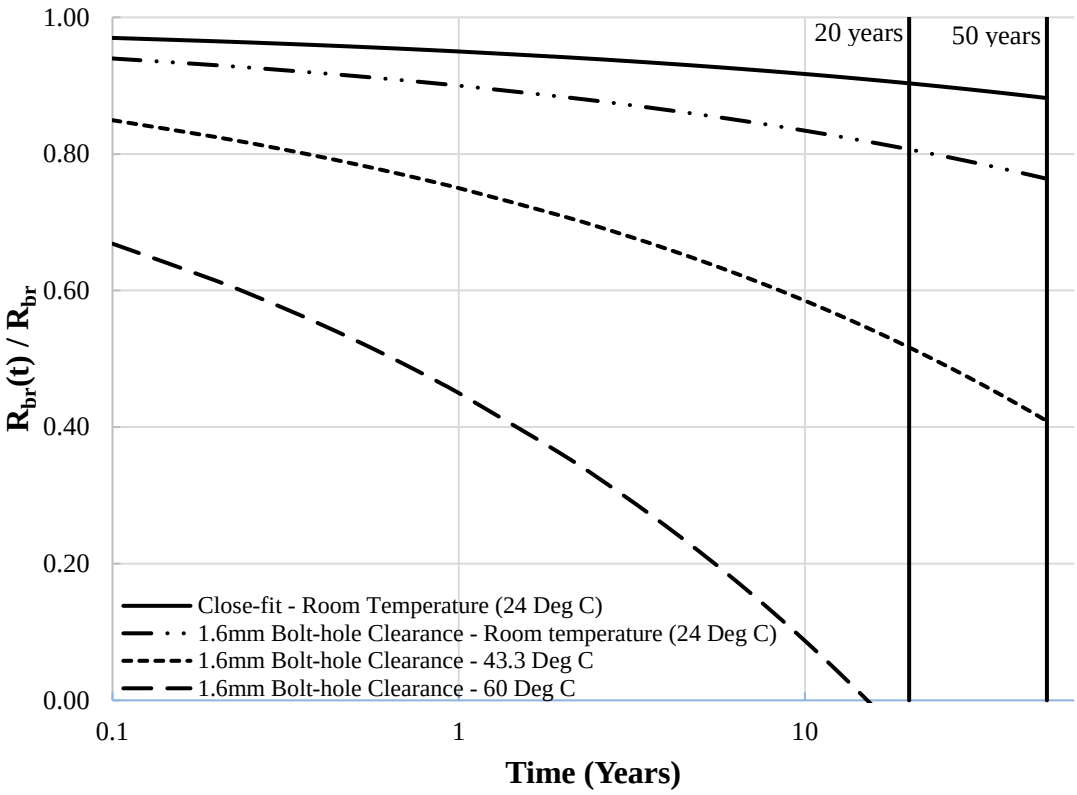

Figure 6.15 Reduction in pin-bearing strength with time - laterally unrestrained connection.

CHAPTER 7

CONCLUSIONS AND RECOMMENDATIONS

7.1 Conclusions

The short and long-term pin-bearing behavior of an E-glass/polyester pultruded FRP composite material was investigated. The investigation involved testing single bolt connections subjected to in-plane loading in tension under a double-lap shear configuration. First, a parametric study was conducted to study the influence of specific connection parameters on short-term pin bearing strength. Then, sustained load tests were conducted for time durations of up to 1,000 hours at various load levels, specific connection conditions, and elevated service temperatures. Finally, based on the short- and long-term experimental investigations, a suitable semi-empirical predictive model was developed for the time-dependent behavior of pin-bearing connections. This model was used to develop a design equation for pin-bearing connections in pultruded materials that accounts for time-dependent behavior. Conclusions drawn from this investigation are summarized below:

a. For laterally unrestrained connections, whether close-fit or a connection with a specified bolt-hole clearance (1.6 mm (1/16 in)), pin-bearing strength reduces with an increase in *d/t* ratio. However, no significant relationship exists between pin-bearing strength and *d/t* ratio for close-fit moderately torqued connections, whether close-fit or a connection with a bolt-hole clearance.

b. For a given *d/t* ratio, an increase in lateral restraint increases short-term pin-bearing strength significantly. Similarly, an increase in bolt-hole clearance reduces pin-bearing strength.

c. The perceived increase in bearing strength achieved by providing lateral restraint through bolt torque is lost or reduced significantly under sustained loading. For instance, in close-fit moderately torqued connections, at a sustained load level of 50% of the mean pin-bearing strength the bolt-hole deformation at 1,000 hours increased by approximately 140% when compared with a laterally unrestrained connection. Therefore, pin-bearing strength in the design of bolted connections should always be computed when there is no lateral restraint in the connection. This aspect must be included in the test standards and any design criteria.

d. Bolt-hole clearance not only influences the short-term pin-bearing strength, but also significantly affects the response under sustained loading. For instance, at a sustained load level of 50% of mean pin-bearing strength for a connection having a 1.6 mm (1/16 in) bolt-hole clearance, the bolt-hole deformation at 1,000 hours increased by approximately 340% when compared with a close-fit connection. A provision for bolt-hole clearance is a practical design consideration and must be included in the test standards. The design of bolted connections should also include the effect of bolt-hole clearance in computing the strength of a connection.

e. The pin-bearing strength for these types of pultruded material is significantly decreased at moderately elevated temperatures. The test results demonstrated that the pin-bearing strength reduced by approximately 33%, and 44% when the test temperature increased from ambient to 43.3, and 60°C (110, and 140°F) respectively.

f. Elevated service temperatures also significantly influence the long-term response of a connection. At a sustained load level of 50% of mean pin-bearing strength the bolt-hole deformation at 1,000 hours increased by

approximately 300% and 900% when the test temperature was increased from ambient to 43.3 and 60°C (110 and 140°F) respectively. Therefore, the effect of temperature on time-dependent behavior should be included in the design of bolted connections.

g. Findley's Power Law model was used to approximate the creep deformation of a bolt-hole loaded in tension under a double-lap shear configuration. The results demonstrated that the Findley model can be applied for approximating the creep deformation of a single pin-bearing connection loaded in tension in pultruded FRP materials.

h. At a sustained load level of 70% of the short-term mean pin-bearing strength, the connection failed before reaching a specified 1,000-hour test duration for the tests conducted at ambient (room) temperature for close-fit moderately torqued connection, and 1.6 mm (1/16 in) bolt-hole clearance laterally unrestrained connection, and for the tests conducted at elevated temperatures of 43.3°C (110°F), and 60°C (140°F) for close-fit laterally unrestrained connections. Therefore, the absolute value of pin-bearing strength after incorporating all the factors should always be less than 70% of the mean pin-bearing strength.

i. Similar to design procedures developed for wood [64] and for pultruded FRP structures [10], the time-dependent amplification factor $k_c(t)$ was developed to predict the total deformation of a single-pin bearing connection to include the long-term deformation under sustained loads. The results of the time-dependent amplification factor $k_c(t)$ compared with experimental results demonstrated that the factor $k_c(t)$ provided a conservative estimate of the creep deformation of a single pin-bearing connection. In simplest form, the factor $k_c(t)$ is shown in Equation (7.1).

$$k_c(t) = \frac{t^{0.22}}{20} \tag{7.1}$$

where

t = time expressed in years

j. A suitable predictive model for time-dependent behavior of pin-bearing connections was developed that provided a conservative estimate for predicting the deformation behavior of a pin-bearing connection under sustained loading. Therefore, a proposed equation for time-dependent pin-bearing strength is given as

$$R_{br}(t) = R_{br}(1 - \Psi_1 \Psi_2 k_c(t)) \tag{7.2}$$

where

$R_{br}(t)$ = time-dependent pin-bearing strength, kN (kip)

R_{br} = short-term pin-bearing strength, kN (kip)

$k_c(t)$ = time-dependent amplification factor accounting for creep

= $\frac{t^{0.22}}{20}$, where *t* is time expressed in years

Ψ_1 = factor accounting for bolt-hole clearance

Ψ_1=1.0 for close-fit connection

Ψ_1=2.0 for 1.6 mm (1/16 in) bolt-hole clearance

Ψ_2 = factor accounting for temperature

Ψ_2=1.0 for room temperature (24°C (75°F))

Ψ_2=2.5 for 43.3°C (110°F) temperature

Ψ_2=5.5 for 60°C (140°F) temperature

7.2 Recommendations for Future Work

The short- and long-term response of single pin-bearing connection for pultruded FRP materials was investigated at normal and elevated service temperatures. This study can be extended in following areas to fill in knowledge gaps.

a. The experimental program presented here involved testing of a connection with coincident direction of pultrusion and direction of loading. The influence of other loading directions with respect to the pultrusion direction on the pin-bearing strength of bolted connections may be investigated.

b. Single-bolt tension connections were investigated in this research. The influence of multiple bolts and rows on the short- and long-term behavior of connections for pultruded materials should be investigated.

c. The experiments in the current study were conducted for close-fit and 1.6 mm (1/16 in) bolt-hole clearance conditions. Tests at other bolt-hole clearance conditions should be conducted to investigate the effect of clearance on connection behavior.

d. The present investigation involved testing of laterally unrestrained and moderately torqued connections. Future research may comprise investigation at other lateral restraint conditions such as lightly torqued, "snug-tightened," and "finger-tight" conditions, to confirm the applicability of the findings of the present work.

e. Tests at other *d/t* ratios are suggested to be conducted to confirm the applicability of the findings of the present research to other connection configurations. For instance, ASCE Pre-Standard [10] specifies a maximum bolt diameter of 25.4 mm (1 in), hence future research may include larger bolt diameters of up to 25.4 mm (1 in) and larger *d/t* ratios of up to 4.

f. The present work included the effect of moderately elevated temperatures on pin-bearing connection behavior - 43.3°C (110°F), and 60°C (140°F). Tests at other elevated temperatures should be conducted to confirm the applicability of the findings of the present work to other potential thermal exposures. The other elevated temperatures may include such temperatures as 32.2°C (90°F), and 50°C (122°F) representing practical thermal exposures and moderately elevated temperature. This can also be extended to cyclic temperature exposure, which is often more representative of real world conditions.

g. The influence of cyclic loading should be investigated relative to the time-dependent behavior of pin-bearing connections.

h. The effects of moisture exposure on long-term pin-bearing connections should be included in future investigations.

APPENDIX A

LOAD-DISPLACEMENT CURVES – SHORT-TERM PIN-BEARING TESTS

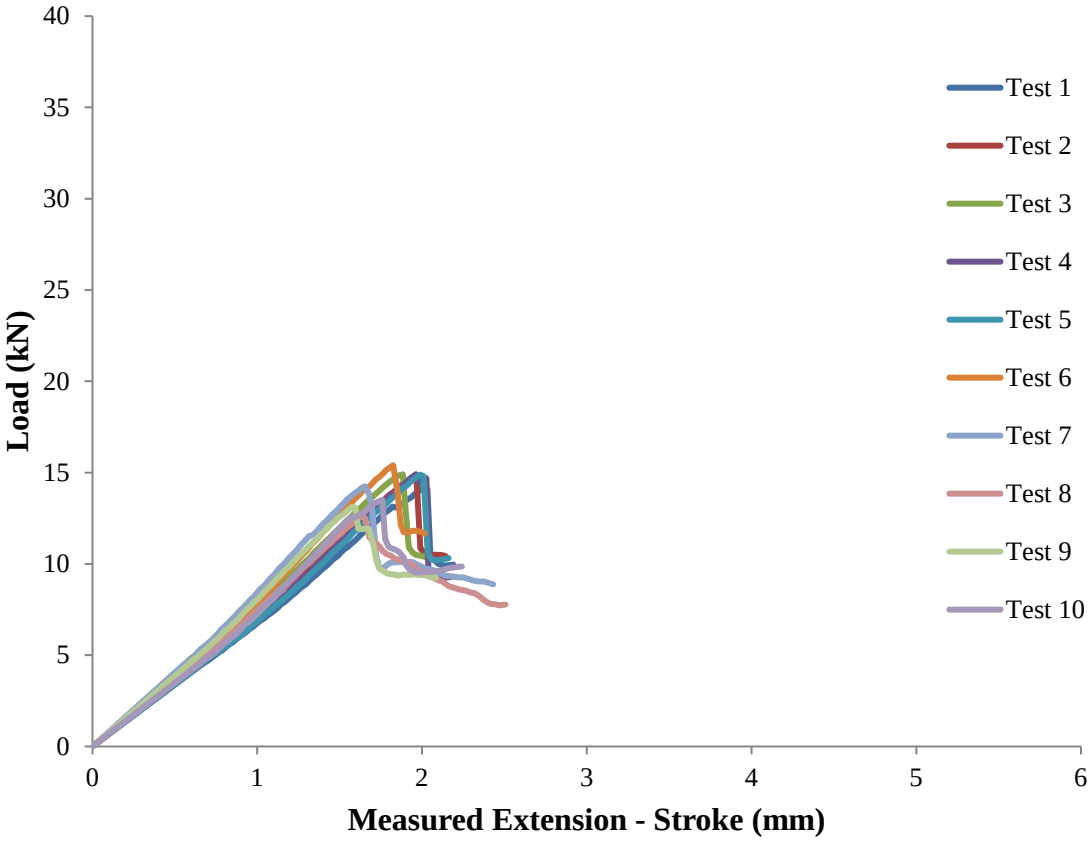

Figure A.1 Load-displacement curves – close-fit, laterally unrestrained specimen tests (6.35 mm (1/4 in) diameter bolt).

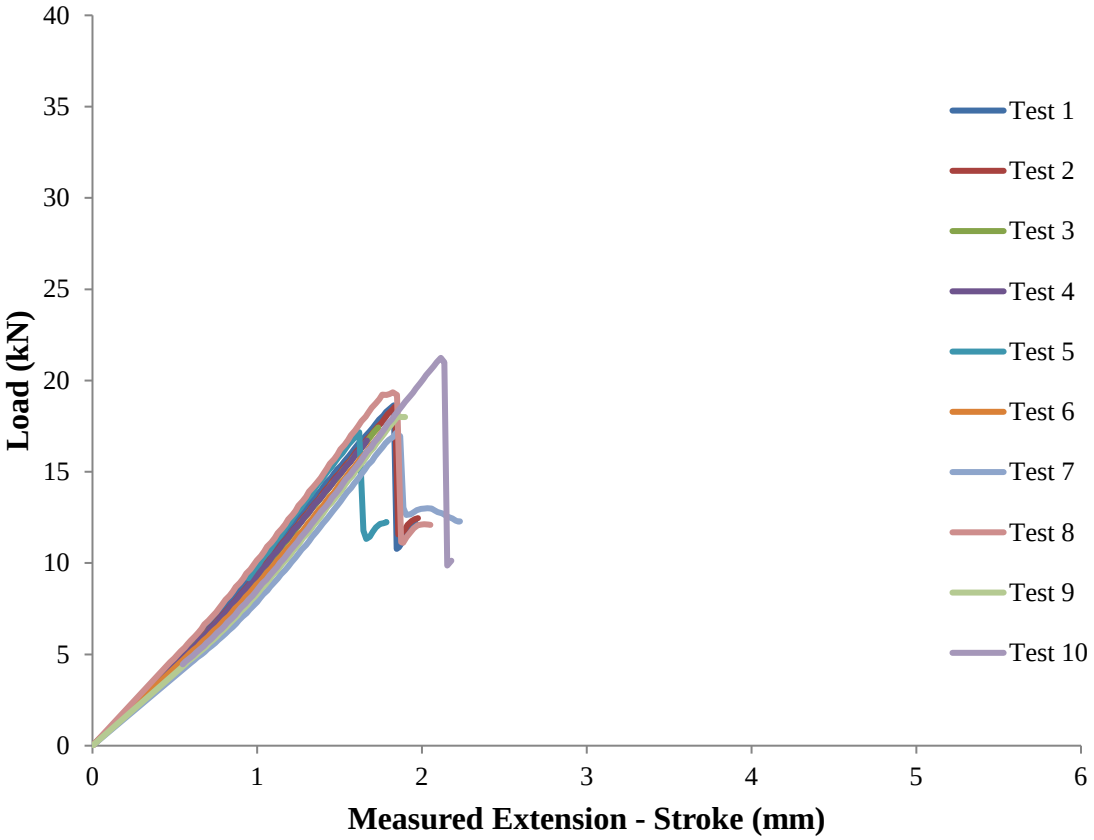

Figure A.2 Load-displacement curves – close-fit, laterally unrestrained specimen tests (9.53 mm (3/8 in) diameter bolt).

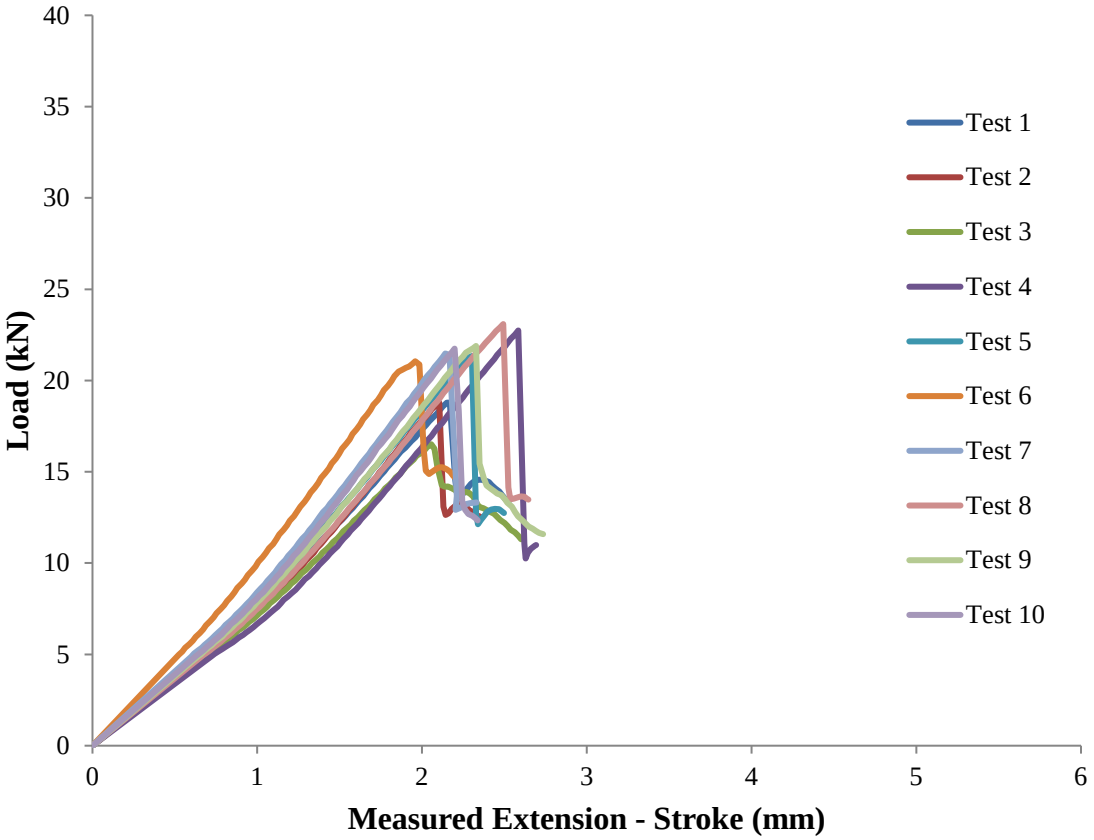

Figure A.3 Load-displacement curves – close-fit, laterally unrestrained specimen tests (12.7 mm (1/2 in) diameter bolt).

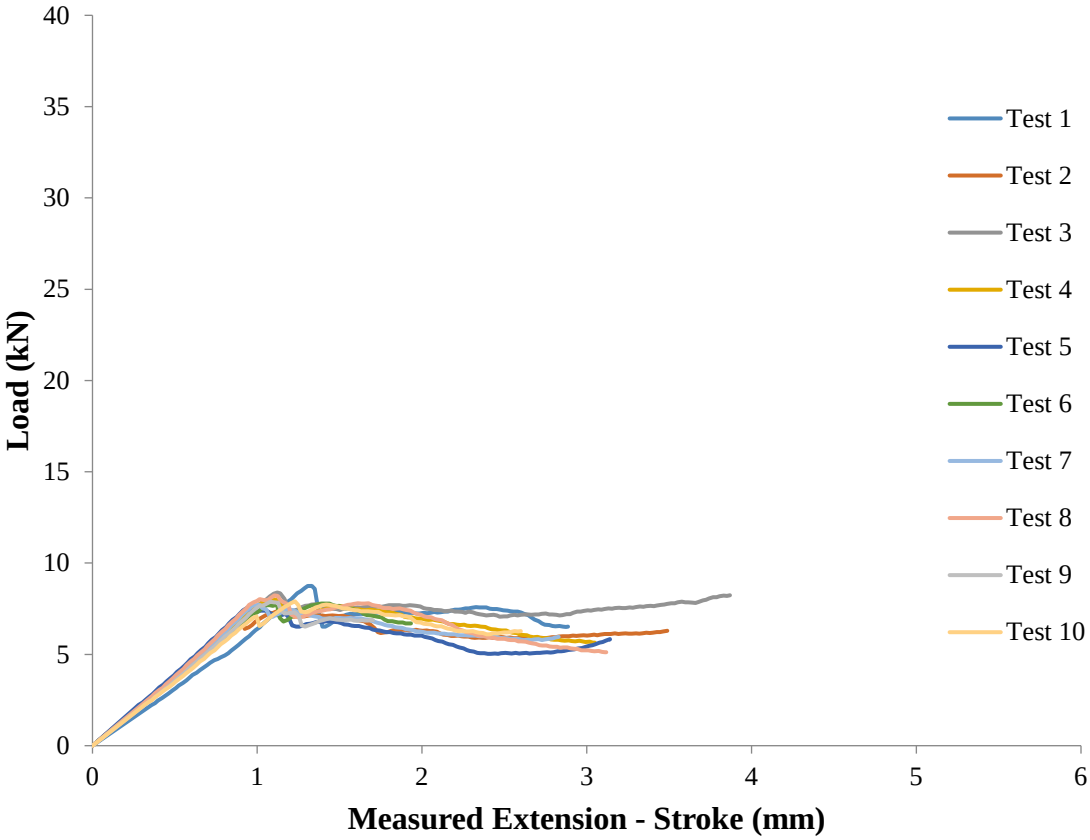

Figure A.4 Load-displacement curves – 1.6 mm (1/16 in) bolt-hole clearance, laterally unrestrained specimen tests (6.35 mm (1/4 in) diameter bolt).

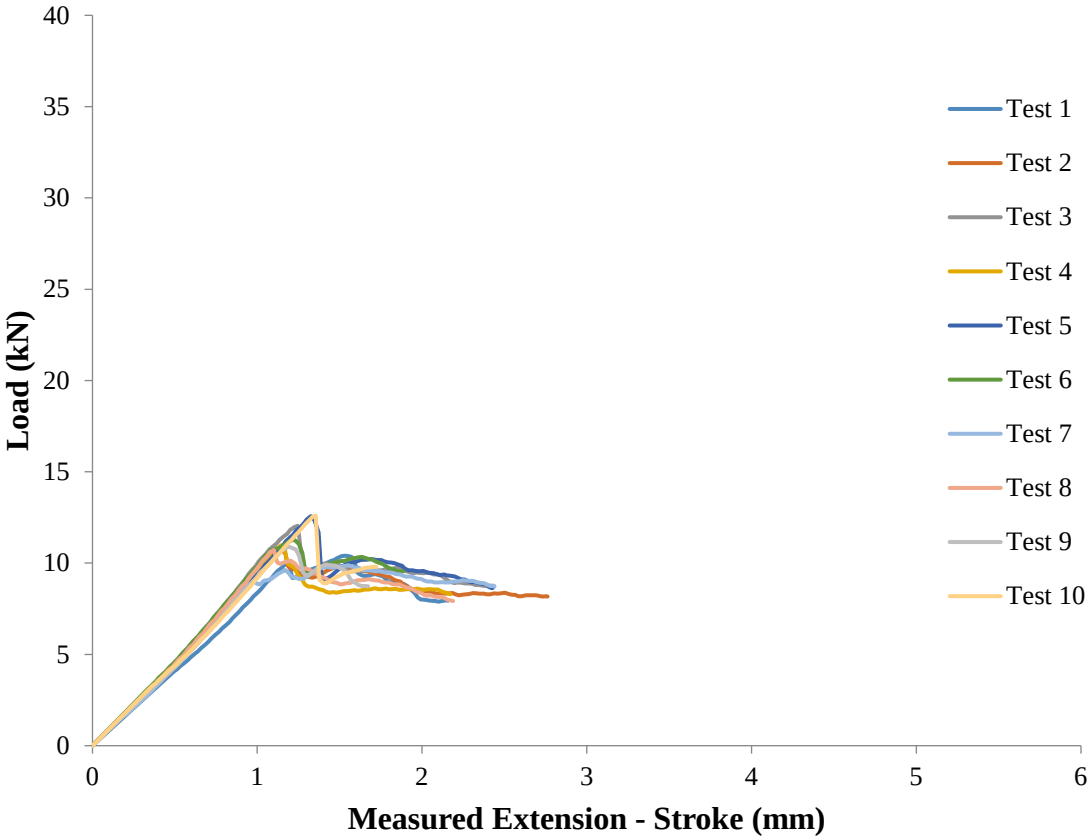

Figure A.5 Load-displacement curves – 1.6 mm (1/16 in) bolt-hole clearance, laterally unrestrained specimen tests (9.53 mm (3/8 in) diameter bolt).

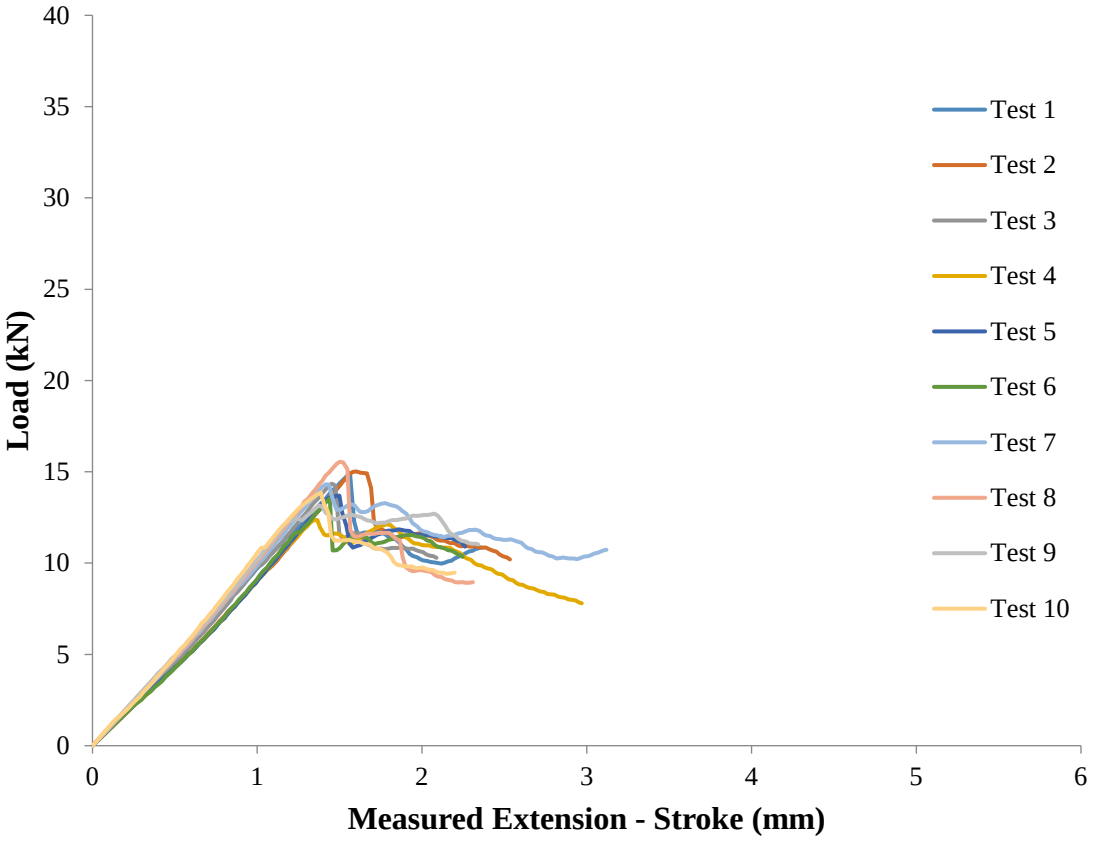

Figure A.6 Load-displacement curves – 1.6 mm (1/16 in) bolt-hole clearance, laterally unrestrained specimen tests (12.7 mm (1/2 in) diameter bolt).

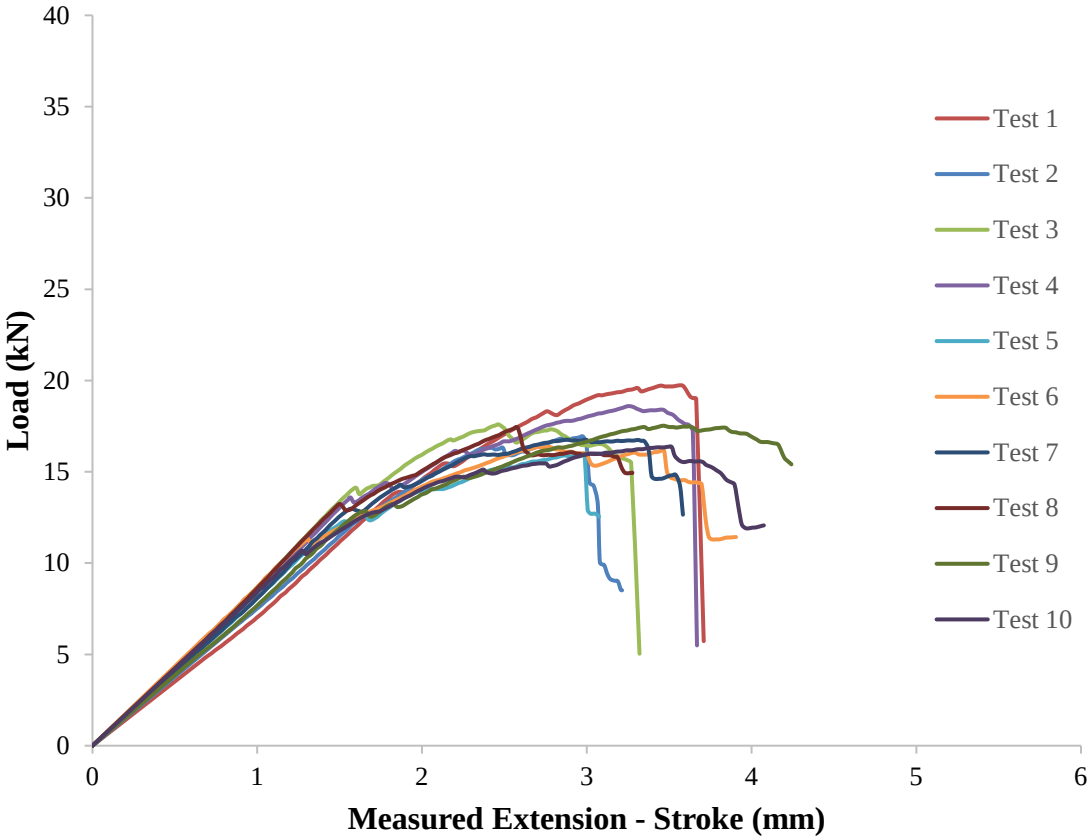

Figure A.7 Load-displacement curves – close-fit, moderately torqued specimen tests (6.35 mm (1/4 in) diameter bolt).

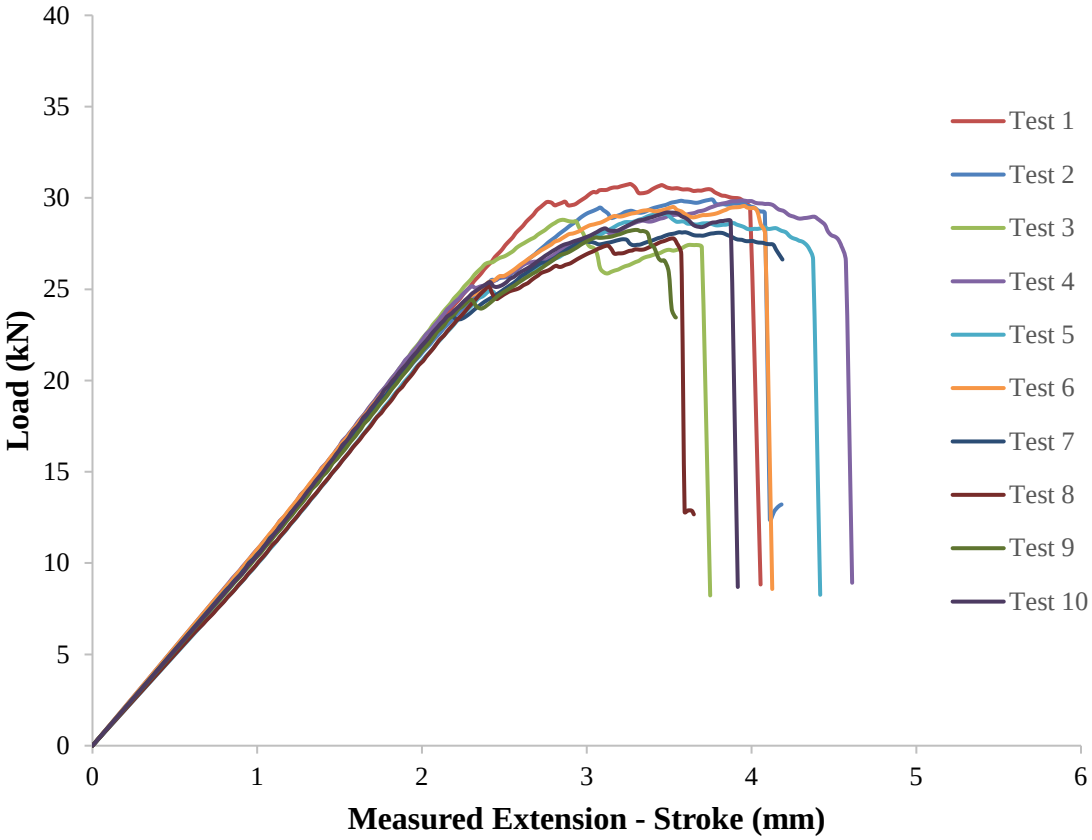

Figure A.8 Load-displacement curves – close-fit, moderately torqued specimen tests (9.53 mm (3/8 in) diameter bolt).

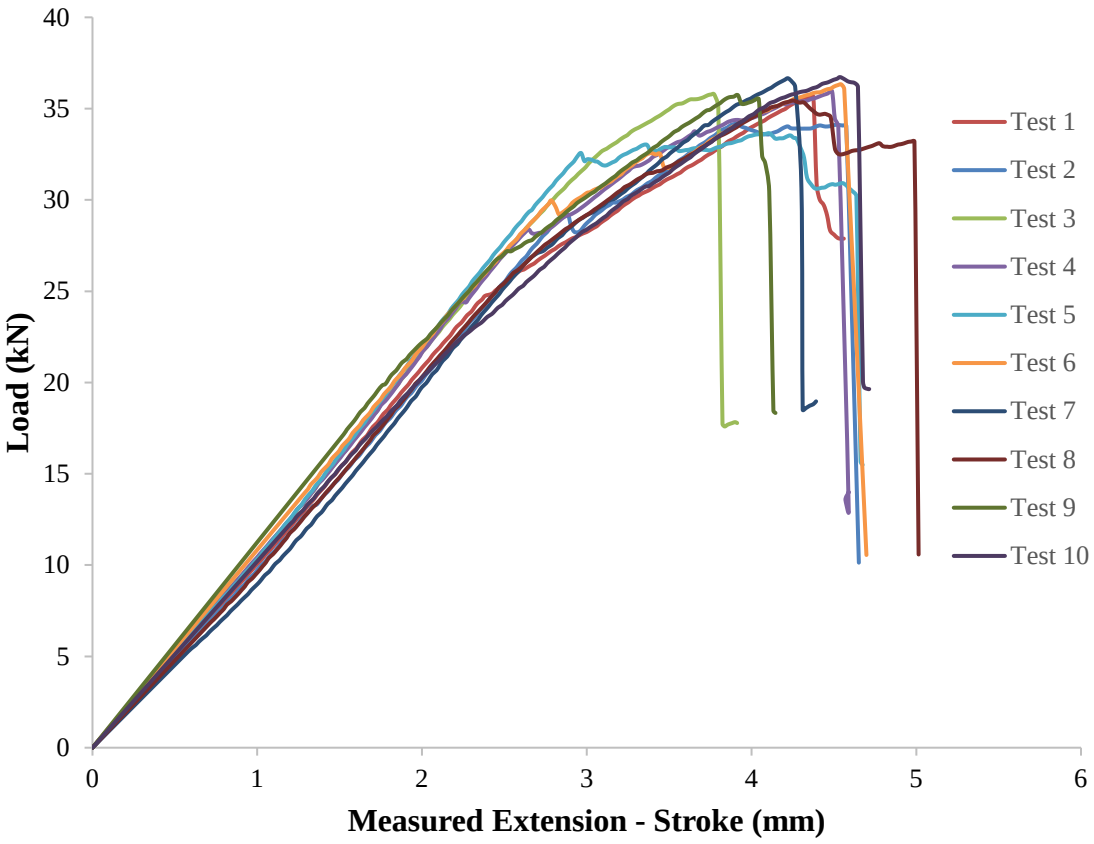

Figure A.9 Load-displacement curves – close-fit, moderately torqued specimen tests (12.7 mm (1/2 in) diameter bolt).

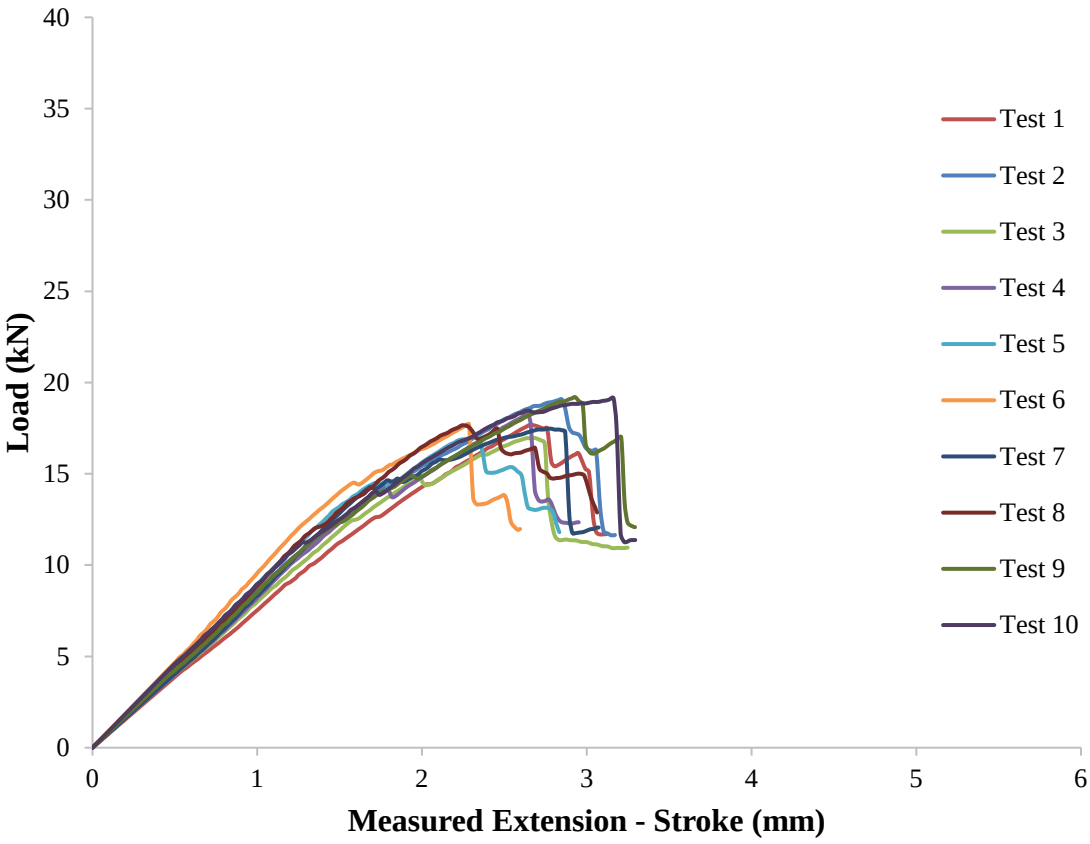

Figure A.10 Load-displacement curves – 1.6 mm (1/16 in) bolt-hole clearance, moderately torqued specimen tests (6.35 mm (1/4 in) diameter bolt).

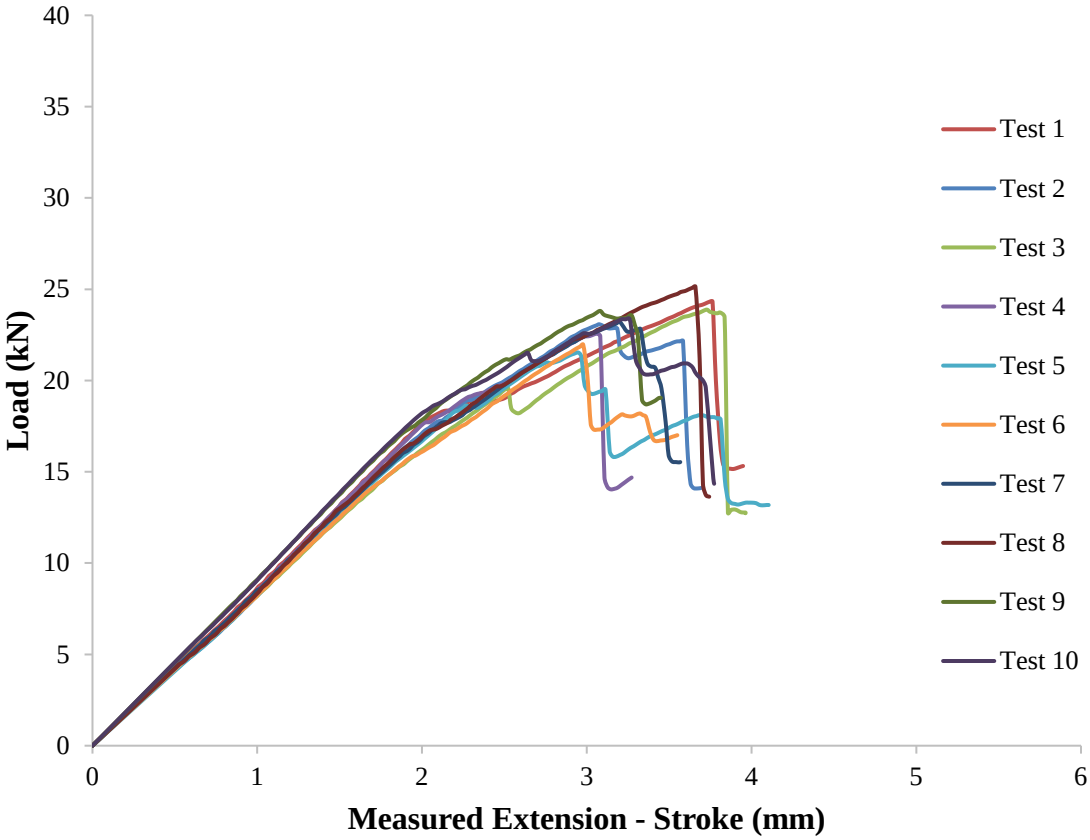

Figure A.11 Load-displacement curves – 1.6 mm (1/16 in) bolt-hole clearance, moderately torqued specimen tests (9.53 mm (3/8 in) diameter bolt).

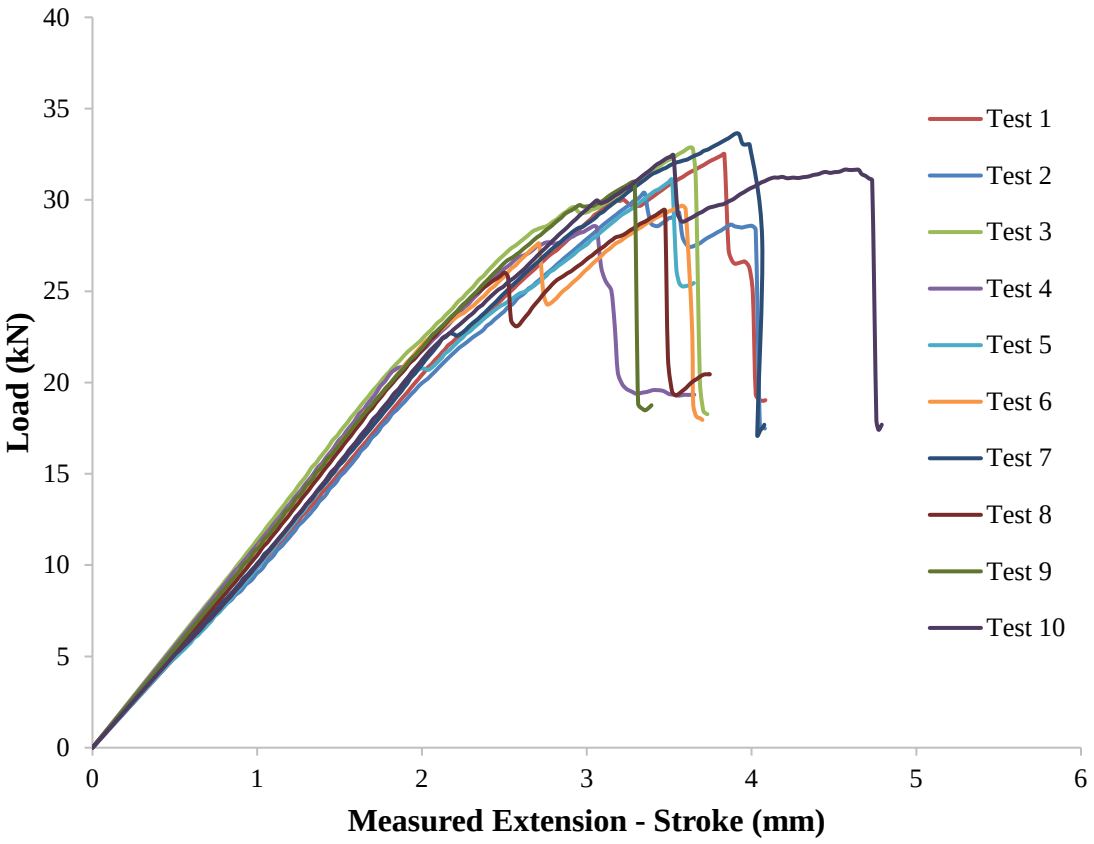

Figure A.12 Load-displacement curves – 1.6 mm (1/16 in) bolt-hole clearance, moderately torqued specimen tests (12.7 mm (1/2 in) diameter bolt).

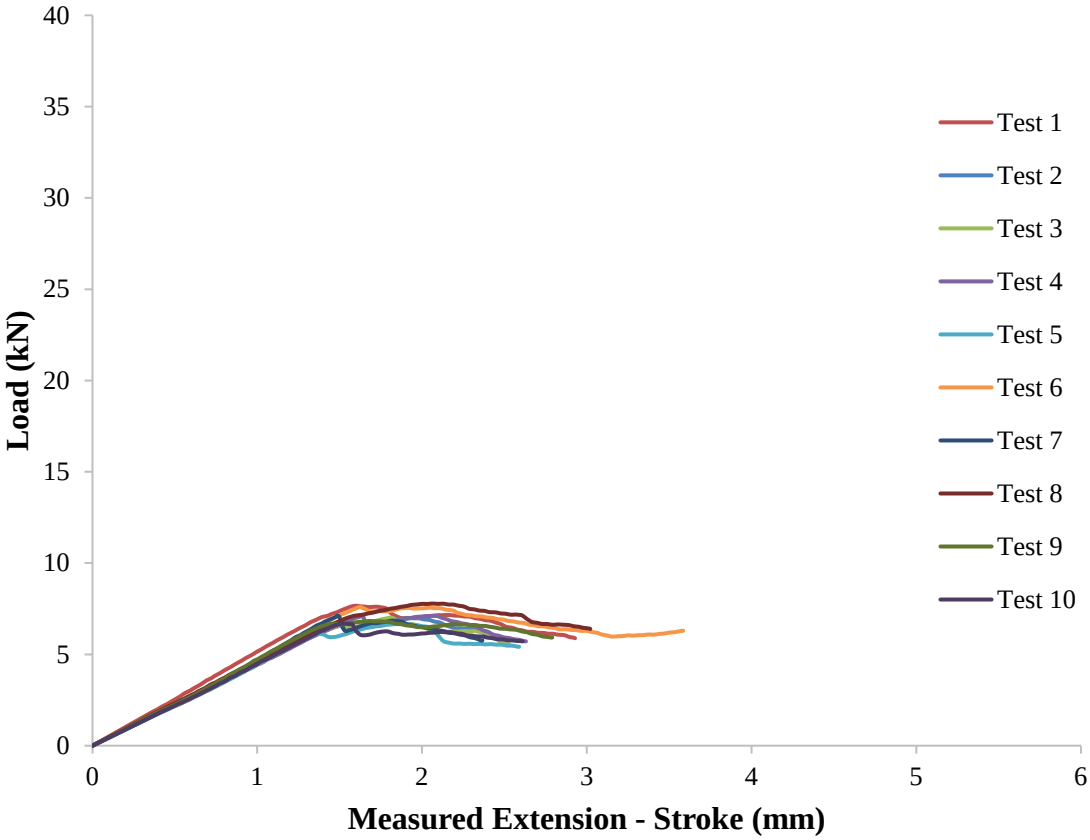

Figure A.13 Load-displacement curves – close-fit, laterally unrestrained specimen tests at 43.3°C (110°F) - (6.35 mm (1/4 in) diameter bolt).

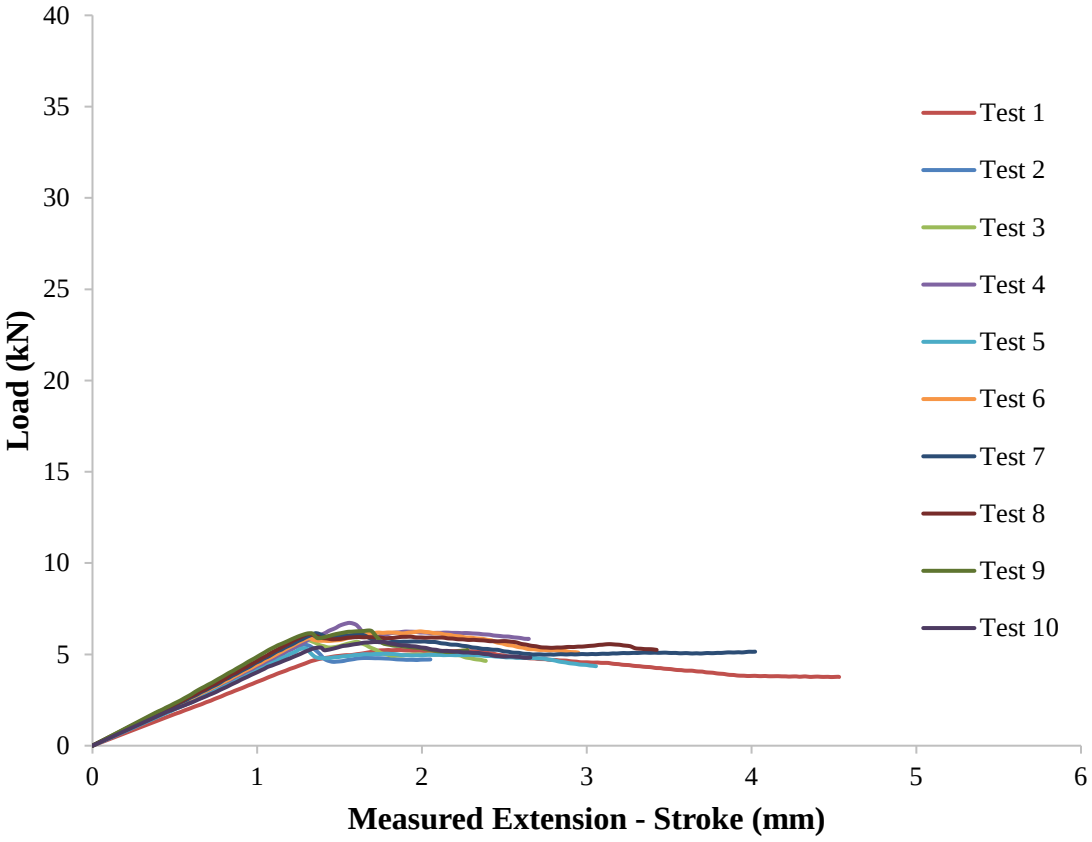

Figure A.14 Load-displacement curves – close-fit, laterally unrestrained specimen tests at 60°C (140°F) - (6.35 mm (1/4 in) diameter bolt).

APPENDIX B

BOLT-HOLE DEFORMATION VS TIME CURVES – CREEP TESTS

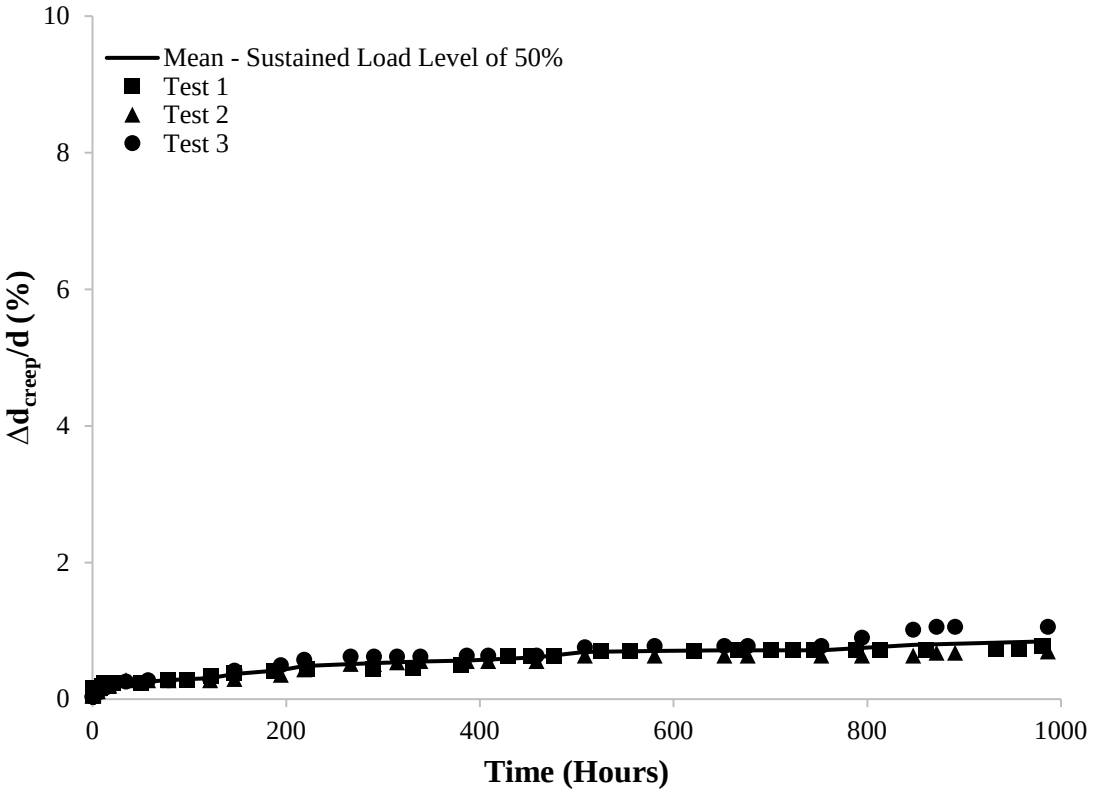

Figure B.1 Creep component of the percent bolt-hole deformation – sustained load level of 50% of mean bearing strength (Case-I - close-fit, laterally unrestrained specimens).

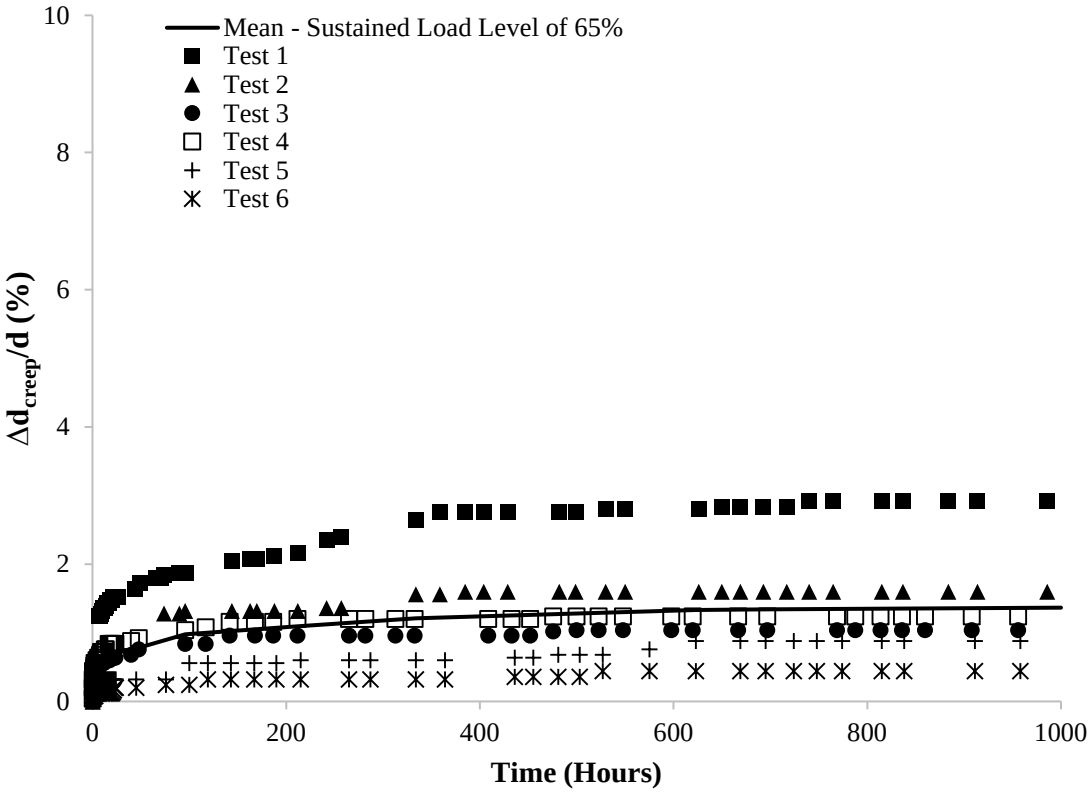

Figure B.2 Creep component of the percent bolt-hole deformation – sustained load level of 65% of mean bearing strength (Case-I - close-fit, laterally unrestrained specimens).

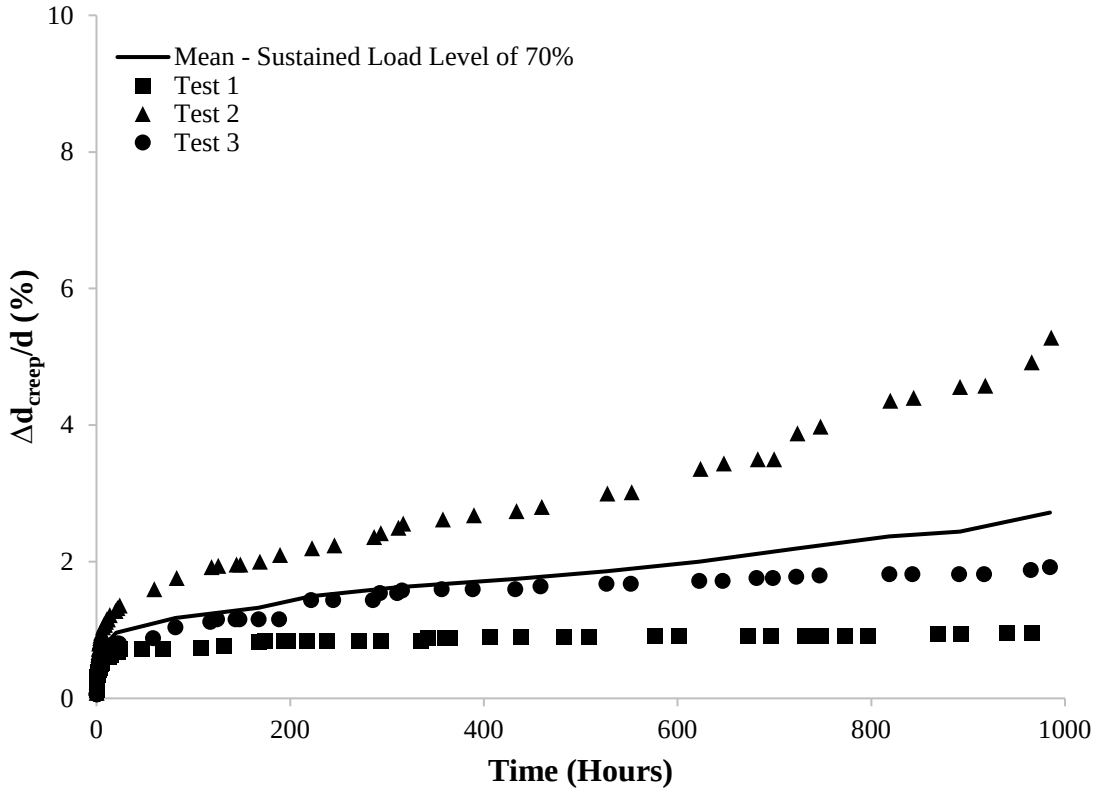

Figure B.3 Creep component of the percent bolt-hole deformation – sustained load level of 70% of mean bearing strength (Case-I - close-fit, laterally unrestrained specimens).

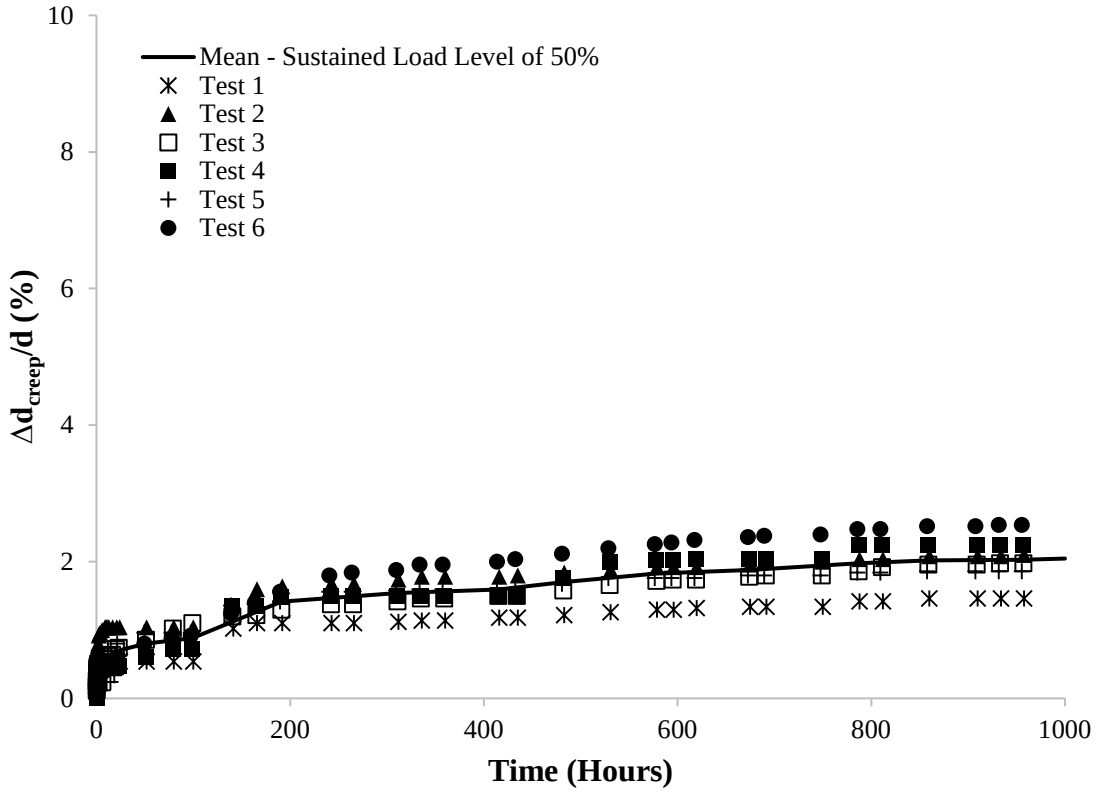

Figure B.4 Creep component of the percent bolt-hole deformation – sustained load level of 50% of mean bearing strength (Case-II - close-fit, moderately torqued specimens).

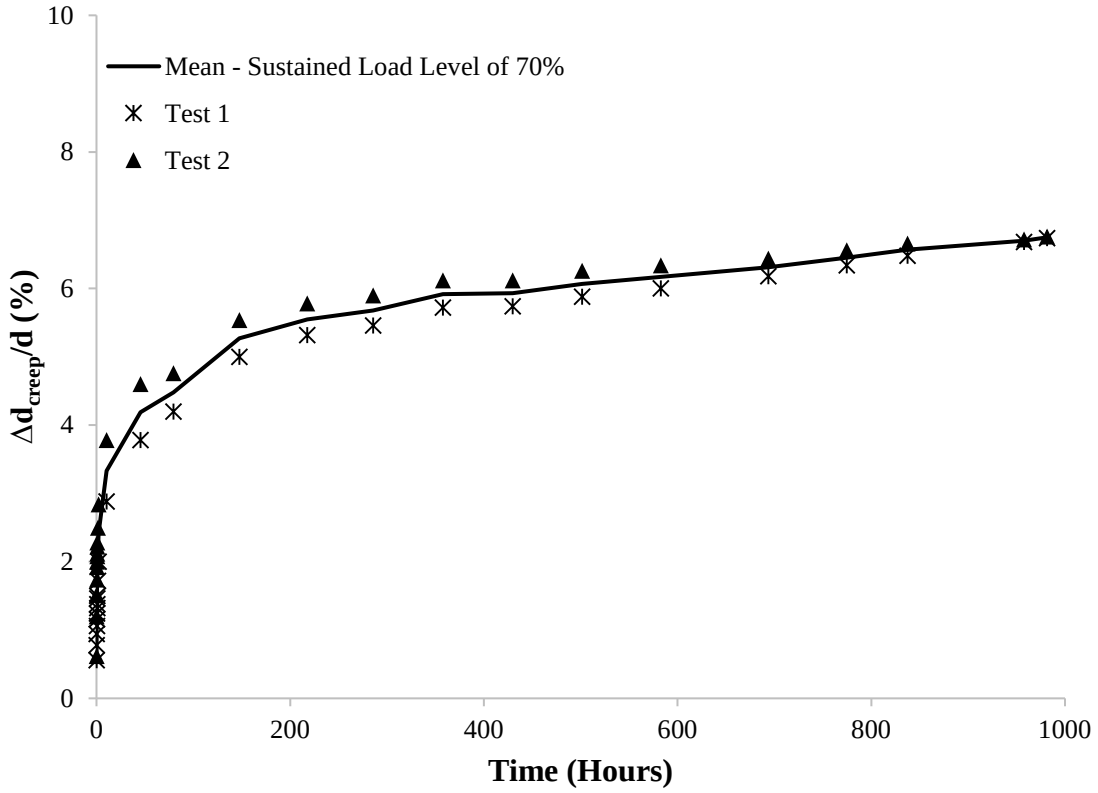

Figure B.5 Creep component of the percent bolt-hole deformation – sustained load level of 70% of mean bearing strength (Case-II - close-fit, moderately torqued specimens).

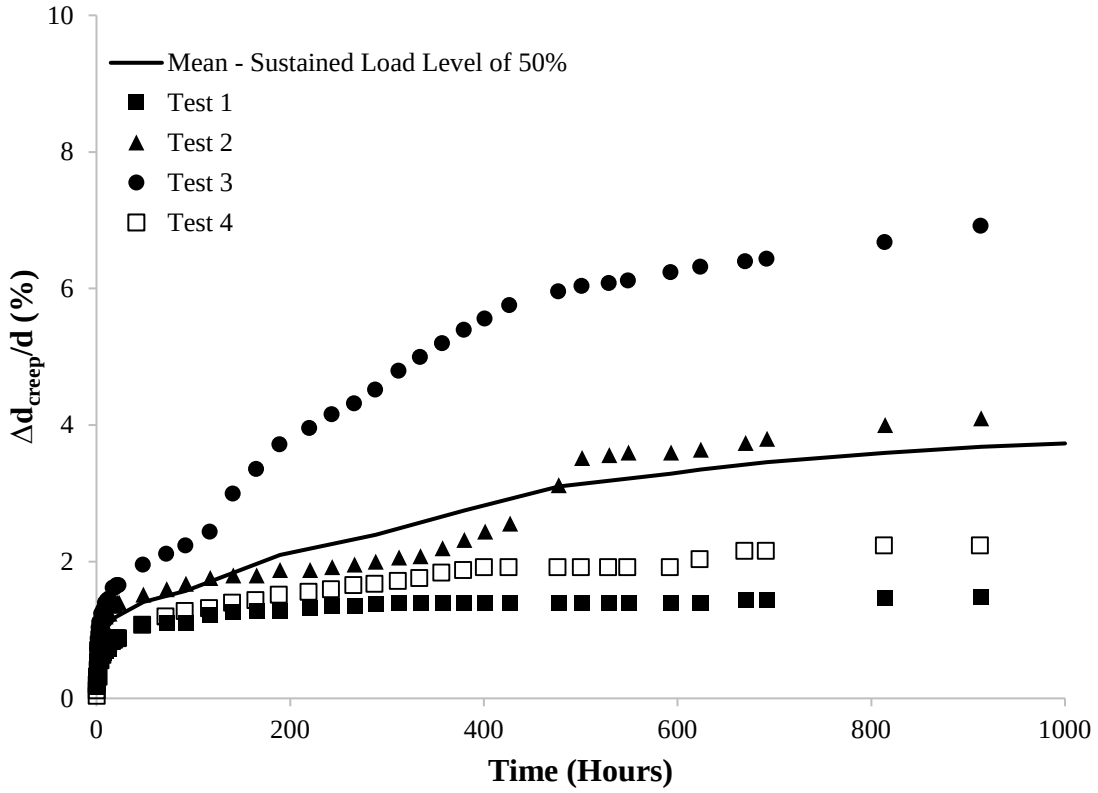

Figure B.6 Creep component of the percent bolt-hole deformation – sustained load level of 50% of mean bearing strength (Case- III - 1.6 mm (1/16 in) bolt-hole clearance, laterally unrestrained specimens).

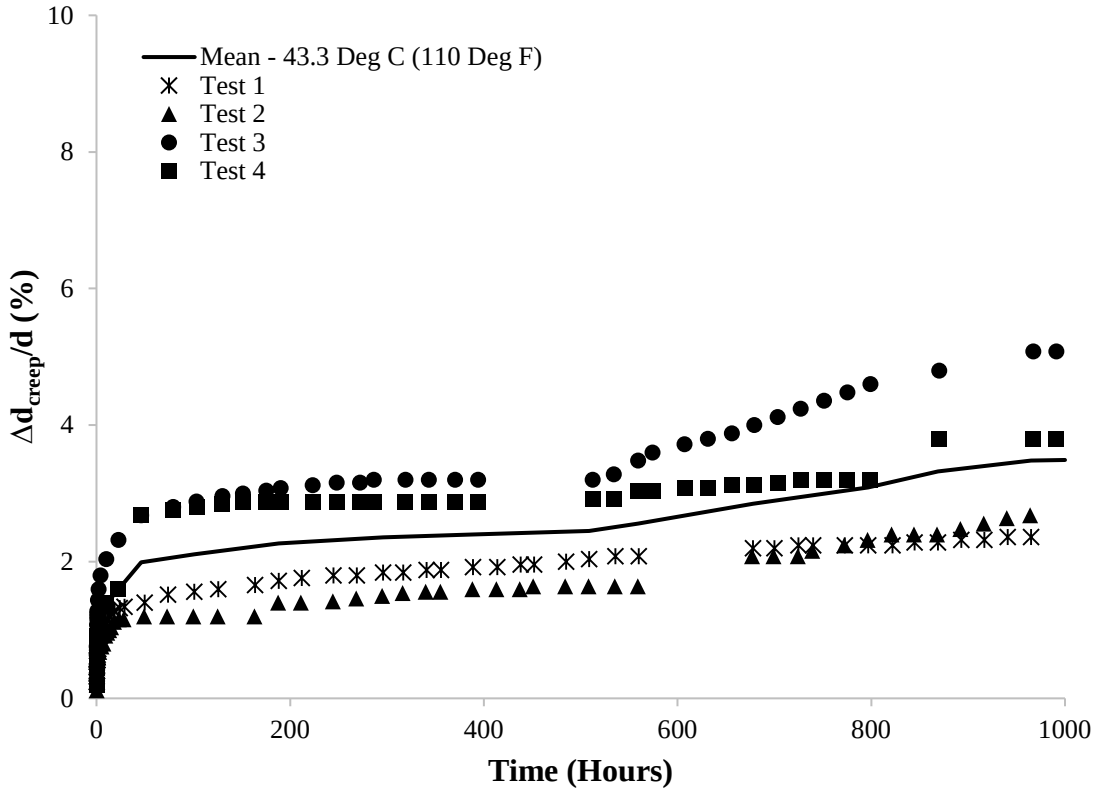

Figure B.7 Creep component of the percent bolt-hole deformation – sustained load level of 50% of mean bearing strength (close-fit, laterally unrestrained specimens at 43.3°C (110°F).

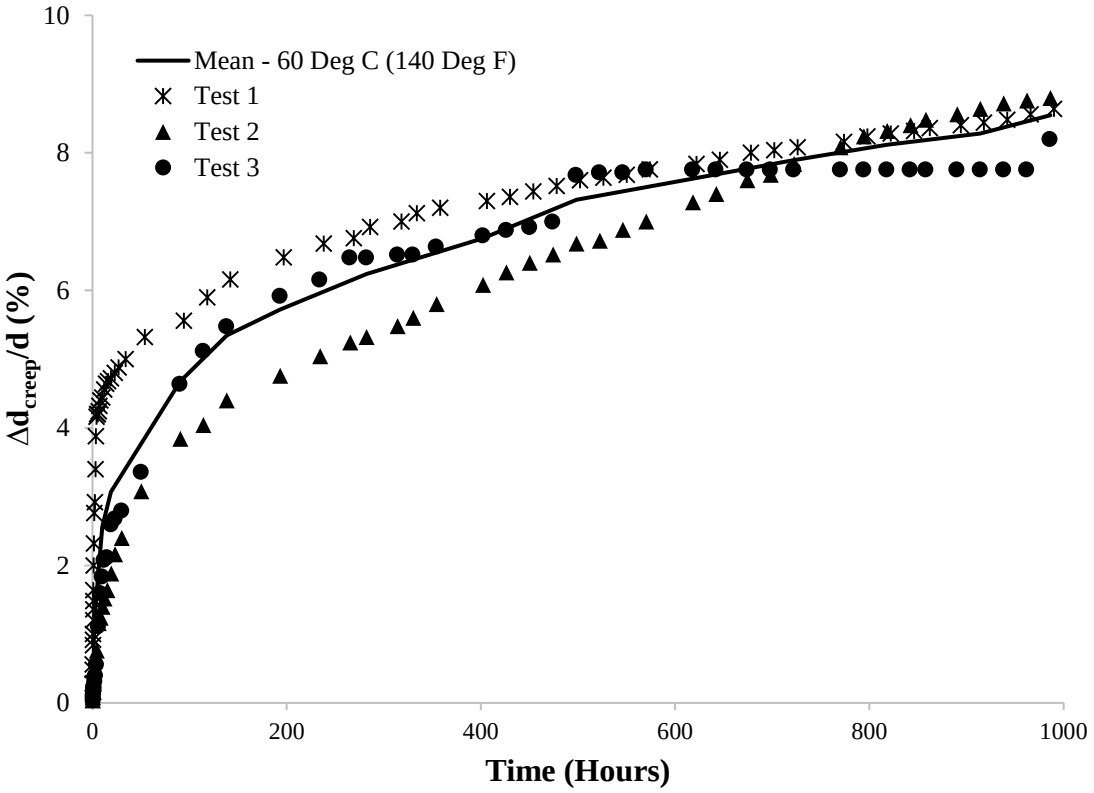

Figure B.8 Creep component of the percent bolt-hole deformation – sustained load level of 50% of mean bearing strength (close-fit, laterally unrestrained specimens at 60°C (140°F).

APPENDIX C

TABULATED RESULTS - CREEP TESTS

Table C.1 Experimental creep data – sustained load level of 50% of mean bearing strength (close-fit, laterally unrestrained specimens).

Test 1		Test 2		Test 3		Average		Findley's Model	
Time (Hours)	**$\Delta d_{creep}/d$ (%)**	**Time (Hours)**	**$\Delta d_{creep}/d$ (%)**	**Time (Hours)**	**$\Delta d_{creep}/d$ (%)**	**Time (Hours)**	**$\Delta d_{creep}/d$ (%)**	**Time (Hours)**	**$\Delta d_{creep}/d$ (%)**
0.10	0.08	0.10	0.06	0.10	0.04	0.10	0.06	0.10	0.04
0.20	0.08	0.20	0.06	0.20	0.04	0.20	0.06	0.20	0.05
0.30	0.08	0.30	0.06	0.30	0.04	0.30	0.06	0.30	0.06
0.40	0.12	0.40	0.06	0.40	0.04	0.40	0.07	0.40	0.07
0.50	0.12	0.50	0.06	0.50	0.04	0.50	0.07	0.50	0.07
0.60	0.12	0.60	0.06	0.60	0.04	0.60	0.07	0.60	0.08
0.70	0.14	0.70	0.06	0.70	0.04	0.70	0.08	0.70	0.08
0.80	0.14	0.80	0.06	0.80	0.04	0.80	0.08	0.80	0.08
0.90	0.14	0.90	0.08	0.90	0.04	0.90	0.09	0.90	0.09
1.00	0.16	1.00	0.08	1.00	0.04	1.00	0.09	1.00	0.09
1.25	0.16	2.50	0.12	2.50	0.06	2.50	0.11	2.00	0.11
1.50	0.16	3.50	0.12	3.50	0.08	3.50	0.12	5.00	0.15

Table C.1 Continued

Test 1		Test 2		Test 3		Average		Findley's Model	
Time (Hours)	**$\Delta d_{creep}/d$ (%)**	**Time (Hours)**	**$\Delta d_{creep}/d$ (%)**	**Time (Hours)**	**$\Delta d_{creep}/d$ (%)**	**Time (Hours)**	**$\Delta d_{creep}/d$ (%)**	**Time (Hours)**	**$\Delta d_{creep}/d$ (%)**
2.00	0.16	4.50	0.12	4.50	0.10	5.50	0.13	10.00	0.18
2.83	0.16	5.50	0.12	5.50	0.10	7.50	0.18	20.00	0.23
3.83	0.16	6.50	0.16	6.50	0.14	9.50	0.19	50.00	0.30
5.83	0.16	7.50	0.18	7.50	0.20	11.50	0.21	100.00	0.38
7.83	0.16	8.50	0.18	8.50	0.20	13.50	0.21	150.00	0.43
9.83	0.20	9.50	0.18	9.50	0.20	11.50	0.21	200.00	0.47
11.83	0.24	10.50	0.20	10.50	0.20	17.50	0.21	250.00	0.51
13.83	0.24	11.50	0.20	11.50	0.20	78.50	0.28	300.00	0.54
17.83	0.24	12.50	0.20	12.50	0.20	121.50	0.31	350.00	0.57
21.83	0.24	13.50	0.20	13.50	0.20	146.50	0.37	400.00	0.60
49.83	0.24	14.50	0.20	14.50	0.20	194.50	0.43	450.00	0.62
77.83	0.28	15.50	0.20	15.50	0.20	218.50	0.49	500.00	0.64
97.83	0.28	16.50	0.20	16.50	0.20	290.50	0.53	550.00	0.66
122.83	0.34	17.50	0.20	17.50	0.20	338.50	0.55	600.00	0.68
145.83	0.38	34.50	0.28	34.50	0.26	386.50	0.57	650.00	0.70
187.83	0.42	57.50	0.28	57.50	0.28	458.50	0.61	700.00	0.72
221.83	0.44	78.50	0.28	78.50	0.28	508.50	0.69	750.00	0.73

Table C.1 Continued

Test 1		Test 2		Test 3		Average		Findley's Model	
Time (Hours)	**$\Delta d_{creep}/d$ (%)**	**Time (Hours)**	**$\Delta d_{creep}/d$ (%)**	**Time (Hours)**	**$\Delta d_{creep}/d$ (%)**	**Time (Hours)**	**$\Delta d_{creep}/d$ (%)**	**Time (Hours)**	**$\Delta d_{creep}/d$ (%)**
289.83	0.44	121.50	0.28	121.50	0.30	580.50	0.71	800.00	0.75
330.83	0.46	146.50	0.30	146.50	0.42	652.50	0.71	850.00	0.77
380.83	0.50	194.50	0.36	194.50	0.50	752.50	0.71	900.00	0.78
428.83	0.64	218.50	0.44	218.50	0.58	847.50	0.79	950.00	0.79
452.83	0.64	266.50	0.52	266.50	0.63	986.50	0.85	1000.00	0.81
476.83	0.64	290.50	0.52	290.50	0.63				
524.83	0.70	314.50	0.54	314.50	0.63				
554.83	0.70	338.50	0.56	338.50	0.63				
620.83	0.70	386.50	0.56	386.50	0.64				
666.83	0.72	408.50	0.56	408.50	0.64				
700.83	0.72	458.50	0.56	458.50	0.64				
723.83	0.72	508.50	0.64	508.50	0.76				
744.83	0.72	580.50	0.64	580.50	0.78				
787.83	0.72	652.50	0.64	652.50	0.78				
812.83	0.72	676.50	0.64	676.50	0.78				
860.83	0.72	752.50	0.64	752.50	0.78				
932.83	0.74	794.50	0.64	794.50	0.90				

Table C.1 Continued

Test 1		**Test 2**		**Test 3**		**Average**		**Findley's Model**	
Time (Hours)	**$\Delta d_{creep}/d$ (%)**	**Time (Hours)**	**$\Delta d_{creep}/d$ (%)**	**Time (Hours)**	**$\Delta d_{creep}/d$ (%)**	**Time (Hours)**	**$\Delta d_{creep}/d$ (%)**	**Time (Hours)**	**$\Delta d_{creep}/d$ (%)**
956.83	0.74	847.50	0.64	847.50	1.02				
980.83	0.78	871.50	0.68	871.50	1.06				
1004.83	0.78	890.50	0.68	890.50	1.06				
		986.50	0.70	986.50	1.06				
		1010.50	0.72	1010.50	1.06				

Table C.2 Experimental creep data – sustained load level of 65% of mean bearing strength (close-fit, laterally unrestrained specimens).

Test 1		Test 2		Test 3,4			Test 5,6			Average		Findley's Model	
					Test 3	Test 4		Test 5	Test 6				
Time (Hours)	$\Delta d_{creep}/d$ (%)	Time (Hours)	$\Delta d_{creep}/d$ (%)	Time (Hours)	$\Delta d_{creep}/d$ (%)	$\Delta d_{creep}/d$ (%)	Time (Hours)	$\Delta d_{creep}/d$ (%)	$\Delta d_{creep}/d$ (%)	Time (Hours)	$\Delta d_{creep}/d$ (%)	Time (Hours)	$\Delta d_{creep}/d$ (%)
0.10	0.16	0.10	0.00	0.10	0.12	0.04	0.10	0.00	0.00	0.10	0.11	0.10	0.32
0.20	0.24	0.20	0.00	0.20	0.16	0.20	0.20	0.04	0.00	0.20	0.16	0.20	0.35
0.30	0.32	0.30	0.04	0.30	0.24	0.32	0.30	0.04	0.00	0.30	0.19	0.30	0.37
0.40	0.40	0.40	0.04	0.40	0.24	0.36	0.40	0.04	0.00	0.40	0.22	0.40	0.39
0.50	0.40	0.50	0.04	0.50	0.28	0.40	0.50	0.04	0.00	0.50	0.23	0.50	0.41
0.60	0.40	0.60	0.04	0.60	0.28	0.40	0.60	0.04	0.00	0.60	0.23	0.60	0.42
0.70	0.40	0.70	0.04	0.70	0.32	0.44	0.70	0.04	0.00	0.70	0.25	0.70	0.43
0.80	0.40	0.80	0.04	0.80	0.32	0.44	0.80	0.12	0.08	1.00	0.25	0.80	0.44
0.90	0.40	0.90	0.04	0.90	0.32	0.44	0.90	0.12	0.08	2.00	0.29	0.90	0.45
1.00	0.40	1.00	0.08	1.00	0.36	0.44	1.00	0.12	0.08	9.83	0.53	1.00	0.45
1.25	0.40	1.25	0.12	1.25	0.36	0.44	1.25	0.12	0.08	20.83	0.69	2.00	0.51
1.50	0.44	1.50	0.12	1.50	0.36	0.48	1.75	0.20	0.08	47.70	0.78	5.00	0.59
1.75	0.44	1.75	0.12	1.75	0.36	0.48	2.00	0.20	0.08	95.83	0.98	10.00	0.66
2.00	0.44	2.00	0.12	2.00	0.36	0.52	3.00	0.20	0.08	211.70	1.09	20.00	0.74

Table C.2 Continued

Test 1		Test 2		Test 3,4			Test 5,6			Average		Findley's Model	
					Test 3	Test 4		Test 5	Test 6				
Time (Hours)	**$\Delta d_{creep}/d$ (%)**	**Time (Hours)**	**$\Delta d_{creep}/d$ (%)**	**Time (Hours)**	**$\Delta d_{creep}/d$ (%)**	**$\Delta d_{creep}/d$ (%)**	**Time (Hours)**	**$\Delta d_{creep}/d$ (%)**	**$\Delta d_{creep}/d$ (%)**	**Time (Hours)**	**$\Delta d_{creep}/d$ (%)**	**Time (Hours)**	**$\Delta d_{creep}/d$ (%)**
2.25	0.44	2.25	0.12	2.25	0.40	0.56	3.50	0.24	0.12	333.83	1.21	50.00	0.86
2.50	0.44	2.50	0.12	2.50	0.40	0.56	4.00	0.24	0.12	432.70	1.25	100.00	0.96
2.75	0.44	2.75	0.12	2.75	0.44	0.56	5.00	0.24	0.12	499.70	1.28	150.00	1.03
3.00	0.44	3.00	0.12	3.00	0.44	0.56	6.00	0.24	0.12	623.00	1.33	200.00	1.08
3.25	0.44	3.25	0.12	4.00	0.48	0.60	7.00	0.28	0.12	695.00	1.34	250.00	1.13
3.50	0.44	3.50	0.16	4.70	0.48	0.60	9.00	0.28	0.12	1000.00	1.37	300.00	1.16
3.75	0.44	3.75	0.16	5.70	0.52	0.64	10.00	0.28	0.12			350.00	1.19
4.83	0.44	4.83	0.16	6.70	0.52	0.64	12.00	0.28	0.12			400.00	1.22
5.83	0.44	5.83	0.16	7.70	0.52	0.68	13.00	0.28	0.12			450.00	1.25
6.83	1.24	6.83	0.16	8.70	0.56	0.72	14.00	0.32	0.12			500.00	1.27
7.83	1.24	7.83	0.20	9.70	0.56	0.72	15.00	0.32	0.12			550.00	1.29
8.83	1.28	8.83	0.20	10.70	0.56	0.72	16.00	0.32	0.12			600.00	1.31
9.83	1.32	9.83	0.20	11.70	0.56	0.72	17.00	0.32	0.12			650.00	1.33
10.83	1.36	10.83	0.24	12.70	0.60	0.76	18.00	0.32	0.12			700.00	1.34
11.83	1.36	73.83	1.28	13.70	0.60	0.76	19.00	0.32	0.12			750.00	1.36
12.83	1.36	89.83	1.28	16.70	0.60	0.84	20.00	0.32	0.12			800.00	1.38

Table C.2 Continued

Test 1		Test 2		Test 3,4			Test 5,6			Average		Findley's Model	
					Test 3	Test 4		Test 5	Test 6				
Time (Hours)	$\Delta d_{creep}/d$ (%)	Time (Hours)	$\Delta d_{creep}/d$ (%)	Time (Hours)	$\Delta d_{creep}/d$ (%)	$\Delta d_{creep}/d$ (%)	Time (Hours)	$\Delta d_{creep}/d$ (%)	$\Delta d_{creep}/d$ (%)	Time (Hours)	$\Delta d_{creep}/d$ (%)	Time (Hours)	$\Delta d_{creep}/d$ (%)
13.83	1.40	95.83	1.32	17.70	0.60	0.84	21.00	0.32	0.14			850.00	1.39
14.83	1.44	143.83	1.32	18.70	0.64	0.84	22.00	0.32	0.16			900.00	1.40
15.83	1.44	162.83	1.32	19.70	0.64	0.84	23.00	0.32	0.20			950.00	1.42
16.83	1.44	169.83	1.32	20.70	0.64	0.84	24.00	0.32	0.20			1000.00	1.43
17.83	1.48	187.83	1.32	21.70	0.64	0.84	45.00	0.32	0.20				
18.83	1.48	211.83	1.32	22.70	0.64	0.84	76.00	0.32	0.24				
19.83	1.48	241.83	1.36	23.70	0.64	0.84	100.00	0.56	0.24				
20.83	1.52	256.83	1.36	39.70	0.68	0.88	119.00	0.56	0.32				
21.83	1.52	333.83	1.56	47.70	0.76	0.92	143.00	0.56	0.32				
22.83	1.52	358.83	1.56	95.70	0.84	1.04	167.00	0.56	0.32				
23.83	1.52	384.83	1.60	116.70	0.84	1.08	190.00	0.56	0.32				
24.83	1.52	403.83	1.60	141.70	0.96	1.16	215.00	0.60	0.32				
25.83	1.52	428.83	1.60	167.70	0.96	1.16	265.00	0.60	0.32				
43.83	1.64	481.83	1.60	186.70	0.96	1.16	287.00	0.60	0.32				
48.83	1.72	498.83	1.60	211.70	0.96	1.20	334.00	0.60	0.32				
65.83	1.80	529.83	1.60	264.70	0.96	1.20	364.00	0.60	0.32				

Table C.2 Continued

Test 1		Test 2		Test 3,4			Test 5,6			Average		Findley's Model	
					Test 3	Test 4		Test 5	Test 6				
Time (Hours)	**$\Delta d_{creep}/d$ (%)**	**Time (Hours)**	**$\Delta d_{creep}/d$ (%)**	**Time (Hours)**	**$\Delta d_{creep}/d$ (%)**	**$\Delta d_{creep}/d$ (%)**	**Time (Hours)**	**$\Delta d_{creep}/d$ (%)**	**$\Delta d_{creep}/d$ (%)**	**Time (Hours)**	**$\Delta d_{creep}/d$ (%)**	**Time (Hours)**	**$\Delta d_{creep}/d$ (%)**
71.00	1.80	549.83	1.60	281.70	0.96	1.20	436.00	0.64	0.36				
73.83	1.84	625.83	1.60	312.70	0.96	1.20	455.00	0.64	0.36				
89.83	1.88	649.83	1.60	332.70	0.96	1.20	481.00	0.68	0.36				
95.83	1.88	668.83	1.60	408.70	0.96	1.20	503.00	0.68	0.36				
143.83	2.04	692.83	1.60	432.70	0.96	1.20	527.00	0.68	0.44				
162.83	2.08	716.83	1.60	451.70	0.96	1.20	575.00	0.76	0.44				
169.83	2.08	739.83	1.60	475.70	1.02	1.24	623.00	0.88	0.44				
187.83	2.12	764.83	1.60	499.70	1.04	1.24	669.00	0.88	0.44				
211.83	2.16	814.83	1.60	522.70	1.04	1.24	695.00	0.88	0.44				
241.83	2.36	836.83	1.60	547.70	1.04	1.24	724.00	0.88	0.44				
256.83	2.40	883.83	1.60	597.70	1.04	1.24	748.00	0.88	0.44				
333.83	2.64	913.83	1.60	619.70	1.04	1.24	774.00	0.88	0.44				
358.83	2.76	985.83	1.60	666.70	1.04	1.24	815.00	0.88	0.44				
384.83	2.76	1004.83	1.60	696.70	1.04	1.24	838.00	0.88	0.44				
403.83	2.76			768.70	1.04	1.24	911.00	0.88	0.44				
428.83	2.76			787.70	1.04	1.24	958.00	0.88	0.44				

Table C.2 Continued

Test 1		Test 2		Test 3,4			Test 5,6			Average		Findley's Model	
					Test 3	Test 4		Test 5	Test 6				
Time (Hours)	**$\Delta d_{creep}/d$ (%)**	**Time (Hours)**	**$\Delta d_{creep}/d$ (%)**	**Time (Hours)**	**$\Delta d_{creep}/d$ (%)**	**$\Delta d_{creep}/d$ (%)**	**Time (Hours)**	**$\Delta d_{creep}/d$ (%)**	**$\Delta d_{creep}/d$ (%)**	**Time (Hours)**	**$\Delta d_{creep}/d$ (%)**	**Time (Hours)**	**$\Delta d_{creep}/d$ (%)**
481.83	2.76			813.70	1.04	1.24	1007.00	0.88	0.52				
498.83	2.76			835.70	1.04	1.24							
529.83	2.80			859.70	1.04	1.24							
549.83	2.80			907.70	1.04	1.24							
625.83	2.80			955.70	1.04	1.24							
649.83	2.84			1001.70	1.04	1.24							
692.83	2.84												
716.83	2.84												
739.83	2.92												
764.83	2.92												
814.83	2.92												
836.83	2.92												
883.83	2.92												
913.83	2.92												
985.83	2.92												
1004.83	2.92												

Table C.3 Experimental creep data – sustained load level of 70% of mean bearing strength (close-fit, laterally unrestrained specimens).

Test 1		Test 2		Test 3		Average		Findley's Model	
Time (Hours)	**$\Delta d_{creep}/d$ (%)**	**Time (Hours)**	**$\Delta d_{creep}/d$ (%)**	**Time (Hours)**	**$\Delta d_{creep}/d$ (%)**	**Time (Hours)**	**$\Delta d_{creep}/d$ (%)**	**Time (Hours)**	**$\Delta d_{creep}/d$ (%)**
0.10	0.12	0.10	0.08	0.10	0.06	0.10	0.09	0.10	0.27
0.20	0.14	0.20	0.16	0.20	0.06	0.20	0.12	0.20	0.31
0.30	0.20	0.30	0.24	0.30	0.06	0.30	0.17	0.30	0.34
0.40	0.24	0.40	0.26	0.40	0.06	0.40	0.19	0.40	0.36
0.50	0.24	0.50	0.30	0.50	0.06	0.50	0.20	0.50	0.38
0.60	0.28	0.60	0.32	0.60	0.32	0.60	0.31	0.60	0.40
0.70	0.30	0.70	0.36	0.70	0.32	0.70	0.33	0.70	0.41
0.80	0.30	0.80	0.36	0.80	0.32	0.80	0.33	0.80	0.42
0.90	0.32	0.90	0.40	0.90	0.34	0.90	0.35	0.90	0.43
1.00	0.32	1.00	0.44	1.00	0.36	1.00	0.37	1.00	0.45
1.08	0.34	1.25	0.48	1.25	0.40	1.25	0.41	2.00	0.52
1.33	0.36	1.50	0.52	1.50	0.40	2.00	0.36	5.00	0.64
1.87	0.38	1.75	0.60	1.75	0.40	2.92	0.59	10.00	0.75
2.37	0.42	2.00	0.64	1.98	0.40	5.48	0.70	20.00	0.89
2.87	0.44	2.25	0.68	2.23	0.44	10.48	0.81	50.00	1.10

Table C.3 Continued

Test 1		Test 2		Test 3		Average		Findley's Model	
Time (Hours)	**$\Delta d_{creep}/d$ (%)**	**Time (Hours)**	**$\Delta d_{creep}/d$ (%)**	**Time (Hours)**	**$\Delta d_{creep}/d$ (%)**	**Time (Hours)**	**$\Delta d_{creep}/d$ (%)**	**Time (Hours)**	**$\Delta d_{creep}/d$ (%)**
3.37	0.44	2.50	0.72	2.48	0.44	20.48	0.96	100.00	1.30
3.87	0.48	2.75	0.74	2.73	0.48	81.48	1.18	150.00	1.44
4.37	0.50	2.92	0.80	2.98	0.52	167.48	1.33	200.00	1.54
4.87	0.50	3.17	0.82	3.23	0.52	221.48	1.49	250.00	1.63
5.37	0.52	3.42	0.82	3.48	0.52	310.48	1.63	300.00	1.70
6.37	0.60	3.67	0.84	3.73	0.56	432.48	1.75	350.00	1.77
7.37	0.60	3.92	0.88	3.98	0.56	526.48	1.86	400.00	1.83
8.37	0.60	4.17	0.92	4.48	0.60	622.48	2.00	450.00	1.88
9.37	0.60	4.67	0.96	5.48	0.62	722.48	2.19	500.00	1.93
10.37	0.60	5.67	0.96	6.48	0.64	818.48	2.37	550.00	1.98
12.37	0.60	6.67	1.04	7.48	0.66	891.67	2.44	600.00	2.02
13.37	0.60	7.67	1.08	8.48	0.68	984.48	2.72	650.00	2.06
14.37	0.64	8.67	1.08	9.48	0.68			700.00	2.10
15.37	0.64	9.67	1.12	10.48	0.68			750.00	2.13
16.37	0.68	10.67	1.16	12.48	0.68			800.00	2.17
17.37	0.68	11.67	1.16	18.48	0.68			850.00	2.20
18.37	0.68	13.67	1.22	20.48	0.80			900.00	2.23

Table C.3 Continued

Test 1		Test 2		Test 3		Average		Findley's Model	
Time (Hours)	**$\Delta d_{creep}/d$ (%)**	**Time (Hours)**	**$\Delta d_{creep}/d$ (%)**	**Time (Hours)**	**$\Delta d_{creep}/d$ (%)**	**Time (Hours)**	**$\Delta d_{creep}/d$ (%)**	**Time (Hours)**	**$\Delta d_{creep}/d$ (%)**
19.37	0.68	19.67	1.28	22.48	0.80			950.00	2.26
20.37	0.68	21.67	1.32	23.48	0.80			1000.00	2.29
21.37	0.68	24.00	1.36	58.48	0.88				
22.37	0.68	59.67	1.60	81.48	1.04				
23.37	0.72	82.67	1.76	117.48	1.12				
24.37	0.72	118.67	1.92	124.48	1.16				
47.37	0.72	125.67	1.94	143.48	1.16				
68.37	0.72	144.67	1.96	147.48	1.16				
108.37	0.74	148.67	1.96	167.48	1.16				
131.37	0.76	168.67	2.00	188.48	1.16				
167.37	0.82	189.67	2.10	221.48	1.44				
174.37	0.84	222.67	2.20	244.48	1.44				
193.37	0.84	245.67	2.24	285.48	1.44				
197.37	0.84	286.67	2.36	292.48	1.54				
217.37	0.84	293.67	2.42	310.48	1.54				
238.37	0.84	311.67	2.50	315.48	1.58				
271.37	0.84	316.67	2.56	356.48	1.60				

Table C.3 Continued

Test 1		Test 2		Test 3		Average		Findley's Model	
Time (Hours)	**$\Delta d_{creep}/d$ (%)**	**Time (Hours)**	**$\Delta d_{creep}/d$ (%)**	**Time (Hours)**	**$\Delta d_{creep}/d$ (%)**	**Time (Hours)**	**$\Delta d_{creep}/d$ (%)**	**Time (Hours)**	**$\Delta d_{creep}/d$ (%)**
294.37	0.84	357.67	2.62	388.48	1.60				
335.37	0.84	389.67	2.68	432.48	1.60				
342.37	0.88	433.67	2.74	458.48	1.64				
360.37	0.88	459.67	2.80	526.48	1.68				
365.37	0.88	527.67	3.00	551.48	1.68				
406.37	0.90	552.67	3.02	622.48	1.72				
438.37	0.90	623.67	3.36	646.48	1.72				
482.37	0.90	647.67	3.44	681.48	1.76				
508.37	0.90	682.67	3.50	698.48	1.76				
576.37	0.92	699.67	3.50	722.48	1.78				
601.37	0.92	723.67	3.88	746.48	1.80				
672.37	0.92	747.67	3.98	818.48	1.82				
696.37	0.92	819.67	4.36	842.48	1.82				
731.37	0.92	843.67	4.40	890.48	1.82				
748.37	0.92	891.67	4.56	916.48	1.82				
772.37	0.92	917.67	4.58	964.48	1.88				
796.37	0.92	965.67	4.92	984.48	1.92				

Table C.3 Continued

Test 1		Test 2		Test 3		Average		Findley's Model	
Time (Hours)	**$\Delta d_{creep}/d$ (%)**	**Time (Hours)**	**$\Delta d_{creep}/d$ (%)**	**Time (Hours)**	**$\Delta d_{creep}/d$ (%)**	**Time (Hours)**	**$\Delta d_{creep}/d$ (%)**	**Time (Hours)**	**$\Delta d_{creep}/d$ (%)**
868.37	0.94	985.67	5.28	1005.48	1.92				
892.37	0.94	1006.67	5.46						
940.37	0.96								
966.37	0.96								
1014.37	0.96								

Table C.4 Experimental creep data – sustained load level of 50% of mean bearing strength (close-fit, moderately torqued specimens).

Test 1			Test 2			Test 3			Average		Findley's Model	
Time (Hours)	**$\Delta d_{creep}/d$ (%)**	**$\Delta d_{creep}/d$ (%)**	**Time (Hours)**	**$\Delta d_{creep}/d$ (%)**	**$\Delta d_{creep}/d$ (%)**	**Time (Hours)**	**$\Delta d_{creep}/d$ (%)**	**$\Delta d_{creep}/d$ (%)**	**Time (Hours)**	**$\Delta d_{creep}/d$ (%)**	**Time (Hours)**	**$\Delta d_{creep}/d$ (%)**
0.10	0.10	0.16	0.10	0.12	0.00	0.10	0.04	0.08	0.10	0.10	0.10	0.20
0.20	0.18	0.28	0.20	0.18	0.04	0.20	0.04	0.12	0.20	0.14	0.20	0.23
0.30	0.22	0.36	0.30	0.26	0.08	0.30	0.04	0.16	0.30	0.19	0.30	0.25
0.40	0.26	0.48	0.40	0.28	0.10	0.40	0.04	0.20	0.40	0.23	0.40	0.27
0.50	0.26	0.50	0.50	0.30	0.12	0.50	0.04	0.20	0.50	0.24	0.50	0.28
0.60	0.34	0.56	0.60	0.34	0.18	0.60	0.04	0.20	0.60	0.28	0.60	0.29
0.70	0.38	0.64	0.70	0.38	0.24	0.70	0.04	0.24	0.70	0.32	0.70	0.30
0.80	0.38	0.64	0.80	0.42	0.28	0.80	0.08	0.24	0.80	0.34	0.80	0.31
0.90	0.38	0.70	0.90	0.42	0.28	0.90	0.08	0.28	0.90	0.36	0.90	0.32
1.00	0.40	0.72	1.00	0.46	0.28	1.00	0.12	0.28	1.00	0.38	1.00	0.33
1.23	0.42	0.76	1.43	0.50	0.42	1.50	0.12	0.28	10.87	0.55	2.00	0.39
1.87	0.42	0.80	1.93	0.50	0.42	3.50	0.12	0.34	20.87	0.69	5.00	0.49
2.37	0.50	0.92	2.93	0.50	0.44	6.50	0.12	0.40	50.93	0.80	10.00	0.58
2.87	0.50	0.94	4.93	0.54	0.44	7.50	0.24	0.40	98.93	0.88	20.00	0.69
3.87	0.50	0.96	7.93	0.58	0.44	8.50	0.24	0.40	190.93	1.42	50.00	0.88
5.87	0.50	1.00	8.93	0.58	0.44	9.50	0.24	0.44	310.93	1.54	100.00	1.07

Table C.4 Continued

Test 1			Test 2			Test 3			Average		Findley's Model	
Time (Hours)	**$\Delta d_{creep}/d$ (%)**	**$\Delta d_{creep}/d$ (%)**	**Time (Hours)**	**$\Delta d_{creep}/d$ (%)**	**$\Delta d_{creep}/d$ (%)**	**Time (Hours)**	**$\Delta d_{creep}/d$ (%)**	**$\Delta d_{creep}/d$ (%)**	**Time (Hours)**	**$\Delta d_{creep}/d$ (%)**	**Time (Hours)**	**$\Delta d_{creep}/d$ (%)**
8.87	0.54	1.04	9.93	0.58	0.44	10.50	0.24	0.44	414.93	1.59	150.00	1.20
9.87	0.54	1.04	10.93	0.62	0.44	14.50	0.24	0.48	481.93	1.70	200.00	1.30
10.87	0.54	1.04	11.93	0.62	0.44	18.50	0.34	0.52	577.93	1.83	250.00	1.39
11.87	0.54	1.04	15.93	0.64	0.46	21.50	0.80	0.60	673.93	1.88	300.00	1.46
12.87	0.54	1.04	19.93	0.72	0.46	49.50	0.96	0.80	786.93	1.98	350.00	1.53
16.87	0.54	1.04	22.93	0.74	0.48	77.50	0.96	0.88	858.93	2.02	400.00	1.59
20.87	0.54	1.04	50.93	0.86	0.60	97.50	0.96	0.92	956.93	2.03	450.00	1.64
23.87	0.54	1.04	78.93	1.02	0.72	139.00	1.36	1.24	1000.00	2.05	500.00	1.70
51.87	0.54	1.04	98.93	1.10	0.72	163.50	1.38	1.40			550.00	1.75
79.87	0.54	1.04	140.43	1.20	1.36	189.50	1.42	1.56			600.00	1.79
99.87	0.54	1.04	164.93	1.22	1.36	240.50	1.56	1.80			650.00	1.83
141.37	1.02	1.36	190.93	1.30	1.48	263.50	1.56	1.84			700.00	1.88
165.87	1.10	1.60	241.93	1.38	1.50	309.50	1.58	1.88			750.00	1.91
191.87	1.10	1.64	264.93	1.38	1.50	333.50	1.60	1.96			800.00	1.95
242.87	1.10	1.68	310.93	1.42	1.50	357.50	1.60	1.96			850.00	1.99
265.87	1.10	1.68	334.93	1.46	1.50	413.50	1.60	2.00			900.00	2.02
311.87	1.12	1.74	358.93	1.46	1.50	432.50	1.60	2.04			950.00	2.06

Table C.4 Continued

Test 1			Test 2			Test 3			Average		Findley's Model	
Time (Hours)	**$\Delta d_{creep}/d$ (%)**	**$\Delta d_{creep}/d$ (%)**	**Time (Hours)**	**$\Delta d_{creep}/d$ (%)**	**$\Delta d_{creep}/d$ (%)**	**Time (Hours)**	**$\Delta d_{creep}/d$ (%)**	**$\Delta d_{creep}/d$ (%)**	**Time (Hours)**	**$\Delta d_{creep}/d$ (%)**	**Time (Hours)**	**$\Delta d_{creep}/d$ (%)**
335.87	1.14	1.78	414.93	1.50	1.50	480.50	1.68	2.12			1000.00	2.09
359.87	1.14	1.78	433.93	1.50	1.50	528.50	1.76	2.20				
415.87	1.18	1.78	481.93	1.58	1.76	576.50	1.76	2.26				
434.87	1.18	1.80	529.93	1.66	2.00	593.50	1.76	2.28				
482.87	1.22	1.84	577.93	1.72	2.02	617.50	1.76	2.32				
530.87	1.26	1.88	594.93	1.74	2.02	672.50	1.80	2.36				
578.87	1.30	1.92	618.93	1.74	2.04	689.50	1.80	2.38				
595.87	1.30	1.92	673.93	1.78	2.04	747.50	1.80	2.40				
619.87	1.32	1.92	690.93	1.80	2.04	785.50	1.84	2.48				
674.87	1.34	1.96	748.93	1.80	2.04	809.50	1.84	2.48				
691.87	1.34	2.00	786.93	1.86	2.24	857.50	1.86	2.52				
749.87	1.34	2.00	810.93	1.92	2.24	907.50	1.86	2.52				
787.87	1.42	2.04	858.93	1.96	2.24	931.50	1.86	2.54				
811.87	1.42	2.04	908.93	1.96	2.24	955.50	1.86	2.54				
859.87	1.46	2.08	932.93	1.98	2.24	1010.50	1.88	2.60				
909.87	1.46	2.08	956.93	1.98	2.24							
933.87	1.46	2.08	1011.93	2.00	2.24							

Table C.4 Continued

Test 1			Test 2			Test 3			Average		Findley's Model	
Time (Hours)	**$\Delta d_{creep}/d$ (%)**	**$\Delta d_{creep}/d$ (%)**	**Time (Hours)**	**$\Delta d_{creep}/d$ (%)**	**$\Delta d_{creep}/d$ (%)**	**Time (Hours)**	**$\Delta d_{creep}/d$ (%)**	**$\Delta d_{creep}/d$ (%)**	**Time (Hours)**	**$\Delta d_{creep}/d$ (%)**	**Time (Hours)**	**$\Delta d_{creep}/d$ (%)**
957.87	1.46	2.10										
1012.87	1.46	2.10										

Table C.5 Experimental creep data – sustained load level of 50% of mean bearing strength (1.6 mm (1/16 in) bolt-hole clearance, laterally unrestrained specimens).

Test 1,2			Test 3		Test 4		Average		Findley's Model	
	Test 1	Test 2								
Time (Hours)	$\Delta d_{creep}/d$ (%)	$\Delta d_{creep}/d$ (%)	Time (Hours)	$\Delta d_{creep}/d$ (%)	Time (Hours)	$\Delta d_{creep}/d$ (%)	Time (Hours)	$\Delta d_{creep}/d$ (%)	Time (Hours)	$\Delta d_{creep}/d$ (%)
0.10	0.16	0.40	0.10	0.32	0.10	0.04	0.10	0.23	0.10	0.31
0.20	0.24	0.50	0.20	0.48	0.20	0.12	0.20	0.34	0.20	0.37
0.30	0.24	0.56	0.30	0.52	0.30	0.20	0.30	0.38	0.30	0.41
0.40	0.28	0.64	0.40	0.58	0.40	0.24	0.40	0.44	0.40	0.44
0.50	0.32	0.68	0.50	0.64	0.50	0.28	0.50	0.48	0.50	0.47
0.60	0.32	0.72	0.60	0.72	0.60	0.32	0.60	0.52	0.60	0.49
0.70	0.36	0.80	0.70	0.74	0.70	0.32	0.70	0.56	0.70	0.51
0.80	0.36	0.80	0.80	0.76	0.80	0.32	0.80	0.56	0.80	0.53
0.90	0.38	0.80	0.90	0.80	0.90	0.32	0.90	0.58	0.90	0.54
1.00	0.40	0.84	1.00	0.80	1.00	0.32	1.00	0.59	1.00	0.56
1.25	0.44	0.88	1.25	0.88	1.58	0.32	2.00	0.68	2.00	0.67
1.50	0.46	0.90	1.75	0.96	2.08	0.32	5.42	0.90	5.00	0.85
1.75	0.46	0.90	2.25	1.04	4.08	0.56	9.42	1.02	10.00	1.01
2.00	0.48	0.92	2.75	1.12	6.08	0.64	19.42	1.19	20.00	1.22

Table C.5 Continued

Test 1,2			Test 3		Test 4		Average		Findley's Model	
	Test 1	Test 2								
Time (Hours)	$\Delta d_{creep}/d$ (%)	$\Delta d_{creep}/d$ (%)	Time (Hours)	$\Delta d_{creep}/d$ (%)	Time (Hours)	$\Delta d_{creep}/d$ (%)	Time (Hours)	$\Delta d_{creep}/d$ (%)	Time (Hours)	$\Delta d_{creep}/d$ (%)
2.42	0.52	0.96	4.75	1.24	8.08	0.72	48.42	1.41	50.00	1.56
2.92	0.52	1.00	6.75	1.30	10.08	0.78	92.42	1.58	100.00	1.88
3.42	0.56	1.04	8.75	1.40	12.08	0.80	189.42	2.10	150.00	2.09
5.42	0.64	1.08	10.75	1.44	16.08	0.84	288.42	2.40	200.00	2.26
7.42	0.66	1.10	12.75	1.46	18.08	0.86	379.92	2.75	250.00	2.41
9.42	0.70	1.20	16.75	1.62	20.08	0.88	477.42	3.10	300.00	2.53
11.42	0.72	1.24	18.75	1.62	22.08	0.88	593.42	3.29	350.00	2.64
13.42	0.72	1.24	20.75	1.66	47.08	1.08	623.92	3.35	400.00	2.74
17.42	0.84	1.36	22.75	1.66	71.08	1.20	692.42	3.46	450.00	2.83
19.42	0.88	1.36	47.75	1.96	91.08	1.28	814.42	3.60	500.00	2.91
21.42	0.88	1.40	71.75	2.12	116.08	1.32	913.42	3.69	550.00	2.99
23.42	0.88	1.40	91.75	2.24	140.08	1.40	1000.00	3.73	600.00	3.06
48.42	1.08	1.52	116.75	2.44	164.08	1.44			650.00	3.13
72.42	1.10	1.60	140.75	3.00	188.08	1.52			700.00	3.20
92.42	1.10	1.68	164.75	3.36	219.08	1.56			750.00	3.26
117.42	1.22	1.76	188.75	3.72	242.08	1.60			800.00	3.32

Table C.5 Continued

Test 1,2			Test 3		Test 4		Average		Findley's Model	
	Test 1	Test 2								
Time (Hours)	$\Delta d_{creep}/d$ (%)	$\Delta d_{creep}/d$ (%)	Time (Hours)	$\Delta d_{creep}/d$ (%)	Time (Hours)	$\Delta d_{creep}/d$ (%)	Time (Hours)	$\Delta d_{creep}/d$ (%)	Time (Hours)	$\Delta d_{creep}/d$ (%)
141.42	1.26	1.80	219.75	3.96	265.08	1.66			850.00	3.37
165.42	1.28	1.80	242.75	4.16	287.08	1.68			900.00	3.43
189.42	1.28	1.88	265.75	4.32	311.08	1.72			950.00	3.48
220.42	1.32	1.88	287.75	4.52	333.08	1.76			1000.00	3.53
243.42	1.36	1.92	311.75	4.80	356.08	1.84				
266.42	1.36	1.96	333.75	5.00	378.58	1.88				
288.42	1.38	2.00	356.75	5.20	400.08	1.92				
312.42	1.40	2.06	379.25	5.40	425.58	1.92				
334.42	1.40	2.08	400.75	5.56	476.08	1.92				
357.42	1.40	2.20	426.25	5.76	500.08	1.92				
379.92	1.40	2.32	476.75	5.96	528.08	1.92				
401.42	1.40	2.44	500.75	6.04	548.08	1.92				
426.92	1.40	2.56	528.75	6.08	592.08	1.92				
477.42	1.40	3.12	548.75	6.12	622.58	2.04				
501.42	1.40	3.52	592.75	6.24	669.08	2.16				
529.42	1.40	3.56	623.25	6.32	691.08	2.16				

Table C.5 Continued

Test 1,2			Test 3		Test 4		Average		Findley's Model	
	Test 1	Test 2								
Time (Hours)	$\Delta d_{creep}/d$ (%)	$\Delta d_{creep}/d$ (%)	Time (Hours)	$\Delta d_{creep}/d$ (%)	Time (Hours)	$\Delta d_{creep}/d$ (%)	Time (Hours)	$\Delta d_{creep}/d$ (%)	Time (Hours)	$\Delta d_{creep}/d$ (%)
549.42	1.40	3.60	669.75	6.40	813.08	2.24				
593.42	1.40	3.60	691.75	6.44	912.08	2.24				
623.92	1.40	3.64	813.75	6.68	1051.08	2.30				
670.42	1.44	3.74	912.75	6.92						
692.42	1.44	3.80	1051.75	7.08						
814.42	1.46	4.00								
913.42	1.48	4.10								
1052.42	1.56	4.10								

Table C.6 Experimental creep data – sustained load level of 50% of mean bearing strength at 43.3°C (110°F) (close-fit, laterally unrestrained specimens).

Test 1		Test 1		Test 3,4			Average		Findley's Model	
					Test 3	Test 4				
Time (Hours)	$\Delta d_{creep}/d$ (%)	Time (Hours)	$\Delta d_{creep}/d$ (%)	Time (Hours)	$\Delta d_{creep}/d$ (%)	$\Delta d_{creep}/d$ (%)	Time (Hours)	$\Delta d_{creep}/d$ (%)	Time (Hours)	$\Delta d_{creep}/d$ (%)
0.10	0.24	0.10	0.12	0.10	0.28	0.20	0.10	0.21	0.10	0.59
0.20	0.32	0.20	0.20	0.20	0.64	0.44	0.20	0.40	0.20	0.67
0.30	0.36	0.30	0.28	0.30	0.76	0.56	0.30	0.49	0.30	0.72
0.40	0.40	0.40	0.32	0.40	0.84	0.64	0.40	0.55	0.40	0.76
0.50	0.48	0.50	0.32	0.50	0.96	0.72	0.50	0.62	0.50	0.79
0.60	0.56	0.60	0.36	0.60	1.08	0.76	0.60	0.69	0.60	0.81
0.70	0.56	0.70	0.40	0.70	1.16	0.80	0.70	0.73	0.70	0.84
0.80	0.56	0.80	0.44	0.80	1.20	0.84	0.80	0.76	0.80	0.86
0.90	0.60	0.90	0.48	0.90	1.24	0.88	0.90	0.80	0.90	0.88
1.00	0.60	1.00	0.52	1.00	1.28	0.92	1.00	0.83	1.00	0.89
1.25	0.64	2.00	0.60	1.67	1.44	1.00	10.17	1.39	2.00	1.01
1.83	0.72	3.00	0.68	2.17	1.60	1.08	46.17	1.99	5.00	1.19
2.83	0.84	5.00	0.76	4.17	1.80	1.36	100.83	2.11	10.00	1.35
3.83	0.92	7.00	0.80	10.17	2.04	1.40	188.33	2.27	20.00	1.53

Table C.6 Continued

Test 1		Test 1		Test 3,4			Average		Findley's Model	
					Test 3	Test 4				
Time (Hours)	$\Delta d_{creep}/d$ (%)	Time (Hours)	$\Delta d_{creep}/d$ (%)	Time (Hours)	$\Delta d_{creep}/d$ (%)	$\Delta d_{creep}/d$ (%)	Time (Hours)	$\Delta d_{creep}/d$ (%)	Time (Hours)	$\Delta d_{creep}/d$ (%)
5.83	1.04	9.00	0.92	22.67	2.32	1.60	295.83	2.36	50.00	1.80
7.83	1.12	11.00	0.96	46.17	2.68	2.68	388.83	2.40	100.00	2.04
9.83	1.16	13.00	1.00	79.17	2.80	2.76	508.83	2.45	150.00	2.19
11.83	1.16	15.00	1.04	103.17	2.88	2.80	559.17	2.56	200.00	2.31
13.83	1.20	18.00	1.12	130.17	2.96	2.84	677.83	2.85	250.00	2.40
15.83	1.24	23.00	1.16	151.17	3.00	2.88	796.83	3.09	300.00	2.48
18.83	1.28	28.00	1.16	175.17	3.04	2.88	868.83	3.32	350.00	2.55
23.83	1.32	49.00	1.20	190.17	3.08	2.88	964.83	3.48	400.00	2.61
28.83	1.34	73.00	1.20	223.17	3.12	2.88	1000.00	3.49	450.00	2.67
49.83	1.40	100.00	1.20	248.17	3.16	2.88			500.00	2.72
73.83	1.52	125.00	1.20	272.17	3.16	2.88			550.00	2.77
100.83	1.56	163.00	1.20	286.17	3.20	2.88			600.00	2.81
125.83	1.60	187.50	1.40	319.17	3.20	2.88			650.00	2.85
163.83	1.66	211.00	1.40	343.17	3.20	2.88			700.00	2.89
188.33	1.72	244.00	1.42	370.17	3.20	2.88			750.00	2.93
211.83	1.76	268.00	1.46	394.17	3.20	2.88			800.00	2.96

Table C.6 Continued

Test 1		Test 1		Test 3,4			Average		Findley's Model	
					Test 3	Test 4				
Time (Hours)	$\Delta d_{creep}/d$ (%)	Time (Hours)	$\Delta d_{creep}/d$ (%)	Time (Hours)	$\Delta d_{creep}/d$ (%)	$\Delta d_{creep}/d$ (%)	Time (Hours)	$\Delta d_{creep}/d$ (%)	Time (Hours)	$\Delta d_{creep}/d$ (%)
244.83	1.80	295.00	1.50	512.17	3.20	2.92			850.00	2.99
268.83	1.80	316.00	1.54	534.17	3.28	2.92			900.00	3.02
295.83	1.84	340.00	1.56	559.17	3.48	3.04			950.00	3.05
316.83	1.84	355.00	1.56	574.17	3.60	3.04			1000.00	3.08
340.83	1.88	388.00	1.60	607.17	3.72	3.08				
355.83	1.88	413.00	1.60	631.17	3.80	3.08				
388.83	1.92	437.00	1.60	656.17	3.88	3.12				
413.83	1.92	451.00	1.64	679.17	4.00	3.12				
437.83	1.96	484.00	1.64	703.17	4.12	3.16				
451.83	1.96	508.00	1.64	727.17	4.24	3.20				
484.83	2.00	535.00	1.64	751.17	4.36	3.20				
508.83	2.04	559.00	1.64	775.17	4.48	3.20				
535.83	2.08	677.00	2.08	799.17	4.60	3.20				
559.83	2.08	699.00	2.08	870.17	4.80	3.80				
677.83	2.20	724.00	2.08	967.17	5.08	3.80				
699.83	2.20	739.00	2.16	991.17	5.08	3.80				

Table C.6 Continued

Test 1		Test 1		Test 3,4			Average		Findley's Model	
					Test 3	Test 4				
Time (Hours)	**$\Delta d_{creep}/d$ (%)**	**Time (Hours)**	**$\Delta d_{creep}/d$ (%)**	**Time (Hours)**	**$\Delta d_{creep}/d$ (%)**	**$\Delta d_{creep}/d$ (%)**	**Time (Hours)**	**$\Delta d_{creep}/d$ (%)**	**Time (Hours)**	**$\Delta d_{creep}/d$ (%)**
724.83	2.24	772.00	2.24	1006.17	5.08	3.80				
739.83	2.24	796.00	2.32							
772.83	2.24	821.00	2.40							
796.83	2.24	844.00	2.40							
821.83	2.24	868.00	2.40							
844.83	2.28	892.00	2.48							
868.83	2.28	916.00	2.56							
892.83	2.32	940.00	2.64							
916.83	2.32	964.00	2.68							
940.83	2.36	1035.00	2.68							
964.83	2.36									
1035.83	2.40									

Table C.7 Experimental creep data – sustained load level of 50% of mean bearing strength at 60°C (140°F) (close-fit, laterally unrestrained specimens).

Test 1		Test 2		Test 3		Average		Findley's Model	
Time (Hours)	**$\Delta d_{creep}/d$ (%)**	**Time (Hours)**	**$\Delta d_{creep}/d$ (%)**	**Time (Hours)**	**$\Delta d_{creep}/d$ (%)**	**Time (Hours)**	**$\Delta d_{creep}/d$ (%)**	**Time (Hours)**	**$\Delta d_{creep}/d$ (%)**
0.10	0.28	0.10	0.04	0.10	0.04	0.10	0.12	0.10	0.70
0.20	0.48	0.20	0.04	0.20	0.08	0.20	0.20	0.20	0.81
0.30	0.56	0.30	0.08	0.30	0.12	0.30	0.25	0.30	0.89
0.40	0.84	0.40	0.08	0.40	0.16	0.40	0.36	0.40	0.94
0.50	0.92	0.50	0.16	0.50	0.16	0.50	0.41	0.50	0.99
0.60	1.00	0.60	0.16	0.60	0.16	0.60	0.44	0.60	1.03
0.70	1.20	0.70	0.16	0.70	0.20	0.70	0.52	0.70	1.07
0.80	1.36	0.80	0.16	0.80	0.20	0.80	0.57	0.80	1.11
0.90	1.48	0.90	0.16	0.90	0.24	0.90	0.63	0.90	1.14
1.00	1.64	1.00	0.16	1.00	0.24	1.00	0.68	1.00	1.17
1.33	2.00	1.17	0.16	1.83	0.32	2.00	1.15	2.00	1.38
1.67	2.32	1.67	0.28	2.50	0.40	2.50	1.28	5.00	1.74
2.00	2.76	2.67	0.52	3.50	0.56	10.00	2.56	10.00	2.10
2.50	2.92	3.33	0.68	5.50	1.12	19.00	3.07	20.00	2.56
3.00	3.40	4.33	0.76	7.50	1.60	90.33	4.68	50.00	3.38

Table C.7 Continued

Test 1		Test 2		Test 3		Average		Findley's Model	
Time (Hours)	**$\Delta d_{creep}/d$ (%)**	**Time (Hours)**	**$\Delta d_{creep}/d$ (%)**	**Time (Hours)**	**$\Delta d_{creep}/d$ (%)**	**Time (Hours)**	**$\Delta d_{creep}/d$ (%)**	**Time (Hours)**	**$\Delta d_{creep}/d$ (%)**
3.50	3.88	6.33	1.16	9.50	1.84	138.33	5.35	100.00	4.22
4.00	4.16	8.33	1.24	11.50	2.08	193.33	5.72	150.00	4.82
4.75	4.20	10.33	1.40	14.50	2.12	282.33	6.24	200.00	5.32
5.33	4.20	12.33	1.52	18.50	2.60	401.50	6.75	250.00	5.74
6.33	4.24	15.33	1.64	22.50	2.68	498.33	7.32	300.00	6.12
7.00	4.32	19.33	1.88	29.50	2.80	618.33	7.63	350.00	6.46
8.00	4.40	23.33	2.16	49.50	3.36	722.33	7.89	400.00	6.77
10.00	4.44	30.33	2.40	89.50	4.64	818.33	8.12	450.00	7.07
12.00	4.56	50.33	3.08	113.50	5.12	914.33	8.28	500.00	7.34
14.00	4.64	90.33	3.84	137.50	5.48	986.33	8.55	550.00	7.60
16.00	4.68	114.33	4.04	192.50	5.92			600.00	7.84
19.00	4.72	138.33	4.40	233.50	6.16			650.00	8.08
23.00	4.80	193.33	4.76	264.50	6.48			700.00	8.30
27.00	4.88	234.33	5.04	281.50	6.48			750.00	8.51
34.00	5.00	265.33	5.24	313.50	6.52			800.00	8.72
54.00	5.32	282.33	5.32	329.50	6.52			850.00	8.92
94.00	5.56	314.33	5.48	353.50	6.64			900.00	9.11

Table C.7 Continued

Test 1		Test 2		Test 3		Average		Findley's Model	
Time (Hours)	**$\Delta d_{creep}/d$ (%)**	**Time (Hours)**	**$\Delta d_{creep}/d$ (%)**	**Time (Hours)**	**$\Delta d_{creep}/d$ (%)**	**Time (Hours)**	**$\Delta d_{creep}/d$ (%)**	**Time (Hours)**	**$\Delta d_{creep}/d$ (%)**
118.00	5.90	330.33	5.60	401.50	6.80			950.00	9.29
142.00	6.16	354.33	5.80	425.50	6.88			1000.00	9.47
197.00	6.48	402.33	6.08	449.50	6.92				
238.00	6.68	426.33	6.26	473.50	7.00				
269.00	6.76	450.33	6.40	497.50	7.68				
286.00	6.92	474.33	6.52	521.50	7.72				
318.00	7.00	498.33	6.68	545.50	7.72				
334.00	7.12	522.33	6.72	569.50	7.76				
358.00	7.20	546.33	6.88	617.50	7.76				
406.00	7.30	570.33	7.00	641.50	7.76				
430.00	7.36	618.33	7.28	673.50	7.76				
454.00	7.44	642.33	7.40	697.50	7.76				
478.00	7.52	674.33	7.60	721.50	7.76				
502.00	7.60	698.33	7.68	769.50	7.76				
526.00	7.64	722.33	7.84	793.50	7.76				
550.00	7.68	770.33	8.08	817.50	7.76				
574.00	7.76	794.33	8.24	841.50	7.76				

Table C.7 Continued

Test 1		Test 2		Test 3		Average		Findley's Model	
Time (Hours)	**$\Delta d_{creep}/d$ (%)**	**Time (Hours)**	**$\Delta d_{creep}/d$ (%)**	**Time (Hours)**	**$\Delta d_{creep}/d$ (%)**	**Time (Hours)**	**$\Delta d_{creep}/d$ (%)**	**Time (Hours)**	**$\Delta d_{creep}/d$ (%)**
622.00	7.84	818.33	8.32	857.50	7.76				
646.00	7.90	842.33	8.40	889.50	7.76				
678.00	8.00	858.33	8.48	913.50	7.76				
702.00	8.04	890.33	8.56	937.50	7.76				
726.00	8.08	914.33	8.64	961.50	7.76				
774.00	8.16	938.33	8.72	985.50	8.20				
798.00	8.24	962.33	8.76	1009.50	8.20				
822.00	8.28	986.33	8.80						
846.00	8.32	1010.33	8.88						
862.00	8.36								
894.00	8.40								
918.00	8.44								
942.00	8.48								
966.00	8.56								
990.00	8.64								
1014.00	8.68								

APPENDIX D

TEST SETUP – DETAILS OF EQUIPMENT

Short-Term Tests at Ambient Temperature

Short-term tensile and bearing tests were conducted using a computer-controlled hydraulic load actuator located in the SEML at the Georgia Institute of Technology. Tests were carried out in "Static Hydraulic Universal Testing System" by INSTRON SATEC™, Model 5590-HVL Series. The machine model is 5591 having a total capacity of 300 kN (67,000 lbf).

Short-Term Tests at Elevated Temperatures

For short-term tests at elevated temperature, an environmental chamber was constructed and placed in the computer-controlled hydraulic load actuator. The chamber was constructed from 38.1 mm (1.5 in) thick duct board and details of various parts used inside the environmental chamber are given below:

a. Finned Strip Heater

Watts	-	475
Volts	-	120
Overall length	-	266.7 mm (10.5 in)
Brand	-	VULCAN
Manufacturer part number	-	OSF1510-475A

b. Thermostat

Manufacturer	-	Johnson Controls
Type	-	Electronic Thermostat

Model	-	A419ABG-3
Range	-	-34 to 100°C (-30 to 212°F)
Differential	-	1 to 30°C (1 to 30°F)

Creep Tests

Creep tests were conducted using a static lever-arm test setup. Details of various parts used in the setup are given below:

a. Deflection Gauge

Brand	-	SHARS Tool Company
Range	-	25.4 mm (1 in)
Graduations	-	0.00254 mm (0.0001 in)

b. Strain Gauge

Brand	-	VISHAY®
Model	-	CEA-06-250UW-350
Type	-	General purpose strain gauge
Grid resistance	-	350 ohms $\pm$0.3%
Gauge factor at 24°C(75°F)	-	2.105 $\pm$0.5%

REFERENCES

[1] Strongwell n.d.:Strongwell Corporation, Bristol, VA. http://www.strongwell.com/about/the-pultrusion-process/ (accessed November 4, 2016).

[2] Mottram JT, Turvey GJ. Physical test data for the appraisal of design procedures for bolted joints in pultruded FRP structural shapes and systems. Prog Struct Eng Mater 2003;5:195–222. doi:10.1002/pse.154.

[3] Mosallam AS. Design guide for FRP composite connections. Reston, VA: American Society of Civil Engineers; 2011.

[4] Turvey GJ, Cooper C. Review of tests on bolted joints between pultruded GRP profiles. Proc Inst Civ Eng - Struct Build 2004;157:211–33.

[5] Thoppul SD, Finegan J, Gibson RF. Mechanics of mechanically fastened joints in polymer-matrix composite structures - A review. Compos Sci Technol 2009;69:301–29. doi:10.1016/j.compscitech.2008.09.037.

[6] Gand AK, Chan TM, Mottram JT. Civil and structural engineering applications, recent trends, research and developments on pultruded fiber reinforced polymer closed sections: A review. Front Struct Civ Eng 2013;7:227–44. doi:10.1007/s11709-013-0216-8.

[7] Coelho AMG, Mottram JT. A review of the behaviour and analysis of bolted connections and joints in pultruded fibre reinforced polymers. Mater Des 2015;74:86–107.

[8] Turvey GJ. Bolted joints in pultruded glass fibre reinforced polymer (GFRP) composites. In: Camanho P, Tong L, editors. Compos. Joints Connect. Princ. Model. Test., Woodhead Publishing Limited; 2011, p. 77–111.

[9] Bank LC. Composites for construction: structural design with FRP materials. Hoboken, NJ: John Wiley & Sons; 2006.

[10] ASCE. Pre-Standard for Load & Resistance Factor Design (LRFD) of Pultruded Fiber Reinforced Polymer (FRP) Structures. American Society of Civil Engineers; 2010.

[11] Mottram JT. Determination of pin-bearing strength for the design of bolted connections with standard pultruded profiles. Proc. 4th Int. Conf. Adv. Compos. Constr. (ACIC 09), Edinburgh, UK: 2009, p. 483–95.

[12] Mottram JT, Zafari B. Pin-bearing strengths for bolted con- nections in fibre-reinforced polymer structures. Proc Inst Civ Eng - Struct Build 2011;164:291–305.

[13] Johnson M, Matthews FL. Determination of safety factors for use when designing bolted joints in grp. Composites 1979;10:73–6.

[14] ASTM D 953-10. Standard test method for bearing strength of plastics. West Conshohocken, PA: ASTM International; 2010. doi:10.1520/D0953-10.

[15] ASTM D 5961/D 5961 M-10. Standard test method for bearing response of polymer matrix composite laminates. West Conshohocken, PA: ASTM International; 2010. doi:10.1520/D5961_D5961M-10.

[16] Rosner CN, Rizkalla SH. Bolted connections for fiber-reinforced composite structural members: experimental program. J Mater Civ Eng 1995;7:223–31.

[17] Turvey GJ. Single-bolt tension joint tests on pultruded GRP plate - effects of tension direction relative to pultrusion direction. Compos Struct 1998;42:341–51.

[18] Stewart WC. Bolted joints. ASME Handb. Second, 1965, p. 328–34.

[19] Collings TA. The strength of bolted joints in multi-directional CFRP laminates. Composites 1977;8:43–55.

[20] Stockdale JH, Matthews FL. The effect of clamping pressure on bolt bearing loads in glass fibre-reinforced plastics. Composites 1976:34–8. doi:10.1016/0010-4361(76)90279-2.

[21] Kretsis G, Matthews FL. The strength of bolted joints in glass fibre/epoxy laminates. Composites 1985;16:92–102.

[22] Cooper C, Turvey GJ. Effects of joint geometry and bolt torque on the structural performance of single bolt tension joints in pultruded GRP sheet material. Compos Struct 1995;32:217–26.

[23] Yuan RL, Liu CJ. Experimental characterization of FRP mechanical connections. Proc. 3rd Int. Conf. Adv. Compos. Mater. Bridg. Struct., Ottawa, Ontario, Canada: The Canadian Society for Civil Engineers, Montreal; 2000, p. 103–10.

[24] ASTM D 953-97. Standard test method for bearing strength of plastics. West Conshohocken, PA: 1997.

[25] Clarke JL, editor. Structural design of polymer composites, EUROCOMP design code and handbook. E&FN Spon, London; 1996.

[26] EN 1990. Eurocode - Basis of structural design. London: British Standards Institution (BSI); 2002.

[27] Abd-El-Naby S, Hollaway L. The experimental behaviour of bolted joints in pultruded glass/polyester material. Part 1: single-bolt joints. Composites 1993;24:531–8.

[28] Sun H-T, Chang F-K, Qing X. The response of composite joints with bolt-clamping loads, Part II: model verification. J Compos Mater 2002;36:69–92. doi:10.1106/002199802023302.

[29] Khashaba UA, Sallam HEM, Al-Shorbagy AE, Seif MA. Effect of washer size and tightening torque on the performance of bolted joints in composite structures. Compos Struct 2006;73:310–7. doi:10.1016/j.compstruct.2005.02.004.

[30] Naik RA, Crews Jr. JH. Stress analysis method for a clearance-fit bolt under bearing loads. AIAA J 1986;24:1348–53.

[31] Yuan RL, Liu CJ, Daley T. Study of mechanical connection for GFRP laminated structures. Proc. 2nd Int. Conf. Adv. Compos. Mater. Bridg. Struct., Montreal, QC, Canada: The Canadian Society for Civil Engineers, Montreal; 1996, p. 951–8.

[32] Lee Y-G, Choi E, Yoon S-J. Effect of geometric parameters on the mechanical behavior of PFRP single bolted connection. Compos Part B 2015;75:1–10.

[33] Erki MA. Bolted glass-fibre-reinforced plastic joints. Can J Civ Eng 1995;22:736–44.

[34] Abd-El-Naby S, Hollaway L. The experimental behaviour of bolted joints in pultruded glass/polyester material. Part 2: Two-bolt joints. Composites 1993;24:539–46.

[35] Hassan NK, Mohamedien MA, Rizkalla SH. Multibolted joints for GFRP structural members. J Compos Constr 1997;1:3–9.

[36] Shivakumar KN, Crews Jr. JH. Bolt clampup relaxation in a graphite/epoxy laminate. Hampton, VA: NASA Technical Memorandum 83268; 1982.

[37] Kallmeyer AR, Stephens RI. Creep elongation of bolt holes subjected to bearing loads in a polymer matrix composite laminate. In: Armanios EA, editor. Compos. Mater. Fatigue Fract. (Sixth Vol. ASTM STP 1285, American Society for Testing and Materials; 1997, p. 452–67.

[38] Turvey GJ, Wang P. Effect of temperature on the structural integrity of bolted joints in pultrusions. Int. Conf. Compos. Constr. - CCC2001, Porto, Portugal: 2001, p. 171–6.

[39] Turvey GJ, Wang P. Failure of pultruded GRP single-bolt tension joints under hot-wet conditions. Compos Struct 2007;77:514–20. doi:10.1016/j.compstruct.2005.08.024.

[40] Strongwell. Design manual. Bristol, VA: Strongwelll Corporation; 2007.

[41] Turvey GJ, Wang P. Thermal preconditioning study for bolted tension joints in pultruded GRP plate. Compos Struct 2007;77:509–13. doi:10.1016/j.compstruct.2005.08.023.

[42] Wu C, Bai Y, Mottram JT. Effect of elevated temperatures on the mechanical performance of pultruded FRP joints with a single ordinary or blind bolt. J Compos Constr 2016;20. doi:10.1061/(ASCE)CC.1943-5614 .0000608.

[43] Kang JO. Fiber reinforced polymeric pultruded members subjested to sustained loads [Ph.D. Thesis]. Atlanta, GA, USA: Georgia Institute of Technology; 2001.

[44] Ye BS, Svenson AL, Bank LC. Mass and volume fraction properties of pultruded glass fibre-reinforced composites. Composites 1995;26:725–31.

[45] Engindeniz M, Zureick A-H. Deflection response of glass fiber-reinforced pultruded components in hot weather climates. J Compos Constr 2008;12:355–63. doi:10.1061/(ASCE)1090-0268(2008)12:3(355).

[46] ASTM D 3039/D 3039 M-14. Standard test method for tensile properties of polymer matrix composite materials. West Conshohocken, PA: ASTM International; 2014. doi:10.1520/D3039_D3039M-14.

[47] Mottram JT. Structural properties of a pultruded E-glass fibre-reinforced polymeric I-beam. In: Marshall IH, editor. Compos. Struct., Elsevier Applied Science; 1991, p. 1–28.

[48] Wang Y, Zureick A-H. Characterization of the longitudinal tensile behavior of pultruded I-shape structural members using coupon specimens. Compos Struct 1994;29:463–72.

[49] Smith KJ. Compression creep of a pultruded E-glass/polyester composite at elevated service temperatures [MS Thesis]. Atlanta, GA, USA: Georgia Institute of Technology; 2005.

[50] ASTM F 606/F 606 M-16. Standard test methods for determining the mechanical properties of externally and internally threaded fasteners, washers, and rivets. West Conshohocken, PA: ASTM International; 2016. doi:10.1520/F0606_F0606M-16.

[51] Zureick A-H, Kahn LF. Rehabilitation of reinforced concrete structures using fiber-reinforced polymer composites. In: Miracle DB, Donaldson SL, editors. ASM Handb. Vol. 21 Compos., ASM International; 2001, p. 906–13.

[52] Web HVAC n.d. http://www.webhvac.com/2010/03/attic-fan-thermostat-settings-how-to-choose/ (accessed February 1, 2017).

[53] ASTM F 436-11. Standard specification for hardened steel washers. West Conshohocken, PA: ASTM International; 2011. doi:10.1520/F0436-11.

[54] Hart-Smith LJ. Design and empirical analysis of bolted or riveted joints. In: Matthews FL, editor. Join. fibre Reinf. Plast., London: Elsevier Applied Science Publishers Ltd.; 1987, p. 227–69.

[55] Mottram JT. Friction and load transfer in bolted joints of pultruded fibre reinforced polymer section. In: Seracino R, editor. Proc. 2nd Int. Conf. FRP Compos. Civ. Eng. (CICE 2004), London: Taylor & Francis plc; 2005, p. 845–50.

[56] Zureick A-H, Bennett RM, Ellingwood BR. Statistical characterization of fiber-reinforced polymer composite material properties for structural design. J Struct Eng 2006;132:1320–7. doi:10.1061/(ASCE)0733-9445(2006)132:8(1320).

[57] Alqam M, Bennett RM, Zureick A-H. Three-parameter vs. two-parameter Weibull distribution for pultruded composite material properties. Compos Struct 2002;58:497–503.

[58] ASTM D 7290 - 06 (Reappoved 2011). Standard practice for evaluating material property characteristic values for polymeric composites for civil engineering structural applications. West Conshohocken, PA: ASTM International; 2011. doi:10.1520/D7290-06R11.

[59] De Silva ART. A theoretical analysis of creep in fibre reinforced composites. J Mech Phys Solids 1968;16:169–86.

[60] Scott DW, Lai JS, Zureick A-H. Creep Behavior of fiber-reinforced polymeric composites: a review of the technical literature. J Reinf Plast Compos 1995;14:588–617.

[61] Lee LS. Creep and time-dependent response of composites. In: Karbhari VM, editor. Durab. Compos. Civ. Struct. Appl., Woodhead Publishing Limited; 2007, p. 150–69.

[62] Findley WN. Creep characteristics of plastics. Symp. Plast. ASTM, 1944, p. 118–34.

[63] Scott DW, Zureick A-H. Compression creep of a putruded E-glass/vinylester composite. Compos Sci Technol 1998;58:1361–9.

[64] EN 1995-1-1. Eurocode 5 - Design of timber structures. Part 1-1: General - Common rules and rules for buildings. London: British Standards Institution (BSI); 2004.

[65] Fan M, Enjily V. Strength and deformation modification factors of wood based composites for engineering design. Open Constr Build Technol J 2008:224–32.

[66] Van De Kuilen JWG. Creep of timber joints. HERON 2008;53:133–55.

[67] Zureick A-H. Polymer composites for infrastructure. In: Reifsnider KL, Dillard DA, Cardon AH, editors. Proc. 3rd Int. Conf. Prog. Durab. Anal. Compos. Syst., Blacksburg, VA, USA: A.A. Balkema, Rotterdam, The Netherlands; 1997, p. 181–4.

VITA

Javaid Anwar was born on November 4, 1978, in Murree, Pakistan, to Mr. and Mrs. Muhammad Arif. He grew up in Pakistan with his two sisters and two brothers. He is married to Humaira Javaid and has three sons—Umar, Ali, and Hashir. He received his bachelor's degree in civil engineering from the National University of Sciences and Technology, Risalpur campus, Pakistan, in April 2000. He has served in the Pakistan Military since 2000. He received his master's degree in Structural Engineering from the National University of Sciences and Technology, Islamabad campus, Pakistan, in March 2011. He won a Fulbright scholarship to pursue a Ph.D. degree in civil engineering from the Georgia Institute of Technology in 2012. He received his master's degree in civil engineering from the Georgia Institute of Technology in December 2014.